LATERAL CAPACITY OF SEGMENTAL MODEL PILES UNDER CYCLIC LOADING

by

Merve Sengez

B.S., Civil Engineering, Yıldız Technical University, 2017

Submitted to the Institute for Graduate Studies in
Science and Engineering in partial fulfillment of
the requirements for the degree of
Master of Science

Graduate Program in Civil Engineering

Boğaziçi University

2019

ACKNOWLEDGEMENTS

The author is greatly indebted to Prof. Gökhan Baykal for his supervision throughout the years go my graduate study at Boğaziçi University. The new idea of variable rigidity piles is first suggested by Prof. Baykal. I am extremely grateful for his assistance, guidance and many valuable suggestions throughout the entire study. Also ı would like to thank Prof. Ayşe Edinçliler and Assoc. Kubilay Keleşoğlu for serving in my committee and their valuable suggestions.

The tests are conducted at the Boğaziçi University Karl Terzaghi soil laboratory with the help of research assistant Uğurcan Erginağ. The author would also like to thank Mr. Erginağ for his kind friendship and support.

The financial support provided by Boğaziçi University Scientific Research Fund (Project No: BAP 18A04P2) is acknowledged. Finally, I would like to express my sincere gratitude to my parents and E. Doğan and my friends for their continuous and unselfish support which contributed immensely to the completion of this work.

ABSTRACT

LATERAL CAPACITY OF SEGMENTAL MODEL PILES UNDER CYCLIC LOADING

Short piles produced with traditional methods are rigid because of the used materials. In this study segmental piles with low rigidity are used. Behavior of these piles are examined under cyclic loading. The segmental pile is formed of the mortar blocks, rubber materials and rescale films which are placed between the mortar blocks and rubber material. The pile is exposed to three point bending test in order to control the target rigidity value. Also with the prescale films stress values are measured. The stress values are used for the moment calculation validation. The stress values are used for the moment calculation validation. Then the segmental pile is placed in the box and around the pile is filled with sand in different density stages. Cyclic loading is made with the antagonistic testing device operate with pneumatic muscles. Displacement values are measured under the applied load. Mortar beam is used for control and the displacement results are compared. From the load-deflection/interface relationship for rubber shore 60 tests shear values corresponding to displacement values are calculated. Shear values are integrated to obtained moment values.

ÖZET

DÖNGÜSEL YÜKLER ALTINDA MODEL KAZIKLARIN YANAL KAPASİTESİ

Geleneksel yöntemlerle üretilen kısa kazıklar, kullanılan malzeme ve donatı özellikleri dolayısyla rijit özelliklere sahiptirler. Bu çalışmada düşük rijitliğe sahip segmental kazıklar kullanılmıştır. Bu tür kazıklar kullanılarak tekrarlı yükler altında kazık davranışları incelenmiştir. Kazık beton bloklar kauçuk malzeme ve bunların arasına yerleştirilen filmlerden oluşmuştur. Oluşturulan kazık sistemine üç nokta eğilme deneyi uygulanarak hedef rijitlik kontrol edilmiştir. Filmlerle stres değerleri de ölçülmüştür. Stres değerleri moment hesaplarının doğrulaması için kullanılmıştır. Kazık çelik kutu içine yerleştirilmiş ve etrafı farklı sıkılıkta kumla doldurulmuştur. Tekrarlı yük pnomatik kasla çalışan antagonistik deney düzeneği ile yüklenmiştir. Uygulanan yük altında yer değiştirme değerleri ölçülmüştür. Kontrol kazığı olarak yekpare beton kazık deneyi ile sonuçlar karşılaştırılmıştır. Kaçuk materyal için yapılan yükleme-yerdeğiştirme/arayüz deneyleri ve yerdeğiştirme değerlerinden yerdeğiştirme değerine karşılık gelen kesme kuvveti hesaplanmıştır. Kesme kuvvetlerinin integrasyonundan moment değerleri de hesaplanmıştır.

TABLE OF CONTENTS

ACKNOWLEDGEMENTS iii
ABSTRACT iv
ÖZET v
LIST OF FIGURES ix
LIST OF TABLES xxii
LIST OF SYMBOLS xxiv
LIST OF ACRONYMS/ABBREVIATIONS xxv
1. INTRODUCTION 1
2. LITERATURE REVIEW 3
2.1. Laterally Loaded Piles 3
2.1.1. Analysis Methods for Laterally Loaded Piles 3
2.1.1.1. Limit Analysis Method 3
2.1.1.2. Subgrade Reaction Method 4
2.1.1.3. Elastic Method 4
2.1.1.4. Soil Reaction-Pile Deflection Method 5
2.1.1.5. Finite Element Method 7
2.2. Pile Properties 8
2.2.1. Active-Passive Piles 8
2.2.2. Long-Short Piles 9
2.3. Laterally Loaded Model Pile Test Studies 10
2.3.1. Model Pile Test Studies Examination 10
2.4. Contact Stress Mapping 34
2.4.1. Contact Stress Mapping Using Precale Films 34
2.4.2. Calibration Study with 4LW Film 42
2.4.3. Application Areas 43
2.5. Large Displacement Constant Contact Area Shear Device 46
2.5.1. New Large Size, Large Displacement Interface Testing System 46
2.5.1.1. Implementation of Pneumatic Muscles 47
2.6. Summary 50

3.METHODOLOGY ……..……..……... 52
3.1. Material Properties ……..…… 52
3.1.1. Concrete Mortar Blocks …… 52
3.1.1.1. Mortar Blocks Production …… 52
3.1.1.2. Compressive Strength of Mortar Blocks …… 53
3.1.2. Shore 60 Rubber …… 53
3.1.3. Aluminium Cylinder Block …… 55
3.1.4. Poorly Graded Sand ……..…… 55
3.2. Measuring Tools and Test Equipment ……..…… 55
3.2.1. Test Equipment …… 55
3.2.1.1. Steel Tension Test …… 55
3.2.1.2. Three Point Bending Test …… 55
3.2.1.3. Large Displacement Constant Contact Area Shear Device …… 57
3.2.1.4. Particle Size Distribution …… 60
3.2.1.5. Relative Density Test…… 60
3.2.1.6. Direct Shear Test ….…… 61
3.2.1.7. Oedometer Test …… 61
3.2.2. Load Cell ……..…… 61
3.2.3. Linear Variable Differential Transducer …… 61
3.2.4. Prescale Film …… 61
3.3. Specimen Preparation ……..……... 62
3.3.1. Experimental Work …… 63
3.3.1.1. Steel Tension Test …… 63
3.3.1.2. Three Point Bending Test …… 64
3.3.1.3. Load-Deflection/Interface Relationship for Sand 64
3.3.1.4. Large Displacement Constant Contact Area Shear Device ……... 64
4. TEST RESULTS AND ANALYSIS …….....…..... 66
4.1. Experimental Test Results of Soil …… 66
4.1.1. Particle Size Distribution …… 66
4.1.2. Relative Density ….……...…… 67
4.1.3. Direct Shear Test …… 67

4.1.4. Constrained Modulus of the Soil …… 70
4.2. Analysis of Segmental Pile Experimental Data ……... 72
4.2.1. Flexural Rigidity of the Segmental Pile ……. 72
4.2.2. The Moment of the Segmental Pile ……... 74
4.2.3. The Deflection of the Top Point of Segmental Pile ……... 83
4.2.4. The Deflection of the Segmental Pile with Depth ……... 89
4.2.5. The Shear Force of the Segmental Pile ……..... 99
4.2.6. Moment Calculation ……..…… 106
5. TEST RESULTS EVALUATION ……. 114
5.1. The Displacement-Soil Density Relationship of the Segmental Pile ….. 114
5.2. The Shear Force-Soil Density Relationship of the Segmental Pile ….. 117
5.3. The Moment-Soil Relative Density Relationship of the Segmental Pile …..... 118
5.4. Test Results Comprehension …….. 119
5.5. Stress Distribution of the Prescale Films …….. 123
6. CONCLUSIONS ……. 124
REFERENCES ……. 126
APPENDIX A: CYCLIC LOAD OF THE SEGMENTAL PILE...……..…….. 132
A.1. Cyclic Load at Mid-Point of the Segmental Pile Deflection Relation-ship ……..……..... 132
A.2. Cyclic Load at End-Point of the Segmental Pile Deflection Relation-Ship ……..……..……. 138
A.3. Slope of the Segmental Pile ……..…… 144
A.4. Comparison of Cyclic Loading Test Results ……. 151
APPENDIX B: MORTAR BLOCKS PROPERTIES...…….. 163
B.1. Mortar Blocks Dimensions ……..……..... 163

LIST OF FIGURES

Figure 2.1. Experimental Set-Up Schematic Diagram …… 12

Figure 2.2. Load – Displacement Curves …… 13

Figure 2.3. Soil Pressure Versus Depth ……..... 13

Figure 2.4. Experimental Set-Up Schematic Diagram ……..... 15

Figure 2.5. Static Loading Case ……..……..… 15

Figure 2.6. Cyclic Loading Case ……..…….. 16

Figure 2.7. Cyclic Loading Case 2 …… 16

Figure 2.8. Experimental Set-Up Schematic Diagram …… 18

Figure 2.9. Normalized Soil Pressure Versus Displacement ……..... 18

Figure 2.10. Experimental Set-Up Schematic Diagram …… 19

Figure 2.11. Test Results of the Study ……. 20

Figure 2.12. Soil Properties.....……. 21

Figure 2.13. Average Lateral Load-Deflection for Group Test (3d Spacing) with Changing Relative Density and Single Pile Test …… 22

Figure 2.14. Average Lateral Load-Deflection for Group Test (6d Spacing) with Changing Relative Density and Single Pile Test …… 22

Figure 2.15. Load Distributin Ratio with Lateral Deflection Variations …… 23

Figure 2.16. Pm - s/d Relationship ……..……... 23

Figure 2.17. Depth Versus Strain …… 24

Figure 2.18. Depth Versus Displacement ……..……... 25

Figure 2.19. Soil Reaction Versus Depth …… 26

Figure 2.20. Static and Cyclic Test Results …… 27

Figure 2.21. Experimental Set-Up Schematic Diagram …… 28

Figure 2.22. Experimental Set-Up Schematic Diagram …… 30

Figure 2.23. Load Versus Displacement ……..……... 30

Figure 2.24. Moment Versus Depth ……..……... 31

Figure 2.25. Experimental Set-Up Schematic Diagram …… 32

Figure 2.26. Photo of The Experimental Set-Up ……. 33

Figure 2.27. Lateral Deflection Versus Load ……. 34

Figure 2.28. Different Types of Prescale Films with Different Pressure Range 36

Figure 2.29. Two Sheet Type ……..…… 37

Figure 2.30. Mono Sheet Type ……..…… 37

Figure 2.31. Explosion of the microcapsules ……. 38

Figure 2.32. The contact pressure versus color intensity calibration curves for sustained pressure…… 39

Figure 2.33. The contact pressure versus color intensity calibration curves for momentary pressure…… 40

Figure 2.34. Calibration Sheet……..…….. 41

Figure 2.35. Typical Stress Map of Geogrid…….….. 41

Figure 2.36. Stress Map-Measurement Display ……. 43

Figure 2.37. Large Displacement Constant Contact Area Shear Device..... 47

Figure 2.38. Rubber Muscle…… 48

Figure 2.39. 40 mm Muscle Load Capacity at Various Air Pressure and Changing Contraction…….……. 49

Figure 2.40. The Right Side View of the Device…… 50

Figure 3.1. Steel Mold …….……... 52

Figure 3.2. Mortar Block Unit …….……... 53

Figure 3.3. Rubber Unit ……. 54

Figure 3.4. Steel Tension Test ……. 56

Figure 3.5. Three Point Bending Test ……. 57

Figure 3.6. The Drawing of Cyclic Actuator……. 58

Figure 3.7. Antagonistic Configuration of the Pneumatic Muscles…….. 58

Figure 3.8. Equilibrium Position as a Function of Gauge Pressure Ratio……. 59

Figure 3.9. Large Displacement Constant Contact Area Shear Device ……. 60

Figure 3.10. Segmental Pile……. 63

Figure 3.11. Schematic View of the Testing Setup……. 65

Figure 4.1. Particle Size Distribution ……. 66

Figure 4.2. Shear versus Horizontal Displacement for Dense Soil…..……. 67

Figure 4.3. Vertical Displacement versus Horizontal Displacement for Dense Soil 68

Figure 4.4. Shear versus Horizontal Displacement for Medium Dense Soil.... 68

Figure 4.5. Vertical Displacement versus Horizontal Displacement for Medium Dense Soil..... 69

Figure 4.6. Shear versus Horizontal Displacement for Loose Soil..... 69

Figure 4.7. Vertical Displacement versus Horizontal Displacement for Loose Soil..... 70

Figure 4.8. Flexural Stress versus Strain ……. 73

Figure 4.9. Flexural Stress versus Strain ……. 73

Figure 4.10. Place of the Prescale Films..... 75

Figure 4.11. Scanned Prescale Films (750 N-Lower Part)…….. 75

Figure 4.12. Scanned Prescale Films (750 N-Upper Part)..... 76

Figure 4.13. Scanned Prescale Films (1500 N-Lower Part).....…….. 76

Figure 4.14. Scanned Prescale Films (1500 N-Upper Part).....……. 77

Figure 4.15. Scanned Prescale Films (2250 N-Lower Part)..... 77

Figure 4.16. Scanned Prescale Films (2250 N-Upper Part)..... 78

Figure 4.17. The Bending Moment Diagram along Segmental Pile Length (750N) ……..... 79

Figure 4.18. The Bending Moment Diagram along Segmental Pile Length (1500N).....……. 79

Figure 4.19. The Bending Moment Diagram along Segmental Pile Length (2250N)…….....…. 80

Figure 4.20. Bending Moment Values Calculated from The Point Bending Test.....……. 81

Figure 4.21. Shear Values Obtained from the Load-Deflection/Interface Relationship for Rubber Shore 60 Tests.....……. 81

Figure 4.22. Moment Values Found from the Shear Values Obtained from Interface Results …….……... 82

Figure 4.23. Segmental Pile with Post-Tension Force 750 N in Loose Soil …. 83

Figure 4.24. Segmental Pile with Post-Tension Force 750 N in Medium-

Dense Soil 84

Figure 4.25. Segmental Pile with Post-Tension Force 750 N in Dense Soil 84

Figure 4.26. Segmental Pile with Post-Tension Force 1500 N in Loose Soil 85

Figure 4.27. Segmental Pile with Post-Tension Force 1500 N in Medium-Dense Soil 85

Figure 4.28. Segmental Pile with Post-Tension Force 1500 N in Dense Soil ... 86

Figure 4.29. Segmental Pile with Post-Tension Force 2250 N in Loose Soil ... 86

Figure 4.30. Segmental Pile with Post-Tension Force 2250 N in Medium-Dense Soil 87

Figure 4.31. Segmental Pile with Post-Tension Force 2250 N in Dense Soil ... 87

Figure 4.32. Mortar Beam in Loose Soil 88

Figure 4.33. Mortar Beam in Medium-Dense Soil 88

Figure 4.34. Mortar Beam in Dense Soil 89

Figure 4.35. Displacement of the segmental Pile with Post-Tension Force 750 N in Loose Soil 90

Figure 4.36. Displacement of the segmental Pile with Post-Tension Force 750 N in Medium-Dense Soil 90

Figure 4.37. Displacement of the segmental Pile with Post-Tension Force 750 N in Dense Soil 91

Figure 4.38. Displacement of the segmental Pile with Post-Tension Force 1500 N in Loose Soil ……. 91

Figure 4.39. Displacement of the segmental Pile with Post-Tension Force 1500 N in Medium-Dense Soil ……... 92

Figure 4.40. Displacement of the segmental Pile with Post-Tension Force 1500 N in Dense Soil ……. 92

Figure 4.41. Displacement of the segmental Pile with Post-Tension Force 2250 N in Loose Soil ……..... 93

Figure 4.42. Displacement of the segmental Pile with Post-Tension Force 2250 N in Medium-Dense Soil ……..… 93

Figure 4.43 Displacement of the segmental Pile with Post-Tension Force 2250 N in Loose Soil ……..……... 94

Figure 4.44. Displacement of the Mortar Beam in Loose Soil……..…....… 94

Figure 4.45. Displacement of the Mortar Beam in Medium-Dense Soil..... 95

Figure 4.46. Displacement of the Mortar Beam in Dense Soil.....……..…….. 95

Figure 4.47. Displacement Values of the Piles in Loose Soil..... 96

Figure 4.48. Displacement Values of the Piles in Medium Dense Soil..... 96

Figure 4.49. Displacement Values of the Piles in Dense Soil..... 97

Figure 4.50. Flowchart of the Shear Force Calculation..... 100

Figure 4.51. Shear of the segmental Pile with Post-Tension Force 750 N in

Loose Soil ……... 100

Figure 4.52. Shear of the segmental Pile with Post-Tension Force 750 N in Medium-Dense Soil …….. 101

Figure 4.53. Shear of the segmental Pile with Post-Tension Force 750 N in Dense Soil ……..……. 101

Figure 4.54. Shear of the segmental Pile with Post-Tension Force 1500 N in Loose Soil ……..……. 102

Figure 4.55. Shear of the segmental Pile with Post-Tension Force 1500 N in Medium-Dense Soil ……..……. 102

Figure 4.56. Shear of the segmental Pile with Post-Tension Force 1500 N in Dense Soil ……..…. 103

Figure 4.57. Shear of the segmental Pile with Post-Tension Force 2250 N in Loose Soil ……..…. 103

Figure 4.58. Shear of the segmental Pile with Post-Tension Force 2250 N in Medium-Dense Soil ……..…. 104

Figure 4.59. Shear of the segmental Pile with Post-Tension Force 2250 N in Dense Soil ……..…. 104

Figure 4.60. Shear of the Mortar Beam in Loose Soil …….. 105

Figure 4.61. Shear of the Mortar Beam in Medium-Dense Soil ……..…. 105

Figure 4.62. Shear of the Mortar Beam in Dense Soil ……..……. 106

Figure 4.63. Moment of the segmental Pile with Post-Tension Force 750 N in

Loose Soil ……..….. 107

Figure 4.64 Moment of the segmental Pile with Post-Tension Force 750 N in Medium-Dense Soil ……..…. 107

Figure 4.65 Moment of the segmental Pile with Post-Tension Force 750 N in Dense Soil ……. 108

Figure 4.66. Moment of the segmental Pile with Post-Tension Force 1500 N in Loose Soil.....……108

Figure 4.67. Moment of the segmental Pile with Post-Tension Force 1500 N in Medium-Dense Soil……..... 109

Figure 4.68. Moment of the segmental Pile with Post-Tension Force 1500 N in Dense Soil ……..…. 109

Figure 4.69. Moment of the segmental Pile with Post-Tension Force 2250 N in Loose Soil ……..…. 110

Figure 4.70. Moment of the segmental Pile with Post-Tension Force 2250 N in Medium-Dense Soil ……..……..… 110

Figure 4.71. Moment of the segmental Pile with Post-Tension Force 2250 N in Dense Soil ……..……. 111

Figure 4.72. Moment of the Mortar Beam in Loose Soil ……..……. 111

Figure 4.73. Moment of the Mortar Beam in Medium-Dense Soil……..…. 112

Figure 4.74. Moment of the Mortar Beam in Dense Soil...……..…. 112

Figure A.1. Segmental Pile with Post-Tension Force 750 N in Loose Soil ... 132

Figure A.2. Segmental Pile with Post-Tension Force 750 N in Medium-Dense Soil ……..…. 132

Figure A.3. Segmental Pile with Post-Tension Force 750 N in Dense Soil ... 133

Figure A.4. Segmental Pile with Post-Tension Force 1500 N in Loose Soil ...133

Figure A.5. Segmental Pile with Post-Tension Force 1500 N in Medium-Dense Soil ……..…. 134

Figure A.6. Segmental Pile with Post-Tension Force 1500 N in Dense Soil... 134

Figure A.7. Segmental Pile with Post-Tension Force 2250 N in Loose Soil... 135

Figure A.8. Segmental Pile with Post-Tension Force 2250 N in Medium-Dense Soil ……..…. 135

Figure A.9. Segmental Pile with Post-Tension Force 2250 N in Dense Soil... 136

Figure A10. Mortar Beam in Loose Soil....……..……. 136

Figure A.11. Mortar Beam in Medium-Dense Soil ……..…. 137

Figure A.12. Mortar Beam in Dense Soil....……..…. 137

Figure A.13. Segmental Pile with Post-Tension Force 750 N in Loose Soil ... 138

Figure A.14. Segmental Pile with Post-Tension Force 750 N in Medium-Dense Soil …….....……. 138

Figure A.15. Segmental Pile with Post-Tension Force 750 N in Dense Soil ... 139

Figure A.16. Segmental Pile with Post-Tension Force 1500 N in Loose Soil... 139

Figure A.17. Segmental Pile with Post-Tension Force 1500 N in Medium-Dense Soil ……..……. 140

Figure A.18. Segmental Pile with Post-Tension Force 1500 N in Dense Soil... 140

Figure A.19. Segmental Pile with Post-Tension Force 2250 N in Loose Soil... 141

Figure A.20. Segmental Pile with Post-Tension Force 2250 N in Medium-Dense Soil.....…….. 141

Figure A.21. Segmental Pile with Post-Tension Force 2250 N in Dense Soil... 142

Figure A.22. Mortar Beam in Loose Soil ……..……. 142

Figure A.23. Mortar Beam in Medium-Dense Soil ……..……. 143

Figure A.24. Slope of the Mortar Beam in Dense Soil ……..……. 143

Figure A.25. Slope of the Segmental Pile with Post-Tension Force 750 N in Loose Soil ……..…….. 144

Figure A.26. Slope of the Segmental Pile with Post-Tension Force 750 N in Medium-Dense Soil ……..……. 144

Figure A.27. Slope of the Segmental Pile with Post-Tension Force 750 N in Dense Soil ……..…. 145

Figure A.28. Slope of the Segmental Pile with Post-Tension Force 1500 N in Loose Soil ……..…. 145

Figure A.29. Slope of the Segmental Pile with Post-Tension Force 1500 N in

Medium-Dense Soil ……..…….. 146

Figure A.30. Slope of the Segmental Pile with Post-Tension Force 1500 N in Dense Soil ……..…. 146

Figure A.31. Slope of the Segmental Pile with Post-Tension Force 2250 N in Loose Soil ……..……. 147

Figure A.32. Slope of the Segmental Pile with Post-Tension Force 2250 N in Medium-Dense Soil …….…… 147

Figure A.33. Slope of the Segmental Pile with Post-Tension Force 2250 N in Dense Soil ……..……. 148

Figure A.34. Slope of the Mortar Beam in Loose Soil ……..…. 148

Figure A.35. Slope of the Mortar Beam in Medium-Dense Soil ……..…. 149

Figure A.36. Slope of the Mortar Beam in Dense Soil ……..…. 149

Figure A.37. All Test Results of Displacement of the Segmental Pile with Post-Tension Force 750 N in Loose Soil …….……..…. 151

Figure A.38. All Test Results of Displacement of the Segmental Pile with Post-Tension Force 750 N in Medium-Dense Soil .....……..…… 152

Figure A.39. All Test Results of Displacement of the Segmental Pile with Post-Tension Force 750 N in Dense Soil....…….…….. 153

Figure A.40. All Test Results of Displacement of the Segmental Pile with Post-Tension Force 1500 N in Loose Soil …….……..……. 154

Figure A.41. All Test Results of Displacement of the Segmental Pile with Post-

Tension Force 1500 N in Medium-Dense Soil .....…….. 155

Figure A.42. All Test Results of Displacement of the Segmental Pile with Post-Tension Force 1500 N in Dense Soil …….…….. 156

Figure A.43. All Test Results of Displacement of the Segmental Pile with Post-Tension Force 2250 N in Loose Soil …….…….. 157

Figure A.44. All Test Results of Displacement of the Segmental Pile with Post-Tension Force 2250 N in Medium-Dense Soil.....……. 158

Figure A.45. All Test Results of Displacement of the Segmental Pile with Post-Tension Force 2250 N in Dense Soil …….…….……. 159

Figure A.46. All Test Results of Displacement of the Segmental Pile with Post-Tension Force Mortar Beam in Loose Soil....…….…. 160

Figure A.47. All Test Results of Displacement of the Segmental Pile with Post-Tension Force Mortar Beam Medium-Dense Soil....……..…. 161

Figure A.48. All Test Results of Displacement of the Segmental Pile with Post-Tension Force Mortar Beam Dense Soil.....……. 162

LIST OF TABLES

Table 2.1. Model Test Studies ……. 11

Table 2.2. Material Properties 33

Table 2.3. Sensitive Film Measurement Ranges 37

Table 3.1. Compressive Strength Test Results ……. 54

Table 3.2. Rubber Properties Details ……. 54

Table 4.1. Loading Situations ……. 70

Table 4.2. Vertical Strain Percentage ……. 71

Table 4.3. Constrained Modulus of Granular Material ……. 72

Table 4.4. Numerical Values of Flexural Rigidity of the Mortar Beam ……. 74

Table 5.1. Displacement of the Pile Model with Post-Tension Force of 750 N in Soil with Various Densities ……..…. 114

Table 5.2. Displacement of the Pile Model with Post-Tension Force of 1500 N in Soil with Various Densities ……..… 114

Table 5.3. Displacement of the Pile Model with Post-Tension Force of 2250 N in Soil with Various Densities ……..… 115

Table 5.4. Displacement of the Pile Model of Mortar Beam in Soil with Various Densities ……..… 115

Table 5.5. Minimum and Maximum Shear Force Values of the Piles.……. 118

Table 5.6. Minimum and Maximum Moment Values of the Piles..... 119

Table 5.7. Results of Segmental pile with post-tension of 2250 N-3K/Cyclic 120

Table 5.8. Results of Segmental pile with post-tension of 2250 120

Table A.1. Minimum and Maximum Slope Values of the Piles ……. 150

Table B.1. Mortar Blocks Dimensions.....,,..... 163

LIST OF SYMBOLS

a	Acceleration
A,B	Emprical adjustment factors
B	Circular plate diameter
b	Pile diameter
c	Undrained shear strength (N/cm^2)
c_a	Average of clay undrained shear strength
d	Diameter of pile (cm)
Dr	Relative density
E	Young Modulus
Es	Soil modulus
E_{sm}	At m point, soil modulus
E50	Secant deformation modulus
E_{30}	Young modulus for test plate with diameter 30 cm
EI	Flexural rigidity
F	Force
H	The distance of P above the ground surface
I	Moment of Inertia
I_p	Shape coefficient
k	Soil modulus N/cm^3
k_h	Subgrade reaction coefficient
ks, kc	Cyclic and static loading constants for stiff clay
k_1,k_2	Soil modulus variation constants
k_{30}	Subgrade reaction for test plate with diameter 30 cm
K_A	Active Earth pressure coefficient
K_p	Passive Earth pressure coefficient
K_o	Earth pressure coefficient at rest
L	Pile length
m	Lateral soil reaction coefficient N/cm^3
M	Mass
M	Moment

n_h	A coefficient up to sand type
N_p	Dimensionless ultimate bearing capacity coefficient
p	Soil reaction
P	Applied Load
P_c	Theoretical ultimate resistance
Pu	Ultimate Bearing Capacity
P_{uc}	For cyclic loading case measured ultimate resistance
P_{us}	For static loading case measured ultimate resistance
Pm,	Reduced ultimate bearing capacity
Pw	The ultimate soil resistance by wedge type failure
p(y)	Soil reaction stress at a significant depth
S	Slope
t	Equal units number
T	Rigidity factor recommended by Matlock and Reese
V	Shear Force
x	Depth
xr	Depth below ground surface to bottom of reduced strength zone
y	horizontal displacement at a significant depth
z	Depth
ν	Poisson ratio
ϕ	Internal friction angle
σ_x	Overburden pressure (N/cm^2)
ε_{50}	Strain at failure
γ'	Soil effective unit weight

LIST OF ACRONYMS/ABBREVIATIONS

ASTM	American society for testing and materials
CRR	Cyclic resistance ratio
CSR	Cyclic stress ratio
LVDT	Linear variable differantial transducer
SPVFR	Segmental pile with variable flexural rigidity

1. INTRODUCTION

Lateral earth pressure, wind, wave and earthquake forces impose lateral loads on pile. Due to the rigid behavior of piles, large cross-section are needed to overcome these forces. Piles with larger flexibility will help to converse these integrity even at larger displacements.

The new technique developed at Boğaziçi University. It requires a new pile construction technique involving alternating concrete blocks and rubber membrane, compressed by an anchor cable passing through the hole at the center of each block. By adjusting the tension force of the anchor cable, the blocks are held together with the imposed normal force due to post tensioning of the cable.

Wave, earthquake and wind forces improve cyclic lateral load on piles. The objective of this study is to assessing the displacement caused by cyclic loads along the segmental pile. Under cyclic lateral loads, behavior of the pile model can be studied with the flexural rigidity control. Allowing the system to flex without breaking under lateral loads is the main benefit of controlling the flexural rigidity. This situation obstructs the collapse of the pile.

In order to obtain these objectives an experimental study is made. With this experimental study behavior of segmental structure in any case has been analyzed.

The next chapters show the outline of the chapters of this thesis. Chapter 2 is the literature review part and it starts with laterally loaded piles. After the introduction of the laterally loaded piles, analyses methods of laterally loaded piles are presented. Some of the analyses methods are explained briefly. In the second part of the literature review short-long pile and active-passive pile cases are presented. After that laterally loaded model pile studies are examined. For the fourth part contact stress mapping applications are presented. The tools used for constact stress mapping is explained briefly. Also the usage areas of contact stress mapping are shown. In the last part large displacement constant contact area shear device which is used for the experimental part of this study is examined. Its

properties are explained briefly. In Chapter 3, the methodology of this study is seen. In this part specimen preparation and implementation of experimental tools are shown. Chapter 4, is a kind of outline of the tests. The test results are shown in this part. On the other hand in Chapter 5, evaluation of the test results which are illustrated in Chapter 4 is presented. Chapter 6 is the last and the conclusion part.

2. LITERATURE REVIEW

2.1. Laterally Loaded Piles

The laterally loaded pile is seen as a part of complex structure rather than a single structural member. For example a laterally loaded pile can be a part of offshore drilling platform.

There are many different kinds of forces which affect the pile foundations laterally. Earthquake, wave forces and lateral soil pressure are examples of the lateral loads. Within these loads wave forces and earthquake are cyclic forces. [3]

In order to make a proper design for a laterally loaded pile, bearing capacity at failure is not the only consideration for engineers. Moment and deflection under working load are also important. [4]

2.1.1. Analysis Methods for Laterally Loaded Piles

In order to make a design for a laterally loaded pile there are five methods. [5]

2.1.1.1. Limit Analysis Method

For this method it is considered that the limiting soil resistance is moving against the pile, in the meantime the ultimate load is placed against the pile. This method requires two assumption.

(i) a soil of fixed strength with depth

(ii) the pile deflects enough to grow the complete soil resistance all along the length noted.

If there are small deflections, that makes second assumption incorrect. [6-8]

2.1.1.2. Subgrade Reaction Method

The aim of this method is obtain subgrade reaction coefficient k_h from the tests in order to make suitable design for piles against horizontal loading. With subgrade coefficient soil reaction can be calculated at a significant depth. [9]

Because of its easiness subgrade reaction method is used widely. It is used on especially beam on elastic foundations assumptions. However this method requires some limitations.

(i) It requires linear soil resistance model but evidence shows that the soil resistance is non-linear.

(ii) Subgrade reaction modulus is not a soil basic soil property, it is a kind of model parameter.

(iii) The springs used to model soil resistance are discontinuous but the the soil is continuous.

(iv) Geometry of pile must be assumed indirectly. [9-13]

2.1.1.3. Elastic Method

It is likely to use an elastic method, if the reaction-pressure connections of a soil are understood.

According to elastic methods, it is considered that soil acts in a sequence of discrete elements. It is counted that this assumption performs without large error when it is applied to laterally loaded pile problems.

Two titles are important to find convincing outcomes from the analysis which requires elastic method. [3]

(i) Full data which identifies the behavior of the soil should be found.

(ii) The differential equation should be solved.

2.1.1.4. Soil Reaction-Pile Deflection Method

Soil reaction-pile deflection method is a numerical model that simulates the soil resistance as predefined nonlinear springs where p is the soil pressure per unit length and y is pile deflection. [15]

In order to obtain laterally loaded pile differential equations, a pile segment is cut and equilibrium equations are applied. Equilibrium equation for moment is shown below.

$$M_{m-1}-M_m-V_m dx=0 \quad (2.1)$$

$$dM-V_m dx=0 \quad (2.2)$$

$$dM/dx-V_m=0 \quad (2.3)$$

There is a differential equation for the solution of the laterally loaded piles which is obtained after differentiating the equations above with respect to x. The equations are shown below.

$$d^2M/dx^2- dV_m/dx=0 \quad (2.4)$$

$$d^2M/dx^2=EI(d^4y)/(dx^4) \text{ and } dV/dx \quad (2.5)$$

$$EI(d^4y)/(dx^4)-p=0 \quad (2.6)$$

y=deflection
x=length along pile
EI=flexural stiffness of pile
p=soil reaction

Equation 2.6. does not contains the impacts of the axial load on flexure. If this impact is in considerable size, the equation has to be expanded.

P value depends on pile-soil interaction and the method mostly adopted to deal with this is the p-y method in which a secant modulus E_s is identified.

$$E_s = -p/y \quad (2.7)$$

E_s depends on; soil stress-strain properities will change with dept, width of pile, deflection of pile.

In these differential equations above, selecting suitable boundary conditions is important in order to provide the satisfaction of the interface between the pile and superstructure. If the superstructure is the simple attendance of the pile, selecting boundary conditions is simple. On the other hand, if there is no attendance, iteration between solutions for the pile and for the superstructure may need. Reason for these iterations is the nonlinear behavior of the soil. [3-14]

While solving the problem of laterally loaded pile, predicting a set of p-y curves is preferable. If it is predictable, Equation 2.6 can easily be solved to yield pile deflection, pile rotation, bending moment, shear and soil reaction for any load supported by pile. However several iterations must be made.

Also, experiments show that reaction of the soil at a point is related to pile deflection at that point not at the points above or below. Therefore for the analyzes, different mechanisms with load-deflection characteristics can be used instead of soil.

The basic equation is written above, again it is shown below.

$$EI(d^4y)/(dx^4)+E_sy=0 \quad (2.8)$$

and in difference form it becomes

$$[EI/(L/t)^2]\,[y_{m+2} - 4y_{m+1} + 6y_m - 4y_{m-1} + y_{m-2}] = - E_{sm}\, y_m \quad (2.9)$$

L= Pile length

t= Pile sections total number

Expressions like that for slope, moment and shear could be written.

$$S_m = [1/2(L/t)] (-y_{m+1} + y_{m-1}) \quad (2.10)$$

$$M_m = [EI/(L/t)^2] (y_{m+1} - 2y_m + y_{m-1}) \quad (2.11)$$

$$V_m = [EI/2(L/t)^3] (-y_{m+2} + 2y_{m+1} - 2y_{m-1} + y_{m-2}) \quad (2.12)$$

Also equations for boundary conditions at the pile base and top can be written as they are seen below.

at pile base=$M_o=V_o=0$

at pile top; P_t and M_t are known (Free head)

at pile top; P_t is known, $S_t= 0$ (Fixed head) [3, 18]

2.1.1.5. Finite Element Method

The finite element method requires lots of facilities like forming interface behavior of pile/soil, 3-D boundary conditions, soil continuity or non-continuity. This method is much more meticulous than other methods. [5]

It is hard in the finite element method to model an endless domain. Mostly, finite element mesh boundaries are set at large enough distances for the boundary impacts to become remissible, at least beyond the theoretical extend of collapse mechanism. On the other hand, Brocklehurst applying this way in his two layer system study. Some considerable errors were found in the finite element results, because of the mesh boundaries close proximity. He had to replace them far away in order to find acceptable results. [16-17]

Clearly it is seen that, this method is still a research appliance. Because it needs too much work for calculating and forming the model. [5]

2.2. Pile Properties

2.2.1. Active-Passive Piles

When soil which moves laterally encounters with the piles which are more stiffer than the soil, it can not move on its lateral movement and it lays on the piles. Unless the piles move forward a little bit, they keep on translating because of the huge movement of the soil coming back. These types of piles are called as passive piles in literature. Passive word implies the soil movement coming to pile. The soil behind and in front of the pile jams with different mechanisms.

There are various methods for passive pile systems solution, but the best way which shows the real behavior of the pile on field is based on displacement. For the other technique which is based on deformation lateral displacement without pile is determined. The most important part is determining both the highest value of the lateral deformation and the variation of lateral deformation connected to time. However it is hard to determine lateral displacement without pile. It is possible to calculate it with finite elements method but the most dependable solutions are found on the field. After obtaining lateral soil movement without pile, the loading situation on the pile is defined based on the pile-soil relative displacement. [18]

Passive piles are good solution for supporting the slopes and avoiding slope movement in poor bearing soils. Soil load transfer coming from lateral soil movements to the piling parts is a serious issue of structure-soil interaction. It is difficult to calculate pile stability when the downward soil movement caused by lateral load distributions happens. [19]

In the passive pile behavior analysis, maximum lateral soil pressure applied to pile is a significant parameter. In the studies, lots of researchers assume that ultimate soil resistance of passive piles are the same as that the values for active piles. Because the relative movement of the soil and pile is alike each other for both situations. Therefore, p_u value between 9 s_u to 12 s_u is derived from the studies of active piles, is used most of the

time for the passive pile analysis. On the other hand, some researchers recommend lower values for p_u for passive pile studies. [20]

Active piles are identified as piles which are exposed to structural or external forces at pile head. Contrary to passive situation, lateral loads acting on active piles are predetermined, they are not affected by the pile existence. [19-21]

2.2.2. Long-Short Piles

Landslide mechanism of a pile under lateral loading depends on the pile length. Short piles are rigid ones and long piles are flexible ones which affects the landslide mechanism. In order to express pile length, length-diameter relationship and the rigidity relation between the pile and soil is important.

Contrary to slender, flexible long piles, short piles diameter or width are wider, but their length is shorter. Also short piles are rigid structural members. For flexible long piles landslide occurs when translation under lateral loading exceeds the critical moment value. The most important factor affecting the lateral load capacity of flexible long pile is bending moment of pile. On the other hand for rigid short piles landslide occurs when a pile starts to turn around a point under lateral loading and lean on the soil causing to soil bearing capacity exceeding.

The analytical solutions recommended by Broms (1964) are classified as the length of piles. For the piles embedded in cohesionless soils;

$L/T<2 \rightarrow$ Short pile

$L/T>4 \rightarrow$ Long pile

$T= [(E\ I)/(\eta_h)]\ ^{(1/5)}$

where

L= Embedded length of pile

T= Rigidity factor recommended by Matlock and Reese

E= Elasticity modulus

I= Moment of inertia

η_h= Subgrade coefficient multiplier

Tomlinson (2001), recommended that if embedded length of pile to diameter of pile ratio (L/D) is less than 10-12, it is a short pile. Santana (2018) expressed that rigid or flexible behavior of an embedded piece is connected to slenderness (L/D) of the embedded part and structure-soil rigidity effect. According to Santana, if the slenderness is less than 6 (L/D<6), it must be accepted as rigid without thinking about structure-soil rigidity effect.. Giannakou (2006) claims that if the slenderness is less than 7,5 (L/D<7,5) it must be counted as rigid pile. Badry and Satyam (2018) said that piles must be classified in two groups under lateral loading. If the slenderness is higher than 30 (L/D>30), it is long pile. On the other hand if the slenderness is less than 20 (L/D<20), it is short. As it is seen above lots of definition is existing for long and short piles. [22-24]

2.3. Laterally Loaded Model Pile Test Studies

This part presents the results of laboratory model tests. The effects of different factors such as, soil type, loading type, pile material and method of installation were studied. The pile responses of different studies are presented in terms of load–deflection curves, bending moment distribution, and shear force distribution.

2.3.1. Model Pile Test Studies Examination

In the table some of the model pile test studies in literature are shown. In the table significant differences between the model pile tests such as, pile material, pile length, soil type and loading type are shown. Below the table brief examination of the tests are made.

Table 2.1. Model Test Studies.

Pile Material	Pile Length (mm)	Diameter of Pile (mm)	Dimensions of Pile (mm)	Single/Group Test	Soil	Loading Type	Reference
Steel	1135	102		Single	Sand	Static	25
Aluminium	1200	32		Single	Sand	Static-Cyclic	26
Steel	295		20x6	Single	Clay	Static	20
Aluminum	850-600		20,8x9,8	Single	Sand	Static-Cyclic	27
Steel	250	12		Group	Sand	Static	28
Steel	1524	102		Single	Sand	Static	29
Aluminium	1200	32		Single	Sand	Static-Cyclic	30
Copper	790	80		Single	Sand	Cyclic	31
Aluminium	750	22		Single	Sand	Static	12
Steel	200	50		Single	Sand	Static	23
Steel-Aluminium-Delrinder	200	50		Single	Sand	Static	32

For the model test, “Lateral Capacity of Model Rigid Piles in Cohesionless Soils” well graded angular dry sand is used.[25] Density values and different friction angles for different density values are found in the study. Friction angles are found with triaxial tests and they are equal to 33,3° for loose state, 39° for medium-dense state and 43° for the dense state.

The embedded part of the pile is equipped with ten pressure transducers. They are attached on each half of the pile in order to measure the soil pressure. Also a load cell is attached to pile base. Diameter of the testing container is equal to 1,83 m. and its height is 2,0 m. The pile stands in the center of the container and the sand is laid in to the device in layers of 50 mm thick. The tests are repeated at various embedment ratios. In Figure 2.1. experimental set-up schematic diagram is shown.

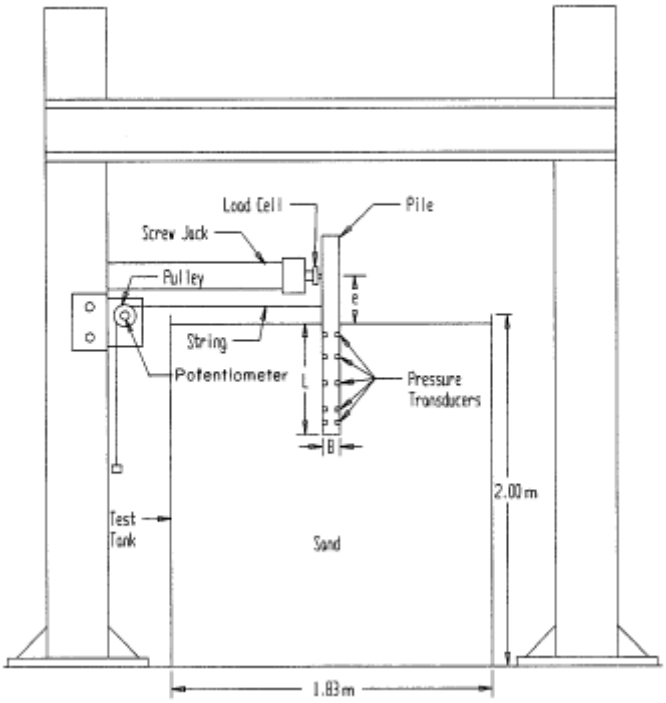

Figure 2.1. Experimental set-up schematic diagram [25].

Screw jack is used for applying the load. The load is measured with the load cell bounded to the jack. Pile top deflection is measured with a ten turn potentiometer which is attached to the pile with cables.

Result of the mentioned study requires the lateral load-pile head deflection and depth- lateral soil pressure distribution graphics which are shown in the Figures 2.2. and 2.3. According to measured soil pressures along pile, a method is recommended in order to predict pile ultimate lateral capacity more accurately. Also this recommended method is compared with the earlier studies.

The recommended method is used to find pile ultimate load capacity from the formula below.

$$Hu = \int 0{,}80\ pBdz \qquad (2.13)$$

Where

Hu= Ultimate Lateral Load Capacity

P= Pressure at a Depth

B= Pile Diameter

The factor 0,80 thought as the non-uniform pressure distribution. [25]

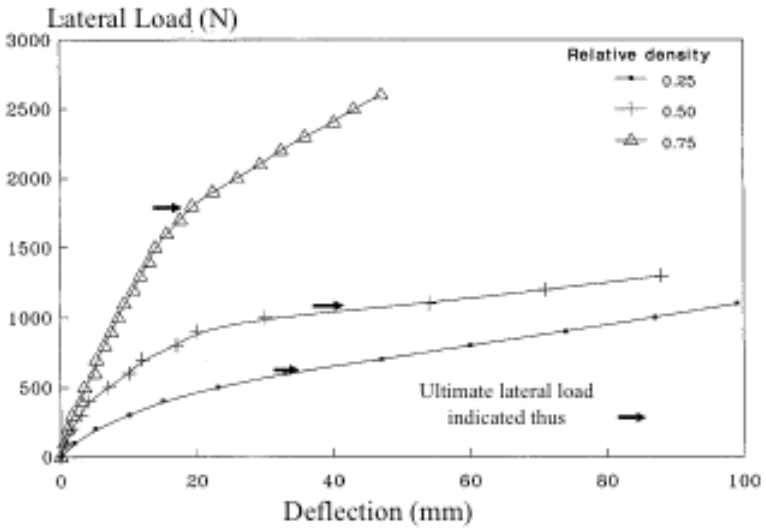

Figure 2.2. Load-Displacement curves [25].

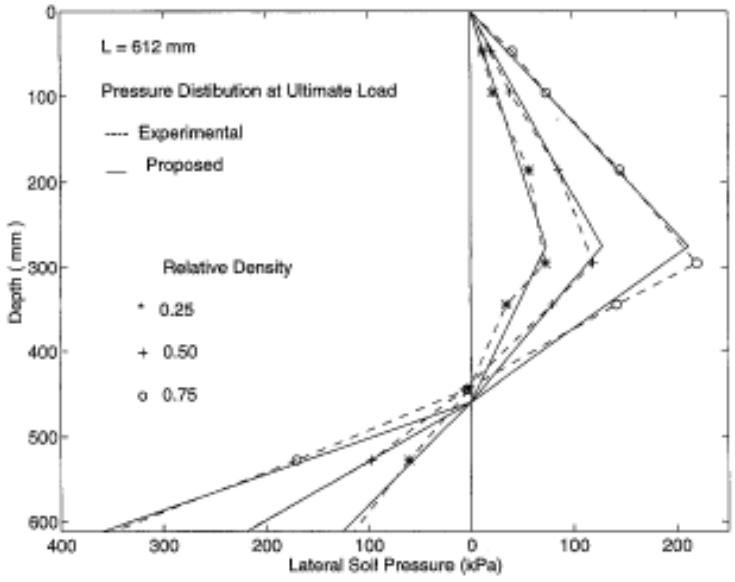

Figure 2.3. Soil pressure versus depth [25].

In “An Experimental Study on Cyclic Loading of Piles in Sand” study, only one density state and the friction angle connected to this density state is used.[26] Also D_{10} value of the sand is found and it is equal to 0,11 mm.

Storage box dimensions are 1x1x0,8 m. Laminar aluminum frames are used for the upper part and a fixed timber box is placed at the lower part. A sand rainer is used in order to fill the storage box. Ten pairs of strain gauges are attached to the pile. In order to protect the gauges an epoxy coverage is used. For the installation of the pile a vertical jack is employed. For the lateral loading steel wire is used. The wire is connected to pile from one side and it is connected to a mass from the other side. It pulls the pile horizontally. The direction of the wire is changed with a pulley. The mass connected to wire is on a jack system. When the force is applied to jack, it moves the mass and the mass pulls the wire. So it causes horizontal movement to pile. In Figure 2.4. experimental set-up schematic diagram is shown.

In Figure 2.4. the first arrow refers the storage box, the second arrow refers the model pile, the third arrow refers the strain gauge wires, the fourth arrow refers LVDT, the fifth arrow refers the steel wire, the sixth arrow refers the pulley, the seventh arrow refers to dead weights, the eightth arrow refers to hydraulic jack and the last arrow refers vertical hydraulic jack.

Three different tests are made. Two of them are cyclic and one of them is static. 50 cycles are made for the cyclic tests. 50 cycles are obtained cumulatively. It is the combination of the ten cycles. Values of each ten cycles are recorded. After the recording of 5 times 10 cycles, it is accepted that a test with 50 cycles is completed. The difference between the test is the value of the applied load. Between the pile and the soil a separation layer called as gap is seen in the cyclic tests.

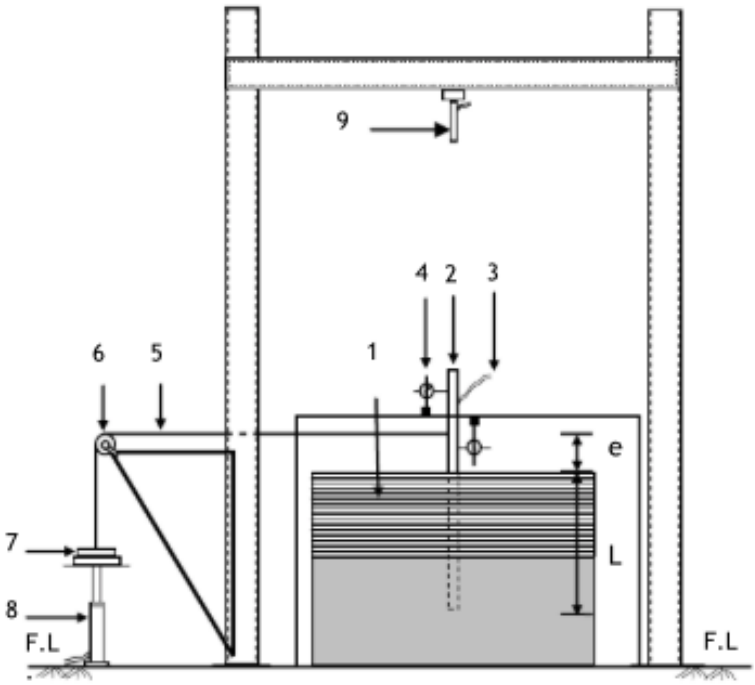

Figure 2.4. Experimental set-up schematic diagram [26].

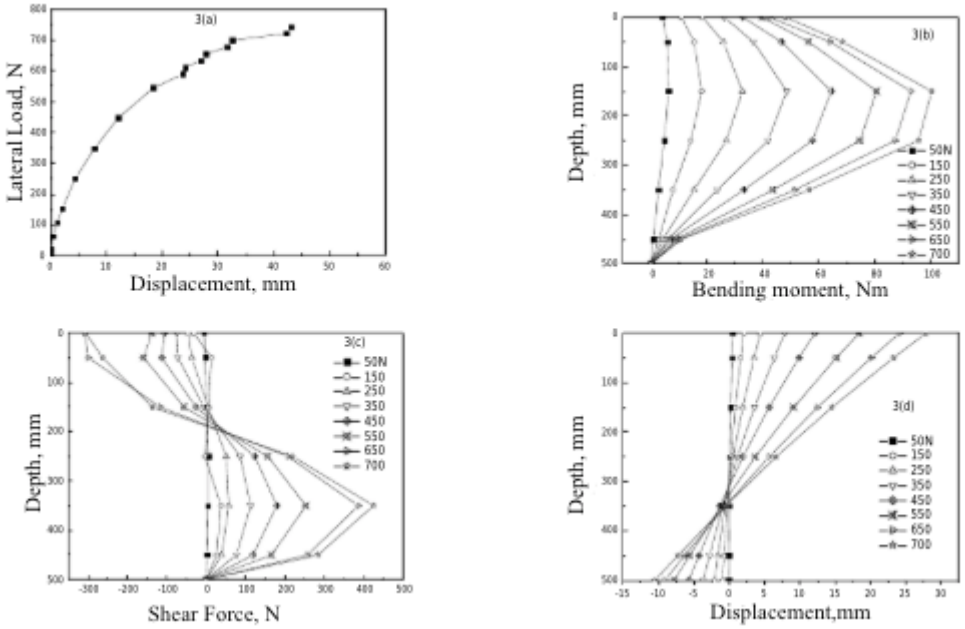

Figure 2.5. Static Loading Case [26].

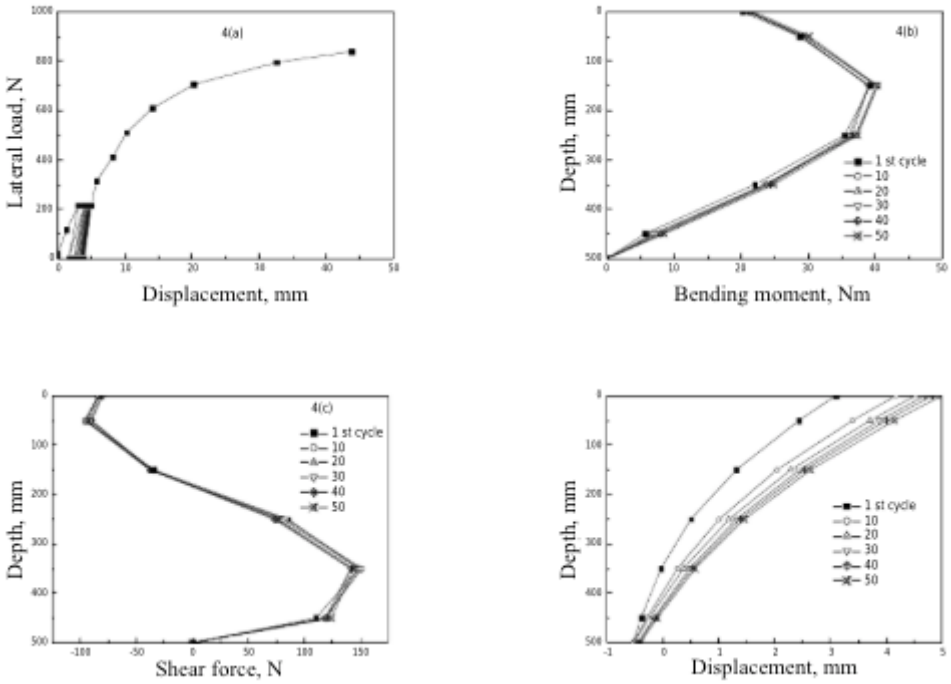

Figure 2.6. Cyclic Loading Case 1 [26].

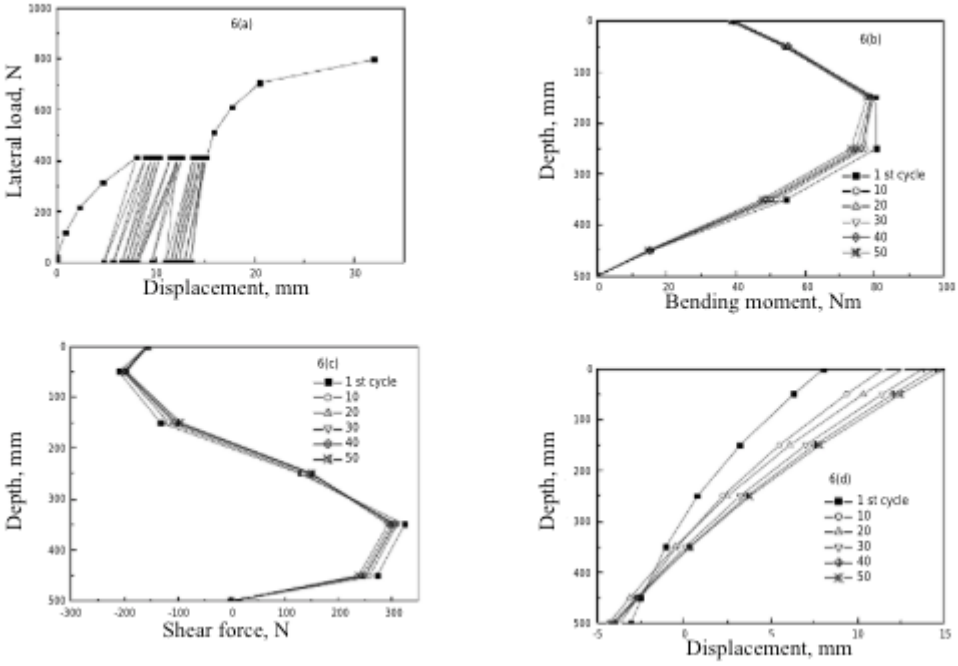

Figure 2.7. Cyclic Loading Case 2 [26].

From the test results, bending moment and shear force of the pile are calculated in the mentioned study. Test results and, calculated moment-shear values versus depth is shown in the Figures 2.5. 2.6. 2.7. [26]

For the static loading case which is shown in Figure 2.5. It is seen that the higher the lateral load is applied, the more displacement is seen. Also maximum moment and shear values are higher when the applied load is higher.

For the cyclic case 1 which is shown in Figure 2.6. The applied force is equal to 200 Newtons and for the second case it is 400 N. Therefore displacement versus depth values get higher nearly 4 times. Also pile head deflection increases 3 times. Therefore both maximum moment and shear values get a higher value. Number of cycle is another parameter affecting the displacement values. When the cycles get higher, displacement values increase. [26]

Clay is used in the third study “Model Tests on Single Piles in Soft Clay”.[20] Tests are made in order to obtain liquid limit, plastic limit, specific gravity and permeability of the soil. Then a slurry is made. Water content of the slurry is %156. After the mixing, the slurry is taken into consolidometer. First 40 kPa is applied then 100 kPa is applied to the slurry. The settlement is measured with LVDT.

The testing device requires a model tank and a sampling box. It is specialized for passive piles. The dimensions of the sampling box is 300x300x200 mm. The slurry is trimmed up to sampling box dimensions and slowly pushed into the box. Square grid lines are drawn on the slurry surface in order to scan the deformation pattern around the pile. A vertical hole is made with a rectangular tube. It is 1 mm larger than the model pile in order to obstruct harm to the pressure transducers attached to pile during the installation. The pile top is fixed and the pile base is restrained.

A cylinder and a hydraulic pump is used for the loading unit. The cylinder maximum stroke is equal to 200 mm. On the back wall of the storage tank the cylinder is screwed. Lateral force applied to box with the cylinder connected to the pump. Also a load cell is attached to the cylinder in order to measure the force. Additionally, there is a LVDT

screwed to front side of the box. It measures the displacement value. In Figure 2.8. experimental set-up schematic diagram is shown.

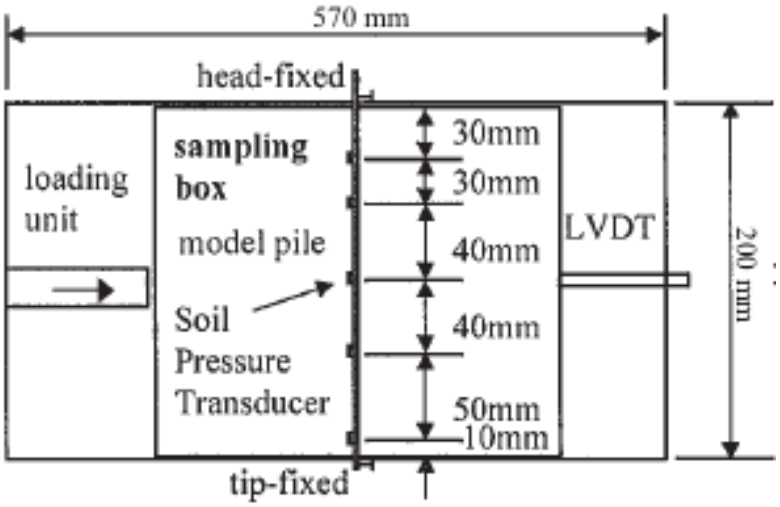

Figure 2.8. Experimental set-up schematic diagram [20].

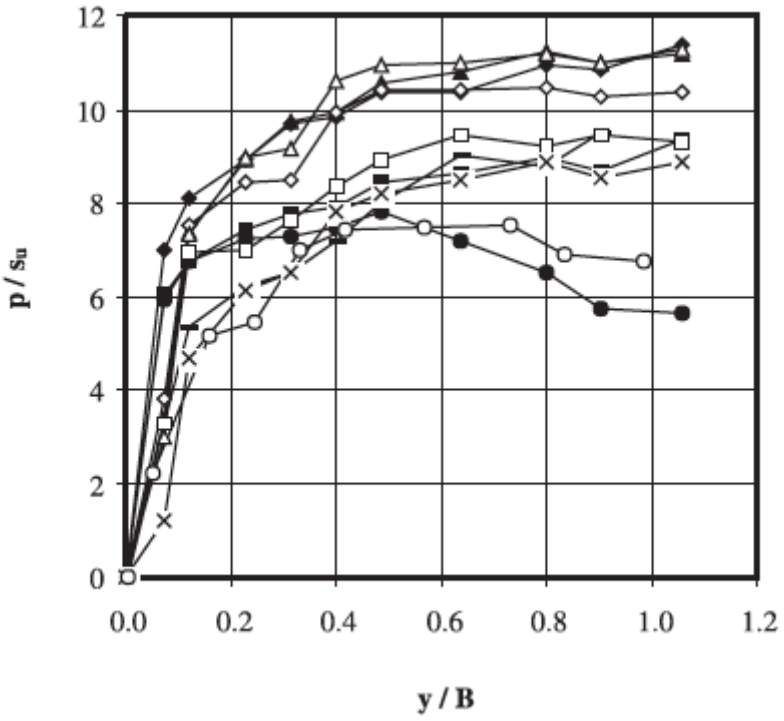

Figure 2.9. Normalized soil pressure versus displacement [20].

In the test soil pressure measured with tranducers and with these values soil pressure versus displacement is plotted. It is shown in Figure 2.9. The ultimate load for the target displacement is measured with the load cell and LVDT. [20]

For the study “The Behaviour of Laterally Loaded Model Piles”, a storage box with the dimensions of 40x70x93 cm. is used.[32] A sand rainer is attached to upper side of the storage box. The pile is placed into the box and fixed with clamps from the top. Measured amount of sand is poured into the box. In this way the density of the sand in the storage box is set. Then the sand rainer is removed. The strain gauge cables are attached to the indicator. The devices for deflection gauge are attached to the point where the lateral load is applied and the test set up is ready. In Figure 2.10. experimental set-up schematic diagram is shown.

The load is applied to the pile. Each time the lateral load is increased by 9,81 N. Both cyclic and static loading are applied to the pile. From the test displacement values versus depth is obtained. From the displacement values slope and moment values are calculated. Also moment values are calculated with a computer program. The values from the calculated moments and the moments found from computer program are compared in this study. [27]

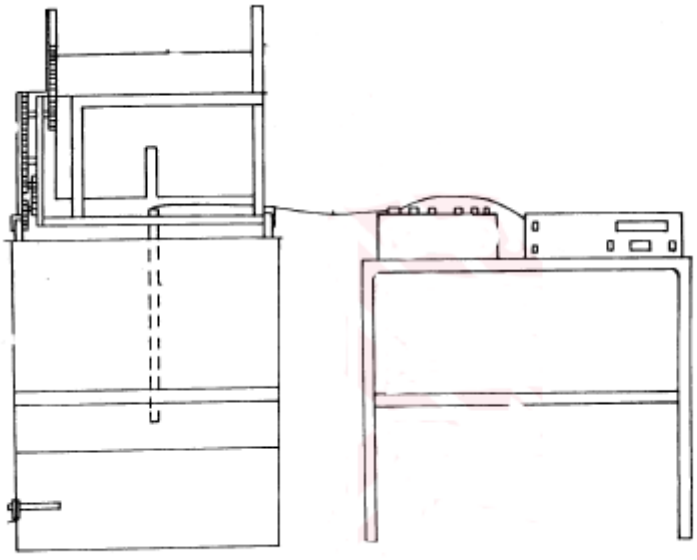

Figure 2.10. Experimental set-up schematic diagram [27].

Measured and calculated values of the first and second tests of this study is shown in Figure 2.11. On the moment diagram first line shows the calculated moment values from the displacement values and the second line is the one found with the computer program.

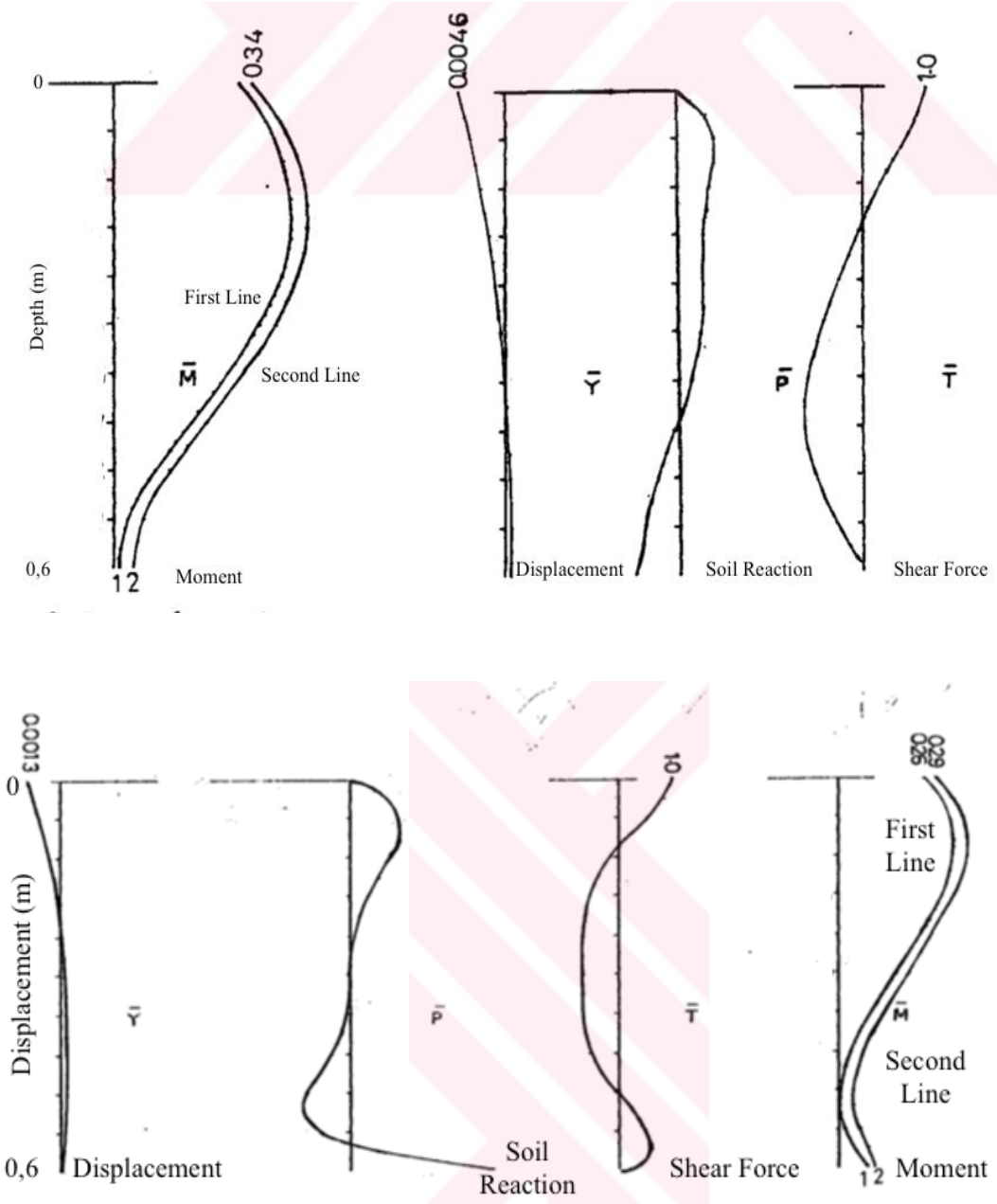

Figure 2.11.Test Results of the Study [27].

Moment diagrams show that directions of the calculated values line and the line found with the computer program are parallel to each other. On the other hand calculated values are always lower than the others.

The displacement values increase with the higher loads. But shear and moment values line direction changes with this difference in the displacement. [27]

“Laboratory Modelling of Laterally Loaded Pile Groups in Sand” is a study about the model group piles. [28] The box dimensions are 0,8x0,8x0,6 m. The grain size distribution, the maximum and minimum void ratio values, curvature coefficient, uniformity coefficient, friction angle in different densities of the sand used in this study. This values are shown in Figure 2.12.

This study aims to show about group effect on the piles subjected to lateral loading. For this aim each test pile group spacing is different. Also there is a control pile, in order to compare the behaviour of the single pile and pile group.

Soil Properties	Values
Specific gravity, G_s	2.67
Mean particle size, d_{50} (mm)	0.26
Uniform coefficient, C_u	2.0
Curvature coefficient, C_c	1.2
Maximum void ratio, e_{max}	1.19
Minimum void ratio, e_{min}	0.81
Peak friction angle, ϕ_{peak} (deg)	40 (D_r=73%) 35 (D_r=50%) 27 (D_r=27%)

Figure 2.12. Soil Properties [28].

The study takes over average load per pile in different densities versus average deflection. It examines this subject both for 3d pile and 6d pile spacing cases. Additionally, ratio of each row load to group lateral load versus lateral deflection is examined. Different values of P-multiplier factor in various pile spacing ratio to pile diameter is examined too. All of thses studies are in the Figures 2.13. 2.14. 2.15. 2.16. [28]

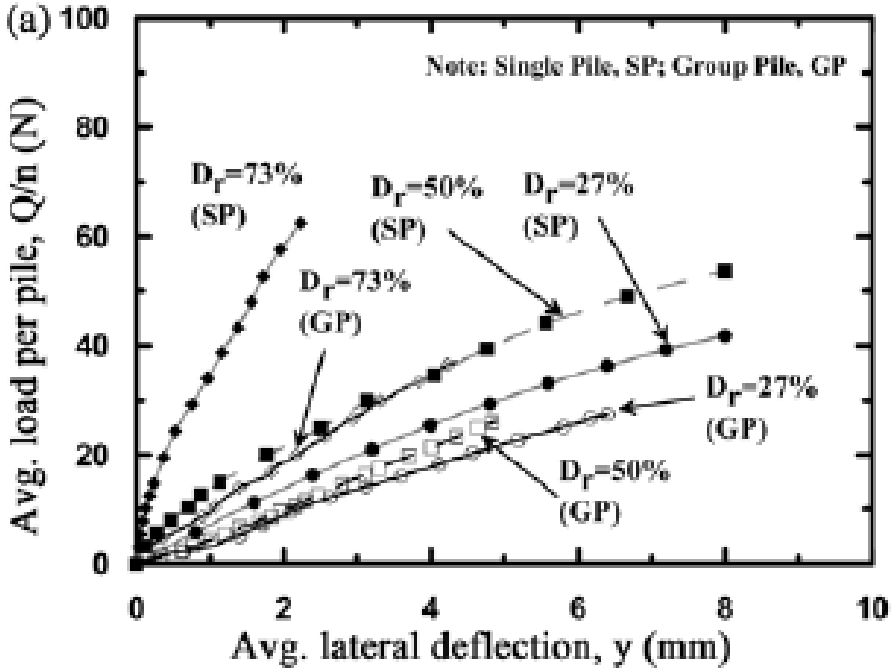

Figure 2.13. Average lateral load-deflection for group tests (3d spacing) with changing relative density and single pile tests [28].

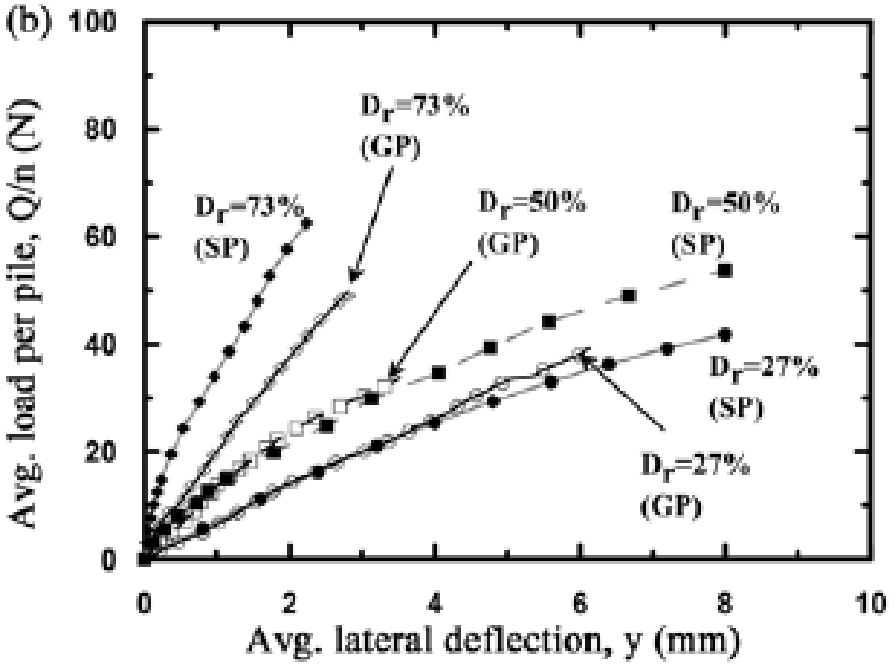

Figure 2.14. Average lateral load-deflection for group tests (6d spacing) with changing relative density and single pile tests [28].

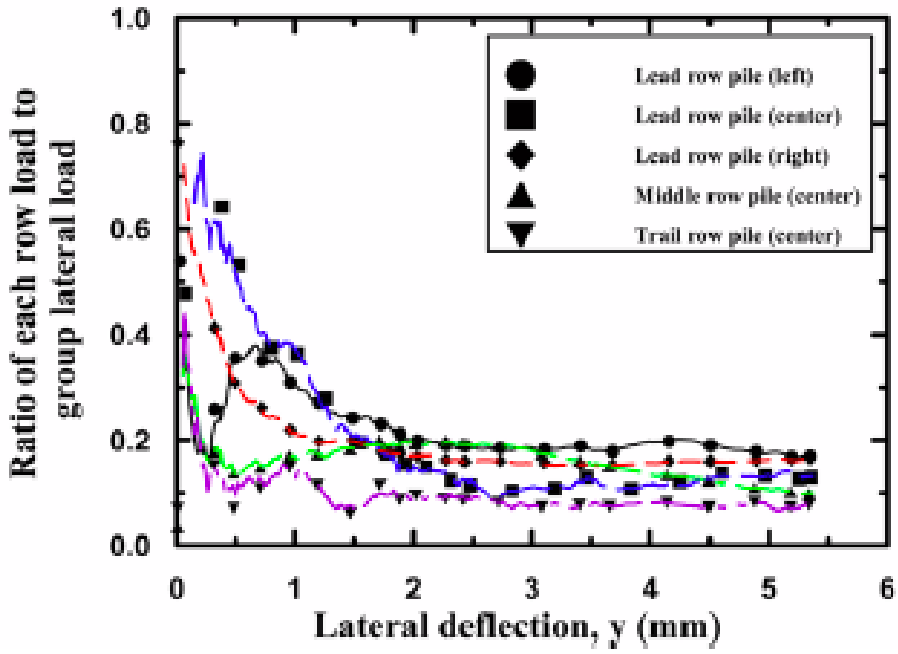

Figure 2.15. Load distribution ratio with lateral deflection variations [28].

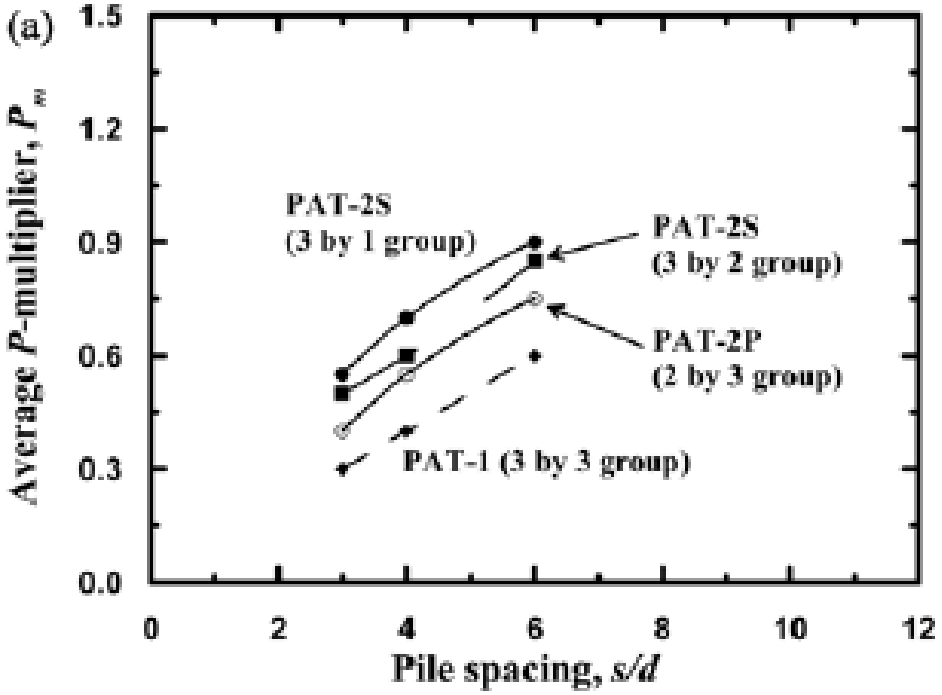

Figure 2.16. Pm-s/d Relationship [28].

In this study pile groups behavior under different densities, different pile spacing is examined. The deflection is affected by different density and pile spacing situations. Also P-multiplier for pile group is affected by the pile spacing. [28]

The study “Interaction Between Laterally Loaded Pile and Surrounding Soil” focuses on imroving understanding of soil-structure interaction for single short, stiff laterally loaded piles by obtaining direct, accurate and simultaneous measurements of compressive soil-pile interaction pressures, lateral movements along the pile length and pressure distribution in the surrounding soil. [29]

For these aims pile is placed inside the box with attached strain gauges and wrapped compression sheets. Then the sand is rained around it. The loads are applied to the pile head. For every load increment, the load is kept constant while the pile lateral displacement is stabilizing. Then the measurements are read.

The displacement of the pile head increases nonlinearly as the load increases. The strain values increases down to a depth of 6D below the surface then they decrease. It shows that maximum moment value is seen at approximately 6D below the ground surface. Depth versus strain and depth versus displacement graphics are shown below.

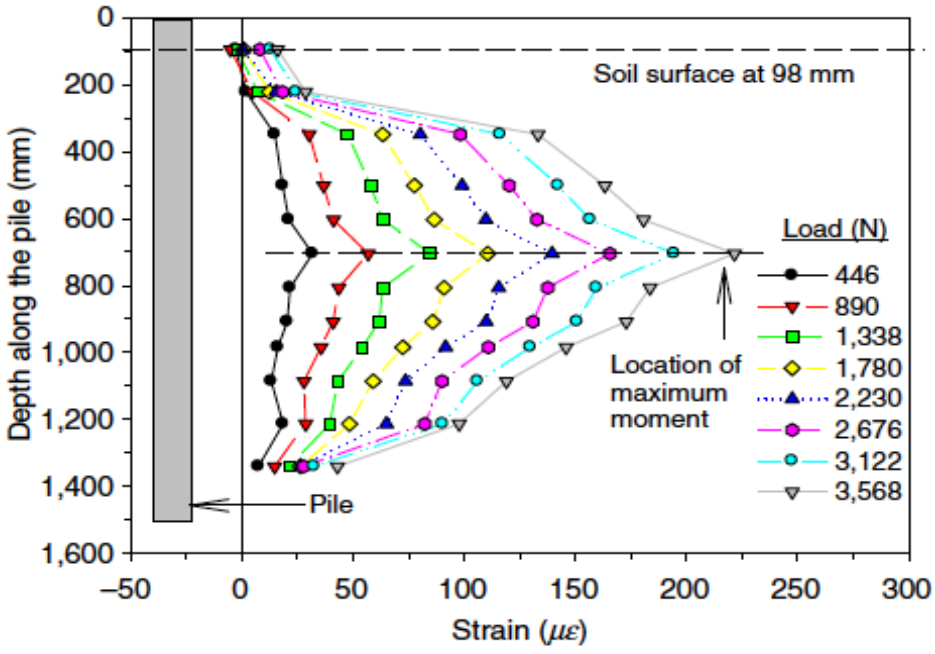

Figure 2.17. Depth versus strain [29].

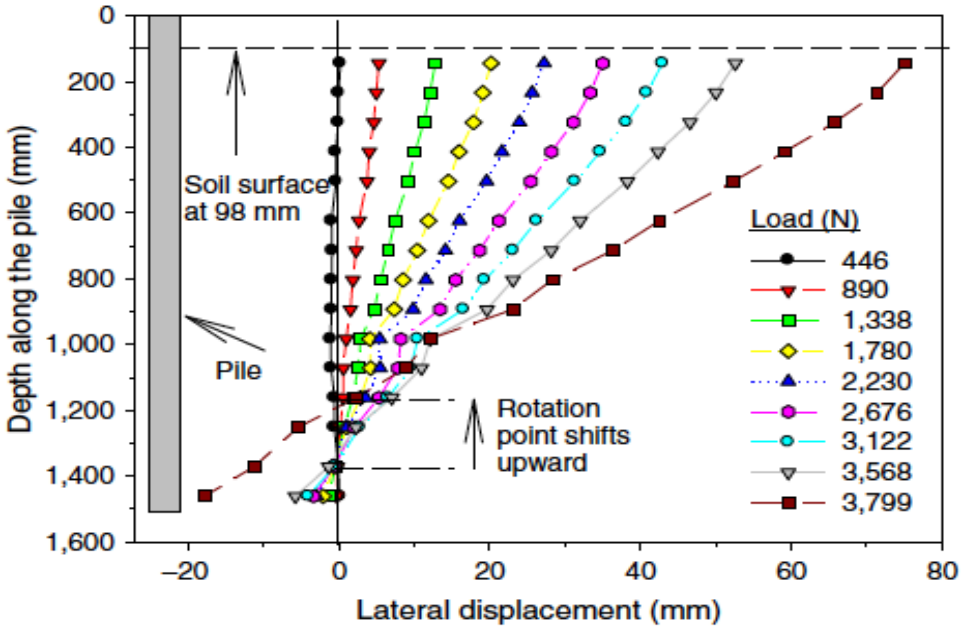

Figure 2.18. Depth versus displacement [29].

Also the measurements are made with pressure sheets. A tactile pressure sheet 0,7 mm thick, consisted of a matrix of small sensing cells that obtained discrete pressure measurements. The tactile pressure sheet sensors are designed to measure compressive stresses only. The color density of these sheets show the pressure it is exposed. The pressure sheets are wrapped around the circumference of the pile. With the pressure sheets soil reaction along the pile is found.

In Figure 2.19 soil reactions measured from these sheets for different applied load values are shown. With these sheets, it is seen that when the load increases soil pressure of the pile on the front side at the top increases. The measured loads from the pressure sheets and the calculated force values are compared in the study. The difference between the measured results and calculated results is less than 12%. [29]

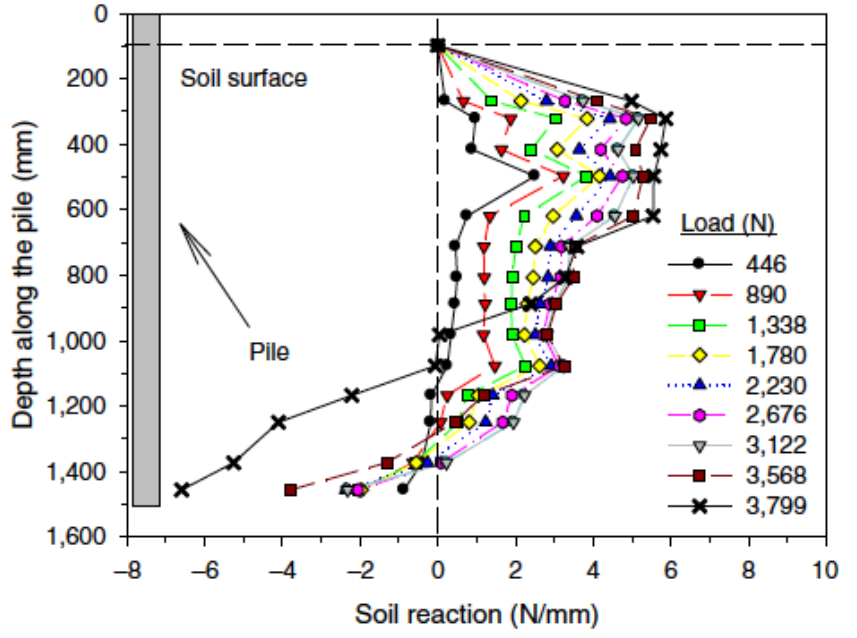

Figure 2.19. Soil reaction versus depth [29].

The study “Response of Static and Cyclic Loaded Rigid Piles in Sand” requires medium-grained, oven dried poorly-graded sand with 38° internal friction angle. [30] Its uniformity coefficient is equal to 2,92 and curvature coefficients is equal to 1,15. The sand is discharged into the storage box with a rainer from 600 mm. height. Dimensions of the storage box is 1x1x0,8 m. The upper part of the box is steel frame and the lower part is timber box.

The same system is also used for “An Experimental Study on Cyclic Loading of Piles in Sand” For the lateral loading the steel wire which is connected to pile is used. The other side of the wire is connected to a mass. The mass connected to wire is on a jack system. When the force is applied to jack, it moves the mass and the mass pulls the wire. The direction of the wire is changed with a pulley. Therefore, the wire moves the pile horizontally.

There are strain gauges attached to pile to make the measurements. Also two dial gauge are used to measure the near surface displacement of the pile.

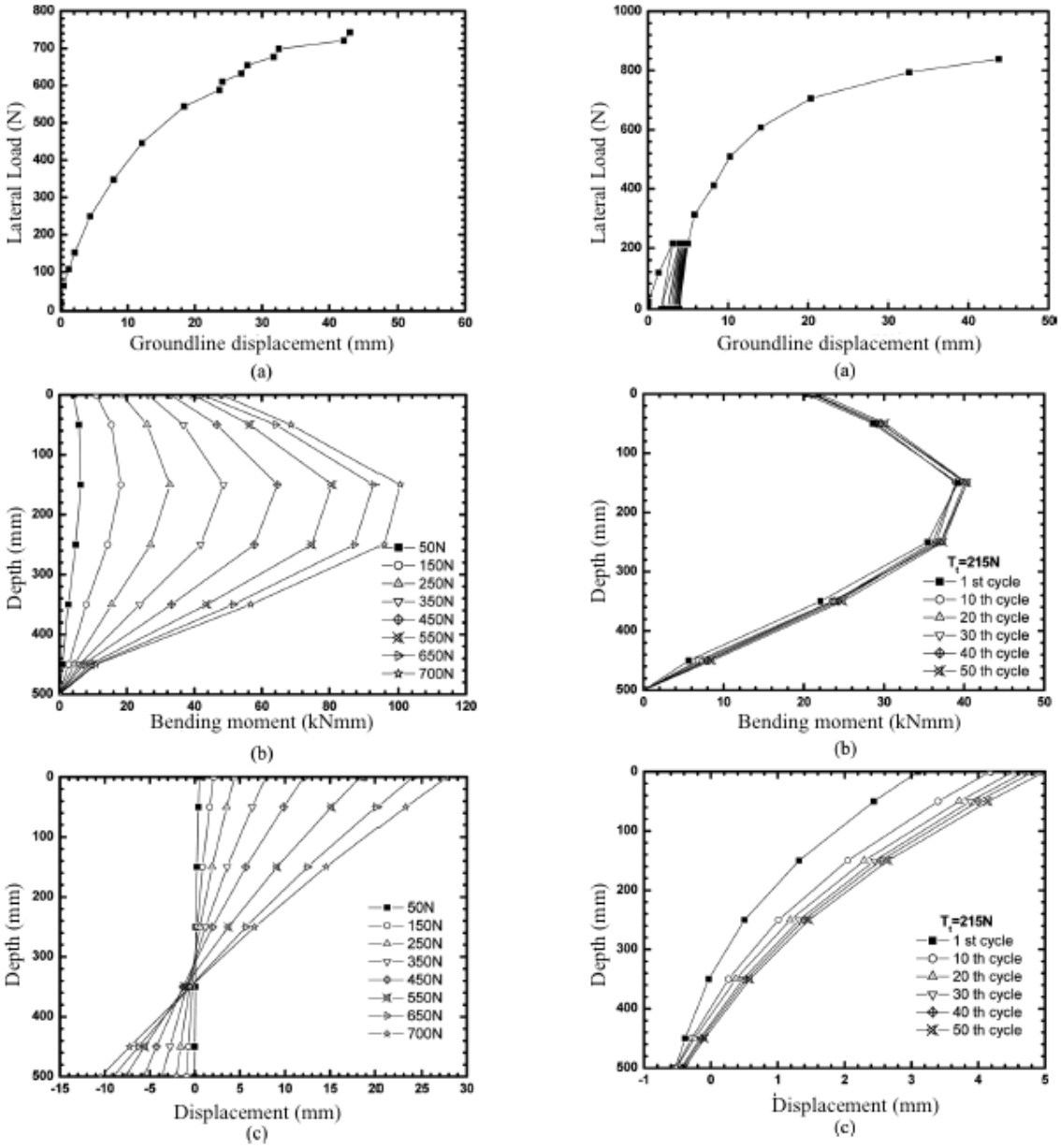

Figure 2.20. Static and Cyclic Test Results [30].

The pile is placed in the center of the box with the help of a vertical jack. Both cyclic and static loads are applied. 20-30-50 cycles applied cumulatively. For both situations displacement values are measured. Moment values are calculated from these displacement values. These values are shown in Figure 2.20.

The accumulated displacement values of pile increases with the higher numbers of cycles. On the other hand a decreasing rate for the displacement values increase is seen.

Maximum moment is nearly linearly related to the lateral applied load, but it is independant to number of cycles. [30]

"Response of Stiff Piles in Sand to Long-Term Cyclic Lateral Loading" searches methods to predict response of the long-term cyclic loading.[31] It is based upon the p-y curves definition. Static soil reaction reduction is considered in this method.

For this aim a test setup is made. Storage box dimensions are 550x600x600 mm. There is a weight and pulley which rotates the rope direction. Also there is lever which carries a motor. The motor rotates the mass and causes the cyclic loading. The motor rotates at 0,106 Hz. frequency. In Figure 2.21. experimental set-up schematic diagram is shown.

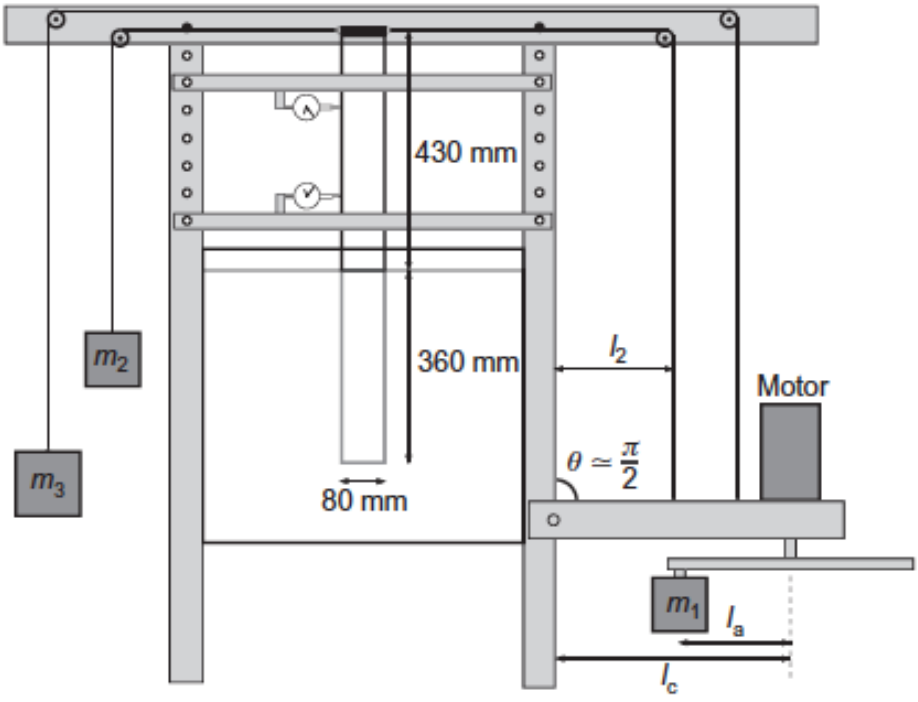

Figure 2.21. Experimental set-up schematic diagram [31].

For these tests, sand properties like minimum and maximum density, friction angle, specific gravity and D_{50} values are obtained. The sand is carefully poured in to the box and the pile is driven into it with a plastic hammer. Strain gauges are attached in order to measure horizontal deflections

A series of tests was conducted on small-scale driven piles subjected to long-term cyclic loading. A typical design of a monopile was adopted and used to quantify realistic pile dimensions and loading ranges. Furthermore, a complete non-dimensional framework for stiff piles in sand is presented and applied to interpret the test results.

The accumulated rotation of a stiff pile is largely affected by the characteristics of the applied cyclic load. Thus parameters characterising the load, other than maximum load levels, are required for accurate predictions.

The tests showed that cyclic loading always increased the pile stiffness, and the increase was found to be independent of relative density. This contrasts with the current methodology of degrading static p–y curves to account for cyclic loading. A method, based on the experimental work carried out, is presented to predict changes in stiffness due to longterm cyclic loading. [31]

In “Investigation of a Laterally Loaded Model Pile Behaviour in Sand by Means of Experimental and Numerical Methods” study, unlike the others mineralogical components of the sand is observed with X-Ray experiments. [12] Also different relative density values and the friction angles are found like the other tests. Also grain size distribution of the sand is plotted. Another difference from the other tests is steel tensile test is applied to the pile. With this test yielding stress and moment of the pile is found.

The box dimensions are 500x700x1000 mm. Glass is used to make the box in order to see the filling applications clearly. The friction angle between the glass and sand is measured. It is lower than 5°. There is a wire connected to pile and a mass from different sides. The lateral load is apllied to the pile with the wire. In Figure 2.22. experimental set-up schematic diagram is shown.

With these tools displacement values are found and from those values moment is calculated. Also with LPILE 4.0 and SAP 2000 programs this test is modeled. All the results are shown in the Figures 2.23. 2.24.

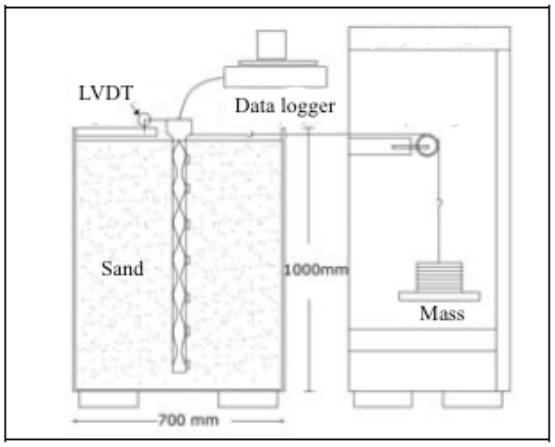

Figure 2.22. Experimental set-up schematic diagram [12].

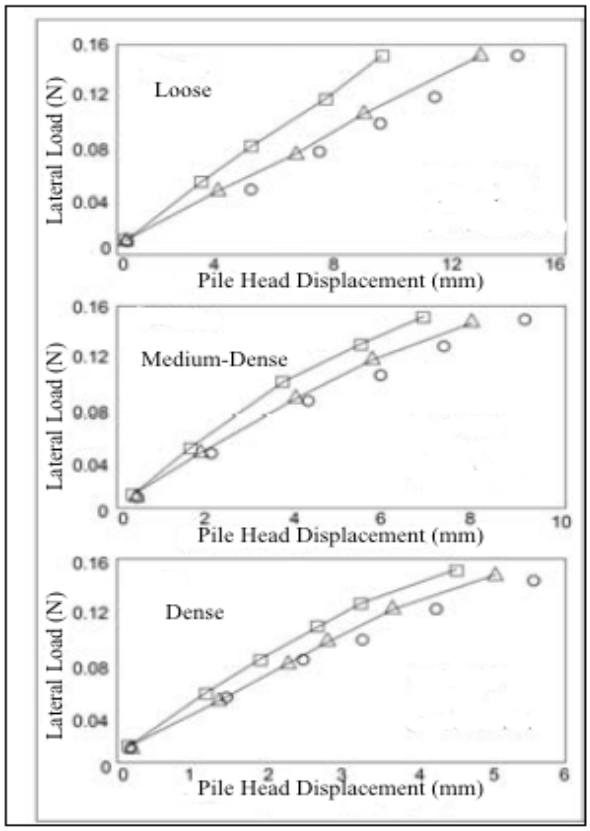

Figure 2.23. Load versus displacement [12].

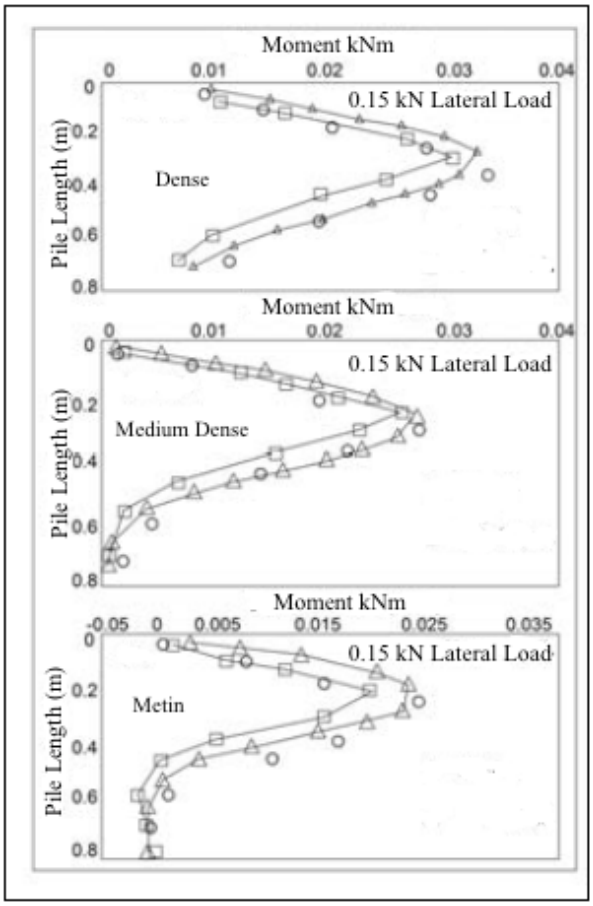

Figure 2.24. Moment versus depth [12].

Results of the experiments, LPILE program and SAP 2000 program are shown in the Figures 2.23. 2.24. It is clearly seen that results found with various techniques are very close to each other. All the results verify each other.[12]

In “Numerical Analysis of Laterally Loaded Battered Rigid Piles” study, the box dimensions are 48x96x50 cm.[23] A motor is used to make the loading. The motor is connected to a loading gear which is attached to load cell. On the other side of the load cell there is rope bounded to the pile. Also LVDTs are attached to the pile to measure the displacement. In Figure 2.25. experimental set-up schematic diagram is shown.

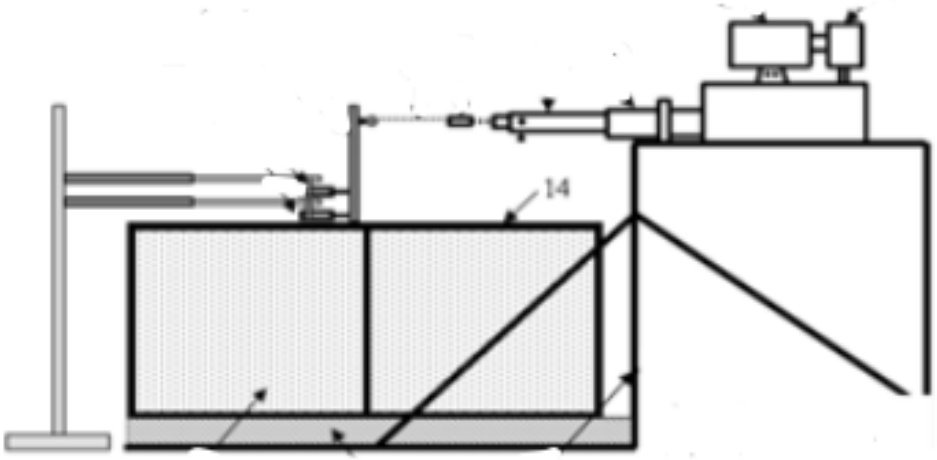

Figure 2.25. Experimental set-up schematic diagram [23].

Dense and loose state of the sand is used in this tests. Internal friction angle of the sand is found for these states and they are equal to 39° - 44°.

Aim of this test is finding the capacity of pile depending on its batter. Because of this aim, behavior of the pile in -20, -15, -10, 0, 10, 15, 20 degrees position are assessed. Displacement values are found in these positions. Also a computer analysis in FEM program is made for this positions.

Minimum load is needed for the significant deflection value for the pile at rest and maximum load is needed for the same significant deflection value for the pile in passive state. In this study soil reaction forces are shown. When the angle gets higher in passive state, the needed force for the significant displacement increases. This situation is valid for the active state too. [23]

In the last study “Experimental Investigation of the Behaviour of the Laterally Loaded Short Piles”, [32] the test setup is exactly the same with the previous test “Numerical Analysis of Laterally Loaded Battered Rigid Piles”. The experimental set-up photo is shown in Figure 2.26.

Dense and loose state of the poorly-graded sand is used in this tests. Internal friction angle of the sand is found for these states. It is equal to 39° for the loose stat and 45° for the dense state. Also grain size distribution and C_u, C_c values are found for the soil. C_u value is equal to 2,78 and C_u value is equal to 1.

Figure 2.26. Photo of the experimental set-up [32].

Three different pile materials are in this study. These materials are steel, aluminum and delrindir. Material properties are shown in the Table below

Table 2.2. Material properties [32].

	Material	D (mm)	L (mm)	γ (kN/m^3)	E (MPa)	ν
Model Pile	Steel	50	200	77	210000	0.25
	Aluminium	50	200	27	70000	0.33
	Delrindir	50	200	14	3100	0.35

Piles are subjected to lateral loading, load displacement values are found for all the materials. Lateral deflection versus load is shown in Figure 2.27.

From the results it is seen that pile material affects the results. For the same load all piles show different displacement values. Applied lateral load-pile head deformation relation shows us that even for the smallest lateral translations, stress-strain behaviour of soil is non-linear. [32]

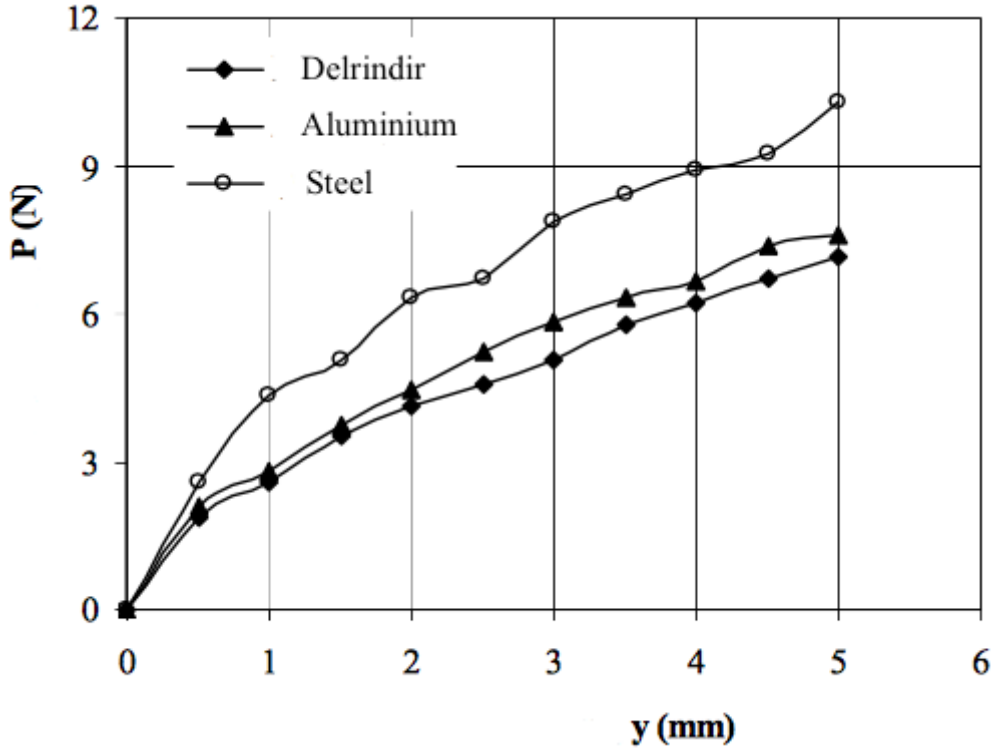

Figure 2.27. Lateral deflection versus load [32].

In the model pile tests, various types of piles and test set-up are used. Soil properities are obtained for each test. Main aim of all these studies is displacement measurement. In most of the tests with the measured displacement values and applied load other porperties such as, moment, soil reaction are derived.

2.4. Contact Stress Mapping

2.4.1. Contact Stress Mapping Using Prescale Films

Load cells are inadequate for illustrating the stress concentration detail of layer areas. Films which are developed for biomedical and medical applications are good option for illustrating the stress concentration details of the areas. The indicator films bring new

opportunities to map the stress concentrations. Innovative films enable easy determination of the pressure distribution. This film reacts to pressure apply and changes color density according to the values of the pressure. Red patches will appear on the film when pressure is applied and the color density changes according to the various pressure levels. Main advantage of the proposed measurement technique is its ability to fully map the contact stresses. The measurement system is unique in a way that, the stress map of the whole area can be obtained continuously. Miniature load cells do not have this capability. Other contact sensors are very expensive, and only provide the stresses over a grid. The adapted technique has a good potential for geotechnical laboratory and field measurements at a reasonable cost. It was interesting to observe and to quantify very high stress concentrations at the contact points of the sample. With the help of this technique, wider areas contact stress distribution can be found. Tactile stress mapping types are summarized below. [33-35]

(i) Real time: The sensors may be used several times. The sensors are relatively more expensive than the sensitive films. The most expensive part of these sensors are their connection hardware to the computers and the software involved for their measurement.

(ii) Sensitive films: The sensors are only used once. The sensors are cheaper however the software is expensive and a dedicated hardware is needed.

(iii) Classical miniature pressure transducers: They are accurate but very expensive and only give the pressure at one point. It is not possible to map the entire interface.

(iv) Other very high technology applications are available but due to their extreme cost they are out of the interest of this study.

Measurement of the pressure value distribution requires two polyester bases. First one requires color forming material, second one requires color development material. It consists polyester base 75 μm, micro encapsulate layer 15 μm and developer layer 15 μm. 21 kg/mm is measured tensile strength for the film. 120% is the elongation value. 0.40 is static friction coefficient of the film. There are eigth types of prescale films available to fulfil varying pressure range.(0.05~300 MPa). Eight types of prescale films are supplied according to pressure level and these are shown in Figure 2.28. However low range films are adequate for geotechnical applications. The high capacity films are

composed of one sheet only. The cross section of the pressure sensitive films are shown in the Figures 2.29. 2.30. Also sensitive film measurement ranges are shown in Table 2.3. The films are available in rolls with protected cover and must be cut to the desired size. Two sheet films are supplied with two rolls which are cut and fit on top of each other. [34,35]

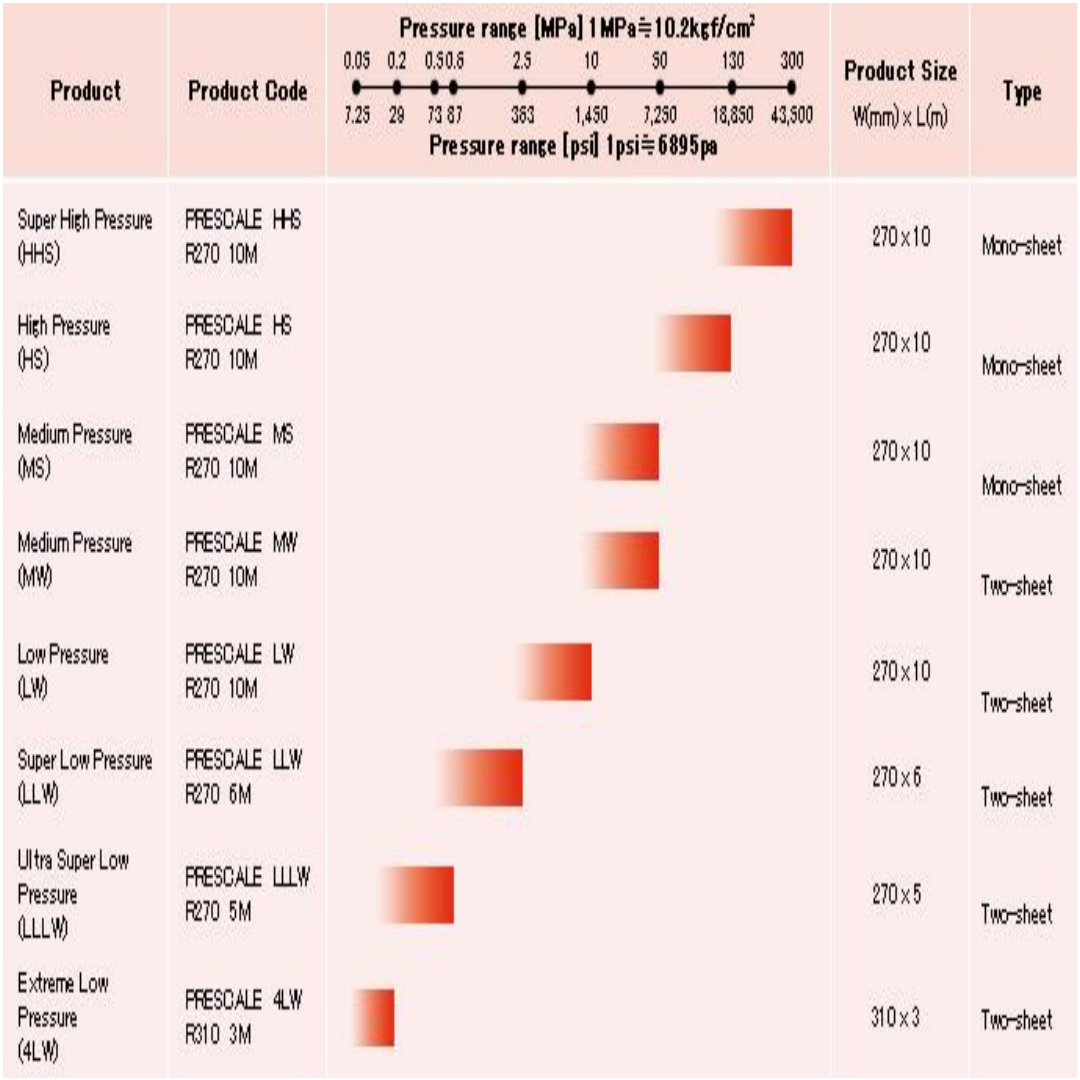

Figure 2.28. Different types of prescale films with different pressure range[35].

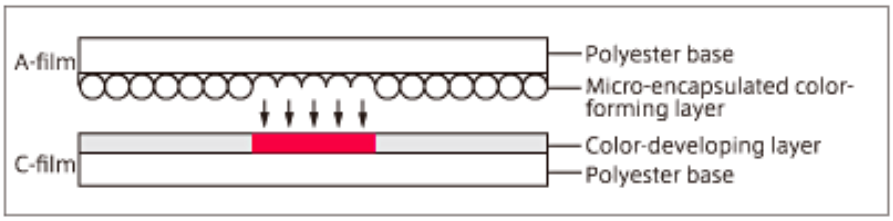

Figure 2.29. Two-Sheet Type [35].

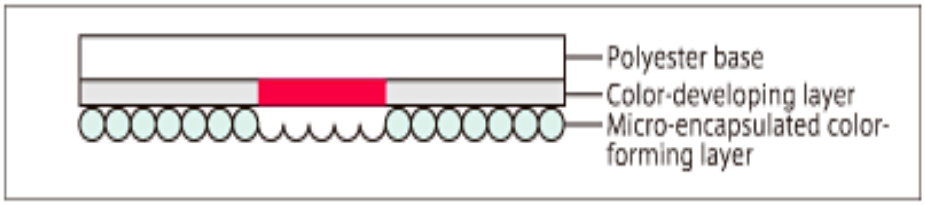

Figure 2.30. Mono-Sheet Type [35].

Table 2.3. Sensitive film measurement ranges [34].

Range	Low	High
Type	MPa	MPa
Extreme Low Pressure	0.05	0.2
Ultra Super Low Pressure	0.2	0.6
Super Low Pressure	0.5	2.5
Low Pressure	2.5	10.0

There is a software to quantify the stress distribution obtained from the films. Color microcapsules are placed inside the films. The microcapsules explode under stress. This process is shown in Figure 2.31. From the density of color, stress distribution can be found. [33]

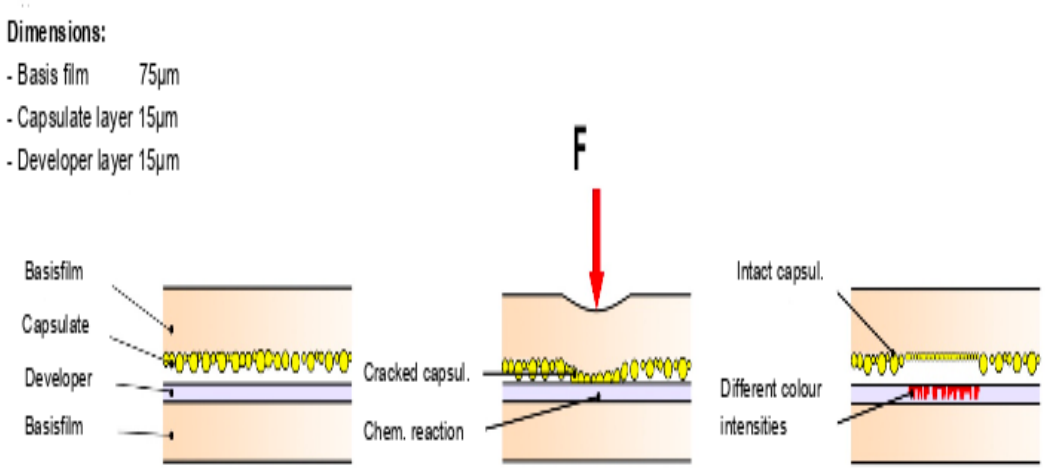

Figure 2.31. Explosion of the microcapsules [35].

Films are too sensitive so gentle handling is an important parameter. Pressure range of the film must be suitable for the aim of the study. Sheets must be cut up to area size. After matching two sheets, they are placed between the surfaces to be measured. Two measurement types are available; sustained and momentary. Two seconds of load application is enough for the momentary type. The relative humidity and temperature is recorded. It is important for the pressure-color intensity relationship. 20 to 30 ºC is recommended range for temperature values. Additionally, 35 to 80% is recommended range for humidity values. The contact pressure versus color intensity calibration curves for sustained pressure are presented in Figure 2.32. for different temperature and relative humidity ranges. Also the contact pressure versus color intensity calibration curves for momentary pressure are presented in Figure 2.33. for different temperature and relative humidity ranges For the software, a special calibration sheet is used. The calibration sheet is shown in Figure 2.34. A scanner cover which is specialized for the dedicated scanner is used. Scanning process must be end within half hour. After this process, the stored image can analyze utilizing several tools. [36]

There is a companion software which can analyze interface stress distribution in a detailed way. The relative stress level magnitudes may easily defined with the software. On the other hand, real stress values need serious calibration. It is easy to define stress concentration of the rough areas. [34]

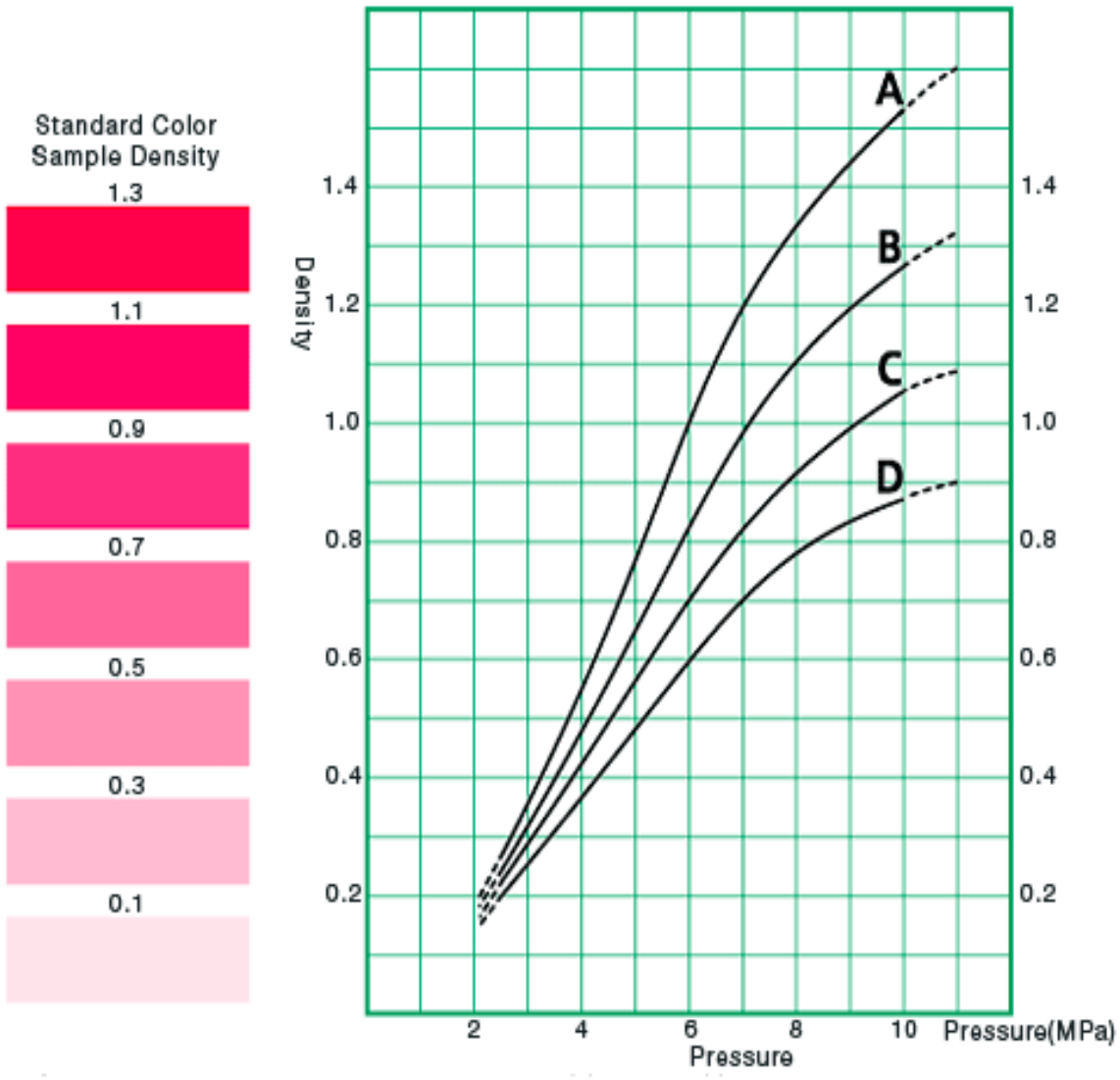

Figure 2.32. The contact pressure versus color intensity calibration curves for sustained pressure (Taking the temperature and humidity condition into consideration, select a curve among A, B, C and D.) [35].

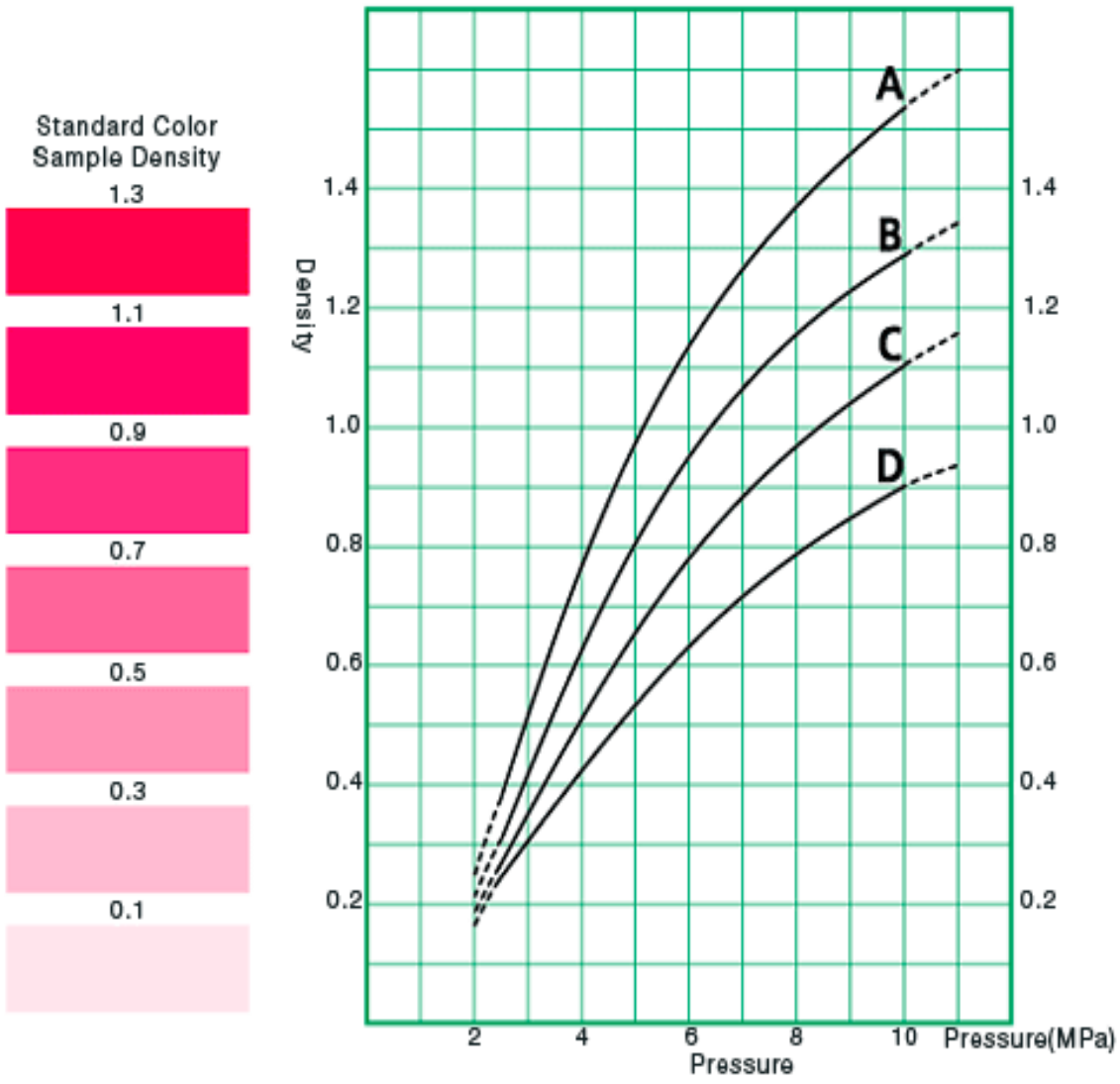

Figure 2.33. The contact pressure versus color intensity calibration curves for momentary pressure (Taking the temperature and humidity condition into consideration, select a curve among A, B, C and D.) [35].

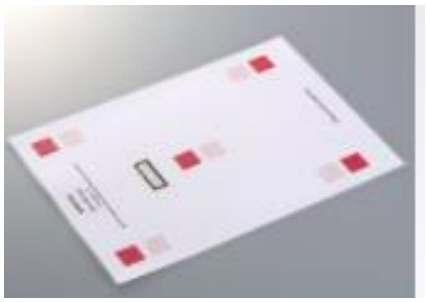

Figure 2.34. Calibration sheet [35].

The software, with a careful and detailed calibration, is a really important agent in order to understand interface behavior. For investigating soil interface stress distribution, pressure sensitive films are satisfactory. With this software the scanned image is analyzed with 2D. The pressure values are presented with a 200 dots per inch resolution (0.125mm). A typical example of the use of the indicator film is presented in Figure 2.35. A geogrid is placed on concrete block and the stress map is produced. Contour maps corresponding to 0.5 Mpa and 2.5 Mpa are derived. The stress values along the x axis and y ordinate are plotted. The 3D wire image and measurement data are obtained [33]

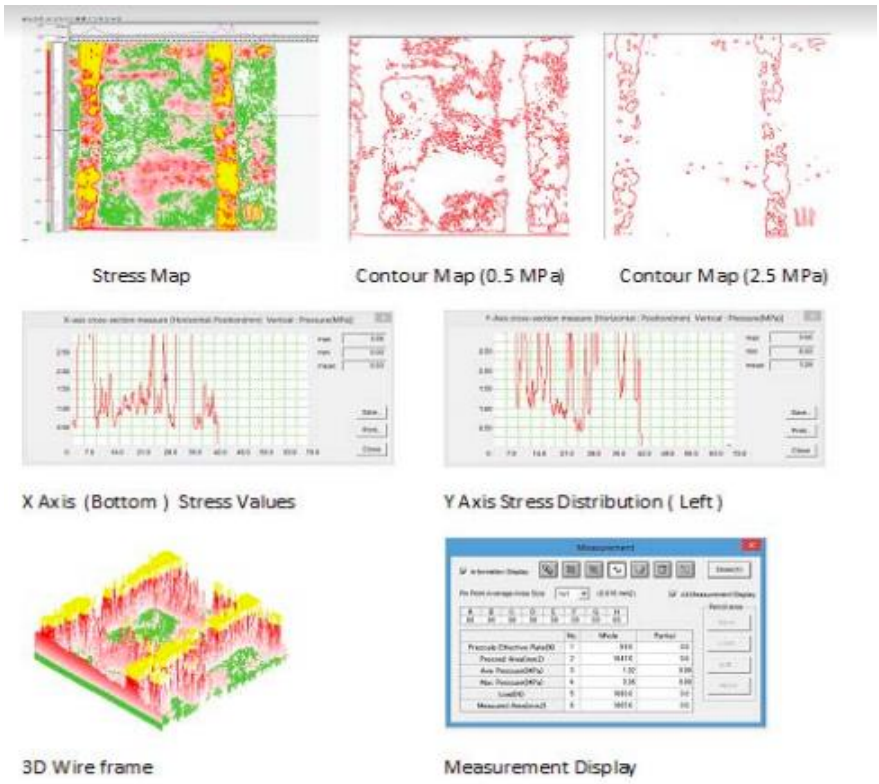

Figure 2.35. Typical stress map of geogrid [35].

It is important to imply that the average contact stresses measured are more realistic closer to the middle range of the film. Based on this information it is recommended to apply loads closer the middle range of the indicator film. Having the lowest stress range between 50 and 200 kPa, stress level of 100-125 kPa seems to be the appropriate range for soil contact applications.

Also, for very low stress levels the indicator films are not appropriate. Although the average stress levels may not be measured accurately at these levels, many other valuable information may be obtained like; any misalignment in the loading mechanism, protrusions or troughs at the contact zone, real contact area, area of voids.

Easy visual check of distribution/uniformity for contact pressure and contact pressure shown with differing concentrations of color can even be converted into numbers are the most important advantages of this method. [34]

2.4.2. Calibration Study with 4LW Film

The indicator film is placed in filter papers on plexiglas blocks and taken in oedometer. With 9X mechanical advantage system, normal load application starts. This systems begins from 25kPa and and rises to 50, 125 and 200 kPa normal contact stresses. 4LW (ultra low sensitivity) indicator film is employed. For two minutes the load continues and then the film is taken. The scanner is calibrated. For the calibration a calibration sheet with special color is used. After this process, it is uploaded to software which is specialized for imagine analyses. The image and corresponding data are found. A typical example of the stress map and measurement display is shown in Figure 2.36. For test results repeatability, effective rate of prescale is important. Mean contact stress is presented on measurement data table in the third raw. Also, 3D software can be employed to generate contact area wired image. [34]

More microspheres explodes with rising stress level. So the area gets more color saturated. It means the more stress applied, the more color saturated view is formed. [34]

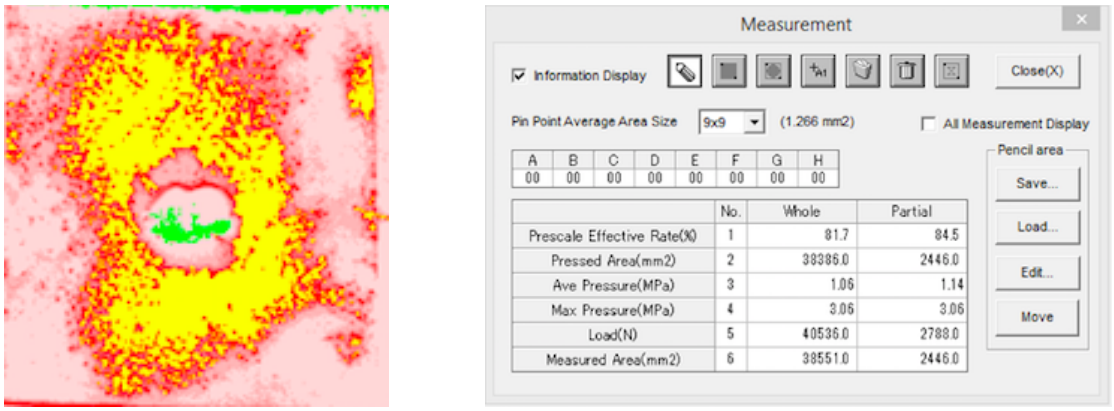

Figure 2.36. Stress map- measurement display [35].

2.4.3. Application Areas

The prescale films are used in biomedical engineering applications. It is used for biological joint loaded articular surfaces interfaces. For this study low pressure films between 2,5-10 MPa is used. Also, for the knee arthroplasty these films are used. It is stated that film provided contact area is 11-36% lower than the ones measured by Kscan. Moreover for the pressures and intraarticular contact area in human knee, these rescale films are used. In another study, with low range and super-low prescale films pressure concentration of human knee is obtained. Additionally, for the prosthetic components and diarthrodial joints pressure these films are used. As it is seen above, for biomedical research these prescale films are used widely.

On the other hand these prescale films are used in pavement engineering. For example, it is used for pavement deformation caused by contact pressure distribution of tire. In contact measurement of tire/road studied, it is also used. Noise modeling of tire/road studies it is used too.[34]

Moreover they are used for the interface behavior studies. While searching for the effects of crushed stone on geomembrane surface under shear stress, the films are used. The stress concentration at the contact points between the crushed stone and geomembrane is measured with these prescale films. With the help of the films, unexpected deformations of geomembranes under low stresses are observed.[37]

Films are also used for obtaining moment values of segmental piles from three point bending test. In the first part films are placed between the blocks and the pile is post-tensioned with the desired value. The prescale films are located in five different positions. These locations are 0, 90.5 mm, 181 mm, 271.5 mm, and 338 mm far away from the base of the pile model. The stress distribution due to the prestress force is estimated. First the average stress distribution is found then the stress distribution of the upper and lower part is found. Later the pile is subjected to three point bending test and the stress on the upper side gets higher. After the test films are taken from the segmental pile, stresses are measured. Again the average stress distribution is found then the stress distribution of the upper and lower part is found. Lateral forces are recorded corresponding to maximum deflection of the pile model. Then the moment values are calculated with these stress values. [2]

Films are used for calender roll pressure balance adjustment too. Calender rolls generally apply pressure using left and right cylinders. If the left/right pressure balance is poor, drift and quality problems occur. Also, nip rolls generally have crowns, change shape when nipping, and are designed to provide uniform nip pressure across the width. If the crown level and roll hardness are not appropriate for the pressure, defects and the rubber roll life can be reduced.

Another usage area for the films is engine cylinder heads gasket seal check. Head gaskets are designed specifically for each type of automobile engine. There was no method for confirming that the combustion gases, cooling water and oil of an engine, were properly sealed inside the cylinder of prototype and new production product of cylinder head gasket, other than by confirmation by operating tests. Placing the prescale film and gasket between cylinder block and cylinder head and then tightening bolts (normally), will be possible to verify the true performance of the gasket.

For chemical mechanical polishing head contact uniformity verification, prescale films are used. Chemical mechanical polishing is a process for polishing the surface of the silicon wafers. It involves mounting a silicon wafer parallel to an abrasive pad, rotating the wafer and pushing it against the abrasive pad along with a polishing slurry. High precision is necessary as the amount of polishing required is extremely small. Prescale is

placed on the abrasive pad, after which the silicon wafer is set in the polishing head and pressure is applied. Pressure is then released, Prescale removed, and resulting colors of impressed Prescale Film are examined.

For verification of brake pads fitting, prescale films are used. Disc brakes serves to reduce or halt the motion of an automobile by means of thefrictional force developed between the discs and bracke pads. If the fit between the discs and the pads is not optimal, serious defects can occur. These includes brake failure, uneven component wear, noises and vibrations. Thus, the proper fitting of brake pads is important for automobile performances, safety and parts life. Prescale can help such verification.

In the manufacturing of the solar cells, modules are formed by cementing the cells to the glass substrate, by mean of a vacuum laminator. If the press pressure is not even when this process is preformed, defects will occur, such as damage to cells or wrinkles in the protective film. Use of Fuji Prescale Film may be indeed helpful in performing such type of important verifications, improving final quality and reducing damages to cells.

Prescale films are used for heat sealing packaging. Poor seals include "imperfect seals that are not bonded" and "false seals that appear to be bonded". False seals, are especially a problem because they cannot be identified visually, and inspection on all items is not possible. Currently, temperature, pressure, time and other parameters are adjusted. If the seal passes later evaluation using the peel strenght test, it is accepted. Altough instruments exist for measuring temperature and time, there is not yet an instrument for measuring pressure; therefore, prescale films constitute a good option for measuring pressure.

They are used for the measurement of pressure distribution. When solder cream is screen printed onto print substrates, any non uniformity in the pressure distribution will result in uneven application of the solder cream. This can result into inadequate conduction and insufficient adhesion (during the subsequent component mounting), or into the abnormal conduction, when there is an excessive solder present. The prescale film may be helpful in measuring such squeegee pressure.

For the backgrind tape lamination pressure check prescale films are used. The process for laminating backgrind tape (protective film), precedes grinding. If thelamination roller pressure distribution is not uniform, the backgrind tape can become wrinkled. If the height of the wafer and the sourronding mounting table are not optimal, wafer cracking and poor backgrind tape lamination occurs. The use of prescale film can help in understanding and check the tape and roller lamination pressure uniformity distribution. [35]

2.5. Large Displacement Constant Contact Area Shear Device

The large size direct shear testing devices are too unwieldly, but they are very useful to investigate the shear and deformation behavior of granular soils in their field sizes. Many types of large size direct shear devices have been developed and new research in achieving better equipment is still popular.

2.5.1. New Large Size, Large Displacement Interface Testing System

A complete versatile and new large size, large displacement interface testing system is designed and manufactured [38,39]. Pneumatic muscles are used for the normal load application, a step motor with reduction gear driven linear actuator is used for the horizontal load application. An antagonistic loading mechanism is also developed by using pneumatic muscles.

This device contains upper and lower parts. Dimensions of the upper box are 0.30 m for length, 0.30 m for width and 0.20 m for depth. The upper box moves on the lower box whose dimesions are 0.90 m for length, 0.30 m for width and 0.60 m for depth. The depth of the bottom box can be adjusted between 0.20 m and 0.40 m. The device is shown in Figure 2.37.

Overall the designed testing system is simple and versatile. It can be examined in three sections. The left section operates independently to apply cyclic loads with precise stress control. The middle section can be used as an independent unit even for tilting table test. The sliding normal load mechanism on the shear box will provide the required confining stress for the tilting table which eliminates the major drawback of very low confining pressures of tilting tables. The third independent section of the testing system is the linear actuator side which can be separated from the system easily. This linear actuator

also can be used for other static or cyclic strain controlled load applications. Another versatile use of the testing system is for model pile testing. The depth of the lower box is adjustable up to 400 mm. The upper box is 200 mm high. This way model pile groups can be tested with 600 mm length subjected to vertical and horizontal loads. Horizontal cyclic loads can be applied either with stress control or strain control. A stress mapping system is used to determine the stresses acting on the interface and on the walls of the device. [37-40]

Figure 2.37. Large displacement constant contact area shear device [40].

The load cells can be used in three places to measure the applied load; under the loading arm and over the soil in the upper box, at the connection point of linear actuator and the top box, at the connection point of the antagonistic cyclic loading system and the top box. [40]

2.5.1.1. Implementation of Pneumatic Muscles

The rubber muscles requires three sections which are shown in Figure 2.38. [41]

(i) Airtight inflatable membrane in the inner section

(ii) A structural web surrounding the inner membrane

(iii) An upper and lower connector where both the membrane and the web are fixed

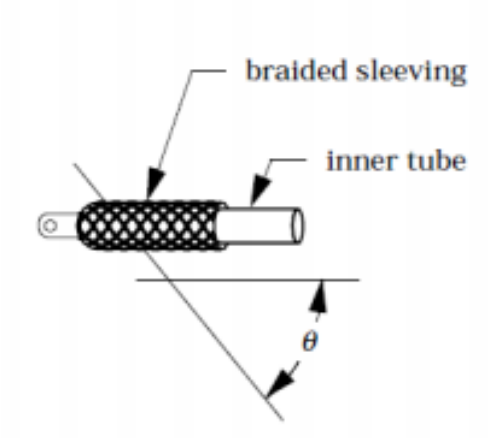

Figure 2.38. Rubber muscle [41].

The normal load is applied with pneumatic muscle actuators. With the help of air pressure these actuators apply forces up to 6.5 KN for a 40 mm diameter muscle. The pneumatic actuators can contract up to 20 per cent of their lengths. In the loading mechanism developed, the bottom connector is attached to a sliding car moving on a rail fixed along the side of the bottom shear box. The top connector is attached to a loading beam in direct contact with the sample enclosed in the upper shear box. By adjusting the air pressure, the desired normal force is obtained. The normal stress is applied by the help of pneumatic artificial muscles, whose diameter is 40 mm and nominal length is 250 mm.

Typical force magnitudes produced corresponding to varying contraction levels are presented in Figure 2.39. For six bar of air pressure the load capacity of one muscle actuator is 4500 N at 5 per cent contraction. At 20 per cent contraction, the load capacity of the muscle actuator decreases to 1500 N. For practical testing conditions the contraction of the muscle actuators are small, so high capacities are easily achieved. Up to three beams with six rubber muscles can be attached providing a theoretical total of 39000 N normal force. This can be achieved even using two 40 mm pneumatic artificial muscles. [41,42]

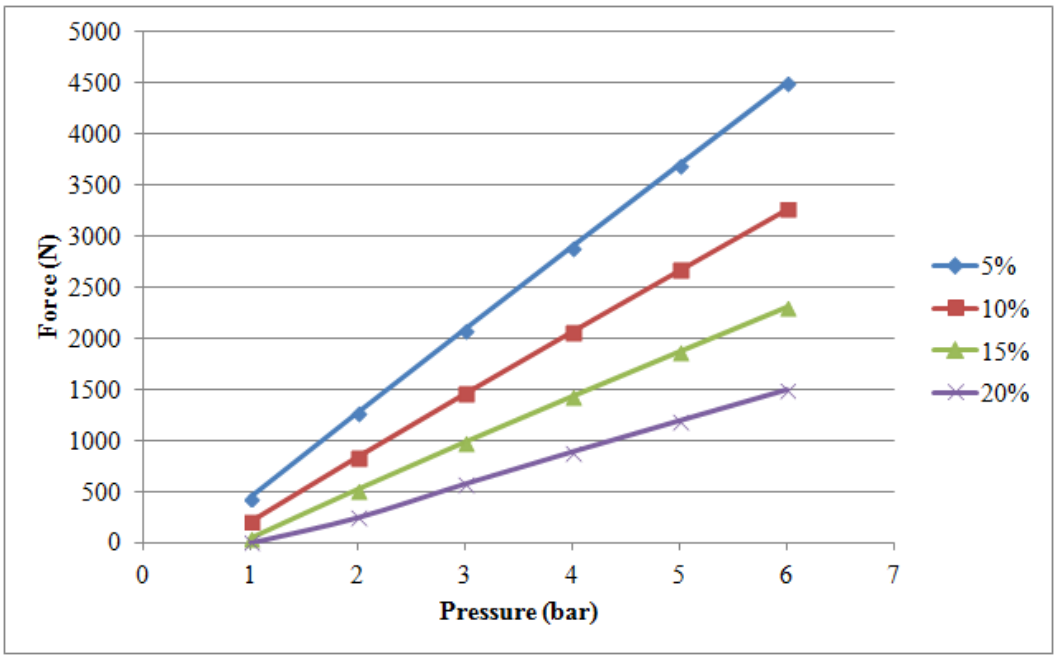

Figure 2.39. 40 mm muscle load capacity at various air pressure and changing contraction [41].

The small size upper box is pulled over the fixed larger bottom box. A stepper motor with reduction gear is used to move the linear actuator as located at the right side of the box. The step motor is controlled by PLC software by the control box shown towards the right end of the equipment. The right side view of the device is shown in Figure 2.40. The capacity of the linear actuator is 15 KN. It can apply shear force up to 167 kPa to the upper box. The PLC software is capable of applying monotonic and cyclic horizontal loads. The software allows control of the direction, displacement rate and frequency of the horizontal load application. The control unit at the left part of the shear box uses PLC software to control the antagonistic loading system.

The antagonistic system is composed of two opposing artificial muscle actuators pulling and pushing against each other to apply cyclic load to the upper box. This provides a stress controlled interface test execution. The maximum horizontal cyclic stress that can be applied by using one set of artificial muscle actuator is 50 kPa. [40-42]

Figure 2.40. The right side view of the device.

2.6. Summary

This chapter contained a review of general information of laterally loaded piles for different soil situations and pile properties. Additionally behavior of buildings under lateral loading is examined.

There are five analyses methods for laterally loaded piles. All methods have their own advantages and disadvantages.

Piles are observed in three different soil situation when they are exposed to lateral loading; soft clay, stiff clay and sand.

Pile properties requires two part; short pile-long pile, active pile-passive pile. Short piles are the rigid ones and long piles are the flexible ones. The force applied to one point, head of pile when it is called as active pile. On the other hand for passive ones, the pile translates with the laterally loaded pile.

Previous laterally model pile studies are examined carefully. A table is made for all the studies. This table gives main introduction like soil type, pile material about the tests. Then all the tests are taken over briefly. Similarities and differencies of the tests are examined and compared.

A review contact stress mapping is presented. Contact stress mapping and the materials used for this system explained briefly. Calibration method is studied. Application areas of contact stress mapping is shown.

At the last part, large displacement constant contact area shear device which is used for the experimental study part of this thesis is examined. Physical properties of the device is defined. Its working principles are examined carefully.

3. METHODOLOGY

3.1. Material Properties

3.1.1. Concrete Mortar Blocks

Concrete mortar blocks are utilized in order to obtain segmental post-tension beam model. For the production of blocks, Portland Cement I is used. Up to ASTM C270 standard specification for unit masonry and mortar, the mix ratios are 1:0,5:3 (cement: water: sand).

3.1.1.1. Mortar Blocks Production

Concrete mortar blocks are molded with dimension 50x50x20 (mm). A steel mold which is shown in Figure 3.1 is used in order to obtain the blocks with the specified dimensions. Also the mortar blocks are shown in Figure 3.2.

Figure 3.1. Steel Mold.

Figure 3.2. Mortar Block Unit.

Block width range is between 4,8-5,1 (cm) and the height range is between 1,8-2,15 (cm). The mass of the concrete blocks are between 92,8-108,56 (gr).

3.1.1.2. Compressive Strength of Mortar Blocks

Compressive strengths of six mortar blocks with 50x50x50 (mm) dimension are are measured. Test results are shown in Table 3.1.

3.1.2. Shore 60 Rubber

Shore 60 rubber is an industrial rubber which is used for any application needing an elastic rubber material and its thickness is equal to 3 mm. It is placed between the mortar blocks in this study. Rubber unit is shown in Figure 3.3. In Table 3.2. properties of rubber shore 60 material are shown.

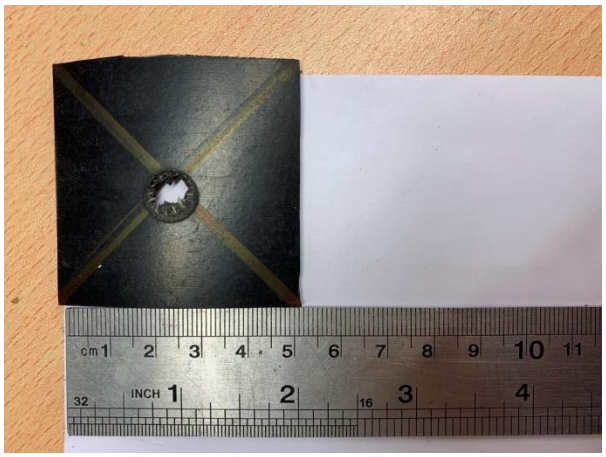

Figure 3.3. Rubber Unit.

Table 3.1. Compressive Strength Test Results.

Sample No	1	2	3	4	5	6	Average values
Load (KN)	52,2	51,2	48,5	47,6	49,4	48,7	49,6
Stress (MPa)	20,88	20,44	19,4	19,04	19,72	19,48	19,8

Table 3.2. Rubber Properties Details.

Rubber Type	Neoprene Rubber 1
General Description	Soft rubber
Style	7797
Colour	Black
Tensile Strenght (KN/m^2)	$10x10^3$
Elongation at Failure (%)	125
Elastic Modulus (MPa)	3
Thickness (t) (mm)	3
Rubber Shore (A)	60

3.1.3. Aluminium Cylinder Block

In this study, aluminum cylinder block is used as the main base of the segmental pile. The high strength wire is pressed into the this block from the tip. Its aim is to hold the concrete mortar blocks and rubber material on the wire under post-tension forces.

3.1.4. Poorly Graded Sand

According to ASTM D3080/D3080M-11 d_{50} value of used material in this study must be equal to 2,5 mm. So the pacticle size distribution is scaled. Uniformity and curvature coefficients are calculated and these are equal to 2,5-1,23. More than half of coarse fraction is smaller than mesh No.4, and curvature and uniformity coefficients are implied. According to theese values the soil is classified as poorly graded sand in USCS.

3.2. Measuring Tools and Test Equipment

3.2.1. Test Equipment

3.2.1.1. Steel Tension Test

Steel tension test is applied to wire which passes through the mortar blocks. Test continues until the determined stress values. Test equipment is shown in Figure 3.4.

3.2.1.2. Three Point Bending Test

Three point bending test is applied according to ASTM D790-17. Rectangular beam specimen is prepared with the dimensions implied above. The specimen is supported on each end point when a load is applied at the middle. With the help of three point bending test, force values corresponding to displacement at the middle is measured. With those values flexural strength and moment values of the pile are calculated. Test equipment is shown in Figure 3.5.

Figure 3.4. Steel Tension Test.

Figure 3.5. Three Point Bending Test.

3.2.1.3. Large Displacement Constant Contact Area Shear Device

A complete new large size, large displacement interface testing system is used in order to apply lateral loads to the pile. A possible use of the proposed large displacement constant contact area shear device is conducting cyclic tests on either structural materials or geosynthetics. Pneumatic muscles are used for the application of the cyclic horizontal loads. 40 mm diameter muscle can be applied up to 6,5 KN. The drawing of the proposed cyclic actuator is shown in Figure 3.6. To create a cyclic motion first the agonist (flexor) muscle is pressurized, thus the upper shear box moves in the direction of the agonist

muscle. In the next step, the antagonist (extensor) muscle is inflated while the agonist muscle is deflated simultaneously, which starts a motion in the reverse direction. [41,42]

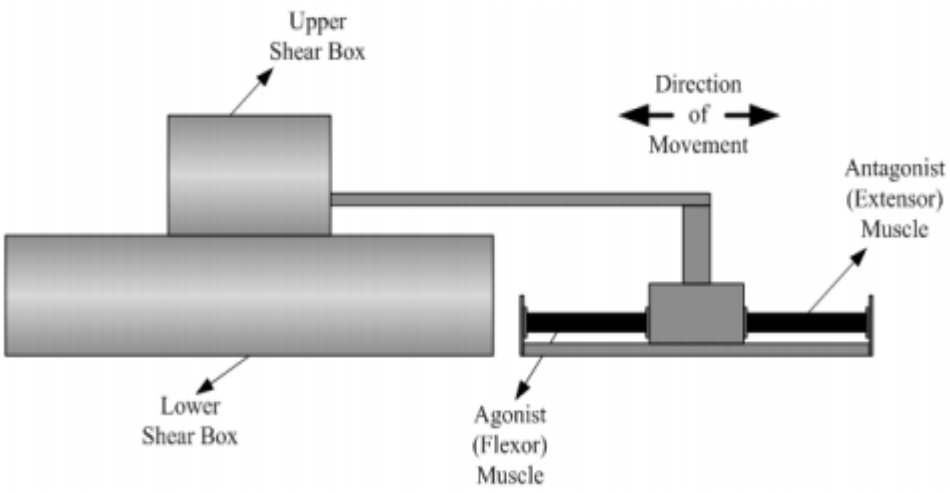

Figure 3.6. The drawing of cyclic actuator [41].

As the pneumatic artificial muscles can only pull, in order to generate a bidirectional motion, two muscles have to be coupled antagonistically. In the cconfiguration, the driving muscle, flexor or agonist, moves the load, while the other one, extensor or antagonist, will act as a brake to stop the load at its desired position. To move the load in the other direction, the muscles change their functions. The antagonistic configuration can generate linear motion as it shown in Figure 3.7. [41,42]

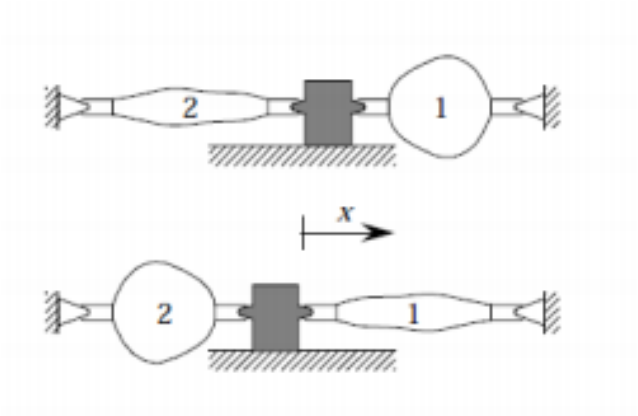

Figure 3.7. Antagonistic configuration of the pneumatic artificial muscles [41].

In this set-up the equilibrium position of the load is determined by the ratio of muscles' gauge pressures. If the load is at its equilibrium position and both pressures are equal, the muscles are at lengths l_1 and l_2. Changing the pressures will break the equilibrium and thus a net force will move the load until a new point of equilibrium is reached at a distance x from the previous equilibrium position. The graphic in Figure 3.8 shows the force characteristics of the muscle pair shown in Figure 3.7. Muscle (1) is at a gauge pressure p while the pressure of muscle (2) varies. As the muscle pressure changes, the force graph of that muscle is scaled accordingly and the equilibrium will move to the new intersection point of the graph. A uniform scaling of both gauge pressures of the muscles will not affect the equilibrium and thus only the ratio of gauge pressures will determine the equilibrium position. [41,42]

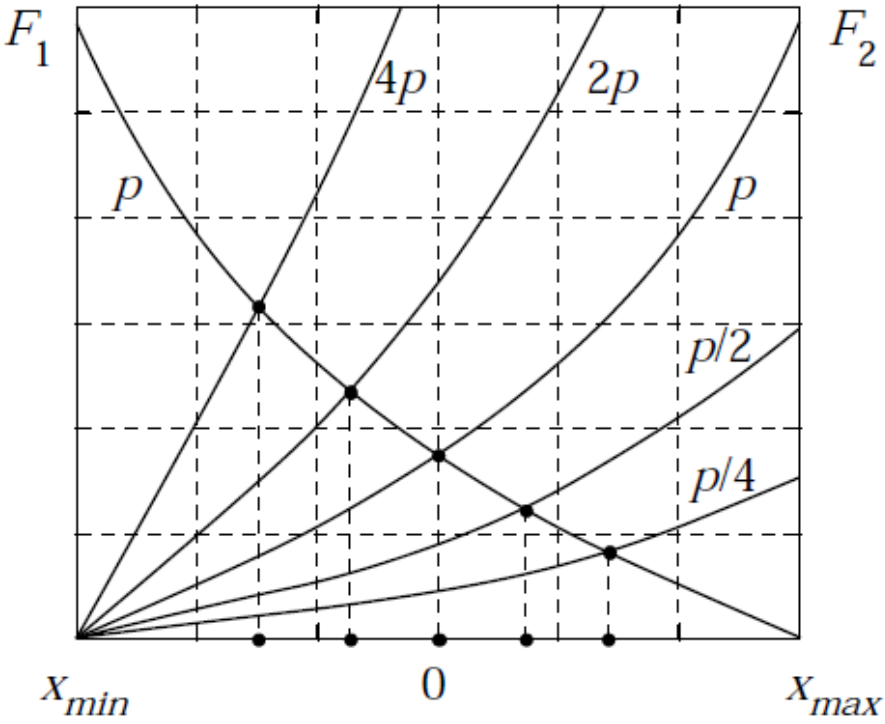

Figure 3.8. Equilibrium position as a function of gauge pressure ratio [41].

The antagonistic system which is explained briefly is used for the experimental part of this study. A new and versatile large displacement constant contact area shear device shows all these specialities. The upper box is pulled over the lower box by the muscle

actuator. Dimensions of the upper part are 0,30x0,30x0,20 m. and dimensions of the lower part are 0,90x0,30x0,60 m. Testing device is shown in Figure 3.9. [38]

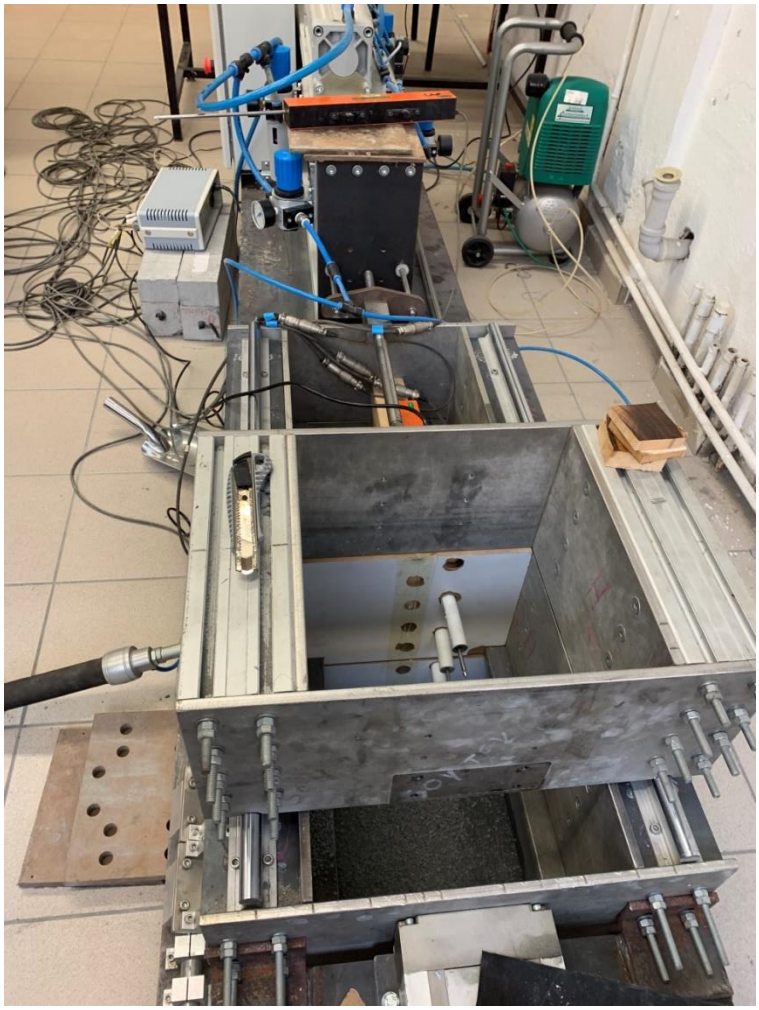

Figure 3.9. Large Displacement Constant Contact Area Shear Device.

3.2.1.4. Particle Size Distribution

In order to obtain particle size distribution and d_{50} value of granular material sieve analysis method according to ASTM D6913/D6913M is used.

3.2.1.5. Relative Density Test

In order to obtain relative density, vibratory table test according to ASTM D4253 is conducted.

3.2.1.6. Direct Shear Test

In order to obtain friction angle of the soil direct shear test up to ASTM D3080/D3080-M is applied to poorly graded sand.

3.2.1.7. Oedometer Test

In order to obtain restrained soil modulus oedometer test is used. This test is conducted according to ASTM D2435/D2435-11.

3.2.2. Load Cell (Tension+Compression)

In this study, S type load cell is used to measure the horizontal forces on the pile head. The S type load cell is developed for use in weight and force measurement applications working with the principle of shear force. It is developed for the measurement of the pulling weight and force, but it can be adapted to pressure systems. Capacity of the load cell is equal to 20 kN

3.2.3. Linear Variable Differential Transducer

It is an electromechanical sensor used to convert mechanical motion or vibrations, specifically rectilinear motion, into a variable electrical current, voltage or electric signals and the reverse. In this study, they are used to measure the displacement of the embedded part of the pile. Five of them are sorted by 8,5 cm from top to bottom.

3.2.4. Prescale Film

Prescale films are developed for illustrating the contact stress concentration details of areas. Relative temperature and humidity values are important for the films. The pressure level is obtained with the color intensity. There is a calibration sheet in order to identify the sheet to the software. In order to understand interface behaviour, careful and detail calibration is important.

3.3. Specimen Preparation

Three segmental pile models are made. Each model requires 13 mortar blocks. The preparation process can be given as follows:

1- Mortar blocks are made w.th the dimensions 50x50x3 (mm).

2- Rubber sheets and prescale films are cut.

3- A hole with 10 (mm) diameter is made at the center of each block, rubber sheet and prescale film.

4- Numbered blocks are placed in vertical direction.

5- Rubber sheets with the dimensions 50x50x3 (mm), prescale films with the dimesions of 50x50 (mm) are placed.

6- Aluminum cylinders are pressed at the end of the high strength wire.

7- For the post-tension application, wire with 3000 N capacity is passed through the rubber and blocks.

8- With steel tension test determined forces are applied and bolts are tightened.

9- Three point bending test is applied then equivalent EI values of the piles are found.

10- Steel wires are attached to pile and LVDTs in order to measure the displacement values.

Figure 3.10. Segmental pile.

3.3.1. Experimental Work

3.3.1.1. Steel Tension Test

Piles with different flexural rigidities is obtained with this test. With steel tension device the wire which passes through the blocks is tensioned until the determined values, then the bolts are tightened. This applied values are 750N, 1500N, 2250N. This test helps the specimen preparation for the following test.

3.3.1.2. Three Point Bending Test

Three point bending test is applied to piles with different flexural rigidities. It supplies values for elasticity modulus in flexural strain, bending, flexural stress and flexural stress-strain response. The rate of loading ise equal to 1mm/min. This test helps the specimen preparation for the following tests.

3.3.1.3. Load-Deflection/Interface Relationship for Sand

Granular material behavior under loading and unloading situation is examined. Both oedometer test and direct shear test are conducted.

For oedometer test poorly graded sand is placed on a oedometer device. A gauge is attached in order to measure displacement. Loading and unloading procedure is made and load-deflection, stress-strain relationships are recorded and plotted.

For direct shear tes the displacement rate is 1 mm/min. Vertical displacements, horizontal forces, horizontal displacements and the vertical force are recorded.

3.3.1.4. Large Displacement Constant Contact Area Shear Device

Each pile which is bounded to linear variable differential transducers with 8,5 cm range is placed into testing device as it is seen in Figure 3.11. Unit weights of the soil for different density stages are known so the box is filled according to these values. Sand is poured into the box with the layers of 5 cm height. The pile is subjected to lateral loading with the piece attached to the pile cap. Applied load is equal to 300 N and it is set with the gauges. The piles are loaded up to 30-50-100 cycles. The force is measured with load cell which is attached to the box and the displacement is measured with linear variable differential transducers.

Force and displacement data are collected with computer and transferred to Excel sheet. With Excel all the graphics are plotted.

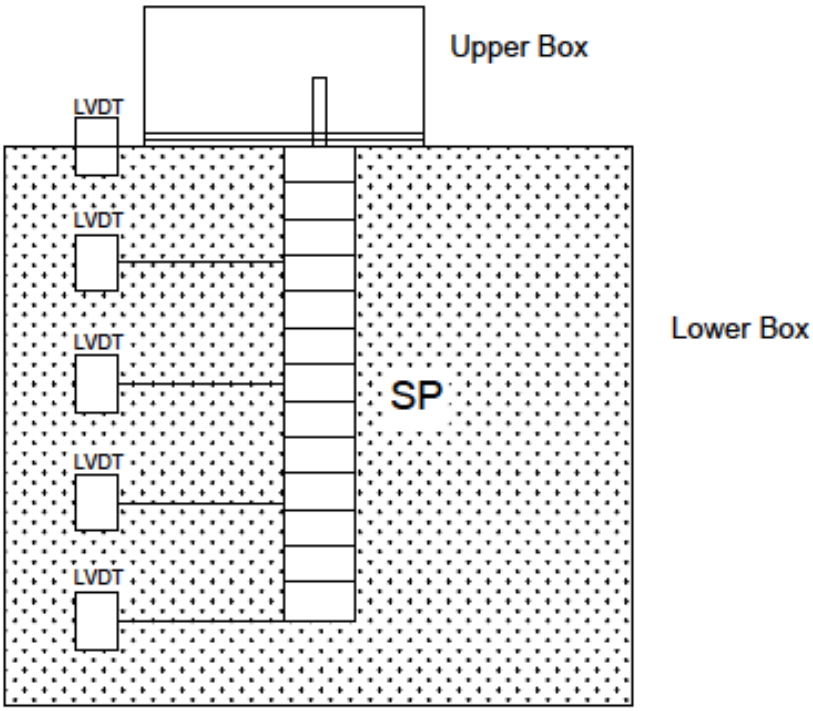

Figure 3.11. Schematic View of the Testing Set-Up.

4. TEST RESULTS AND ANALYSIS

In this chapter, test results on segmental pile subjected to lateral load are presented. The results for cyclic loading are presented. Displacement, slope, shear force and bending moment due to lateral forces are obtained. Also results of soil tests are shown. Grain size distribution, friction angle and elasticity modulus are presented.

4.1. Experimental Test Results of Soil

4.1.1. Particle Size Distribution

According to ASTM D6913/D6913-M D_{50} value of the soil must be equal to 2,5 mm. So, soil is subjected to sieve analyzes test according to ASTM D6913/D6913M. The grain seze distribution of the soil which is used for the tests are shown below in Figure 4.1. C_c value of the soil is equal to 1,23 and C_u value of the soil is equal to 2,5.

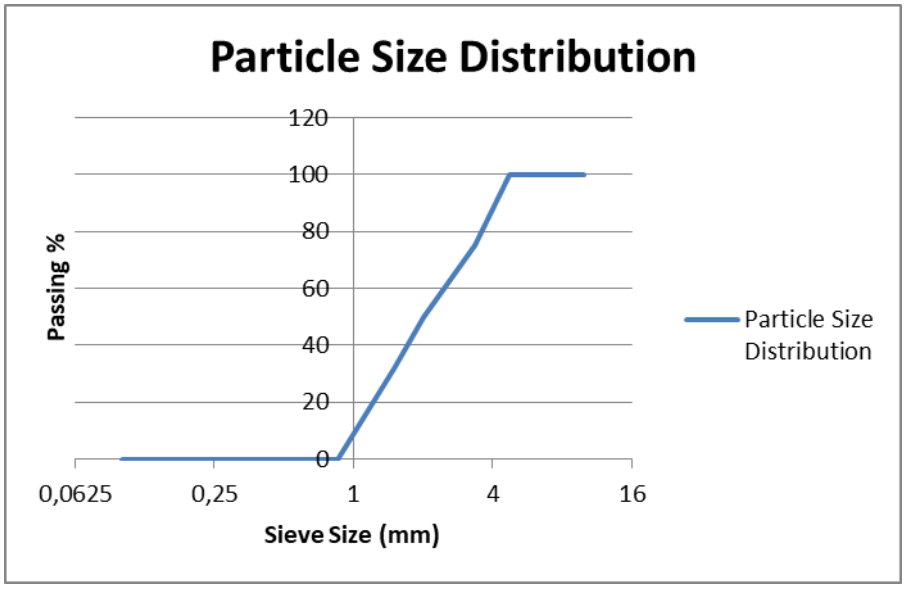

Figure 4.1. Particle Size Distribution.

4.1.2. Relative Density

Relative density tests are made according to ASTM D4253. 4073,5 g poorly graded sand is used for the test. The test is conducted three times. The weight of the SP is equal to 4060,8 g. First, the volume of the SP is equal to 2820 cm^3. After the shaking it is equal to 2580 cm^3. It is seen that soil density is equal to 1,44 g/cm^3 for the loose state, 1,51 g/cm^3 for the medium-dense state and 1,57 g/cm^3 for the dense state. Also, emax-emin values are calculated and they are equal to 0,61-0,55.

4.1.3. Direct Shear Test

In order to obtain friction angle of the soil with different densities direct shear test is conducted. The results of the test are shown in Figures 4.2. 4.3. and 4.4. The friction angle of the soil is equal to 45,7 º for loose state, 47,12 º for medium dense state and for dense state 49,23º . Also dilation results are shown in Figures 4.5. 4.6. and 4.7.

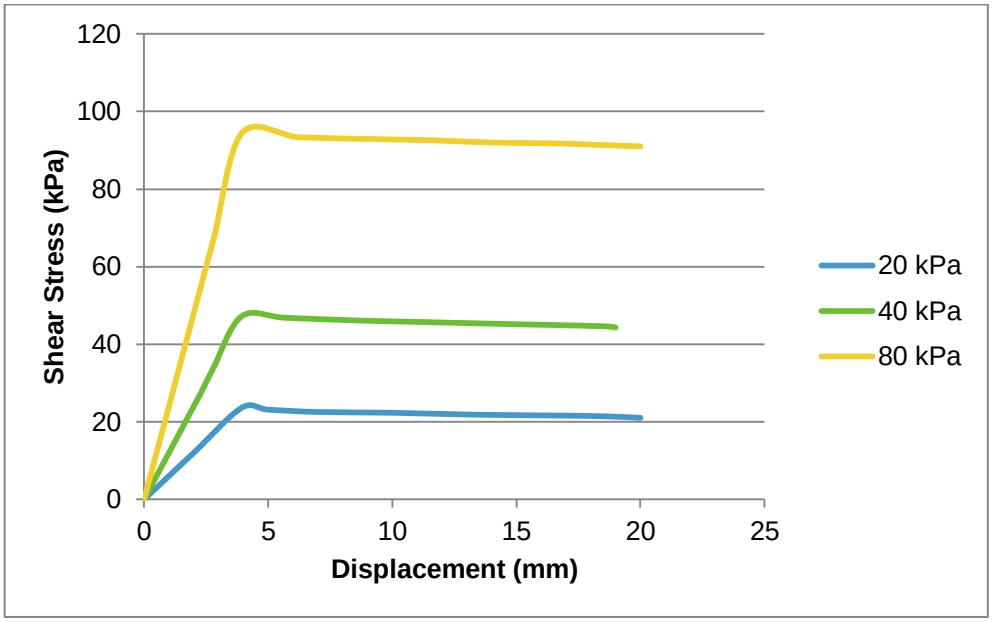

Figure 4.2. Shear versus Horizontal Displacement for Dense Soil.

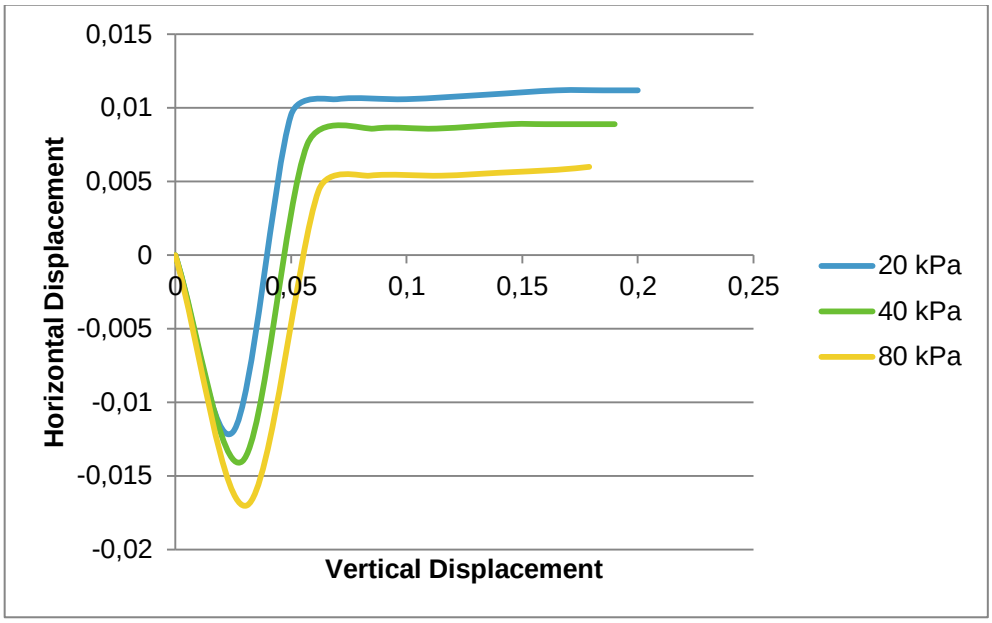

Figure 4.3. Vertical Displacement versus Horizontal Displacement for Dense Soil.

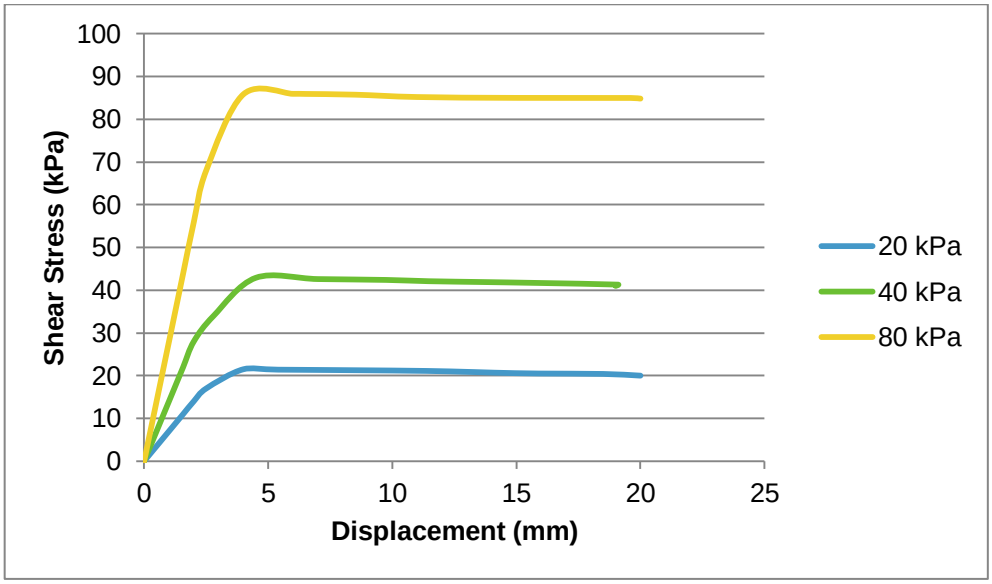

Figure 4.4. Shear versus Horizontal Displacement for Medium - Dense Soil.

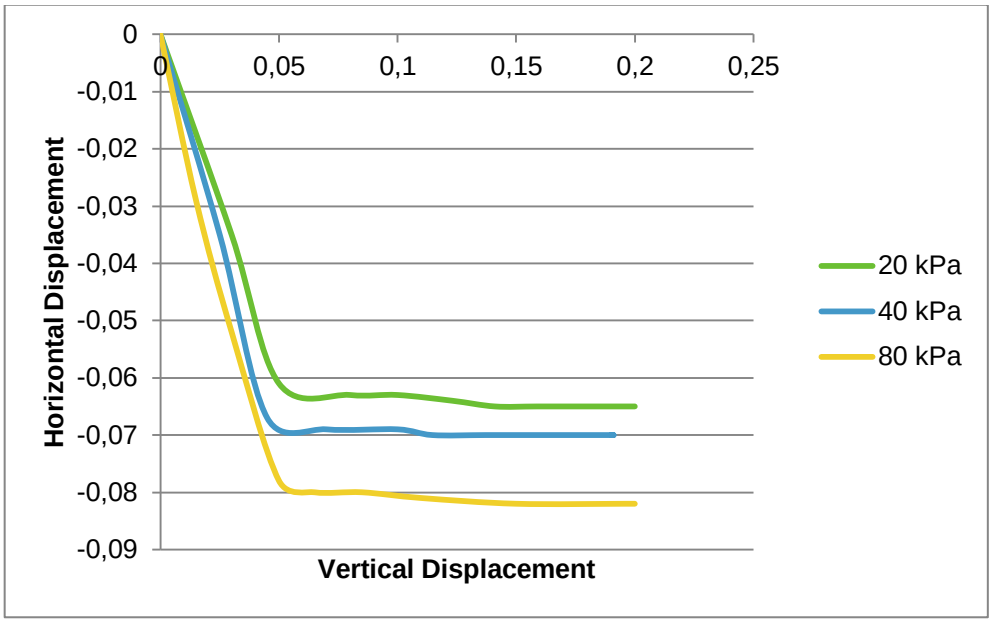

Figurre 4.5. Vertical Displacement versus Horizontal Displacement for Medium Dense Soil.

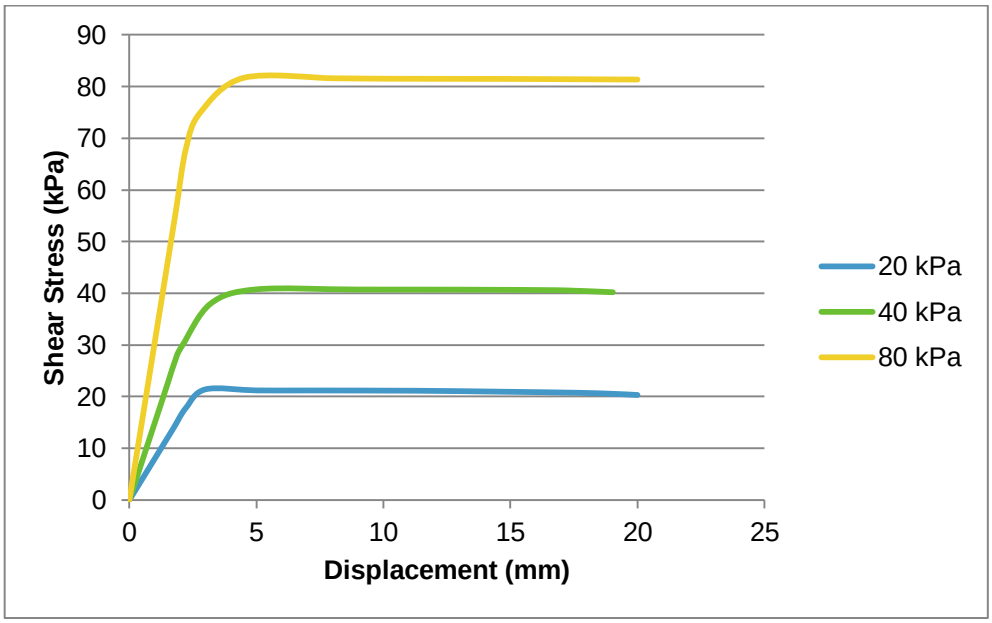

Figurre 4.6. Shear versus Horizontal Displacement for Loose Soil.

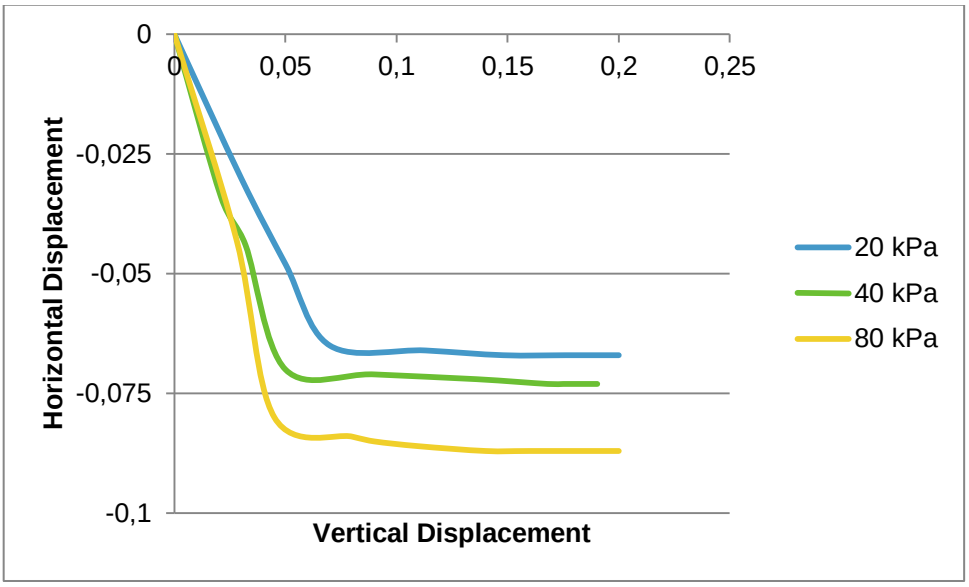

Figurre 4.7. Vertical Displacement versus Horizontal Displacement for Loose Soil.

4.1.4. Constrained Modulus of the Soil

Constrained modulus of the soil is obtained by odoemeter test. The testing procedure consisted in a gradual increase in loading from 25 to 1600 kPa at time intervals of approximately 0.1, 0.25, 0.5, 1, 2, 4, 8, 15 and 30 min and 1 hour, each time increasing the load following stabilization of sample strain. Results of loading situations are shown below in Table 4.1. In Table 4.2. vertical strain percentage is shown. Also, in Table 4.3. constrained modulus of SP is shown.

Table 4.1. Loading Situations.

	25 kPA	50 kPA	100 kPA	200 kPA	400 kPA	800 kPA	1600 kPA
Time	**Settlement**	**Settlement**	**Settlement**	**Settlement**	**Settlement**	**Settlement**	**Settlement**
0 sec	0	0	0	0	0	0	0
5 sec	0,04	0,15	0,19	0,2	0,32	0,48	0,68
10 sec	0,04	0,15	0,19	0,2	0,32	0,48	0,68
20 sec	0,04	0,15	0,19	0,2	0,34	0,48	0,68

Table 4.1. Loading Situations (cont.).

60 sec	0,04	0,15	0,19	0,2	0,34	0,48	0,68
120 sec	0,04	0,16	0,2	0,21	0,34	0,49	0,68
240 sec	0,04	0,16	0,2	0,21	0,34	0,49	0,68
480 sec	0,04	0,16	0,2	0,21	0,34	0,49	0,69
900 sec	0,04	0,16	0,2	0,22	0,34	0,49	0,69
1800 sec	0,04	0,16	0,21	0,22	0,35	0,49	0,69
3600 sec	0,04	0,16	0,21	0,22	0,35	0,5	0,69

Table 4.2. Vertical Strain Percentage.

	25 kPA	**50 kPA**	**100 kPA**	**200 kPA**	**400 kPA**	**800 kPA**	**1600 kPA**
Time	**Strain %**	**Strain %**	**Strain %**	**Strain %**	**Strain %**	**Strain %**	**Strain %**
0 sec	0	0	0	0	0	0	0
5 sec	0,18	0,65	0,85	0,86	1,39	2,08	3,97
10 sec	0,18	0,65	0,86	0,89	1,39	2,1	3,97
20 sec	0,19	0,67	0,86	0,90	1,47	2,1	3,97
60 sec	0,2	0,68	0,86	0,90	1,47	2,10	3,97
120 sec	0,2	0,69	0,86	0,91	1,5	2,13	3,98
240 sec	0,2	0,69	0,86	0,91	1,5	2,13	3,98
480 sec	0,20	0,71	0,89	0,91	1,51	2,13	3,98
900 sec	0,20	0,71	0,89	0,95	1,51	2,13	3,98
1800 sec	0,20	0,71	0,91	0,95	1,52	2,16	3,98
3600 sec	0,20	0,71	0,91	0,97	1,52	2,17	3,98

Table 4.3. Constrained Modulus of Granular Material.

Strain	ΔБ (kPa)	Es=ΔБ/ε (MPa)
0,002	25	12,5
0,007	50	7,14
0,009	100	11,11
0,010	200	20
0,015	400	26,66
0,022	800	36,36

4.2. Analysis of Segmental Pile Experimental Data

4.2.1. Flexural Rigidity of the Segmental Pile

Analysis of segmental pile is shown using the experimental data. The data is recorded during the tests. The main aim is to obtain elasticity modulus of segmental pile which is exposed to three point bending test. Then with these results and large displacement constant contact area shear device results; slope, bending moment and shear force of the segmental pile is found. In three point bending test, stress strain curve is constructed and EI is calculated. The EI in equivalent EI for segmental beam. Figure 4.5. shows the stress/strain relation of the pile model and the mortar beam which is used as a control pile.

The failure of segmental pile with post-tension force 750 N took place at flexural stress of 0,6 MPa corresponding to 0,0025 strain. Flexural stress value at failure of the pile model is increased nearly 2 times 3 times and 5,5 times when using segmental pile with post-tension force of 1500 N and 2250 N, mortar beam respectively. The pile model with post-tension force of 750 the strain is 0,0025. It is nearly 5 times more than the mortar beam strain at failure. In order to obtain the EI value of the mortar beam, the general equation is shown below in Table 4.4.

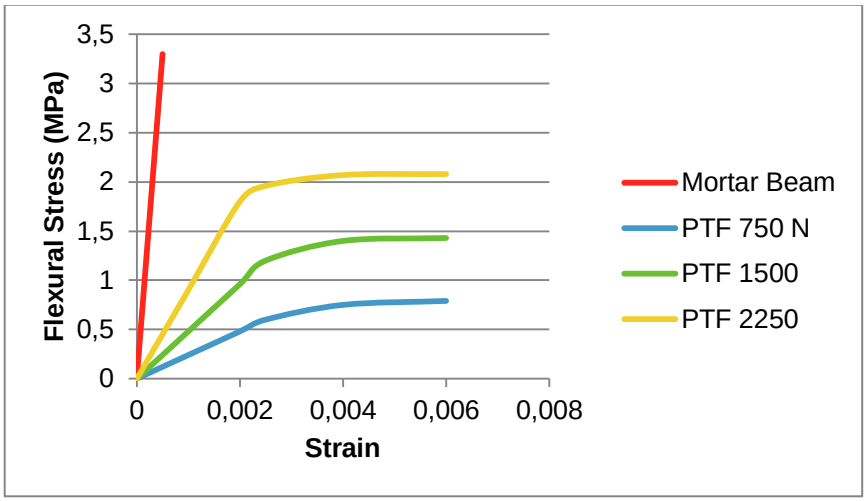

Figure 4.8. Flexural Stress versus Strain.

“”

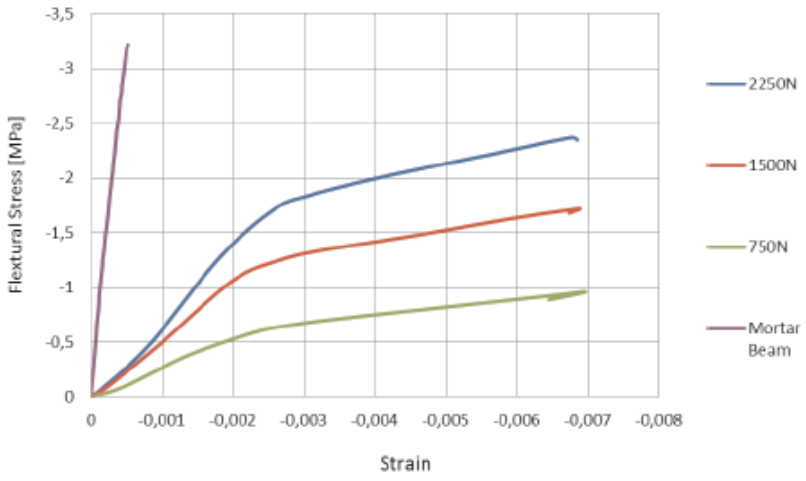

Figure 4.9. Flexural Stress versus Strain [2].

In the Figures 4.8. 4.9. first one is from this study and second one is from referenced study. In both studies a mortar beam and segmental piles with post tension force 750-1500.2250 N are used. In the Figures 4.8. 4.9. it is seen that the results nearly coincide to each other. Also the mentioned ratios of failure stresses verify each other. In both studies slope of the mortar beam line is steeper than the others and the mortar beam line is the only one reaches 3 MPa flexural stress. In both studies, strain values at failure for segmental piles are nearly same. However, the strain values corresponding to flexural stresses are different in each study. Yet, the difference is not too much.

In order to calculate pile model flexural rigidity, general deflection equation of simple support beam subjected to point load at the middle of the span is used.

$$\delta=[PL^3/48EI] \quad (4.1.)$$

Table 4.4. Numerical Values of Flexural Rigidity of the Mortar Beam.

Force	**Deflection (mm)**	**EI (KNm²)**
0,19	3,7	0,42
0,25	4,2	0,48
0,36	4,8	0,57

EI average of the mortar beam is equal to 0,49 KNm².

4.2.2. The Moment of the Segmental Pile

Due to the segmental pile discontinuity, moment values can not be found from the displacement values caused by the cyclic loading. So, in order to validate the moment capacity of segmental pile, prescale films are used. Prescale films are placed between the blocks and rubber material before the post-tension step. Then the wire is post-tensioned with the wanted values and piles are exposed to three point bending test. Test results are shown in the previous papers. After the tests prescale films are examined and stress values are determined with a computer program. Then moment values are calculated. Prescale films scanned views and moment graphics are shown below.

$$\sigma = \frac{N}{A} \mp \frac{M}{W} \quad (4.1)$$

Where σ is the stress (KN/m^2), N is the normal force (KN), M is the moment (KNm), W is the section modulus (m^3) and A is the area (m^2).

In Figure 4.10. the schmatic diagram shows the place of the numbered prescale films.

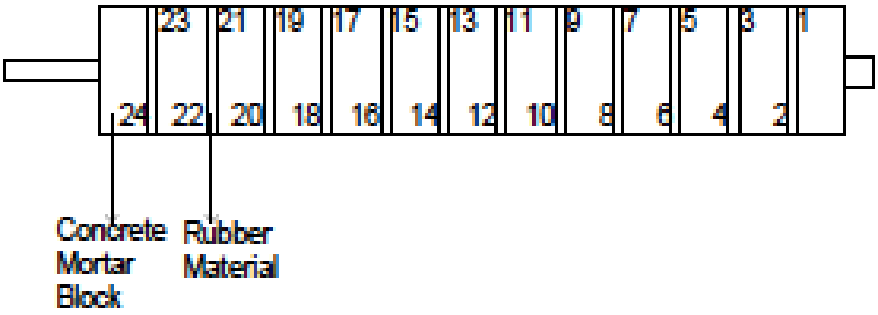

Figure 4.10. Place of the Prescale Films.

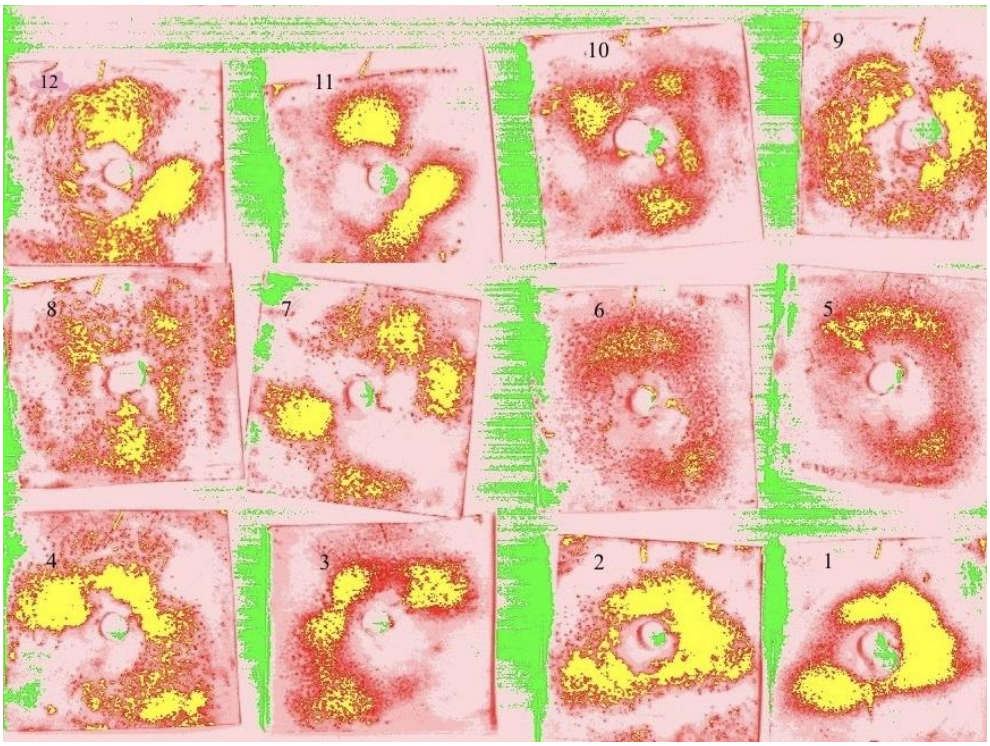

Figure 4.11. Scanned Prescale Films (750N-Lower Part).

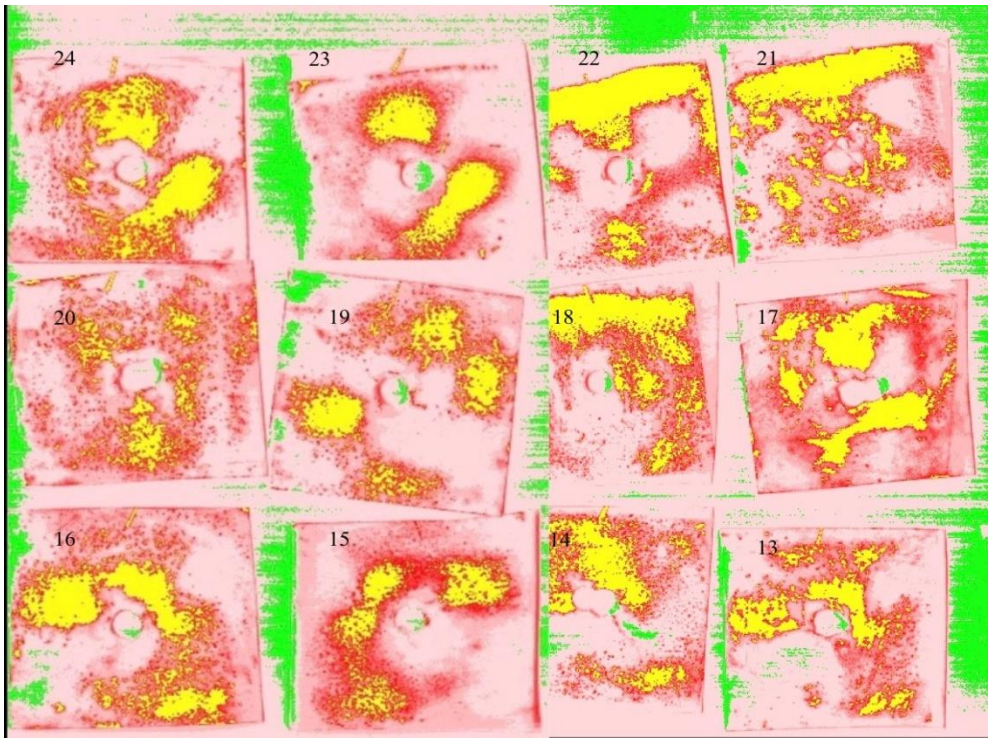

Figure 4.12. Scanned Prescale Films (750N-Upper Part).

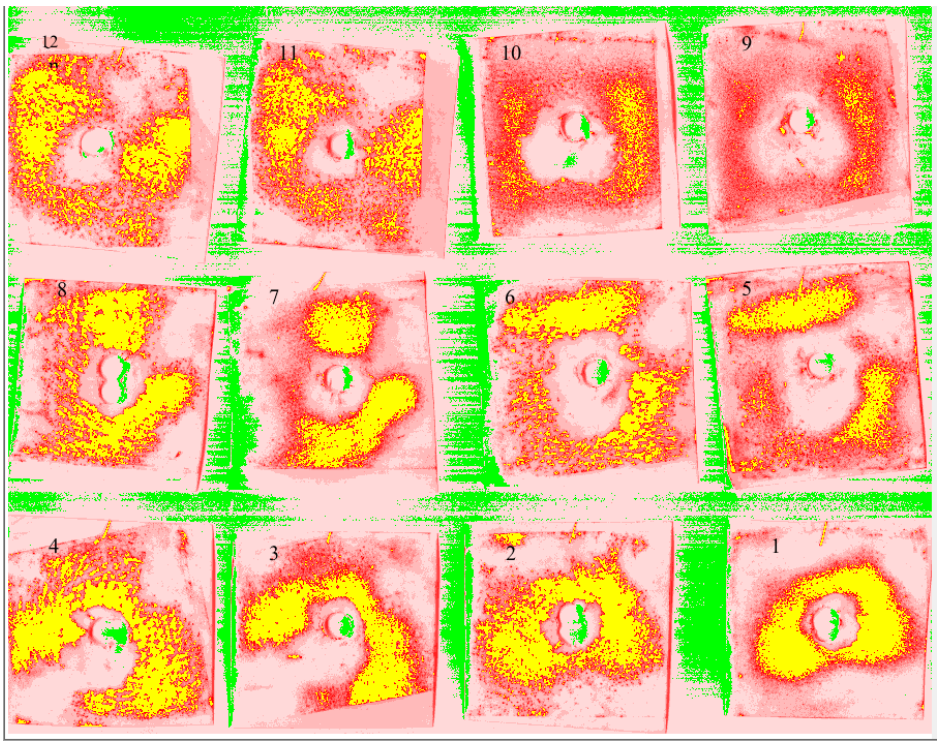

Figure 4.13. Scanned Prescale Films (1500N-Lower Part).

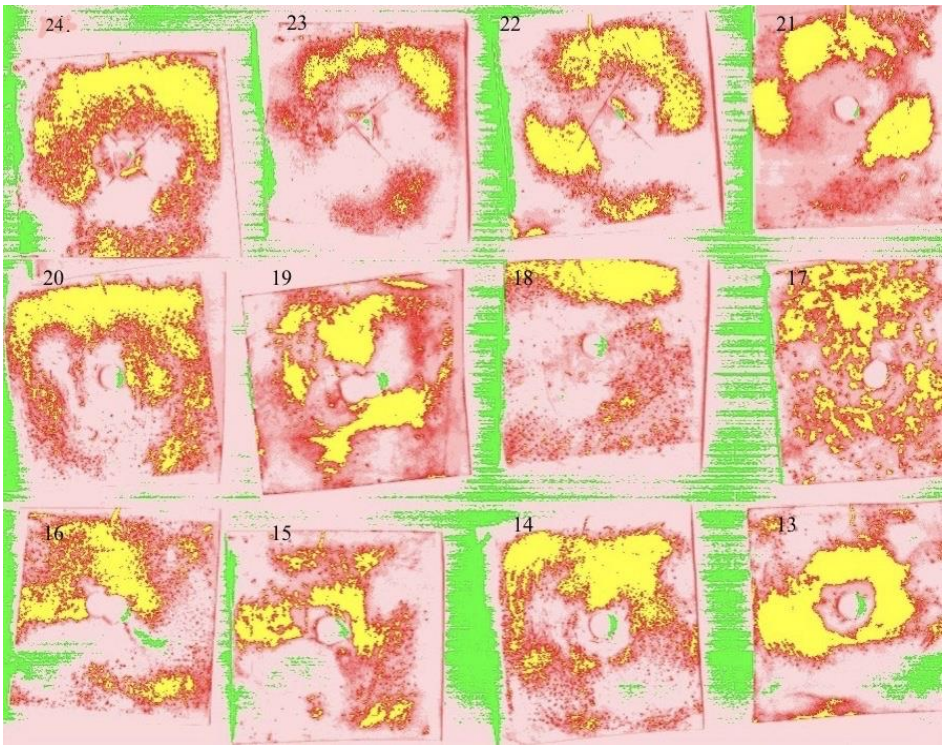

Figure 4.14. Scanned Prescale Films (1500N-Upper Part).

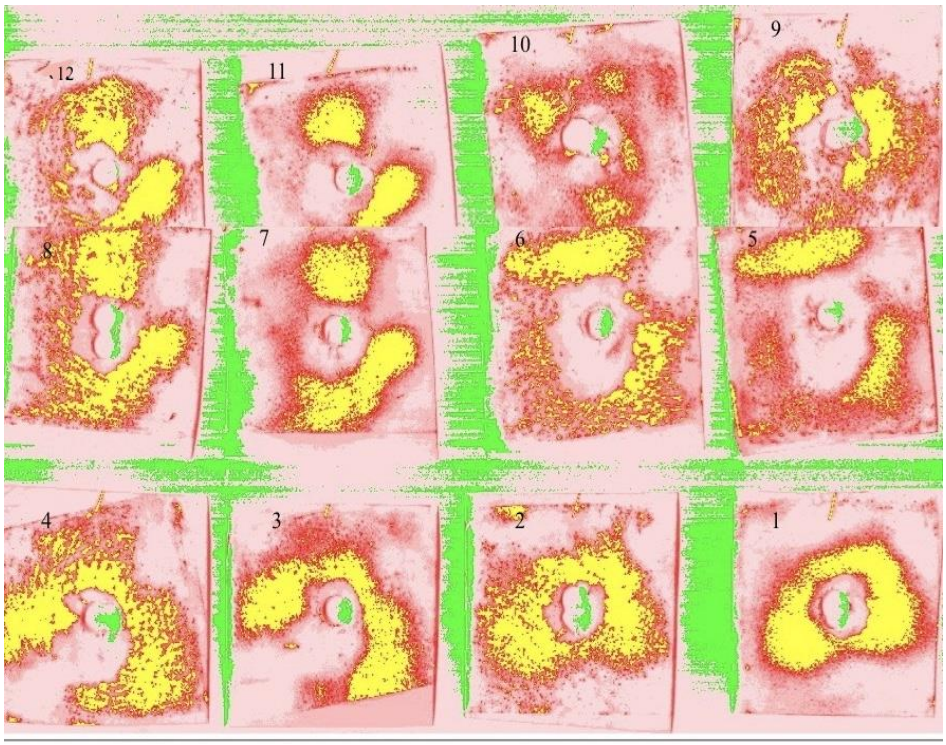

Figure 4.15. Scanned Prescale Films (2250N-Lower Part).

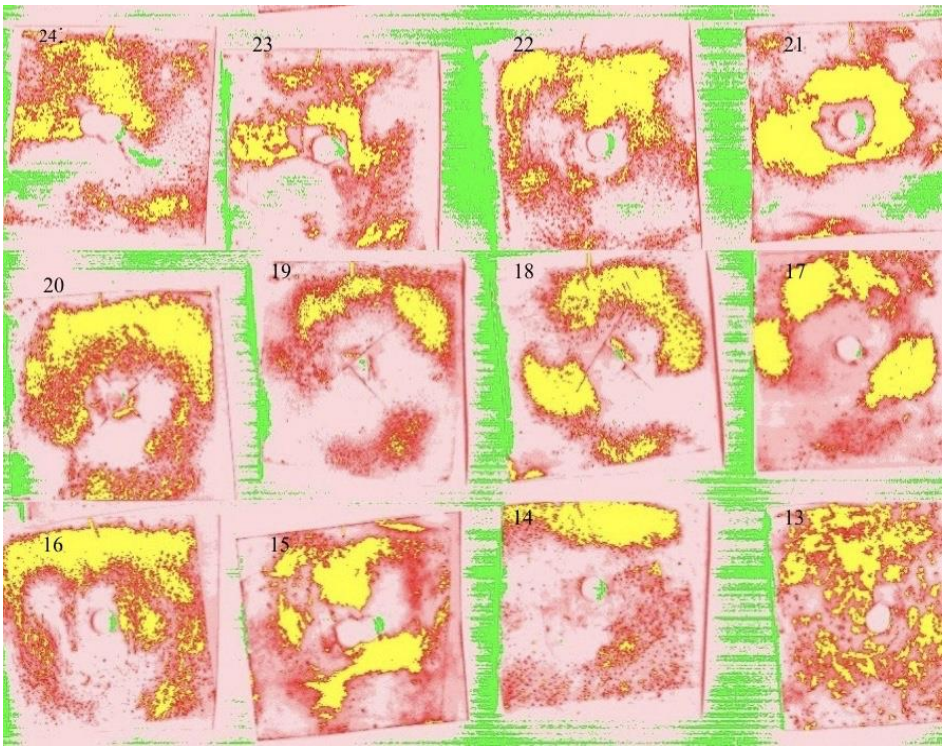

Figure 4.16. Scanned Prescale Films (2250N-Upper Part).

Yellow color shows that the capacity of the film in exceeded. Green color shows that the measurement is lower than the capacity of the film. The films in the Figures 4.11. 4.12. 4.13. 4.14. 4.15. and 4.16 are goes from the pile base to top. All of them scanned in the same marked direction in order to prevent confusion.

First of all, in the films it is seen that when the post tension is higher, yellow areas are wider. This means the flexural capacity of the pile is higher as expected. Yellow areas are wider in the upper parts of the films. Because the pile was exposed to three point bending test and the pressure due to squeeze in that part is higher. Color of the film changes with the pressure. On the other hand in the lower part of the films yellow color is not that common, that part is more in red shade. This shows that the pressure at that part is lower than the upper part.

The moment values calculated from the pressures at the films. They are shown in Figures 4.17. 4.18. 4.19.

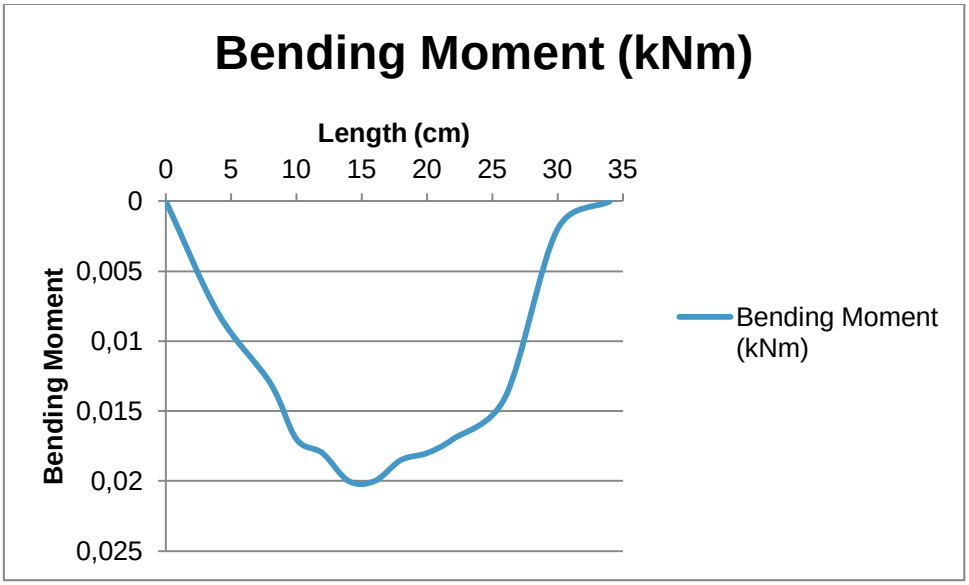

Figure 4.17. The Bending Moment Diagram Along Segmental Pile Length (750N).

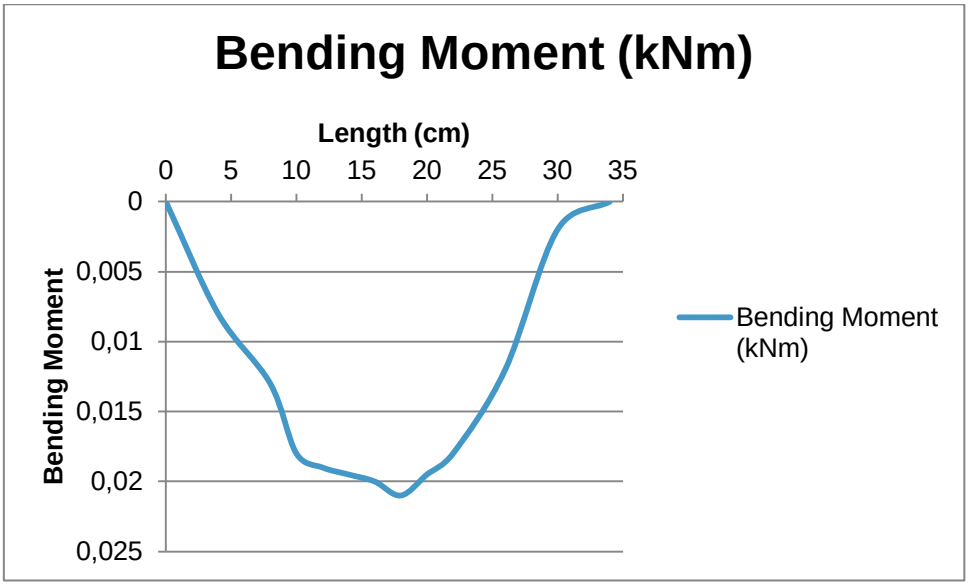

Figure 4.18. The Bending Moment Diagram Along Segmental Pile Length (1500N).

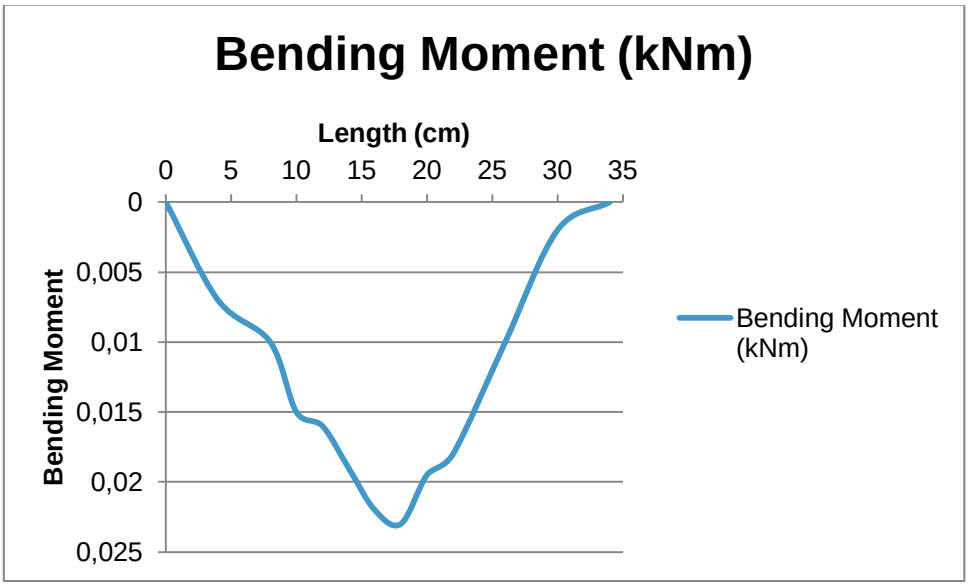

Figure 4.19. The Bending Moment Diagram Along Segmental Pile Length (2250N).

It is seen that there is a breaking point at 30 cm. depth for all the moment graphics and the peak point depth is close to each other. Only, a little difference like 1-2 cm. is seen at the first graphic peak point.

Bending moments are also calculated from the maximum force applied to pile when it was exposed to three point bending test.

$$M=PL/4 \qquad (4.2)$$

Where P is the normal force (KN), M is the moment (KNm), L is the length of pile (m).

The applied forces and deflection values corresponding to them are measured in three point bending test. With this results segmental pile moment is calculated.

Bending moment values which are calculated from the measured values of three point bending test are shown in Figure 4.20. The moment values are calculated with the measured maximum forces. This calculation is made with an assumption. While

calculating, the segmental piles are assumed as a continuous pile and the formula in Equation 4.2. is used for the calculation. The result with this assumption is nearly 20 % higher than the maximum moment results obtained from prescale films. The difference between the maximum values are higher when the post-tension force is lower.

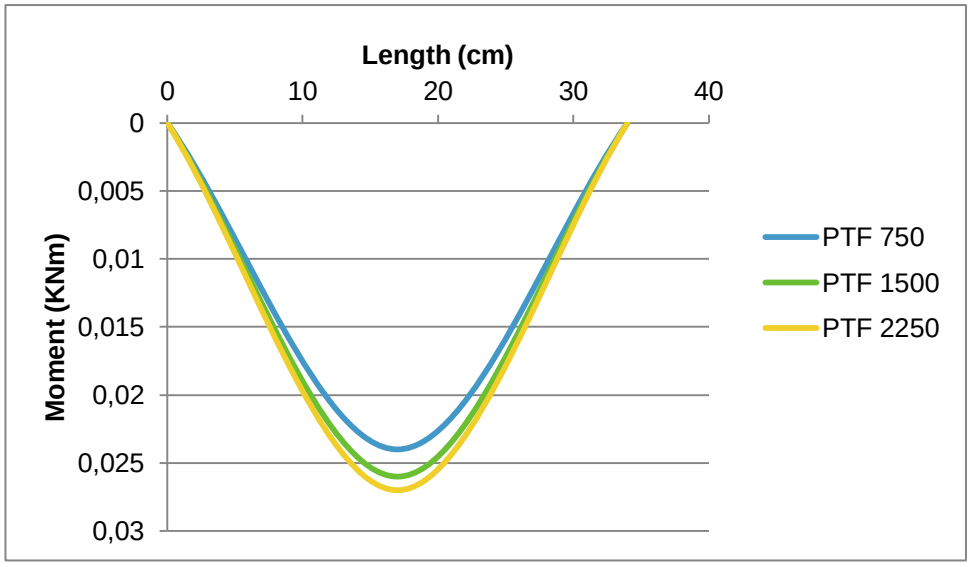

Figure 4.20. Bending Moment Values Calculated from the Three Point Bending Test.

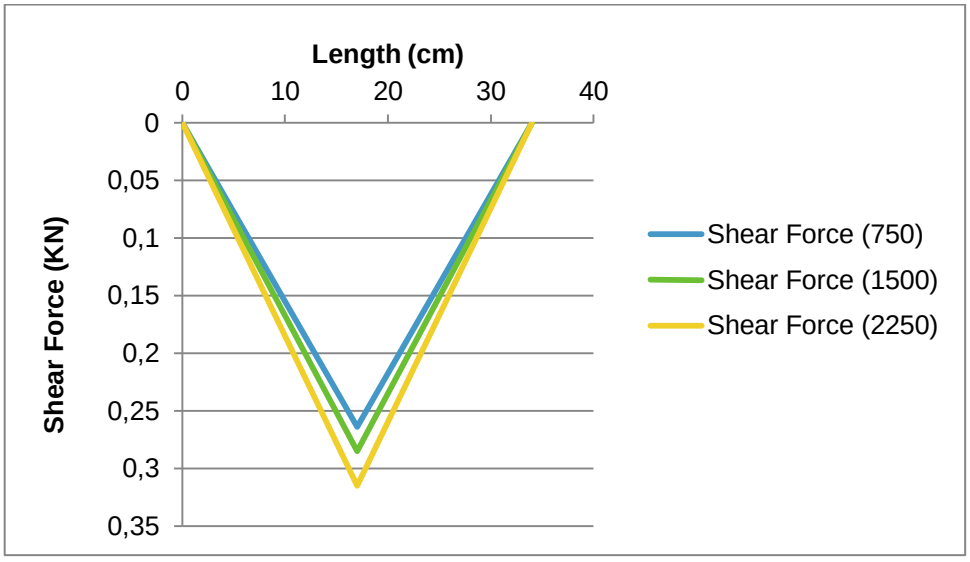

Figure 4.21. Shear Values Obtained from the Load-Deflection/Interface Relationship for Rubber Shore 60 tests.

In three point bending test the force applied to the middle of the pile and the deflection values are known. Whic are you used to calculate the shear stress values. Shear values are obtained from the Load-Deflection/Interface Relationship for Rubber Shore 60 tests and displacement results [2]. With the values obtained from the referenced paper, shear values are calculated relatively.

The shear values which are obtained from the Load-Deflection/Interface Relationship for Rubber Shore 60 tests are close to the values applied in the bending test. The Figure above is drawn relatively for each block so it is normal that the form of the Figure does not coincide with the one single force shear diagram. From these shear values moment values are found.

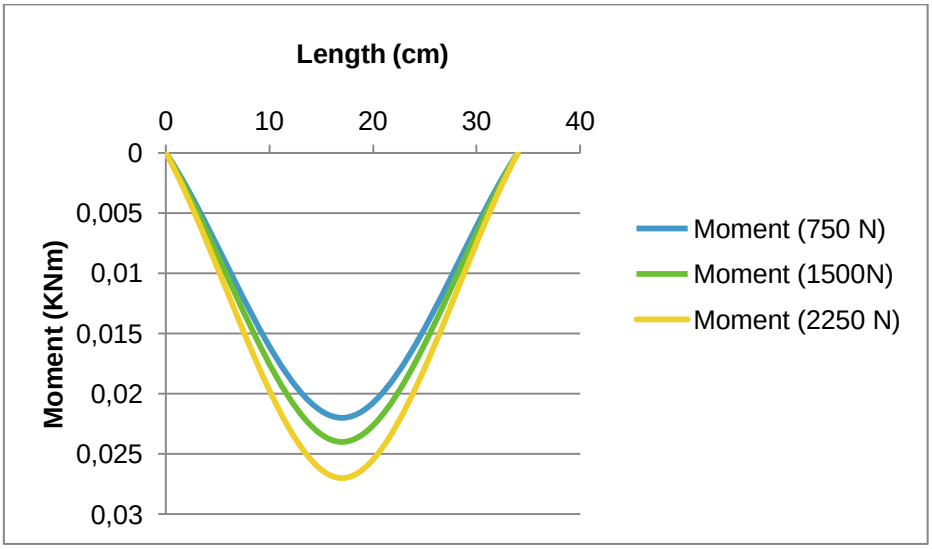

Figure 4.22. Moment Values Found from the Shear values Obtained from Interface Results..

Values obtained from the shear values from the Load-Deflection/Interface Relationship for Rubber Shore 60 tests, results are very close to previous ones. But the maximum moment values are lower than the ones found from the applied force in three point bending test. On the other hand they are higher than the ones found with the prescale films. Therefore it is seen that moment values of these three tests nearly support each other.

4.2.3. The deflection of the Top Point of Segmental Pile

In the Figures 4.23. 4.24. 4.25. 4.26. 4.27. 4.28. 4.29. 4.30 4.31. 4.32. 4.33. 4.34. deflections of the top point of segmental pile and mortar beam in loose, medium-dense and dense soil under cyclic loading are shown. For all states the applied force is equal to 300N for cyclic loading then piles are loaded up to 600 N with static loading. In the Figures, it is clearly seen that the deflection decreases when the soil is denser. Also it gets lower when the post tension force rises and for the mortar beam lowest values are seen. Additionally for all pile types in dense soil state cycle intervals are very frequent. A reduction at the frequency is seen between the cycles of Segmental Pile with Post-Tension Force 1500 N in loose soil. It may be caused by instant soil movement or read-out error of the system.

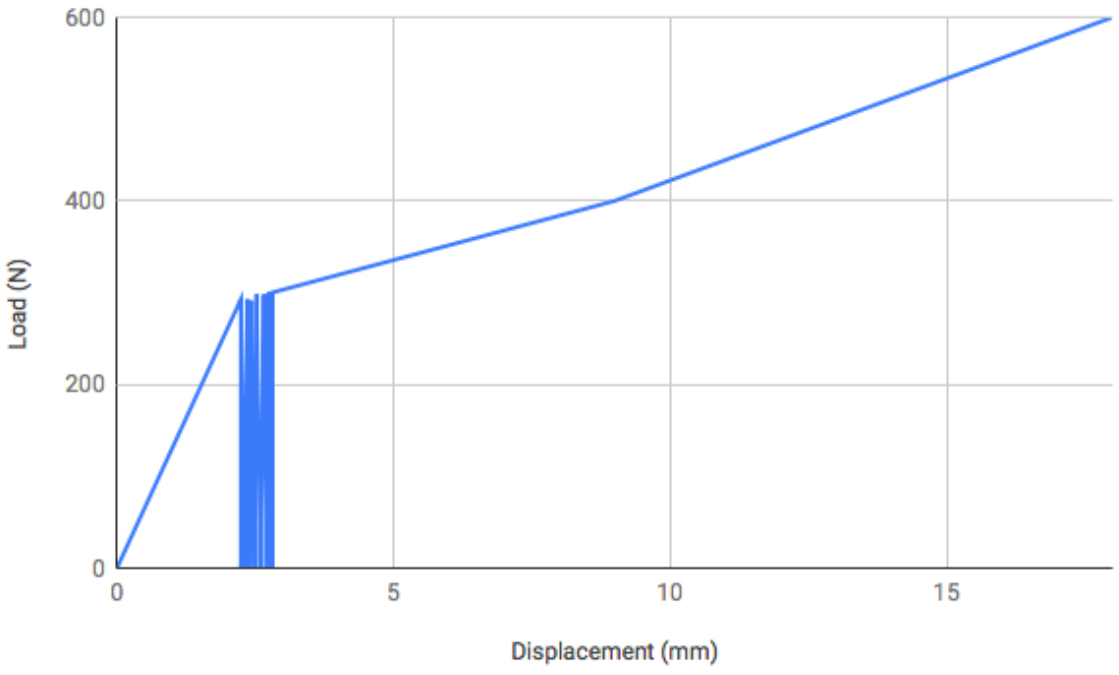

Figure 4.23. Segmental Pile with Post-Tension Force 750 N in Loose Soil.

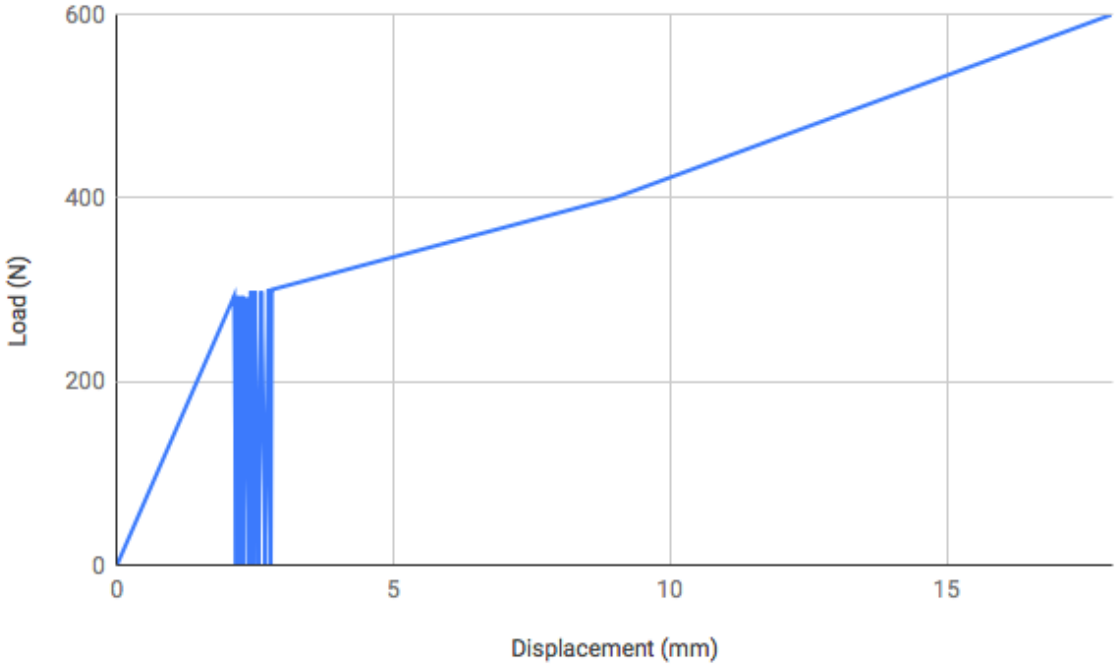

Figure 4.24. Segmental Pile with Post-Tension Force 750 N in Medium-Dense Soil.

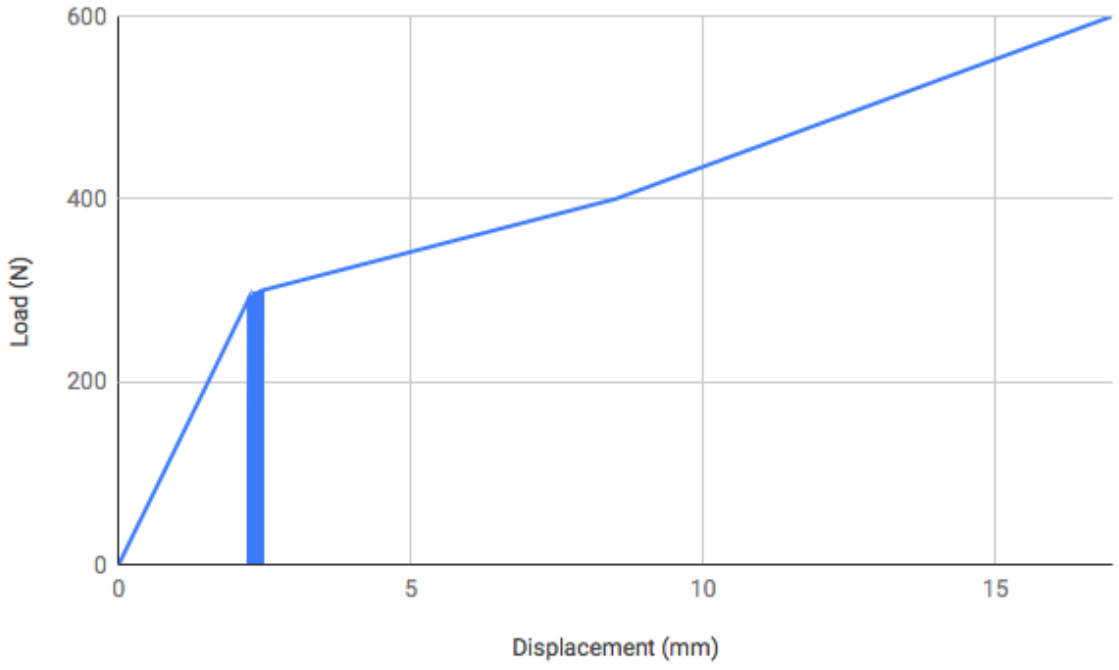

Figure 4.25. Segmental Pile with Post-Tension Force 750 N in Dense Soil.

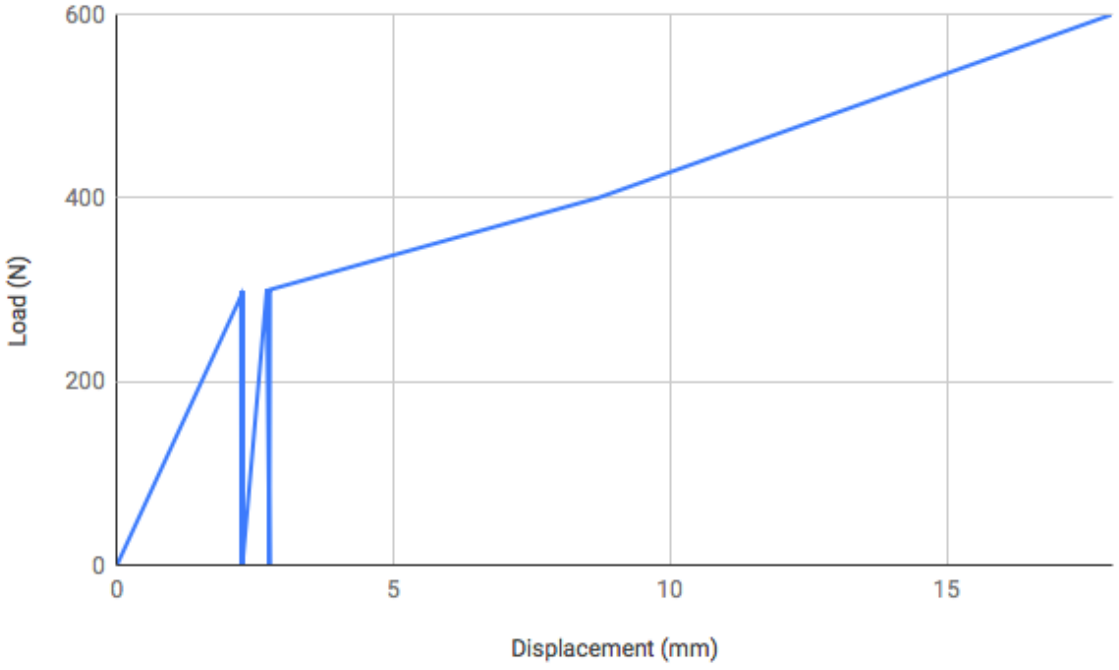

Figure 4.26. Segmental Pile with Post-Tension Force 1500 N in Loose Soil.

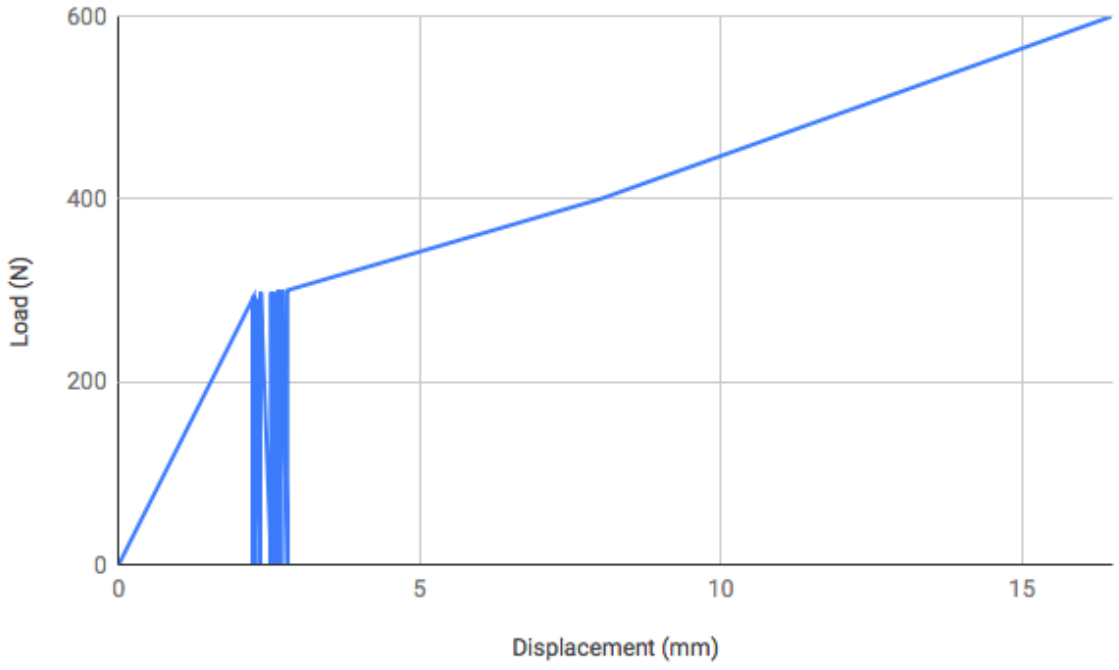

Figure 4.27. Segmental Pile with Post-Tension Force 1500 N in Medium-Dense Soil.

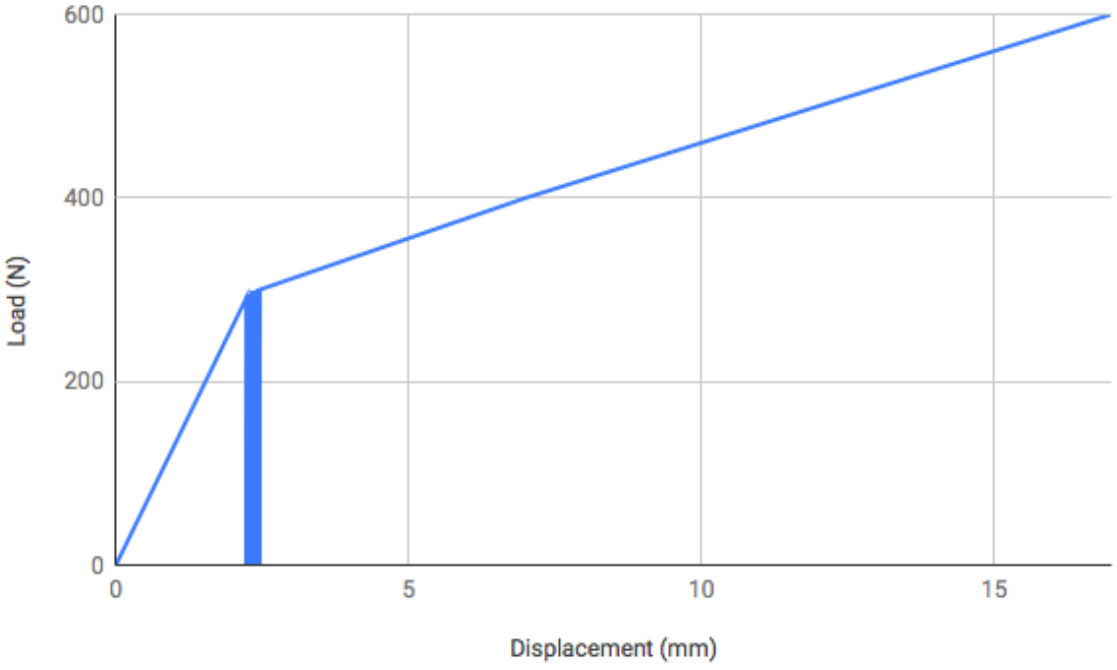

Figure 4.28. Segmental Pile with Post-Tension Force 1500 N in Dense Soil.

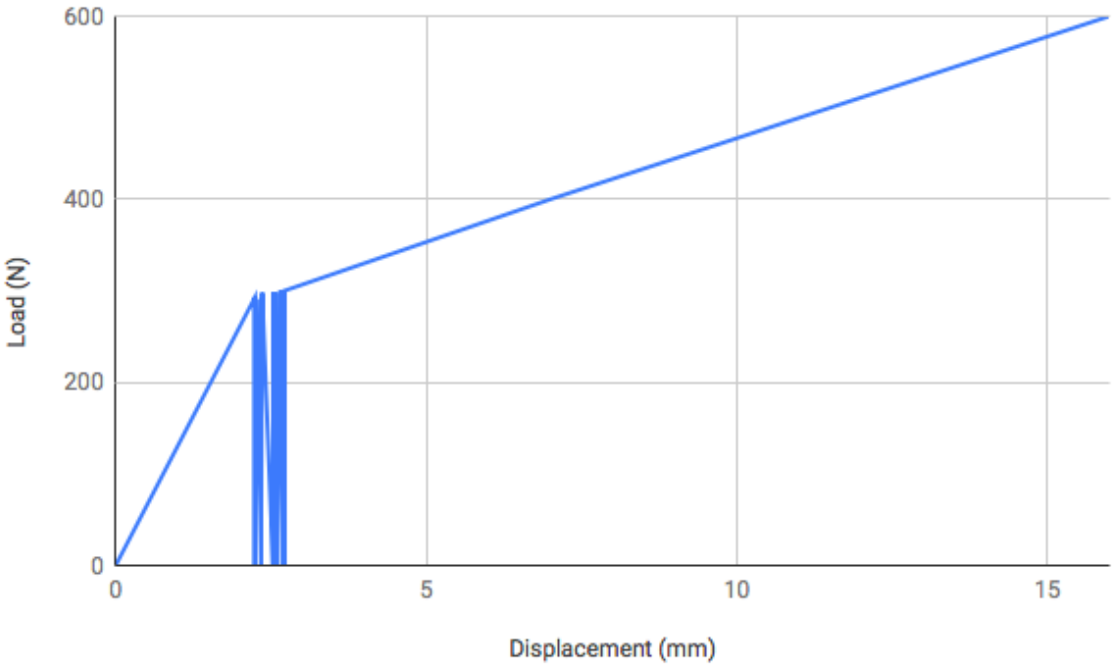

Figure 4.29. Segmental Pile with Post-Tension Force 2250 N in Loose Soil.

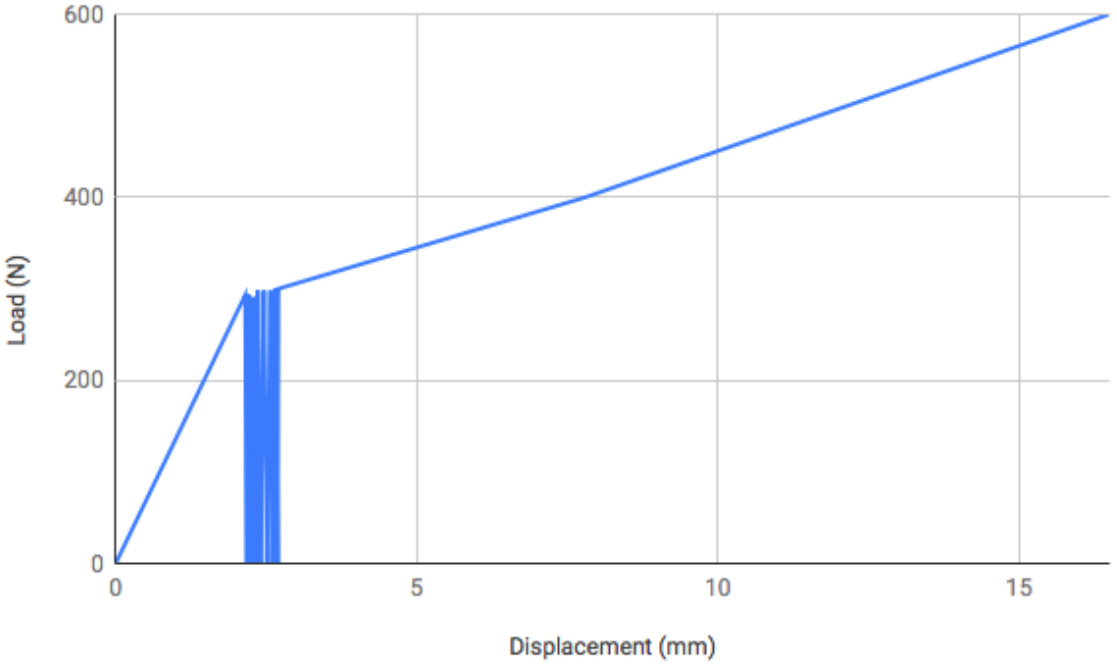

Figure 4.30. Segmental Pile with Post-Tension Force 2250 N in Medium-Dense Soil.

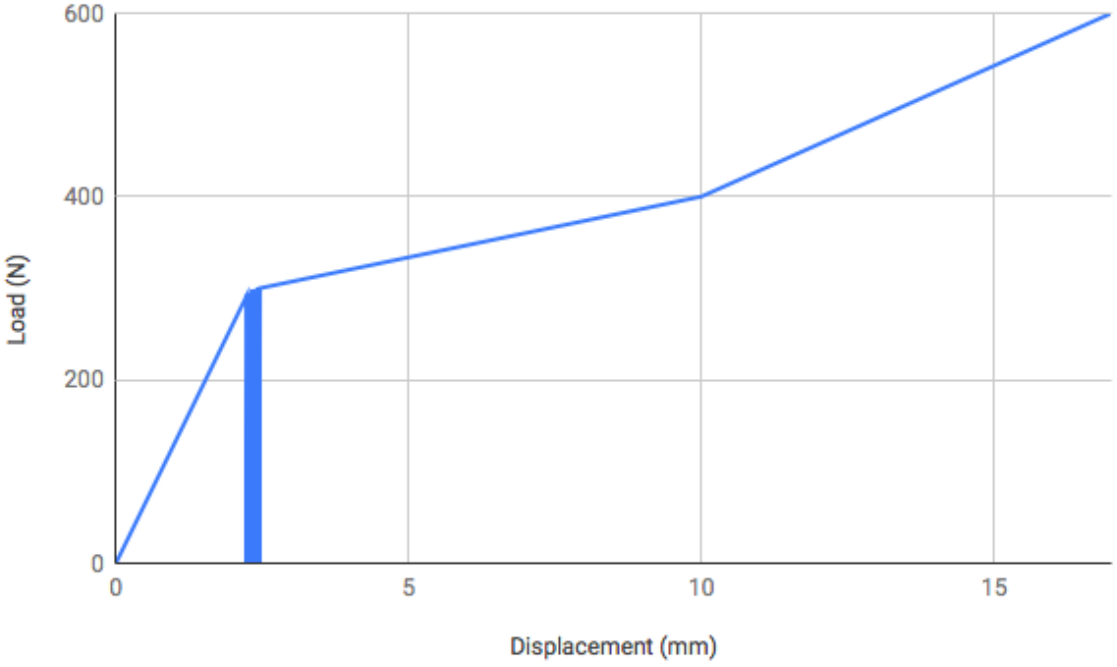

Figure 4.31. Segmental Pile with Post-Tension Force 2250 N in Dense Soil.

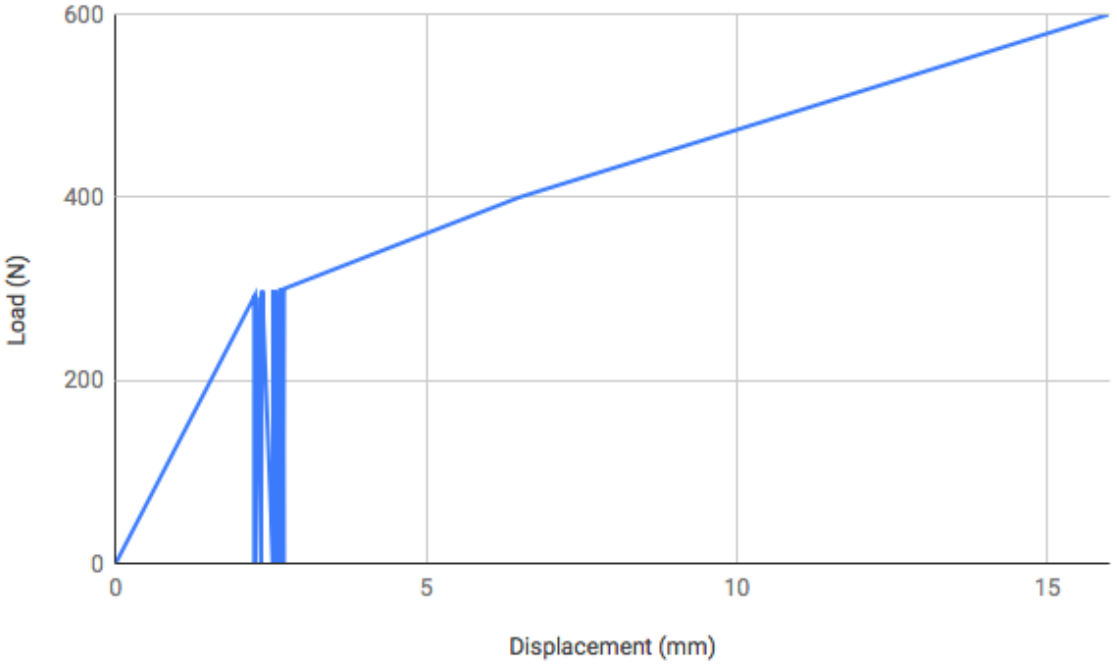

Figure 4.32. Mortar Beam in Loose Soil.

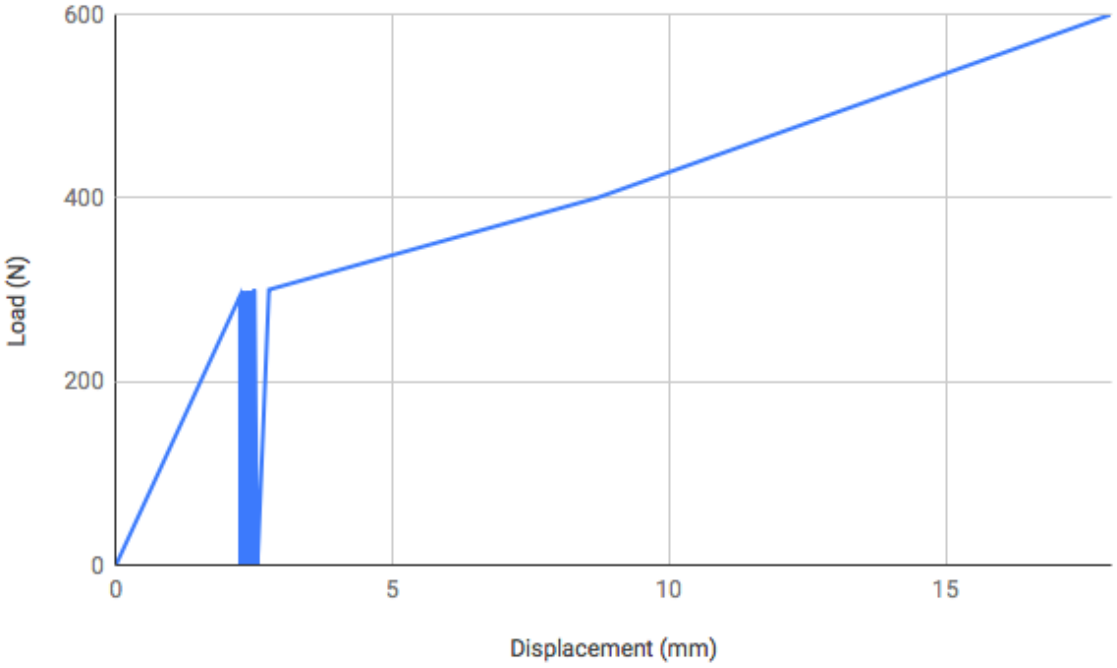

Figure 4.33. Mortar Beam in Medium-Dense Soil.

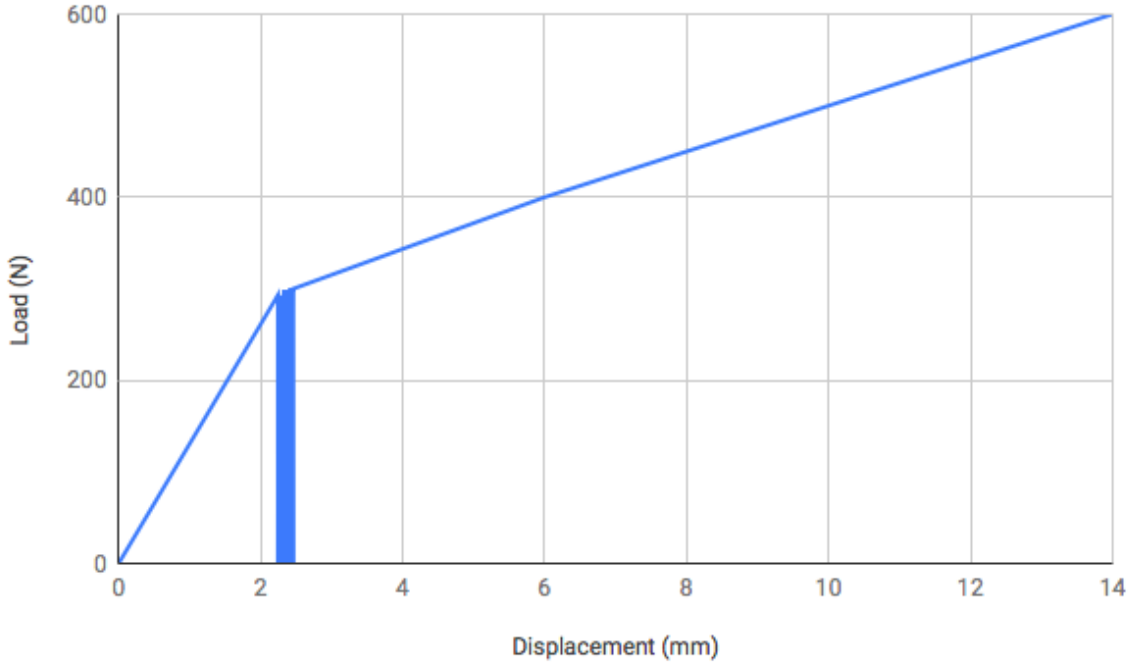

Figure 4.34. Mortar Beam in Dense Soil.

The lowest displacement values for cyclic loading are observed for the mortar beam. Values of segmental pile with post-tension force 2250 N are close to those of the mortar beam. Still, they are higher than the mortar beam values. With the first cycle all the pile heads relocate more than 2 mm. and after the loading procedure all of the displacement values of pile heads are between 2-3 mm.

4.2.4. The deflection of the Segmental Pile with Depth

It is assumed that before the loading is applied the vertical pile axis is on zero. After the loading top of the pile goes to positive direction and pile base goes to negative direction. This shows that piles act like a short pile and rotate with the loading. The displacement values are magnified in the graphics. Actually, when it is considered the largest displacement difference between the pile top and base is under 6 mm. The lines show that the displacements are not straight lines. Displacement values of the piles for different cyclic conditions are nearly the same but of course the values get higher when the number of cycles increases. Like the top point values above, the displacement values decrease when soil is denser for the same kind of pile. Also, the values decrease when the

pile is stiffer. Direction of the deflection line for 30 and 50 cycles are nearly the same and direction of the deflection line for 100 cycles is very close to them.

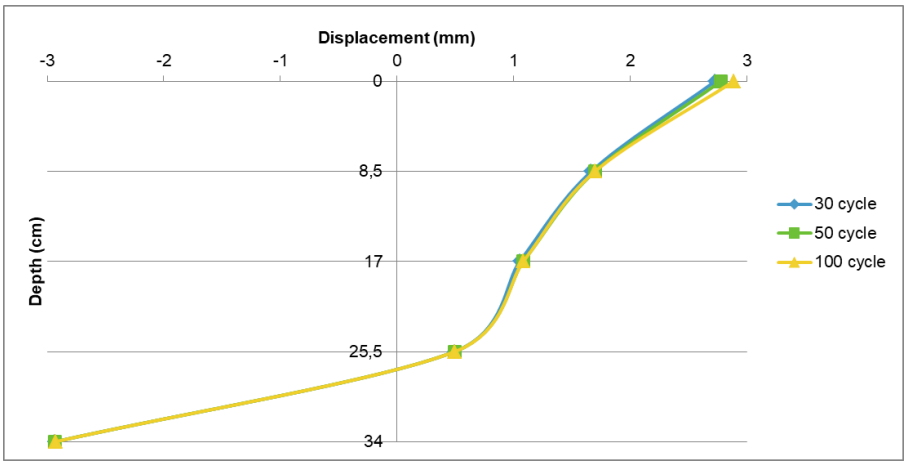

Figure 4.35. Displacement of the Segmental Pile with Post-Tension Force 750 N in Loose Soil.

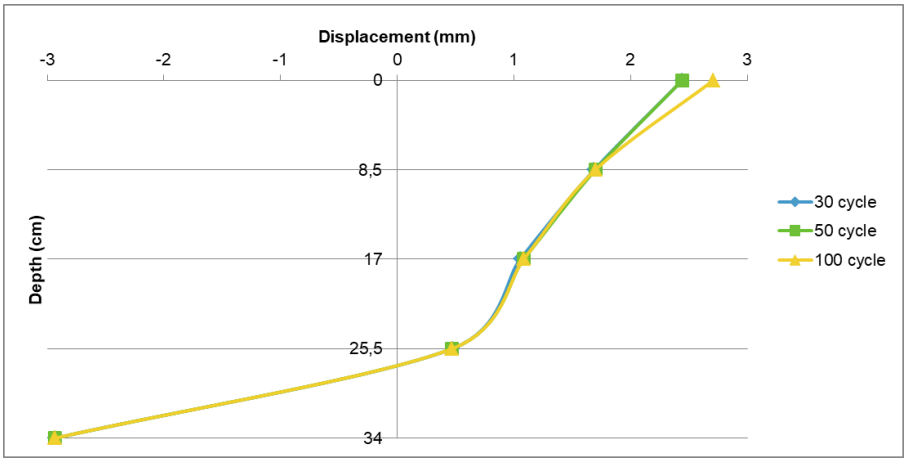

Figure 4.36. Displacement of the Segmental Pile with Post-Tension Force 750 N in Medium-Dense Soil.

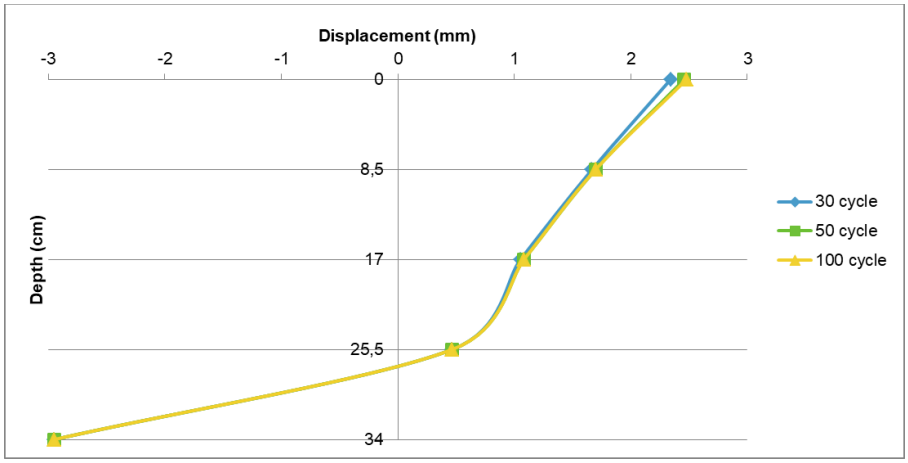

Figure 4.37: Displacement of the Segmental Pile with Post-Tension Force 750 N in Dense Soil.

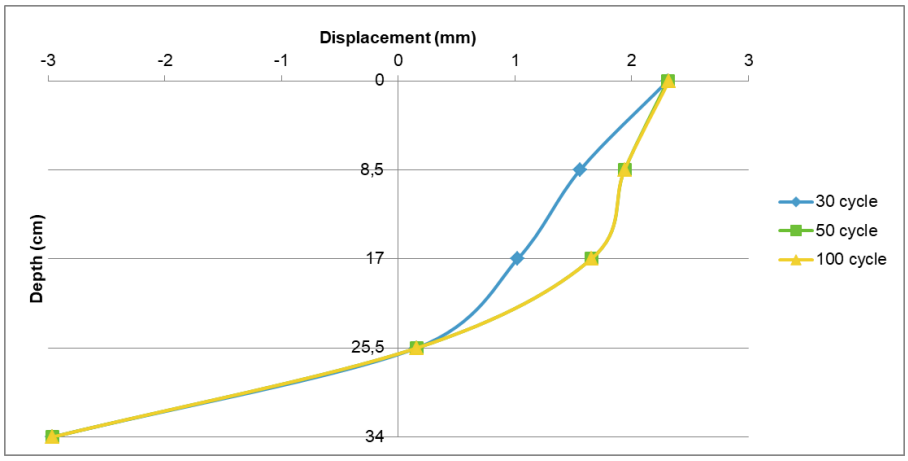

Figure 4.38. Displacement of the Segmental Pile with Post-Tension Force 1500 N in Loose Soil.

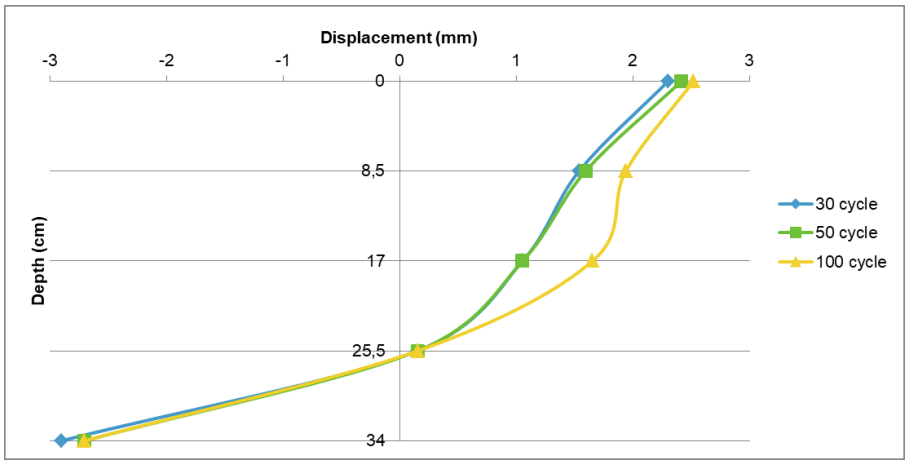

Figure 4.39: Displacement of the Segmental Pile with Post-Tension Force 1500 N in Medium-Dense Soil.

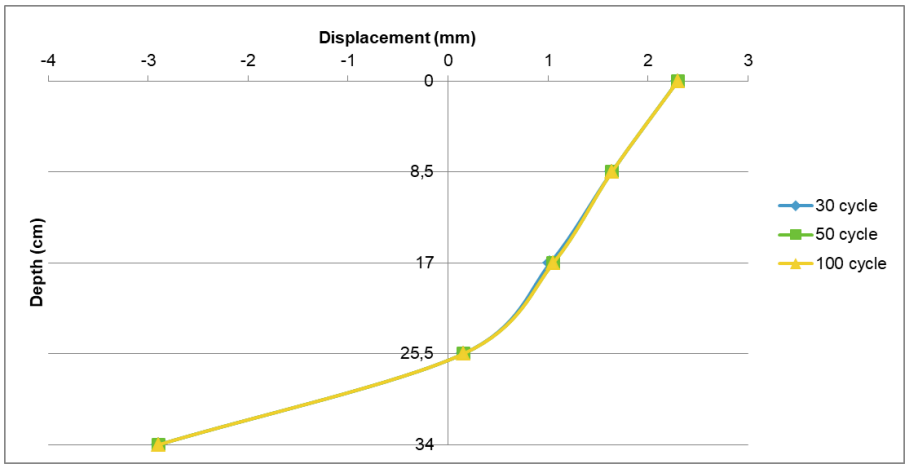

Figure 4.40. Displacement of the Segmental Pile with Post-Tension Force 1500 N in Dense Soil.

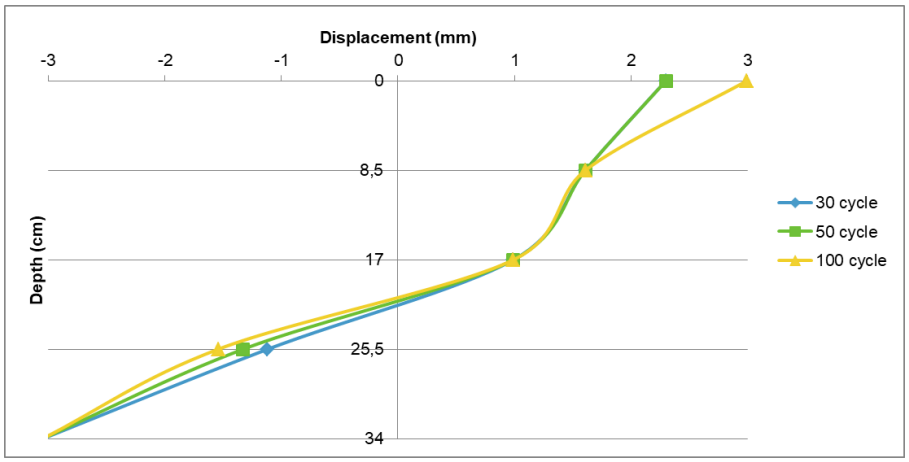

Figure 4.41. Displacement of the Segmental Pile with Post-Tension Force 2250 N in Loose Soil.

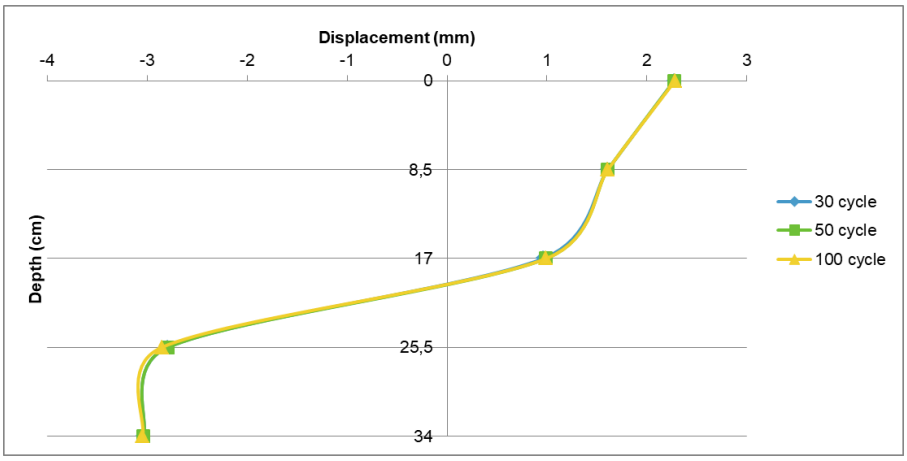

Figure 4.42. Displacement of the Segmental Pile with Post-Tension Force 2250 N in Medium-Dense Soil.

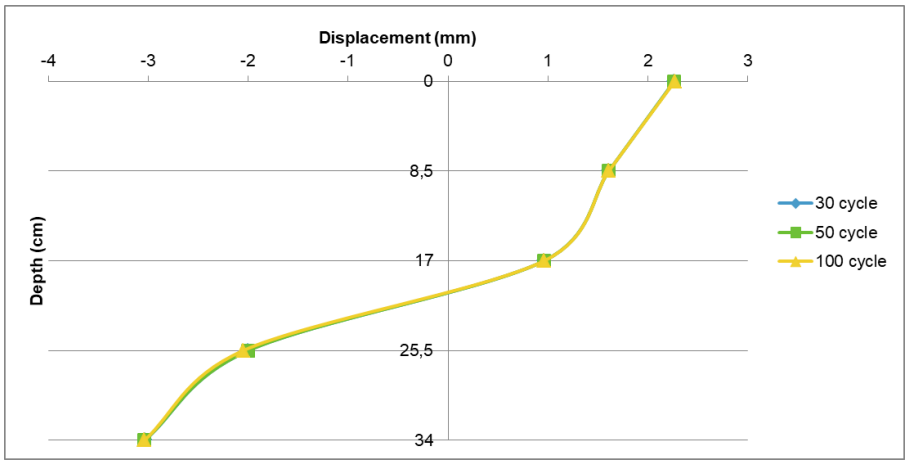

Figure 4.43. Displacement of the Segmental Pile with Post-Tension Force 2250 N in Dense Soil.

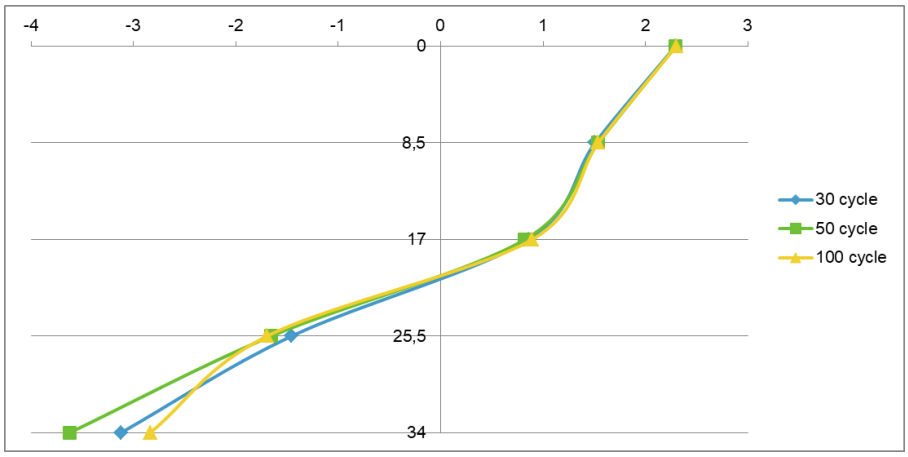

Figure 4.44. Displacement of the Mortar Beam in Loose Soil.

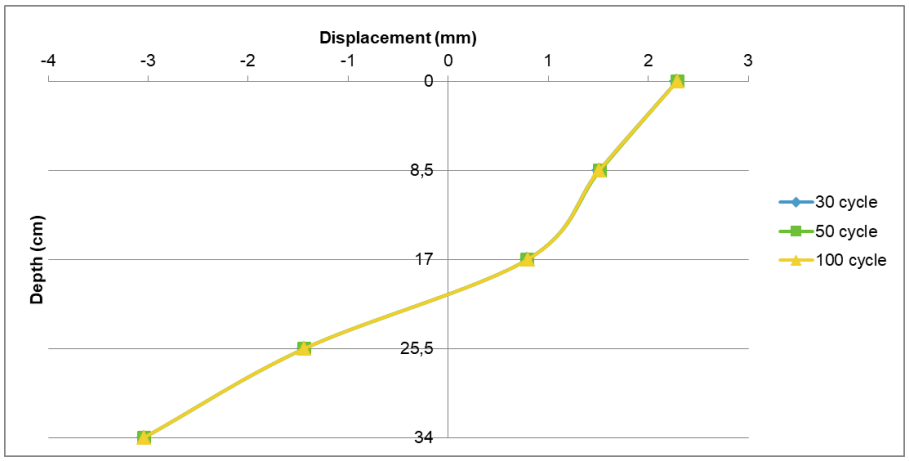

Figure 4.45. Displacement of the Mortar Beam in Medium-Dense Soil.

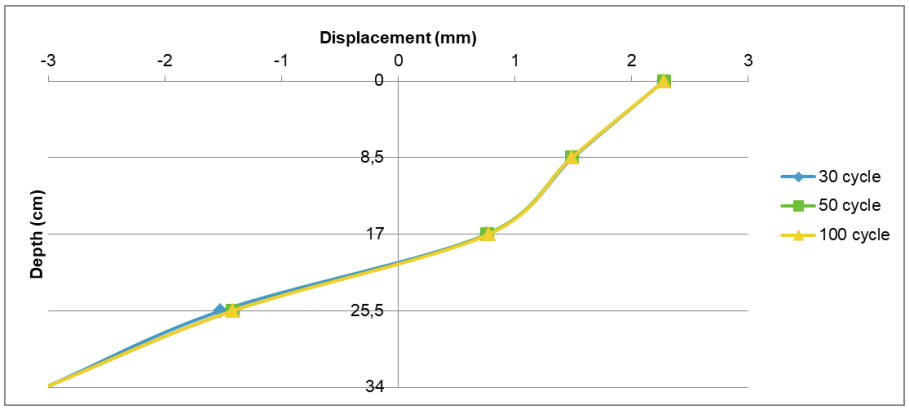

Figure 4.46. Displacement of the Mortar Beam in Dense Soil.

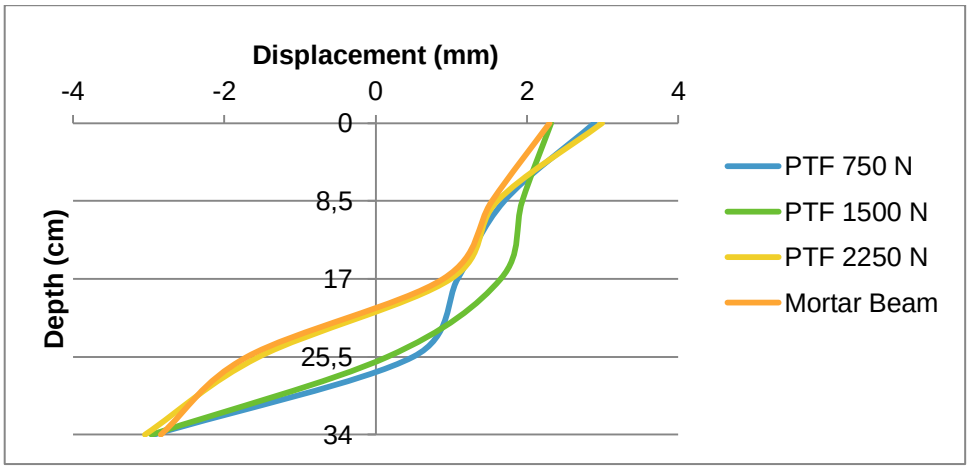

Figure 4.47. Displacement Values of the Piles in Loose Soil.

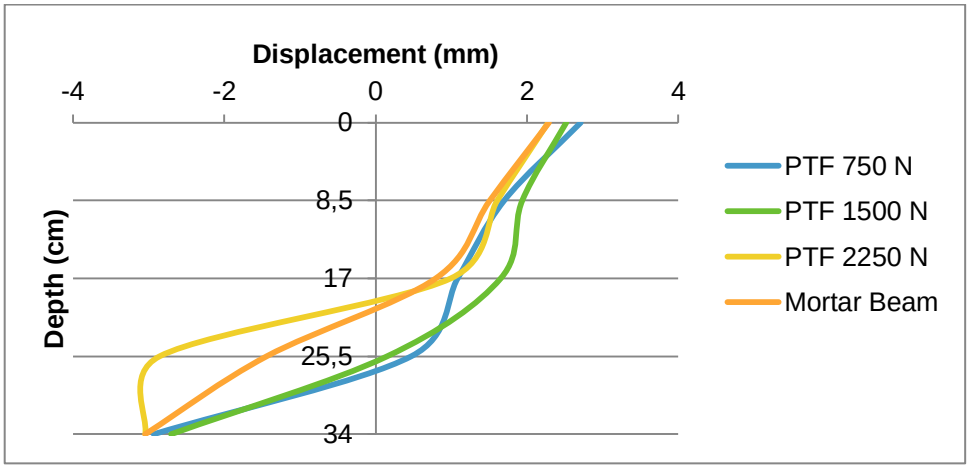

Figure 4.48. Displacement Values of the Piles in Medium-Dense Soil.

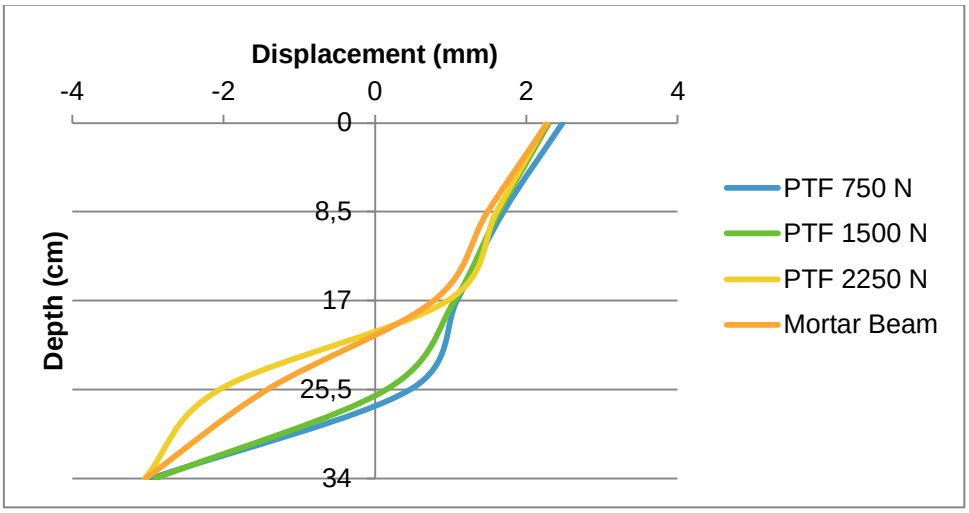

Figure 4.49. Displacement Values of the Piles in Dense Soil.

The pile with post tension force 750 N and 1500 N rotate at a depth under 25,5 cm but the mortar beam and the pile with post tension force 2250 N rotate at a depth under 17 cm.

A straight line is seen under 25,5 cm depth for the pile with post-tension force 750 N. After that inclination of the line changes and it approaches to vertical direction. Displacement lines goes in nearly the same direction for different cyclic cases, except 100 cycles in medium-dense soil. A deviation is shown there. The pile head deflects more than the other cycles after 100 cycles.

A straight line is seen under 25,5 cm depth for the pile with post-tension force 1500 N. After that the inclination of the line changes and it approaches to vertical direction. The reasons for that may be the same with pile with post-tension force 750 N. The striking part of this segmental pile is the difference between the displacement values for different cycles in loose and medium-dense soil. It starts with the change of inclination. Still, the displacements of the top points are close to each other but between points where the inclination change and pile top the lines goes with a different direction. Between these points pile deflects more for 100 cycles. However the increase in deflection at that points do not affect the pile head displacement. Reason for that may the soil reaction or pile

deformation after lots of cycles. On the other hand the displacement values for different cycles in dense soil are parallel to each other.

Pile with post tension force 2250 N acts different for various densities. In loose soil it is nearly a straight line. A little difference is seen for the top point after 100 cycles of loading. The striking part of this segmental pile is seen at 25,5 cm. depth in medium-dense soil. The displacement value at that depth is very close to the lowest measurement point unlike the other displacement values in different densities. In dense soil. The inclination of the lines for each soil type and number of cycles at mid-point is changes and gets closer to the vertical direction.

The direction of the mortar beam lines are nearly straight as expected. The inclination of lines change a little at 17 cm. depth but it is not that much. So that does not need to be taken into consideration. Maybe the screw inside of it to attach it to the device is affecting.

In Figure 4.40. displacement values of the different piles for 100 cycles in loose soil is shown. It is seen that the difference between the displacement values at the top and the tip is higher when the post tension force is lower. The lowest difference is seen for the mortar beam. Lines of the pile with post tension force 2250 N and mortar beam are nearly parallel to each other up to the depth at 8,5 cm. From that depth line of the pile with post tension force 2250 N changes. Its pile head deflects more.

In Figure 4.41. displacement values of the different piles for 100 cycles in medium-dense soil is shown. It is seen that all the piles displacement line inclination is different. But the displacement value at the pile base is nearly same for all off them. Lines of the pile with post tension force 750 N and pile with post tension force 1500 N are nearly parallel to each other up to the depth at 25,5 cm. Then their lines inclination are changed. Still their head displacement value is very close. . Lines of the pile with post tension force 2250 N and mortar beam start with a different inclination. However after the depth at 17 cm their lines are parallel to the each other up to pile head.

In Figure 4.42. displacement values of the different piles for 100 cycles in dense soil is shown. It is seen that the displacement value at the pile base is nearly same for all off

the piles. After the depth at 17 cm inclination of all lines is parallel. Up to this point from the pile base lines of the pile with post tension force 750 N and pile with post tension force 1500 N are nearly parallel to each other. Also up to this point from the pile base lines of the pile with post tension force 2250 and the mortar beam are nearly parallel to each other.

4.2.5. The Shear Force of the Segmental Pile

Shear force values of the segmental pile is shown below. Shear values are obtained from the Load-Deflection/Interface Relationship for Rubber Shore 60 tests and displacement results.[2] The Figures below are drawn relatively for each block used the values in referenced paper. Calculated shear force values just about to coincide with the applied force. (This shear calculation method is also used in related reference and results are paralel to each other.)

For this calculations the stress affecting each pile is found. 300-600-900 kPa are the normal stress values applied to each block of the segmental piles. Then displacement of the each block is found from the graphics above. Difference between the displacement values are calculated. From the referenced paper the force value corresponding to that displacement difference value under same normal stress is read and accepted as the shear force value at that point. Shear forces of the blocks are found based on displacement difference from the previous block. So, the shear force value is calculated cumulatively. The place of the base point is accepted as zero and from the displacement of the upper blocks the shear force increases and reaches the applied force. The applied force in this tests is equal to 300 N. and the values of the calculated forces are very close to that value. Except the one result, the range of the calculated shear force values are between 290-313 N. The calculated values at top where the force applied are shown in part 5.

A flowchart is made for explaining the calculations of the shear force. It is shown in Figure 4.50. It shows all the calculation steps clearly. Each part of the calculation is defined in that flowchart.

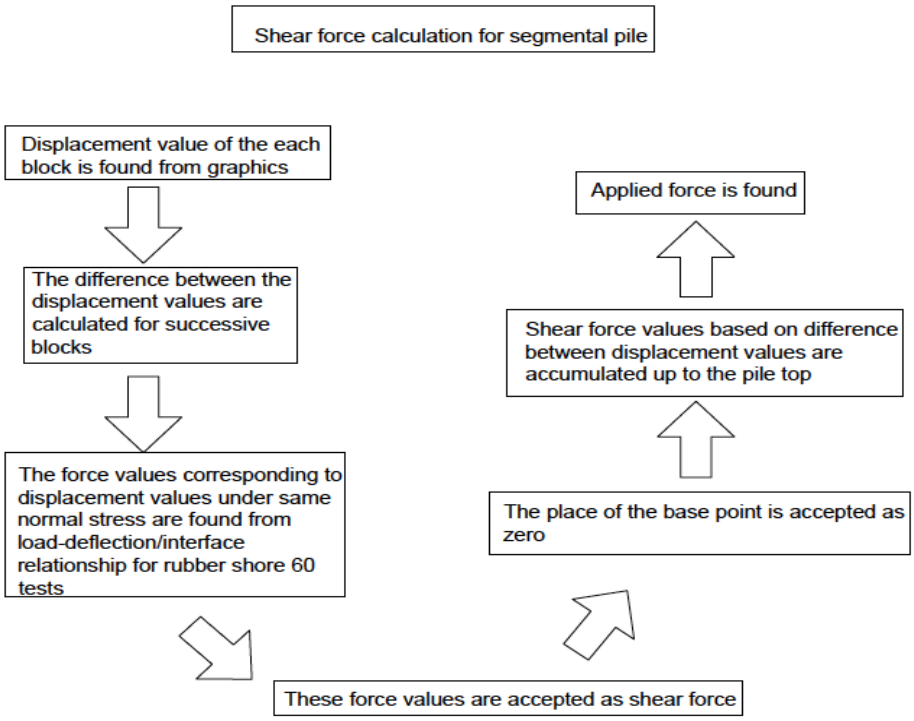

4.50. Flowchart of the Shear Force Calculation.

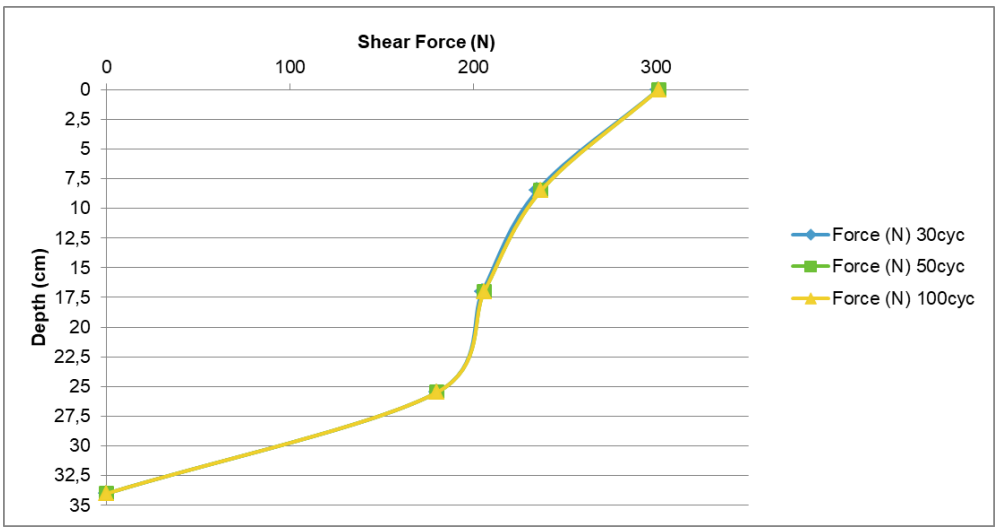

Figure 4.51. Shear of the Segmental Pile with Post-Tension Force 750 N in Loose Soil.

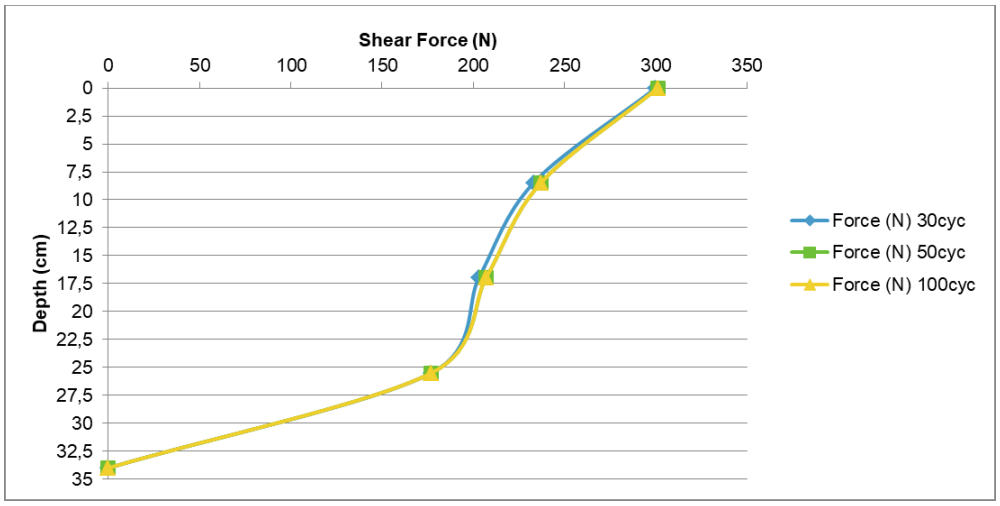

Figure 4.52. Shear of the Segmental Pile with Post-Tension Force 750 N in Medium-Dense Soil.

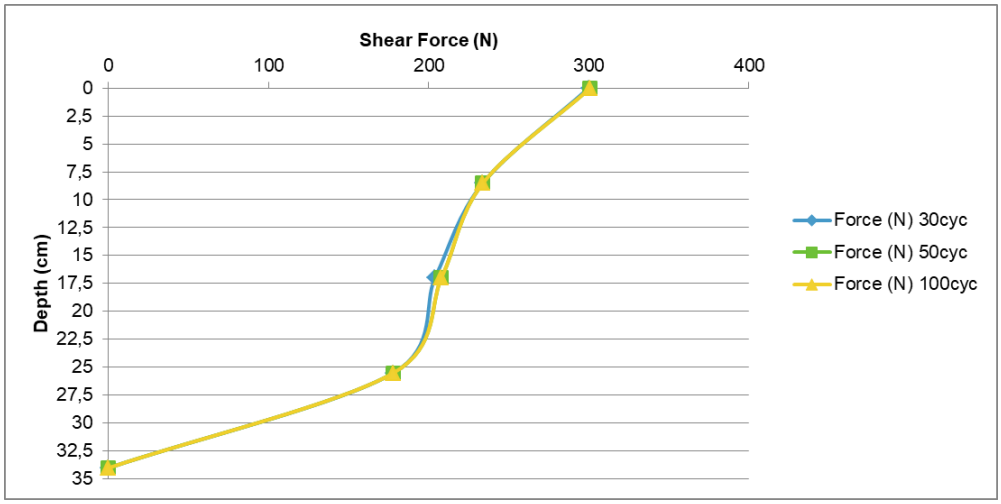

Figure 4.53. Shear of the Segmental Pile with Post-Tension Force 750 N in Dense Soil.

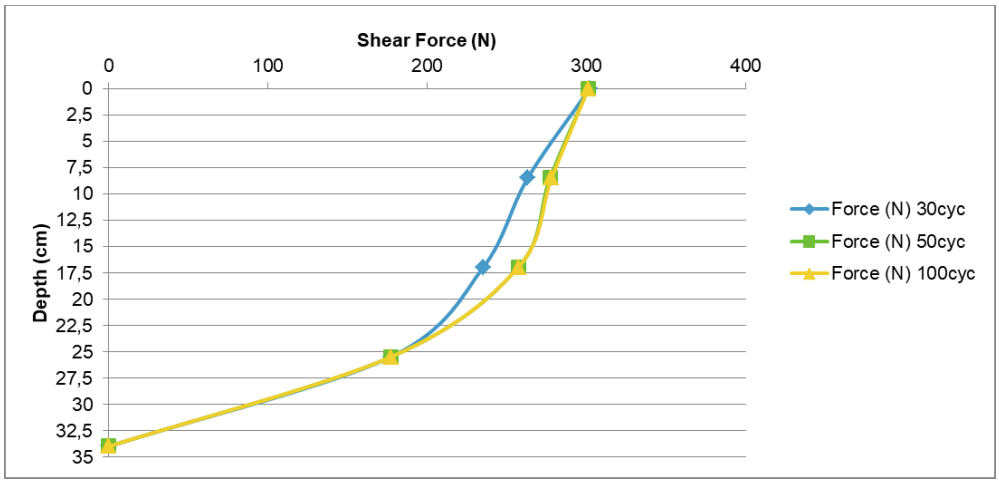

Figure 4.54. Shear of the Segmental Pile with Post-Tension Force 1500 N in Loose Soil.

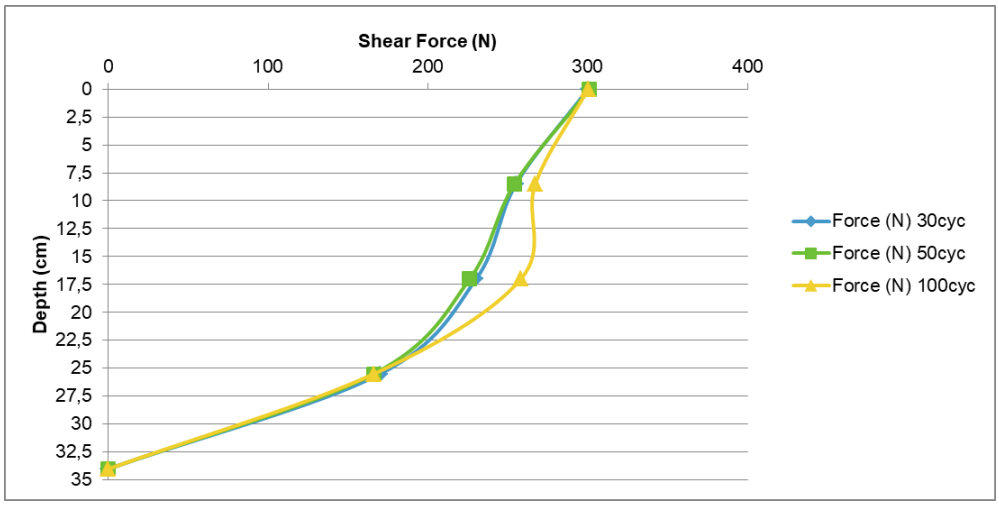

Figure 4.55. Shear of the Segmental Pile with Post-Tension Force 1500 N in Medium-Dense Soil.

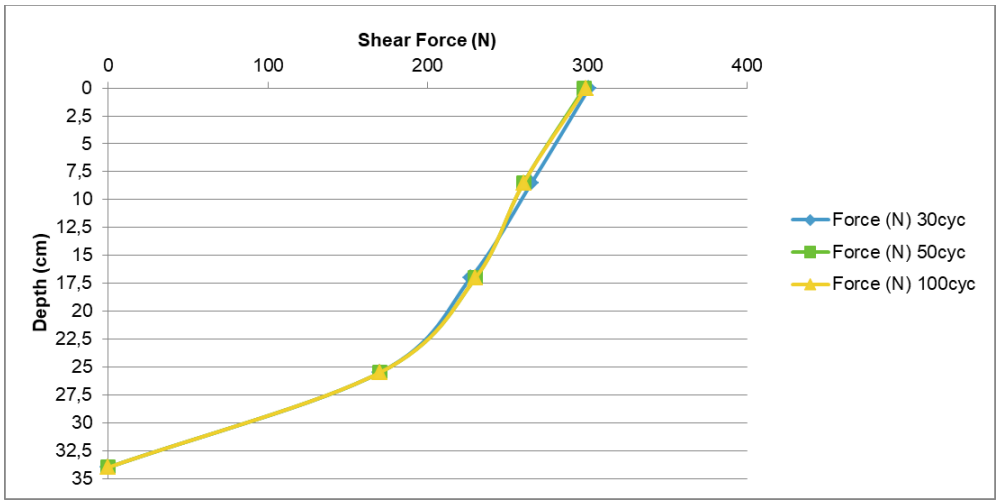

Figure 4.56. Shear of the Segmental Pile with Post-Tension Force 1500 N in Dense Soil.

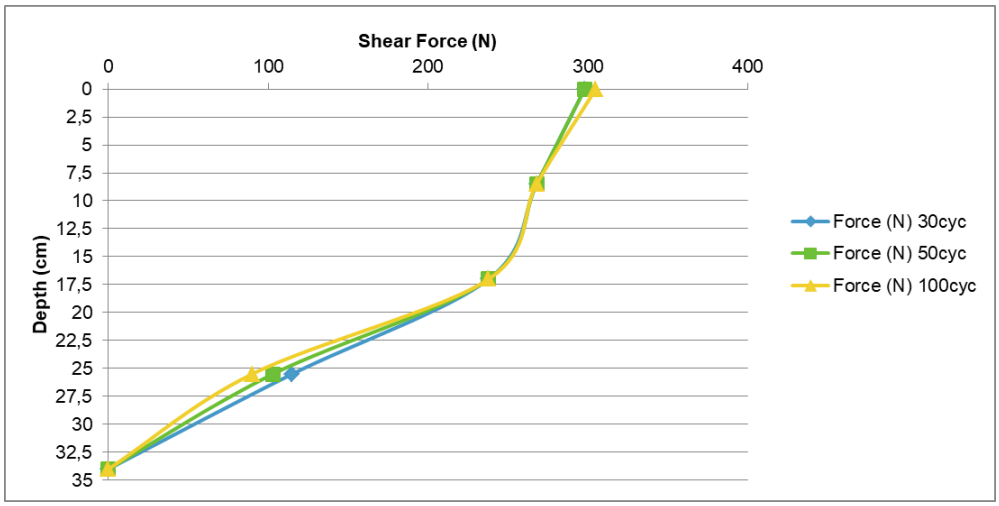

Figure 4.57. Shear of the Segmental Pile with Post-Tension Force 2250 N in Loose Soil.

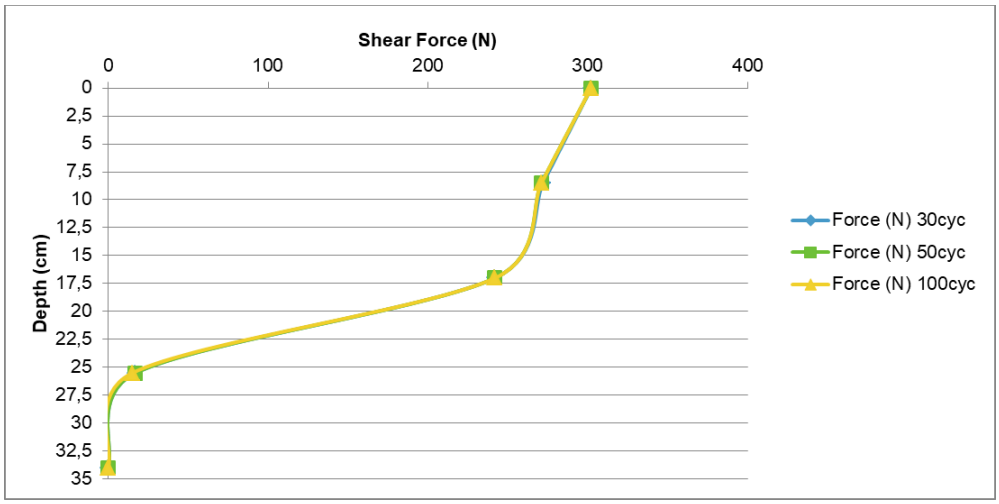

Figure 4.58. Shear of the Segmental Pile with Post-Tension Force 2250 N in Medium-Dense Soil.

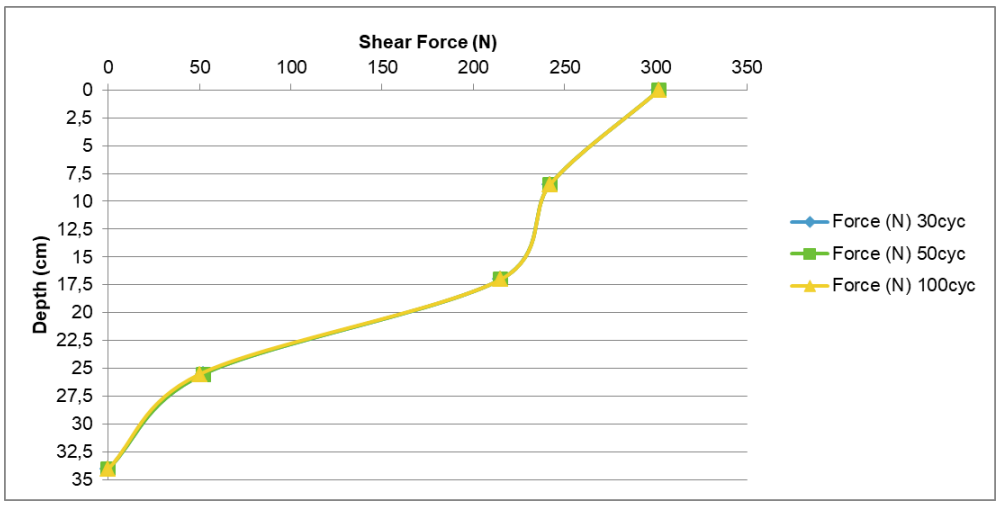

Figure 4.59. Shear of the Segmental Pile with Post-Tension Force 2250 N in Dense Soil.

In the Figures it is seen that the shear force lines are parallel to the displacement lines. Because the calculation method is based on displacement.

On the other hand shear values of the mortar beam is also calculated from the displacement values with beam formulas. This formulas are suitable for the entire beam.

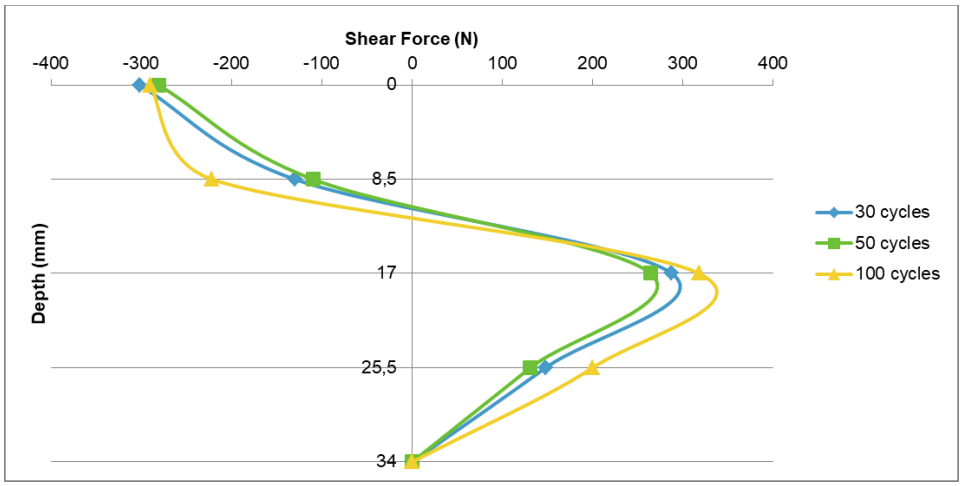

Figure 4.60. Shear of the Mortar Beam in Loose Soil.

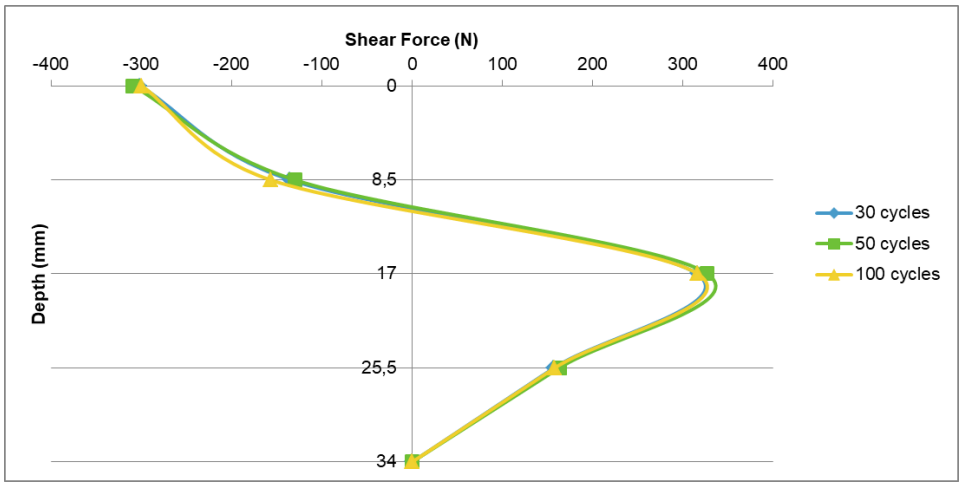

Figure 4.61. Shear of the Mortar Beam in Medium-Dense Soil

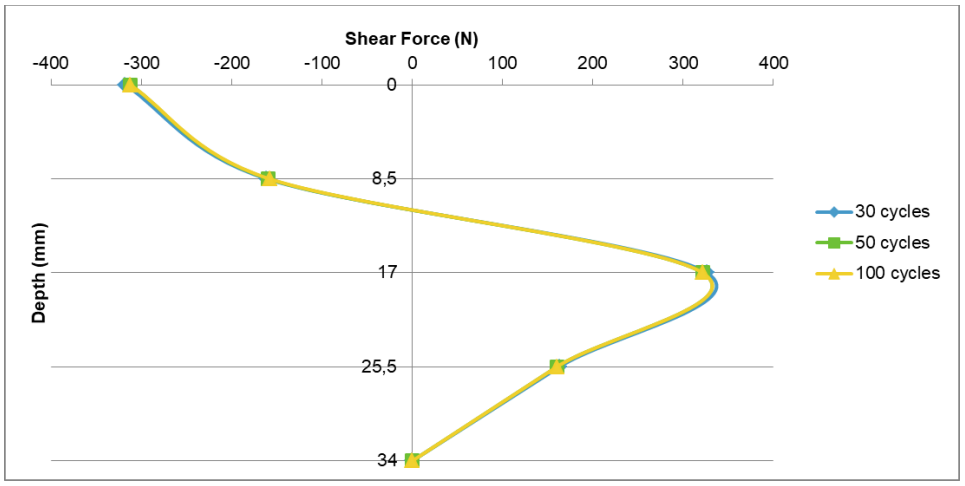

Figure 4.62. Shear of the Mortar Beam in Dense Soil.

Shear values reach 300 N at the top point which is the applied force to the pile from the top. The applied force value and the shear force value fit each other. Then it approaches to zero because of the loads coming from the soil. At the pile base shear force is equal to zero.

4.2.6. Moment Calculation

Moment values for segmental pile are calculated from the shear results which are calculated from the Load-Deflection/Interface Relationship for Rubber Shore 60 tests and displacement results. After the shear force calculation, results are plotted versus depth and for the moment values, area of the shear force graphics are calculated. The values are found as it is expected for the piles fixed at the top-free at the base and loaded at the pile top. The moment is equal to zero at the base point and it increases up to pile head.

On the other hand moment values of the mortar beam is also calculated from the displacement values with beam formulas. This formulas are applicable for continuous beam.

.

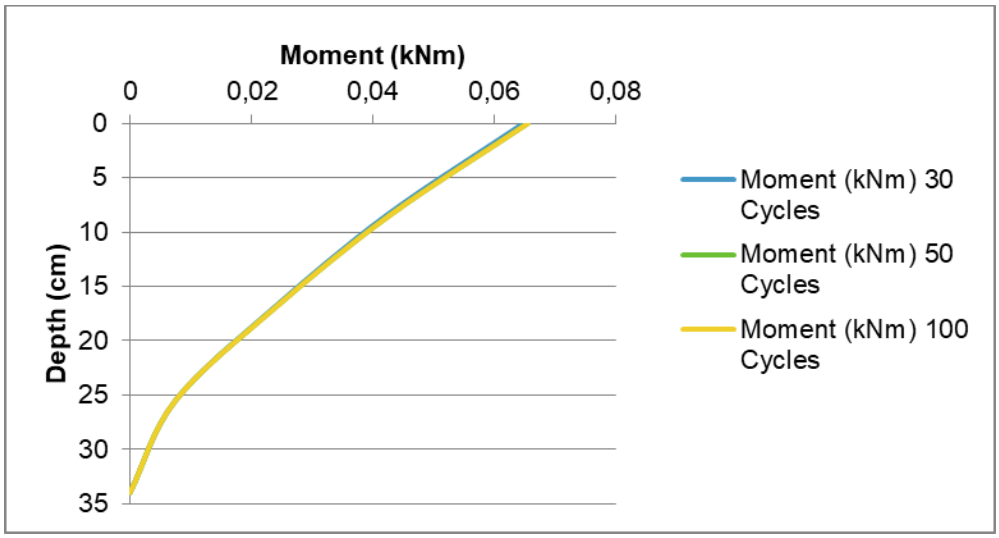

Figure 4.63. Moment of the Segmental Pile with Post-Tension Force 750 N in Loose Soil.

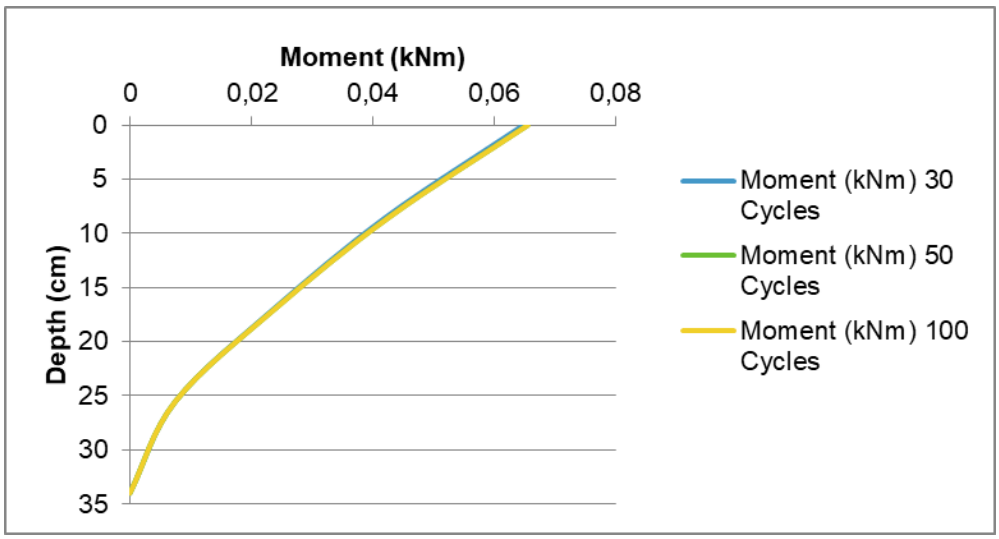

Figure 4.64. Moment of the Segmental Pile with Post-Tension Force 750 N in Medium - Dense Soil.

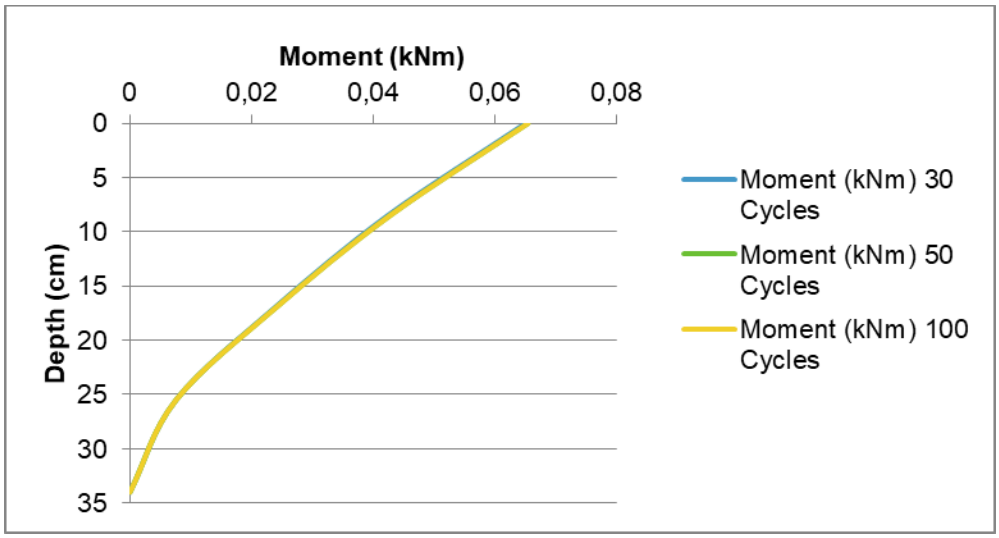

Figure 4.65. Moment of the Segmental Pile with Post-Tension Force 750 N in Dense Soil.

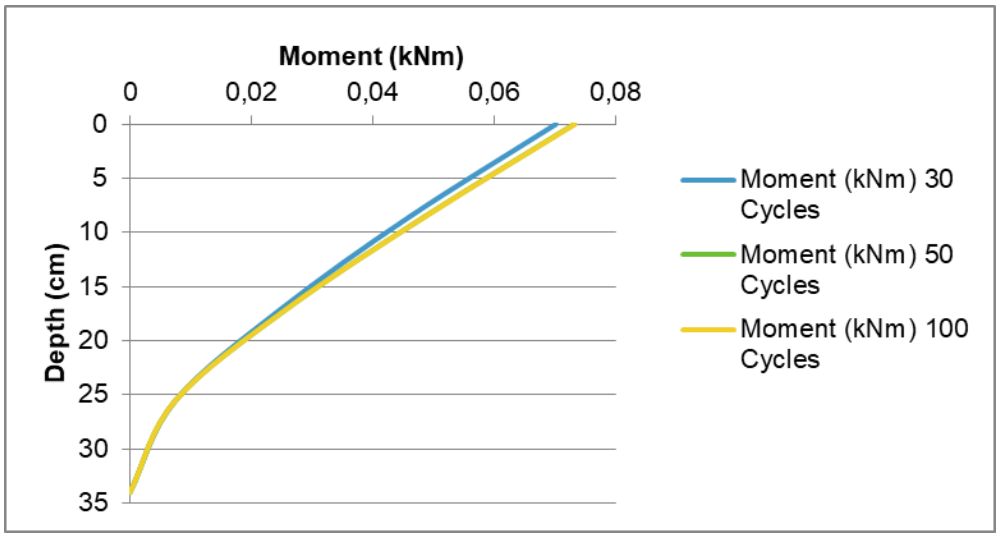

Figure 4.66. Moment of the Segmental Pile with Post-Tension Force 1500 N in Loose Soil.

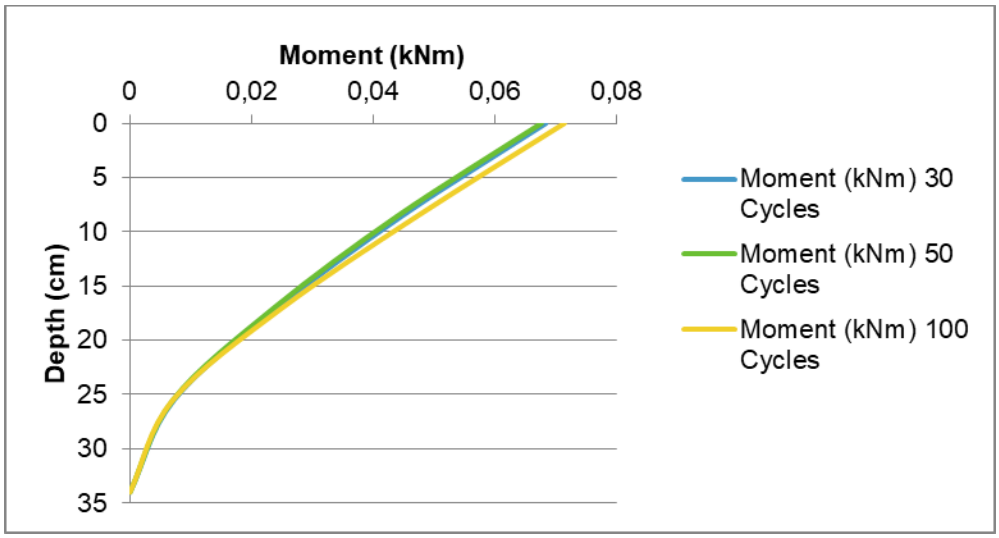

Figure 4.67. Moment of the Segmental Pile with Post-Tension Force 1500 N in Medium - Dense Soil.

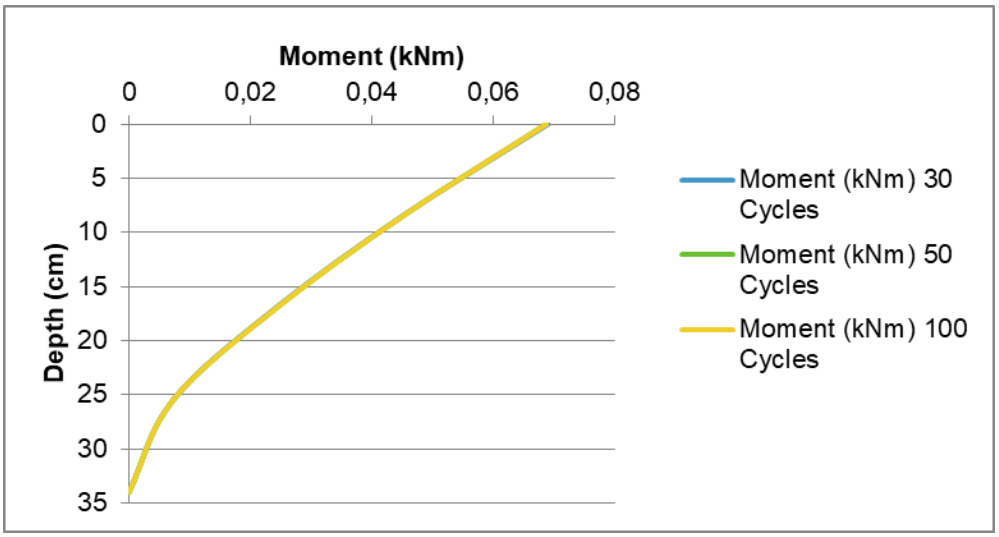

Figure 4.68. Moment of the Segmental Pile with Post-Tension Force 1500 N in Dense Soil.

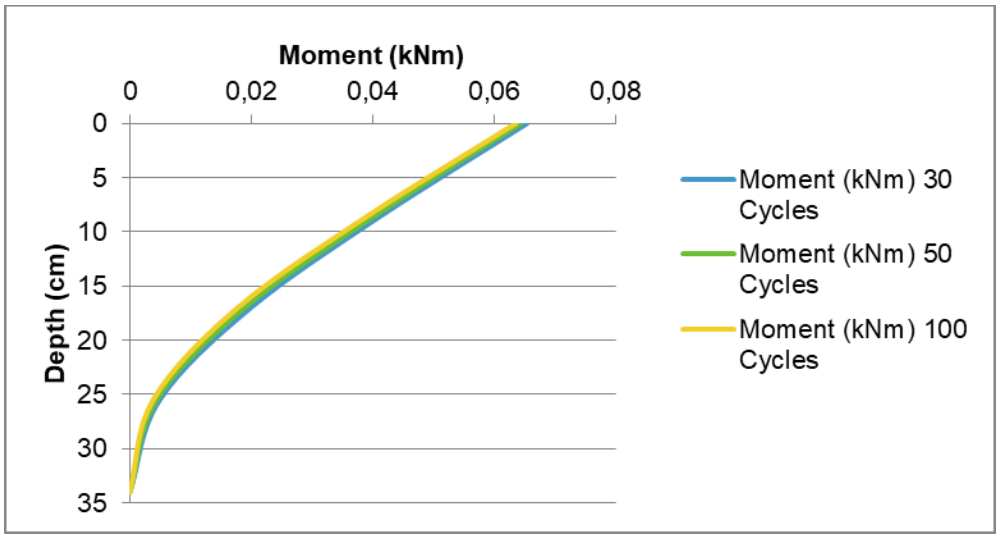

Figure 4.69. Moment of the Segmental Pile with Post-Tension Force 2250 N in Loose Soil.

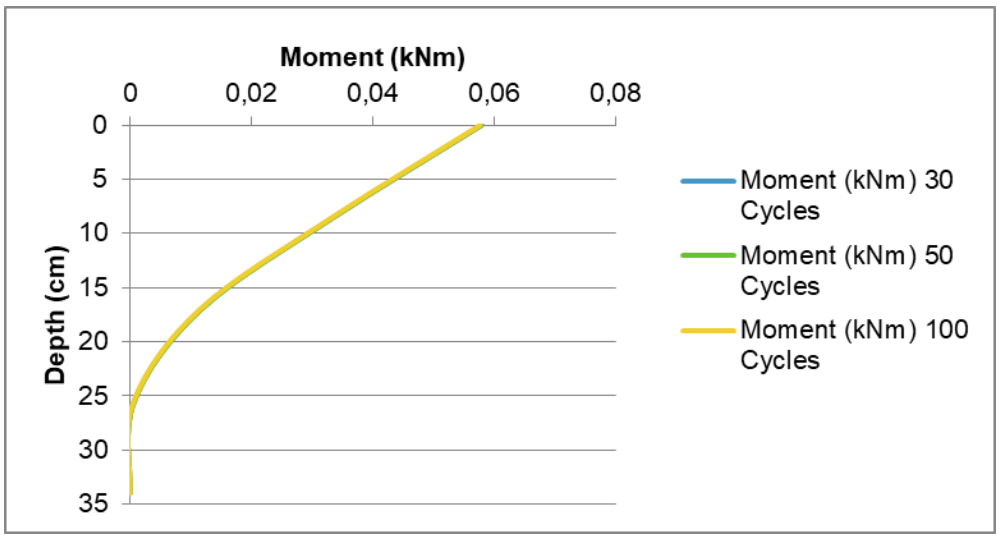

Figure 4.70. Moment of the Segmental Pile with Post-Tension Force 2250 N in Medium - Dense Soil

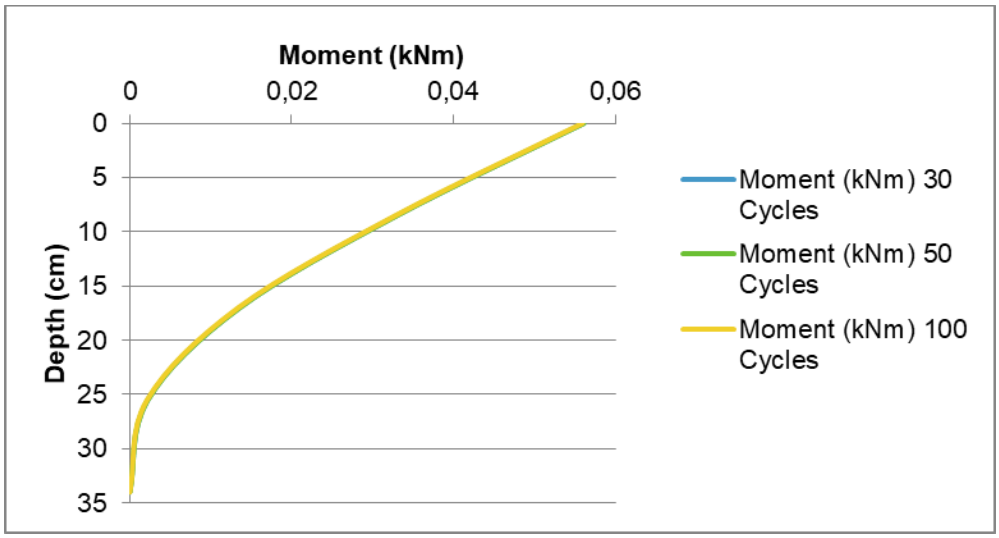

Figure 4.71. Moment of the Segmental Pile with Post-Tension Force 2250 N in Dense Soil.

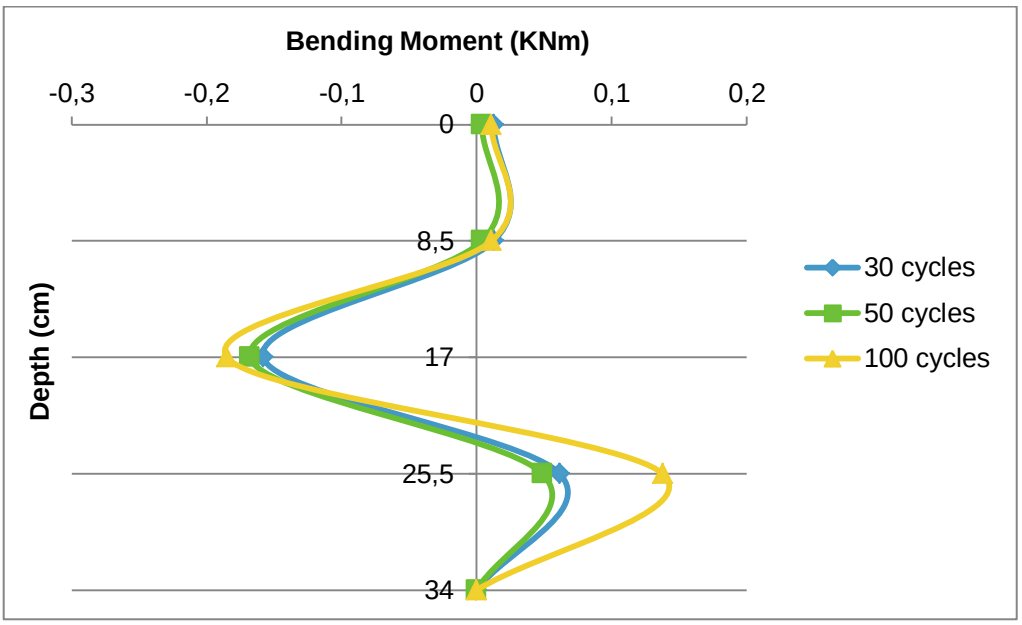

Figure 4.72. Moment of the Mortar Beam in Loose Soil.

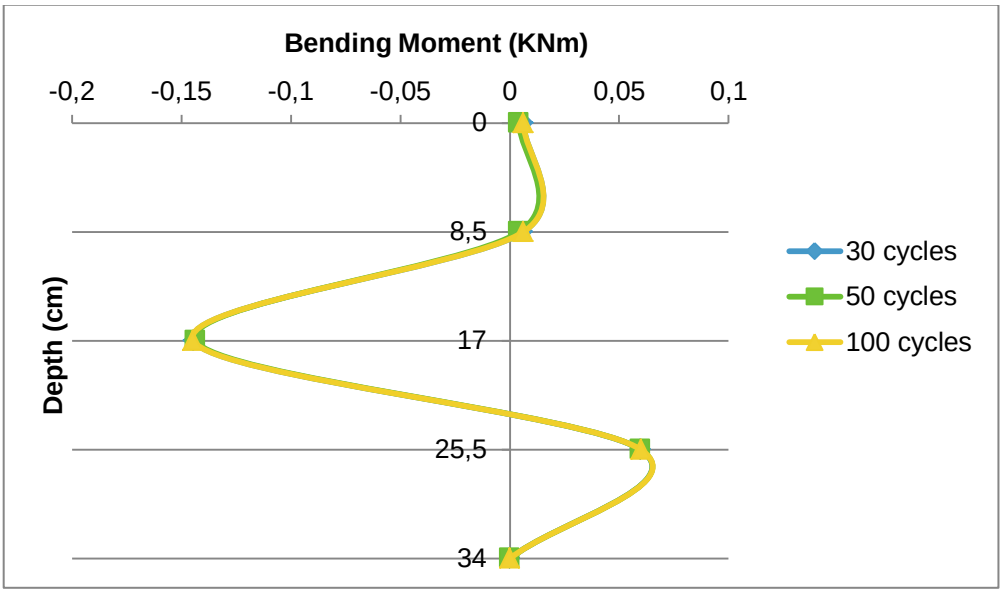

Figure 4.73. Moment of the Mortar Beam in Medium-Dense Soil.

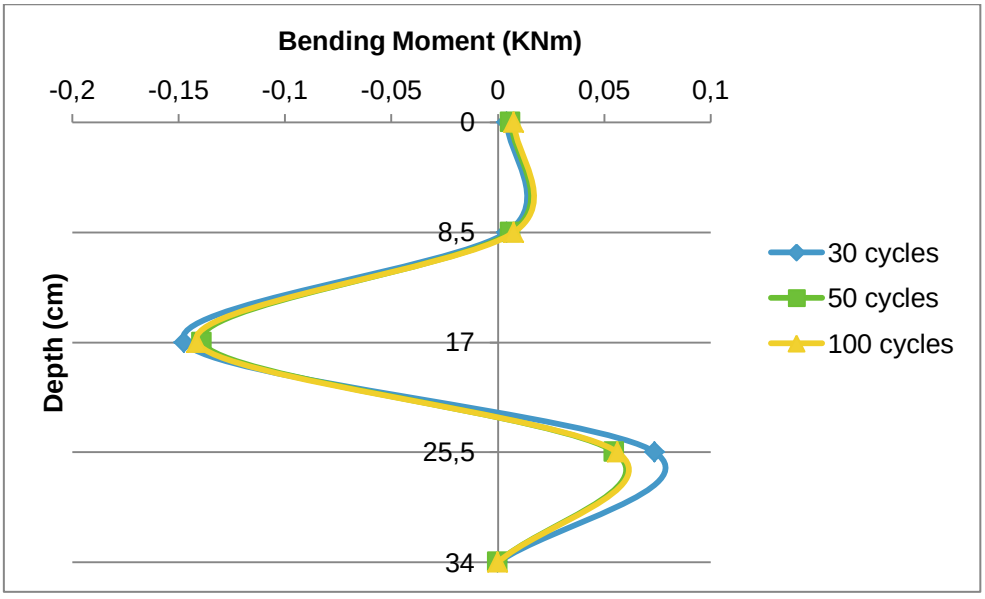

Figure 4.74. Moment of the Mortar Beam in Dense Soil.

Moment value for the segmental pile with post-tension force 750 N at the top point is higher than 0,06 KNm for each density. Values for different densities are very close to each other.

Moment value for the segmental pile with post-tension force 1500 N in loose state is close to 0,08 KNm at the top point. However the moment value at the pile head decreases when the soil is denser.

Moment value for the segmental pile with post-tension force 2250 N at pile head is higher than 0,06 KNm, but the values decrease under 0,06 KNm when the soil is denser. In the medium-dense state moment values are very close to zero under the depth at 25,5 cm. The reason for that is the displacement values of the segmental pile. A different direction is seen under that depth.

Moment values at the base for all pile types are equal to zero. Because base of the pile is free.

Mortar beam moment line directions are very close to each other. Because the displacement values are close. The moment lines are found as expected for the mortar beam.

5. TEST RESULTS EVALUATION

5.1. The Displacement-Soil Density Relationship of the Segmental Pile

The tables of displacement under various cyclic loads versus depth are shown below.

Table 5.1. Displacement of the Pile Model with Post-Tension Force of 750 N in Soil with Various Densities.

Depth (cm)	30 Cycles/Loose (mm)	50 Cycles/Loose (mm)	100 Cycles/Loose (mm)	30 Cycles/Medium-Dense (mm)	50 Cycles/Medium-Dense (mm)	100 Cycles/Medium-Dense (mm)	30 Cycles/Dense (mm)	50 Cycles/Dense (mm)	100 Cycles/Dense (mm)
0	2,73	2,78	2,89	2,44	2,44	2,71	2,34	2,46	2,48
8,5	1,66	1,69	1,69	1,68	1,69	1,69	1,66	1,69	1,69
17	1,05	1,08	1,08	1,05	1,08	1,08	1,05	1,08	1,08
25,5	0,49	0,49	0,49	0,47	0,47	0,47	0,46	0,46	0,46
34	-2,93	-2,93	-2,93	-2,93	-2,93	-2,93	-2,94	-2,94	-2,94

Table 5.2. Displacement of the Pile Model with Post-Tension Force of 1500 N in Soil with Various Densities.

Depth (cm)	30 Cycles/Loose (mm)	50 Cycles/Loose (mm)	100 Cycles/Loose (mm)	30 Cycles/Medium-Dense (mm)	50 Cycles/Medium-Dense (mm)	100 Cycles/Medium-Dense (mm)	30 Cycles/Dense (mm)	50 Cycles/Dense (mm)	100 Cycles/Dense (mm)
0	2,30	2,30	2,31	2,30	2,41	2,51	2,29	2,29	2,29
8,5	1,55	1,93	1,93	1,53	1,59	1,93	1,63	1,63	1,63
17	1,02	1,65	1,65	1,05	1,05	1,65	1,02	1,05	1,05
25,5	0,15	0,15	0,15	0,15	0,15	0,15	0,15	0,15	0,15
34	-2,96	-2,96	-2,96	-2,90	-2,70	-2,70	-2,89	-2,89	-2,89

Table 5.3. Displacement of the Pile Model with Post-Tension Force of 2250 N in Soil with Various Densities.

Depth (cm)	30 Cycles/Loose (mm)	50 Cycles/Loose (mm)	100 Cycles/Loose (mm)	30 Cycles/Medium-Dense (mm)	50 Cycles/Medium-Dense (mm)	100 Cycles/Medium-Dense (mm)	30 Cycles/Dense (mm)	50 Cycles/Dense (mm)	100 Cycles/Dense (mm)
0	2,29	2,29	2,99	2,27	2,27	2,27	2,26	2,26	2,26
8,5	1,60	1,60	1,60	1,60	1,60	1,60	1,60	1,60	1,60
17	0,99	0,99	0,99	0,96	0,99	0,99	0,96	0,96	0,96
25,5	-1,11	-1,32	-1,54	-2,79	-2,79	-2,85	-2,00	-2,00	-2,05
34	-3,04	-3,04	-3,04	-3,03	-3,03	-3,04	-3,03	-3,03	-3,03

Table 5.4. Displacement of the Pile Model of mortar beam in Soil with Various Densities.

Depth (cm)	30 Cycles/Loose (mm)	50 Cycles/Loose (mm)	100 Cycles/Loose (mm)	30 Cycles/Medium-Dense (mm)	50 Cycles/Medium-Dense (mm)	100 Cycles/Medium-Dense (mm)	30 Cycles/Dense (mm)	50 Cycles/Dense (mm)	100 Cycles/Dense (mm)
0	2,29	2,29	2,29	2,28	2,28	2,28	2,27	2,27	2,27
8,5	1,50	1,53	1,53	1,50	1,51	1,50	1,49	1,48	1,48
17	0,85	0,82	0,89	0,79	0,79	0,79	0,76	0,76	0,77
25,5	-1,45	-1,65	-1,69	-1,44	-1,44	-1,44	-1,52	-1,42	-1,42
34	-3,12	-3,62	-2,83	-3,04	-3,04	-3,04	-3,02	-3,02	-3,02

For all the pile models, generally the displacement values decrease and the values are more close to zero when the soil gets in a denser state. The difference between the displacement values for different cycles at same depth is not too much except the model pile post-tension of 1500 N. for loose and medium dense state. For loose state at depth 17, a difference higher than the others is seen when number of cycles increase from 30 to 50 and for medium dense state at depth 8,5, a difference higher than the others is seen when

number of cycles increase from 50 to 100. Also the values for the model pile post-tension of 2250 N and mortar beam show similarity between each other.

For segmental pile with post-tension of 750 N pile head displacement values in loose soil change in order of one in a hundred millimeter with the increasing number of cycles. However there is no change in base point displacement values with the increasing number of cycles. For medium-dense soil pile head displacement values do not change with 30 cycles and 50 cycles but for 100 cycles it increases in order of one in a hundred millimeter. Still there is no change in base point displacement values with the increasing number of cycles. Even the displacement values at the base are same with values for loose soil. Also for dense state pile head displacement values change in order of one in a hundred millimeter with the increasing number of cycles. Once again there is no change in base point displacement values with the increasing number of cycles. But the values are different from the loose and medium-dense state values.

For segmental pile with post-tension of 1500 N pile head displacement values in loose soil can be counted as equal with the increasing number of cycles. Also there is no change in base point displacement values with the increasing number of cycles. So, increasing number of cycles do not affect the displacement values at tip points for loose state. On the other hand for medium-dense state pile head displacement values change in order of one in a hundred millimeter with the increasing number of cycles. At pile base displacement values do not change with 50 cycles and 100 cycles but for 30 cycles it changes in order of one in a hundred millimeter. For dense state here is no change in top point displacement values with the increasing number of cycles and also here is no change in base point displacement values with the increasing number of cycles.

For segmental pile with post-tension of 2250 N pile head displacement values in loose soil do not change with the increasing number of cycles. Also pile base displacement values do not change with the increasing number of cycles. Additionally, for medium-dense state pile head displacement values do not change with the increasing number of cycles. Pile base displacement values can be counted as equal with the increasing number of cycles. So, increasing number of cycles do not affect the displacement values at tip points for medium-dense state. For the dense state displacement values at pile base and top

do not change with the increasing number of cycles as well. But pile head displacement values are different from the values for medium-dense soil. Still pile base displacement values are same with the values for medium-dense soil.

For mortar beam pile head displacement values in loose soil do not change with the increasing number of cycles. However at the pile base displacement values change in order of one in a ten millimeter with the increasing number of cycles. It is a striking point. The reason for that may be read-out error. But for the medium-dense state pile head and base displacement values do not change with the increasing number of cycles. Again for the dense state pile head and base displacement values do not change with the increasing number of cycles.

5.2. The Shear Force-Soil Density Relationship of the Segmental Pile

The table of shear force-soil density under various cyclic loads is shown below. Values are calculated relatively up to displacement values so minimum values are started with zero. For these calculations Load-Deflection/Interface Relationship for Rubber Shore 60 tests are used from the referenced paper. [2] Difference between the displacement values for each block are calculated. From the referenced paper the force value corresponding to that displacement value under same normal stress is read and assumed as the shear force value at that point. The values are accumulated up to the top point and applied force value is nearly found.

It is seen that except the segmental pile with post-tension of 1500 N in dense state, shear values increase with number of cycles. In this exception the decreasing value is not very different from the previous value. This decrease is seen between the 50 cycles to 100 cycles. The decrease is in order of one in a ten Newton. So it is not a big difference. For 30 cycles shear values increase with the higher post tension forces. This situation is not valid for other number of cycles. Still the lower shear values are usually seen at lower post tension forces. Mostly the shear values lower than 300 N are seen at post-tension of 750 N and 1500 N. For the segmental pile with post-tension of 2250 N, the shear values are higher than 300N.

Table 5.5. Minimum and Maximum Shear Force Values of the Piles.

		30 Cycles Shear (N)	50 Cycles Shear (N)	100 Cycles Shear (N)
Post-Tension 750 N	**Loose**	Min: 0	Min: 0	Min: 0
		Max: 290,14	Max: 297	Max: 300,12
	Medium-Dense	Min: 0	Min: 0	Min: 0
		Max: 292,47	Max: 292,71	Max: 304,09
	Dense	Min: 0	Min: 0	Min: 0
		Max: 282,32	Max: 290,04	Max: 299,54
Post-Tension 1500 N	**Loose**	Min: 0	Min: 0	Min: 0
		Max: 299,76	Max: 305,01	Max: 305,89
	Medium-Dense	Min: 0	Min: 0	Min: 0
		Max: 291,88	Max: 294	Max: 301,02
	Dense	Min: 0	Min: 0	Min: 0
		Max: 295,38	Max: 295,81	Max: 295,52
Post-Tension 2250 N	**Loose**	Min: 0	Min: 0	Min: 0
		Max: 302,67	Max: 306,07	Max: 308,75
	Medium-Dense	Min: 0	Min: 0	Min: 0
		Max: 304,28	Max: 304,88	Max: 305,1
	Dense	Min: 0	Min: 0	Min: 0
		Max: 305,82	Max: 308,17	Max: 313,36

Soil densities do not affect the calculated shear force values too much. Also, all the values nearly coincides with applied force 300. Except the segmental pile with post-tension of 750 N in dense state for 30 cycles and the segmental pile with post-tension of 2250 N in dense state for 100 cycles the calculated shear force values are between 290 to 310 N. These exceptional values are equal to 282,32 N for the segmental pile with post-tension of 750 N and 313,36 N the segmental pile with post-tension of 2250 N. Actually these values are not significantly different from the applied load. This shows us that nearly all the values coincide with the applied force 300 N.

5.3. The Moment-Soil Relative Density Relationship of the Segmental Pile

Moment values for segmental pile are calculated from the area of shear force graphics. The moment is equal to zero at the base point, because the pile base is free. Then it increases up to pile head connected to shear force values.

Table 5.6. Minimum and Maximum Moment Values of the Piles.

	30 cyc (kNm)	50 cyc (kNm)	100 cyc (kNm)
PTF 750 N (Loose)	0,06	0,06	0,06
PTF 750 N (Medium-Dense)	0,06	0,06	0,06
PTF 750 N (Dense)	0,06	0,06	0,06
PTF 1500 N (Loose)	0,07	0,07	0,07
PTF 1500 N (Medium-Dense)	0,06	0,06	0,07
PTF 1500 N (Dense)	0,06	0,06	0,06
PTF 2250 N (Loose)	0,06	0,06	0,06
PTF 2250 N (Medium-Dense)	0,05	0,05	0,05
PTF 2250 N (Dense)	0,05	0,05	0,05

In the table maximum moment value is equal to 0,07 kNm and minimum moment value is equal to 0,05 kNm. In the table it seen that soil relative densities do not affect the calculated moment values. Because it is seen that there is not a variation parallel to the soil relative density. Post tension forces do not affect moment values too. Also there is no variation for moment values parallel to the post tension forces. When the highest moment values are seen for the segmental pile with post-tension of 1500 N, the lowest moment values are seen for the segmental pile with post-tension of 2250 N.

Only for the number of cycles a difference is seen with the increasing numbers. It can not be seen for all the cases clearly, yet it is clearly seen for the the segmental pile with post-tension of 1500 N in medium dense state.

5.4. Test Results Comprehension

Previous study results for the segmental pile with post-tension of 2250 N for cyclic loading is shown below in Table 5.7. [2] Results of this study is shown in Table 5.8.

Table 5.7. Results of Segmental pile with post-tension of 2250 N-3K/Cyclic [2].

Analysis Method	Deflection (mm)	Position	Slope (Degree)	Position	Bending.M (KN.m)	Position	Shear Force (N)	Position
Exp	Min: 0 Max: 4	Tip Top	Min:-.053 Max:-0.32	Top Tip	Min:0 Max:0.013	Top Tip	Min:0 Max:200	Tip Top
P.F-Post Top point Load	-	-	-	-	Min:0.0025 Max:0.02	Top Tip	-	-
L.Pile	Min: 0 Max: 4.15	Tip Top	Min:-.049 Max:-0.57	Tip Top	Min: 0 Max:0.0541	Top and Tip 3D	Min:0 Max:200	Tip Top
NDM	Min: 0 Max: 2.62	Tip Top	Min:0 Max:-.012	Tip Top	Min:0 Max:0.0168	Top and Tip 3D	Min:0 Max:200	Tip Top

Table 5.8. Results of Segmental pile with post-tension of 2250 N.

	Deflection (mm)	Difference Between the Deflection Values (mm)	Shear Force (N)	Moment (kNm)
Loose	2,99-Top -3,04-Tip	6,03	308,75-Top 0-Tip	0,06-Top 0-Tip
Medium-Dense	2,27-Top -3,04-Tip	5,31	305,1-Top 0-Tip	0,05-Top 0-Tip
Dense	2,26-Top -3,03-Tip	5,29	313,36-Top 0-Tip	0,05-Top 0-Tip

In the previous study the pile is fixed at the tip and loaded at the free top point. In this study the pile is fixed and loaded at the top. The pile base is free. According to experimental results in the previous study the pile is stable at the fixed point. It deflects up to the top point. The deflection at the top point is 4 mm. The difference between the deflection values is equal to 4 mm. In this study it is assumed that before the loading is applied the vertical pile axis is on zero. After the loading top of the pile goes to positive direction and pile base goes to negative direction. In loose state pile head deflects 2,99 mm after 100 cycles and pile base deflects -3,04 mm after 100 cycles. The difference between

the deflection values is equal to 6,03 mm. In medium dense state after 100 cycles, pile head deflects 2,27 mm and pile base deflects -3,04 mm. The difference between the deflection values is equal to 5,31 mm. In dense state after 100 cycles, pile head deflects 2,26 mm and pile base deflects -3,03 mm. The difference between the deflection values is equal to 5,29 mm. The difference between deflection values are 32-50 % higher than the previous study in all density states. Also the deflection is seen at the all points in this study unlike the previous one.

According to experimental results in the previous study, the force is applied at the top point so the maximum shear force value is measured at the top point and it is equal to 200 N. The minimum shear force value is at the base. The difference between the deflection values corresponding to this shear force value is equal to 4 mm. In this study the applied shear force is 300 N and the calculated shear values for different density states are equal to 308,75 N for loose state, 305,1 N for medium-dense state and 313,36 N for dense state at the top point. Also for this study the minimum shear force value is at the base. The shear force is nearly 50% higher than the previous study at the top point.

According to experimental results in the previous study, the maximum bending moment is measured at the base point and it is equal to 0,013 kNm. The minimum bending moment value is at the top and it is equal to zero. Because the pile top is free. In this study the maximum bending moment is measured at the top point and it is equal to 0,06 kNm for loose state, 0,05 kNm for medium-dense state and 0,05 kNm for dense state. In this study the minimum bending moment value is at the pile base for all density states and it is equal to zero. Because the pile base is free. The maximum moment values calculated in this study are nearly four times higher than the previous study.

According to L. Pile results in the previous study the pile deflects up to the top point from the zero. The deflection at the top point is 4,15 mm. The difference between the deflection values is equal to 4,15 mm. The difference between the deflection values for this study is implied before. The difference between deflection values are 27-45 % higher than the previous study in all density states.

According to L. Pile results in the previous study, the force is applied at the top point so the maximum shear force value is measured at the top point and it is equal to 200 N. Shear force values for this study are implied before. Again the shear force is nearly 50% higher than the previous study at the top point.

According to L. Pile results in the previous study, minimum bending moment value is seen at top and tip. However the maximum bending moment value is seen for 3D and it is equal to 0,0541 kNm. Unlike L. Pile results, in this study minimum moment value is only seen at the base point and maximum moment value is seen at the pile top. Still the maximum moment values are very close to each other.

According to NDM results in the previous study the pile deflects up to the top point from the zero. The deflection at the top point is 2,62 mm. The difference between the deflection values is equal to 2,62 mm. The difference between the deflection values for this study is implied before. The difference between deflection values are 230-202 % higher than the previous study in all density states. The ratio of the difference is striking.

According to NDM results in the previous study, the force is applied at the top point so the maximum shear force value is measured at the top point and it is equal to 200 N. Shear force values for this study are implied before. Again the shear force is nearly 50% higher than the previous study at the top point.

According to NDM results in the previous study, minimum bending moment value is seen at top and tip. However the maximum bending moment value is seen for 3D and it is equal to 0,0168 kNm. Unlike NDM results, in this study minimum moment value is only seen at the base point and maximum moment value is seen at the pile top. The maximum moment values of this study are nearly 4 times higher than the previous study. On the other hand in the previous study the bending moment values from experimental results and NDM method is very close to each other.

5.5. Stress Distribution of the Prescale Films

First of all results of stress distribution of the segmental pile with post-tension of 750 N subjected to three point bending test are examined. The average stress at the upper part of the films is 1.4 MPa and in the lower part is 1.18 MPa. Due to the loading condition, the segmental pile develops convex curve. The stress values of twenty four prescale films are recorded; and the average stress is 1.29 MPa.

The results of stress distribution of the segmental pile with post-tension of 1500 N subjected to three point bending test are examined. The average stress at the upper part of the films is 1.2 MPa and in the lower part is 1.29 MPa. Due to the loading condition, the segmental pile develops convex curve. The stress values of twenty four prescale films are recorded; and the average stress is 1.35 MPa.

The results of stress distribution of the segmental pile with post-tension of 2250 N subjected to three point bending test are examined. The average stress at the upper part of the films is 1.52 MPa and in the lower part is 1.4 MPa. Due to the loading condition, the segmental pile develops convex curve. The stress values of twenty four prescale films are recorded; and the average stress is 1.46 MPa.

6. CONCLUSIONS

The following conclusions are limited to the experimental setup used in this study. Although with the soil and testing device the real life conditions simulated for loose, medium-dense and dense state. There may be different situations on the field and the real behavior of the pile and the soil will be different.

In the experiments with the segmental pile it is obtained that changing the density state causes a small decrease in the displacement.

Changing the rigidity state causes a decrease in the displacement. Displacement values of the segmental piles with post-tension force of 750 N and 1500 N are close to each other. Also displacement values of the segmental pile with post tension-force 2250 N and mortar beam are close to each other.

Increasing the cyclic loading numbers causes a small increase in the displacement. But that does not represent expected degradation under cyclic loading for real soil.

From the Load-Deflection/Interface Relationship for Rubber Shore 60 tests measured displacement values, shear forces are calculated. For this calculation shear forces corresponding to displacement values are accumulated from base to top. After this calculations applied force is nearly obtained.

From the shear force graphics area moment values are calculated.

For checking the shear and moment results accuracy, prescale films are used. Pile with prescale film is exposed to three point bending test. The results calculated from the prescale films and load-deflection/interface relationship for rubber shore 60 tests coincide.

For future research it is recommended that the beam displacements should be measured in more locations. The beam used in this study was fixed from one side. A ball

joint type connection is recommended to have zero moment at the tip of the segmental beam.

REFERENCES

1. Manfred R. Hausmann, *Engineering Principle of Ground Modification*, McGrow-Hill International press, London, 1989.

2. Yahia, Y.İ.O., *An Experimental Study on the Behavior of Segmental Pile with Variable Flexural Rigidity*, Ph.D. Thesis, Boğaziçi University, 2015.

3. Baykal, G., *A Study on Numerical Analysis of Laterally Loaded Piles*, M.S. Thesis, Boğaziçi University, 1982.

4. Zhang, C., Yu, J., Huang, M., *Winkler Load-Transfer Analysis for Laterally Loaded Piles*, www..nrcreserchpress.com/cgj, accessed in 2006.

5. Fan, C.C. And Long, J.H., Assessment of Existing Methods for Predicting Soil Response of Laterally Loaded Piles in Sand, *Computers and Geotechnics*, Vol 32, pp. 274-289, 2005.

6. Matlock, H. And Reese, L.C., Generalized Solutions for Laterally Loaded Piles, *Journal of Soil Mechanics and Foundation Engineering Division*, ASCE, Vol. 86, pp.63-91, 1960.

7. Matlock, H., Correlations for Design of Laterally Loaded Piles in Soft Clay, *Proceedings of Second Annual Offshore Technology Conference*, Houston, Texas, Paper 1204, pp. 577-594, 1970.

8. Qin, H., Oh, E., Guo, W. D., Dai, P.F., Upper Bound Limit Analysis of Lateral Pile Capacity, *International Conference on State of the Art Pile Foundation and Pile Cast Histories*, 2013.

9. Honjo, Y., Zaika, Y., Pokharel, G., Estimation of Subgrade Reaction Coefficient for Horizontally Loaded Piles by Statical Analyses, *Soils and Foundations*, Vol. 45, No. 3, pp. 51-70, Japanese Geotechnical Society, June 2005.

10. Terzaghi, K., *Theoretical Soil Mechanics*, John Wiley and Sons, USA, 1943.

11. Terzaghi, K., Evaluation of Coefficients of Subgrade Reaction, *Journal of Geotechnique*, Vol. 5, pp. 297-326, 1955.

12. Terzi, N.U., Kılıç, H., Gültekin, S., Investigation of a Laterally Loaded Model Pile Behaviour in Sand by Means of Experimental and Numerical Methods, Pamukkale University Engineering Faculty, *Journal of Engineering Sciences*, Vol. 1, No. 15, pp. 119-127, 2009.

13. Meyer, B.J., Reese, L.C., *Analysis of Single Piles Under Lateral Loading*, Research Report 244–1, Project 3-5-78-244, Centre for Transportation Research, University of Texas, 1–182, 1979.

14. Reese, L.C., Cox, W.R., Koop, F.D., Analysis of Laterally Loaded Piles in Sand, *6th Offshore Technology Conference, Houston*, OTC 2080, Vol. 2, pp. 473-483, 1974.

15. Ashour, M., Norris, G., Lateral Loaded Pile Response in Liquefiable Soil, *Journal and Geoenvironmental Engineering*, ASCE, Vol. 129, No. 6, June 1, 2003.

16. Brocklehurst, C.J., *Finite Element Studied of Reinforced and Unreinforced Two-Layer Soil Systems*, Ph.D. Thesis, University of Oxford, U.K., 1993.

17. Chaudhry, A.R., *Static Pile-Soil-Pile Interaction in Offshore Pile Groups*, Ph.D. Thesis, University of Oxford, U.K., 1994.

18. Keleşoğlu, M.K., Çinicioğlu S.F., *A Deformation Based Solution for Soil-Structure Load Sharing Mechanism in Case of Laterally Loaded Passive Piles*, http://www.imo.org.tr/resimler/ekutuphane/pdf/10812.pdf, accessed in 2012.

19. Özçelik, Ç., Yıldırım S., Experimental Investigation of Piles Behaviour Subjected to Lateral Soil Movement, *İMO Teknik Dergi*, writing 423, pp. 6867-6887, 2014.

20. Pan, J.L., Goh, A.T.C., Wong, K.S., Teh, C.I., *Model Tests on Single Piles in Soft Clay*, www..nrcreserchpress.com/cgj, accessed in 2000.

21. Özçelik, Ç., *Şevlerde Yanal Yüklü Kazıkların Laboratuar Koşullarında Modellenmesi*, M.S. Thesis, Yıldız Technical University, 2007.

22. İmançlı, G., Kahyaoğlu, M.R., Özden, G., Limit State Moment Functions for Laterally Loaded Single Piles in Local OC Clay, *Pammukkale Üniversitesi Mühendislik Bilimleri Dergisi*, Vol 15, No 3, pp. 4-5-416, 2009.

23. Mısır, G., Laman, M., *Yanal Yüklü Eğik Rijit Kazıkların Sayısal Analizi*, http://dergipark.gov.tr/download/article-file/554071, accessed in 2019.

24. Uncuoğlu, E., Laman, M., Yıldız, A., *The analysis of the laterally loaded piles by theoretical methods and Plaxis 3D*, http://www.imo.org.tr/resimler/ekutuphane/pdf/10823.pdf, accessed in, 2017.

25. Prasad, V.S.N., Chari, T.R., Lateral Capacity of Model Rigid Piles in Cohesionless Soils, *Soils and Foundation*, Vol. 39, No. 2, pp. 21-29, 1999.

26. Qin, H., And Guo, W.,D., An Experimental Study on Cyclic Loading of Piles in Sand, *10th ANZ Conference on Geomechanics*, Vol. 1, January 2007.

27. Dinçer, E., *Yatay Yük Etkisindeki Model Kazıkların Davranışı*, Ph.D. Thesis, İstanbul Technical University, 1986,

28. Kim, B.T., Yoon G.L., Laboratory Modeling of Laterally Loaded Pile Groups in Sand, *KSCE Journal of Civil Engineering*, Vol. 15, pp. 65-75, 2011.

29. Hai Lin, S.M., Lusu Ni, S.M., Muhannad T., Suleiman, A.M., Interaction Between Laterally Loaded Pile and Surrounding Soil, , *Journal and Geoenvironmental Engineering*, ASCE, Vol. 141, No. 4, June 1, 2015.

30. Qin, H., Guo, W.D., Response of Static and Cyclic Laterally Loaded Rigid Piles in Sand, *Marine Georesources Geotechnology*, Vol. 34, pp. 138-153, 2014.

31. Leblanc, C., Houlsby, G.T., Byrne, B.W., Response of Stiff Piles in Sand to Long-Term Cyclic Lateral Loading, *Geotechnique*, Vol. 60, pp. 79-90, 2010.

32. Brown, D., Reese, L., O'Neill, M., Cyclic Lateral Loading of a Large-Scale Pile Group, *Journal and Geotechnical Engineering*, ASCE, Vol. 113, No. 11, November, 1987.

33. Baykal, G., *Three Techniques for the Study of Soil Structure Interface Properties; 3D Roughness Parameter; Contact Stress Mapping; Artificially Manufactured Sand, Soil-Structure Interaction Underground Structures and Retaining Walls*, Boğaziçi University, İstanbul, 2014.

34. Baykal, G., Contact Stress Mapping in Geotechnical Engineering, *4th International Conference on New Developments in Soil Mechanics and Geotechnical Engineering*, Near East University, Nicosia, North Cyprus, 2-4 June 2016.

35. Fujifilm Corporation, *Pressure Distribution Mapping System for PRESCALE FOD-8010 Ver. 10*, 2007.

36. Baykal,G., Pressure Mapping System for Geosynthetic Interfaces. *IGS World Conference*, Berlin, 2014.

37. Baykal, G., Elmas, B., Keklik, A., Pürüzlü ve Pürüzsüz *Geomembranın, Düşük Normal Gerilme Altında Büyük Deplasmanlardaki Davranışı, Yedinci Ulusal Geosentetikler Konferans*ı, Boğaziçi Üniversitesi, İstanbul, 11-12 Mayıs 2017.

38. Baykal, G., Large Displacement, Constant Contact Area Geosynthetic-Soil Interface Direct Shear Test Device, *Proceedings of the 19th International Conference on Soil MechanCs and Geotechnical Engieering*, Seoul, 2017

39. Baykal, G., *Development of Soil-Structure Interface Testing System Using pneumatic muscles*, BAP 5580 project, Boğaziçi University, İstanbul, 2015.

40. Baykal, G., Large Size-Large Displacement Residual Direct Shear Test Device Development, *Proceedings of the 19th International Conference on Soil Mechanics and Geotechnical Engieering*, Seoul, 2017.

41. Yıldız, A., *Utilization of Pneumatic Artificial Muscles on a Direct Shear Test Setup*, M.S. Thesis, Boğaziçi University, 2010.

42. Baykal, G., Implementation of Pneumatic Muscles in Geotechnical Laboratory Equipment Development, *4th International Conference on New Developments in Soil Mechanics and Geotechnical Engineering*, Near East University, Nicosia, North Cyprus, 2016.

43. ASTM, *C270-19 Standard Specification for Mortar for Unit Masonry*, West Conshohocken, PA,

44. ASTM, *D3080 / D3080M - 11 Standard Test Method for Direct Shear Test of Soils Under Consolidated Drained Condition*, West Conshohocken, PA, 2011

45. ASTM, *D6913/D6913M Standards Standard Test Methods for Particle-Size Distribution (Gradation) of Soils Using Sieve Analysis*, West Conshohocken, PA,

46. ASTM, *D4253-16 Standard Test Methods for Maximum Index Density and Unit Weight of Soils Using a Ultimate resistance per length*, West Conshohocken, PA,

47. ASTM, *D2435/D2435M – 11 Standard Test Methods for One-Dimensional Consolidation Properties of Soils Using Incremental Loading*, West Conshohocken, PA

APPENDIX A: CYCLIC LOAD OF THE SEGMENTAL PILE

A.1. Cyclic Load at Mid-Point of the Segmental Pile Deflection Relationship

The load-displacement relations at mid-point of pile model subjected to lateral cyclic load are shown below. In the Figures, it is seen that the deflection decreases when the soil is denser. Also it gets lower when the post tension force rises and for the mortar beam lowest values are seen.

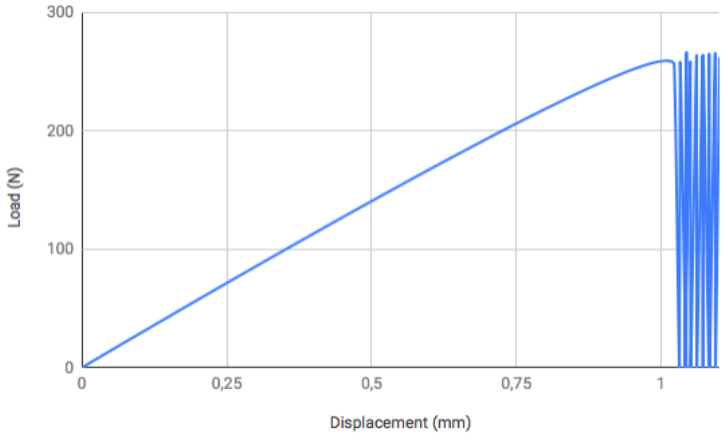

Figure A.1. Segmental Pile with Post-Tension Force 750 N in Loose Soil.

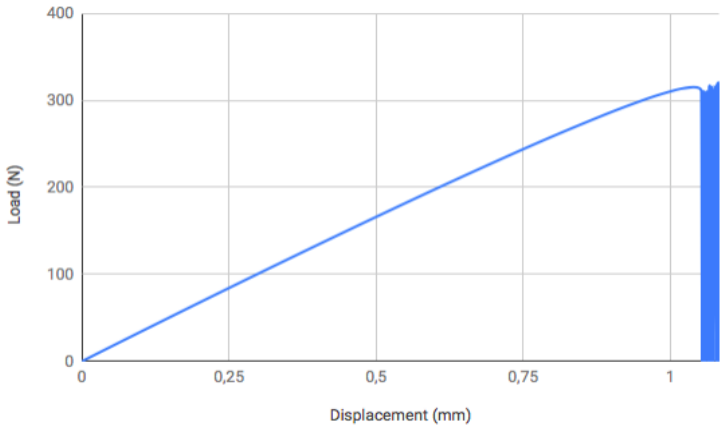

Figure A.2. Segmental Pile with Post-Tension Force 750 N in Medium-Dense Soil.

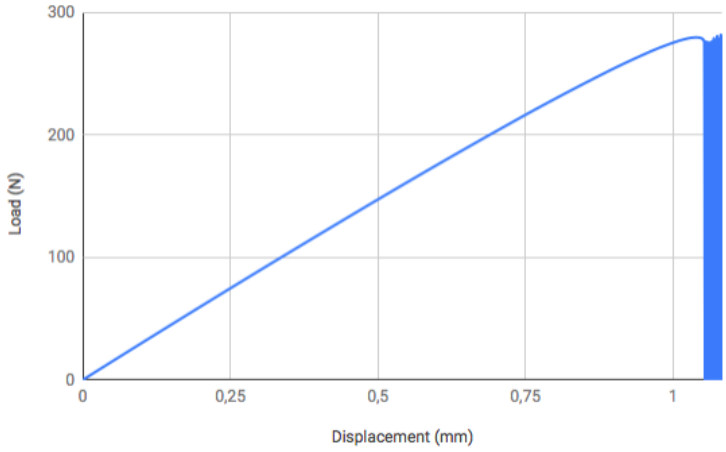

Figure A.3. Segmental Pile with Post-Tension Force 750 N in Dense Soil.

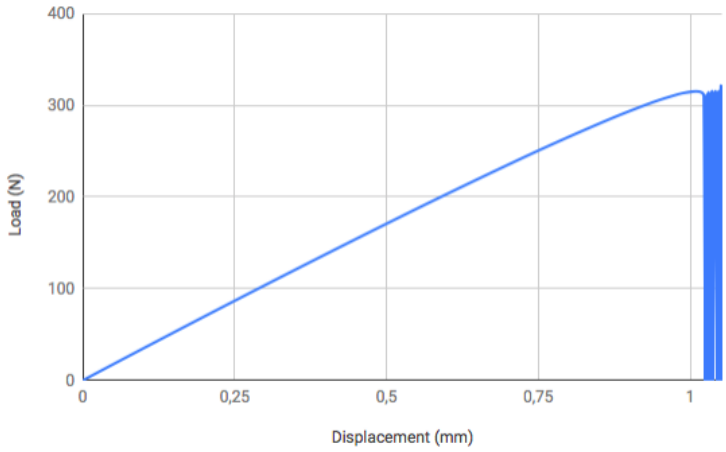

Figure A.4. Segmental Pile with Post-Tension Force 1500 N in Loose Soil.

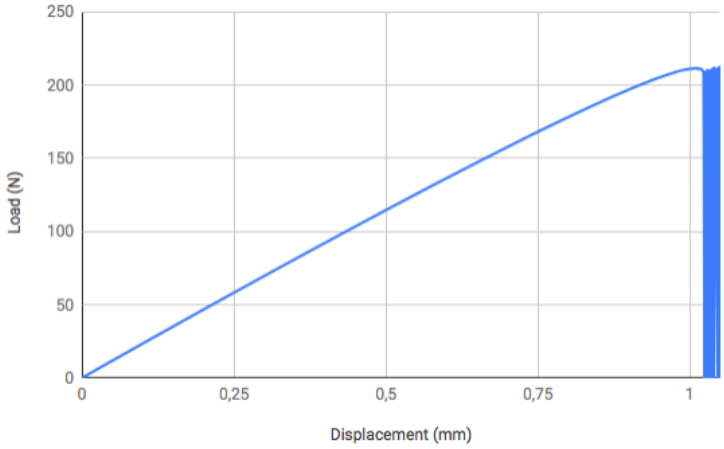

Figure A.5. Segmental Pile with Post-Tension Force 1500 N in Medium-Dense Soil.

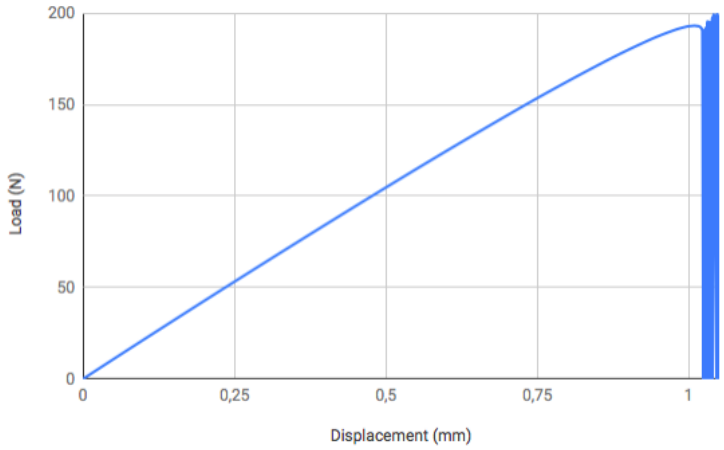

Figure A.6. Segmental Pile with Post-Tension Force 1500 N in Dense Soil.

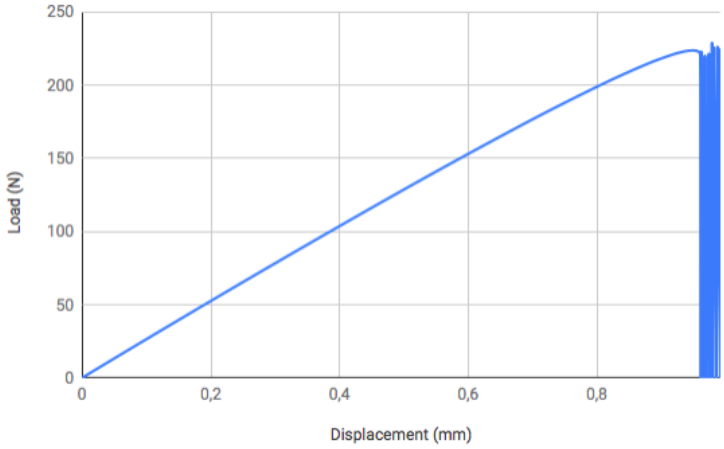

Figure A.7. Segmental Pile with Post-Tension Force 2250 N in Loose Soil.

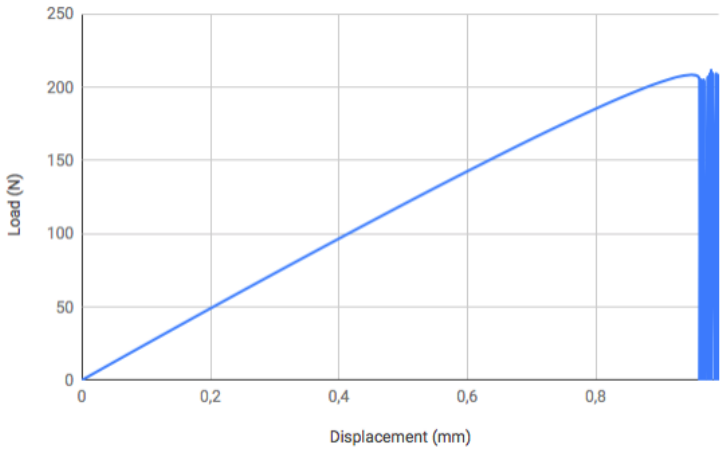

Figure A.8. Segmental Pile with Post-Tension Force 2250 N in Medium-Dense Soil.

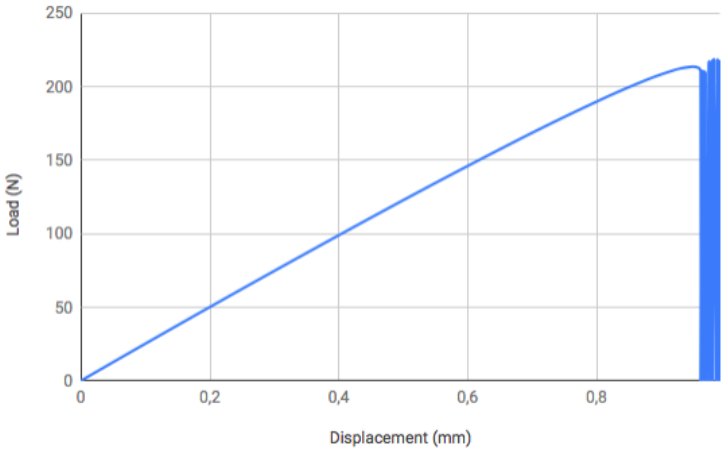

Figure A.9. Segmental Pile with Post-Tension Force 2250 N in Dense Soil.

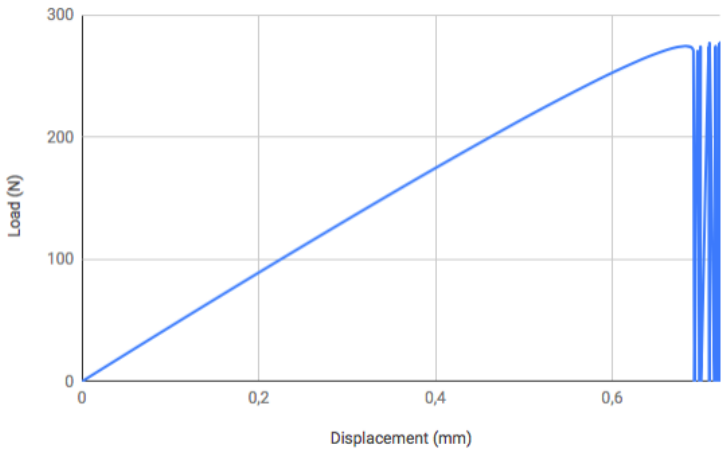

Figure A.10. Mortar Beam in Loose Soil.

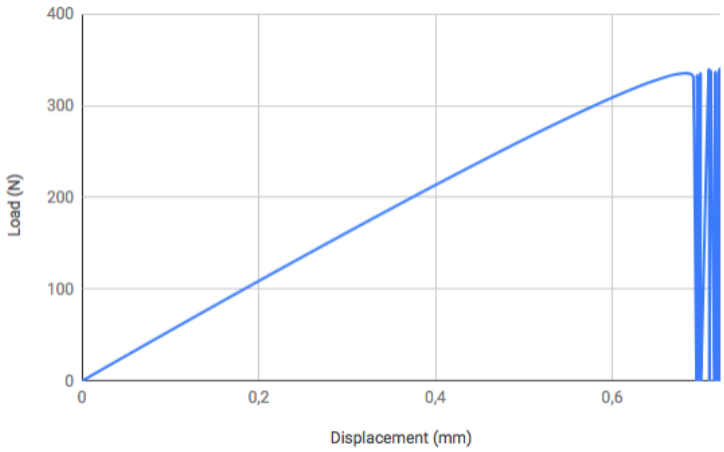

Figure A.11. Mortar Beam in Medium-Dense Soil.

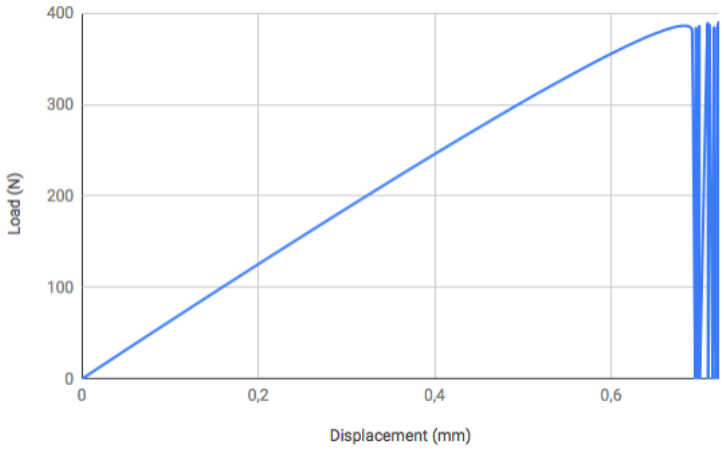

Figure A.12. Mortar Beam in Dense Soil.

According to Figures above the deflection values at mid-point for the model pile post-tension 750 N and 1500 N are higher than 1 mm. The deflection values at mid-point for the model pile post-tension 2250 N is between 0,8-1 mm. Furthermore the deflection values at mid-point for the mortar beam is lower than 0,8 mm.

A.2. Cyclic Load at End-Point of the SEgmental Pile Deflection Relationship

The load-displacement relations at the end-point of pile models subjected to lateral cyclic load are shown below. In the Figures, it is seen that the cycling interval decreases when the soil is denser. Especially, this situation is seen on the mortar beam.

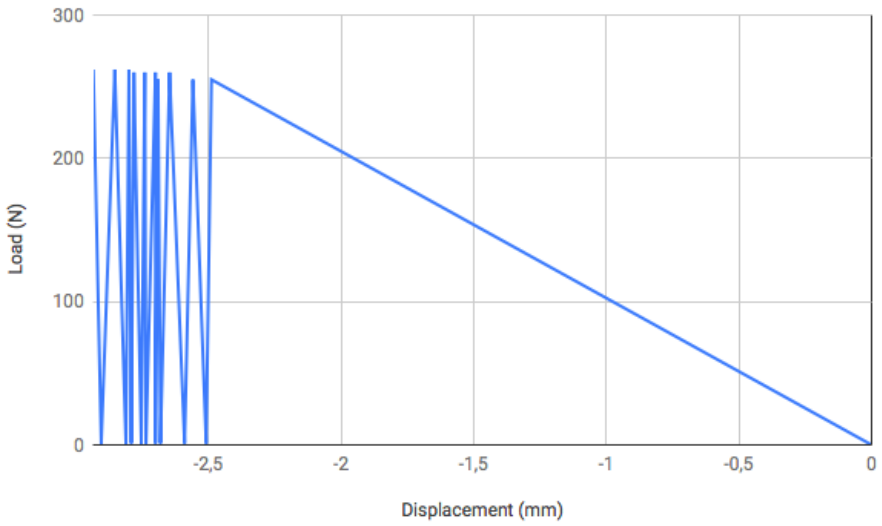

Figure A.13. Segmental Pile with Post-Tension Force 750 N in Loose Soil.

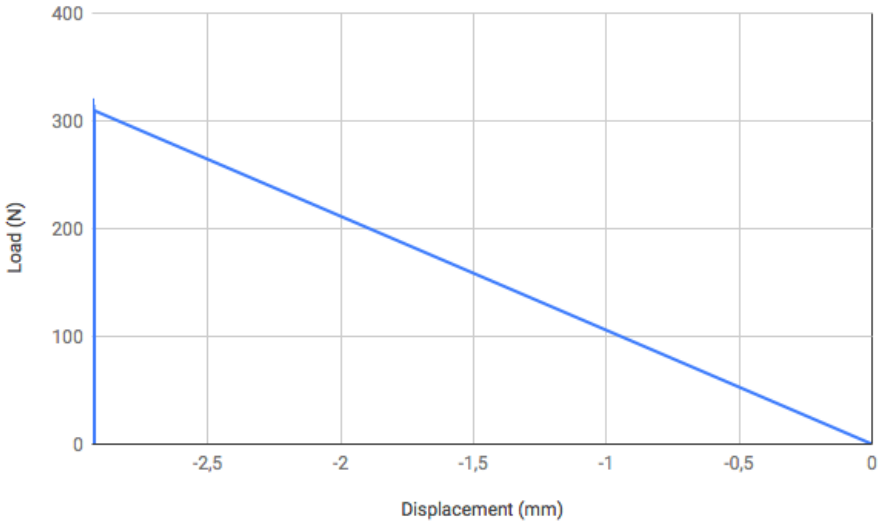

Figure A.14. Segmental Pile with Post-Tension Force 750 N in Medium - Dense Soil.

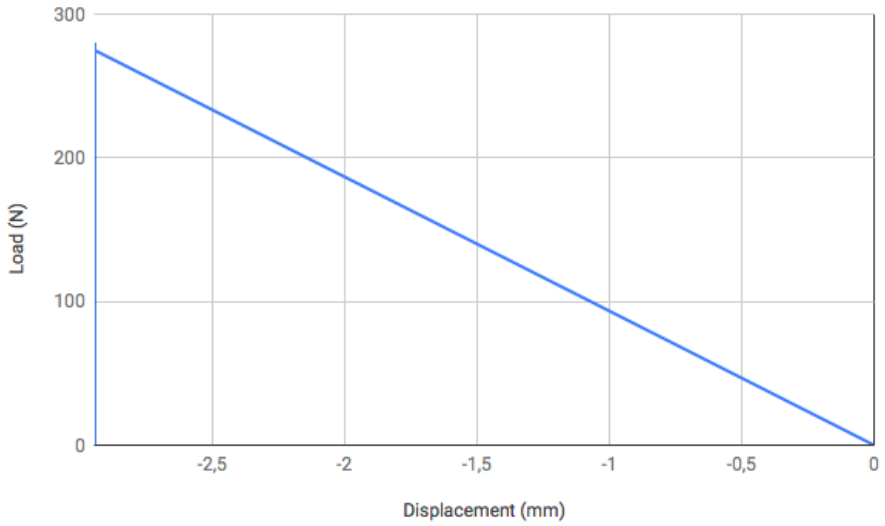

Figure A.15. Segmental Pile with Post-Tension Force 750 N in Dense Soil.

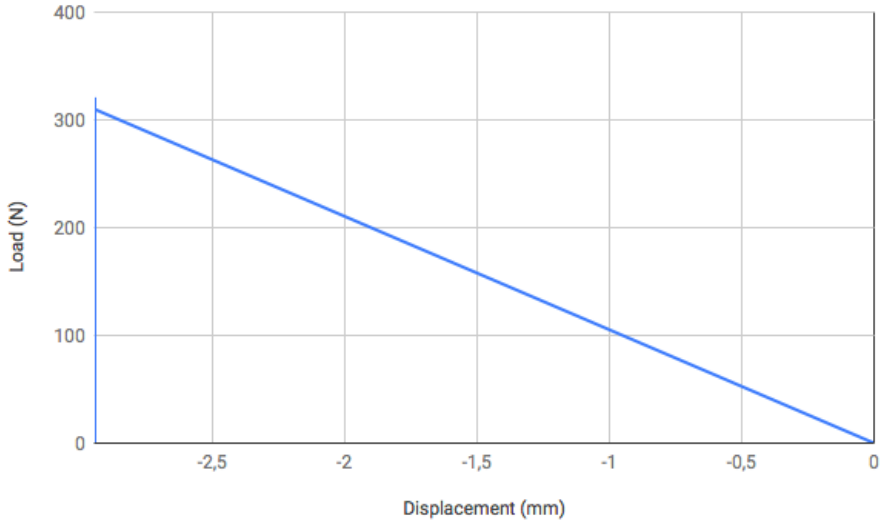

Figure A.16. Segmental Pile with Post-Tension Force 1500 N in Loose Soil.

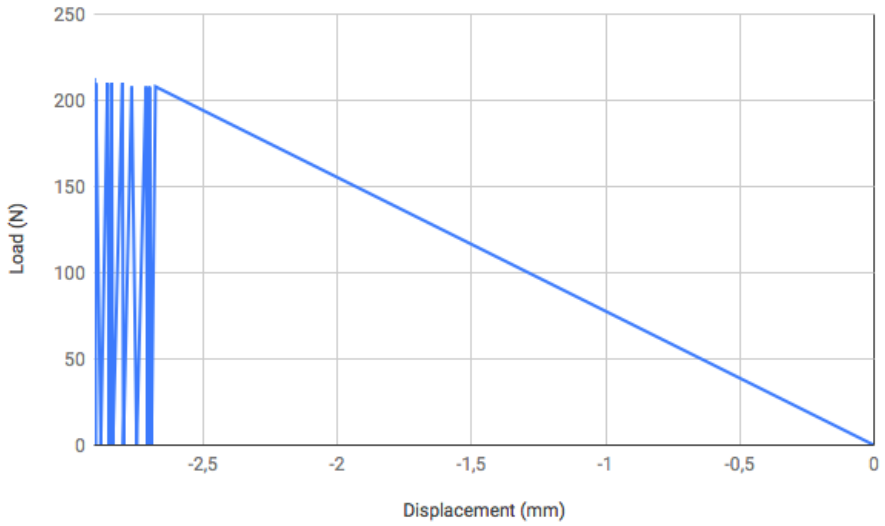

Figure A.17. Segmental Pile with Post-Tension Force 1500 N in Medium - Dense Soil.

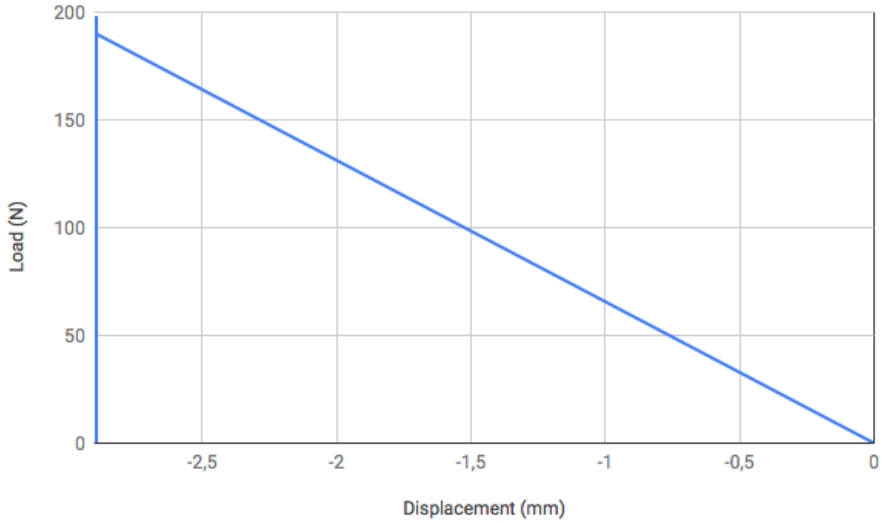

Figure A.18. Segmental Pile with Post-Tension Force 1500 N in Dense Soil.

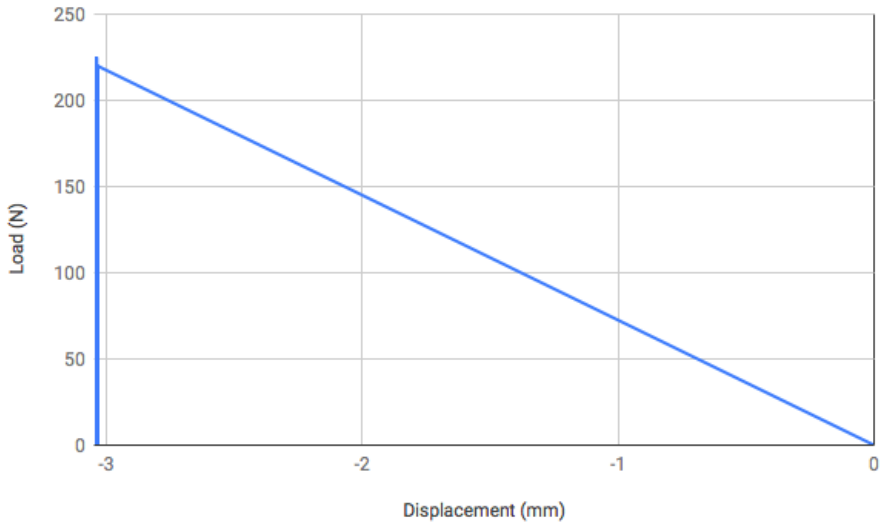

Figure A.19. Segmental Pile with Post-Tension Force 2250 N in Loose Soil.

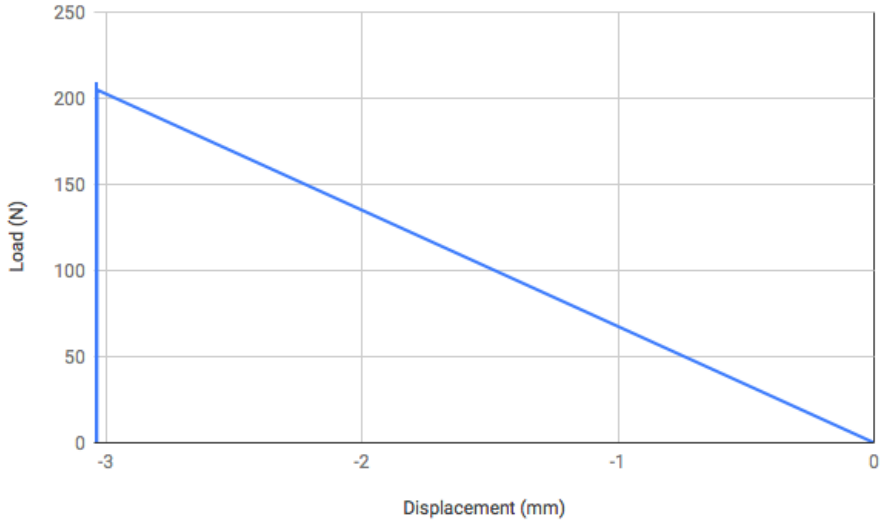

Figure A.20. Segmental Pile with Post-Tension Force 2250 N in Medium - Dense Soil.

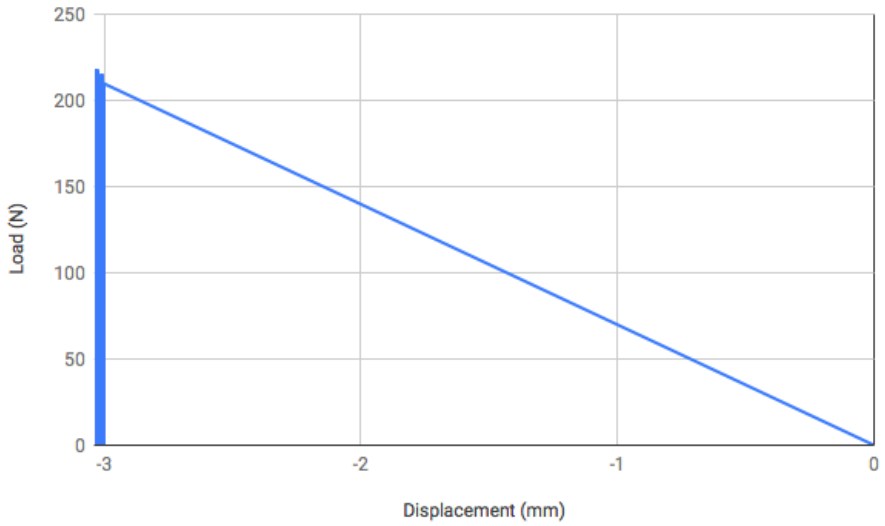

Figure A.21. Segmental Pile with Post-Tension Force 2250 N in Dense Soil.

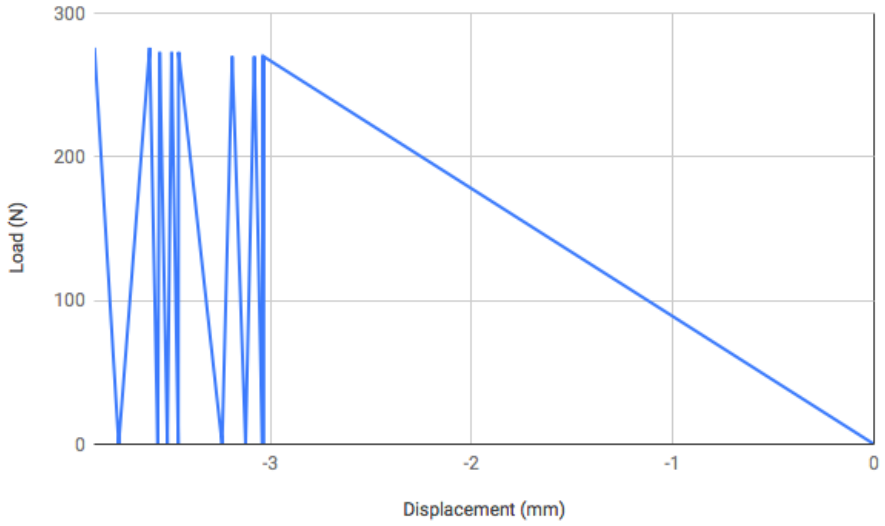

Figure A.22. Mortar Beam in Loose Soil.

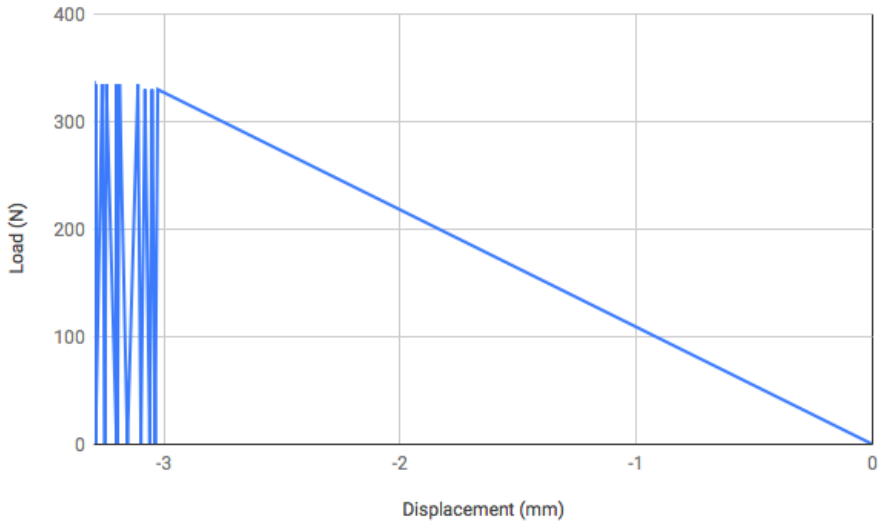

Figure A.23. Mortar Beam in Medium - Dense Soil.

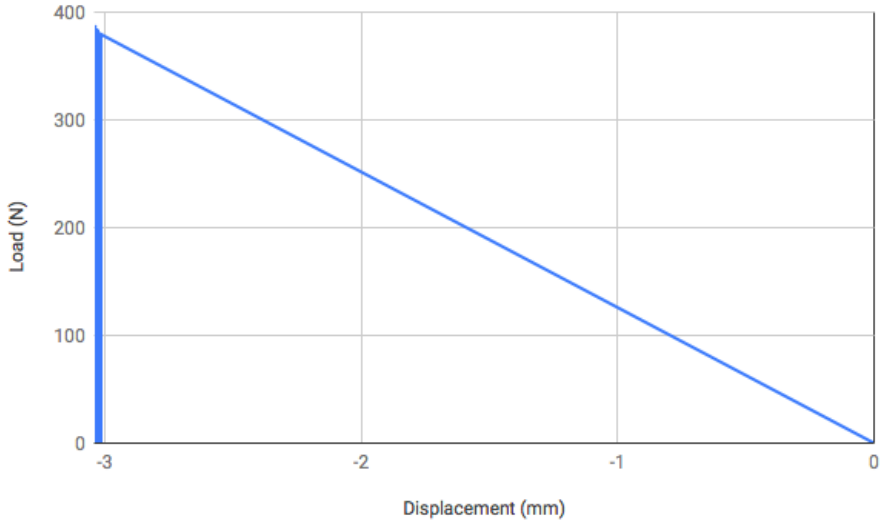

Figure A.24. Mortar Beam in Dense Soil.

According to Figures above the deflection values at the end-point for the model pile post-tension with 750 N and 1500 N are are between -2,5-3 mm. The deflection values at the end-point for the model pile post-tension with 2250 N and the mortar beam are higher than -3 mm.

A.3. Slope of the Segmental Pile

The slope values of pile model subjected to lateral cyclic load are shown below. According to boundary conditions, at top of pil slope is equal to 0 for fixed head conditions.

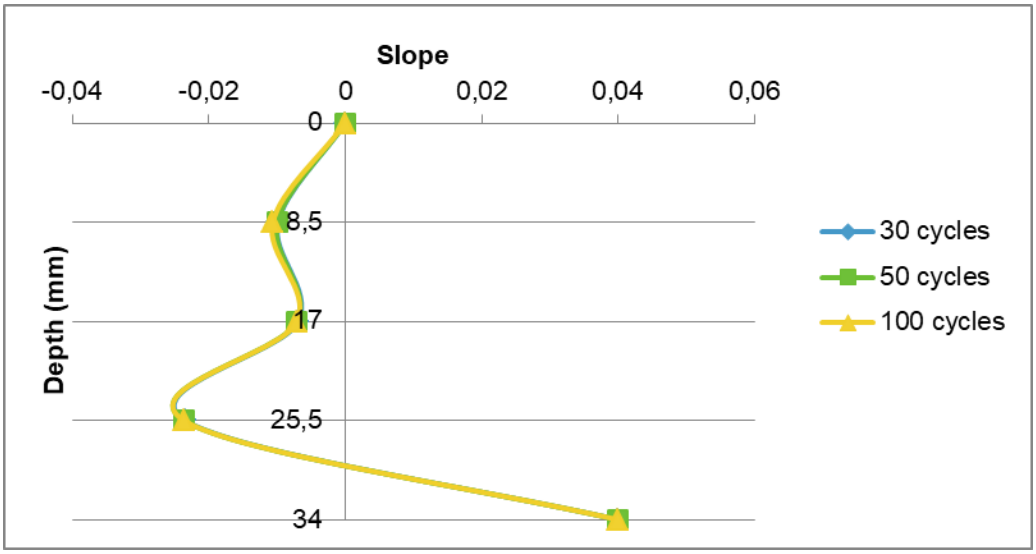

Figure A.25. Slope of the Segmental Pile with Post-Tension Force 750 N in Loose Soil.

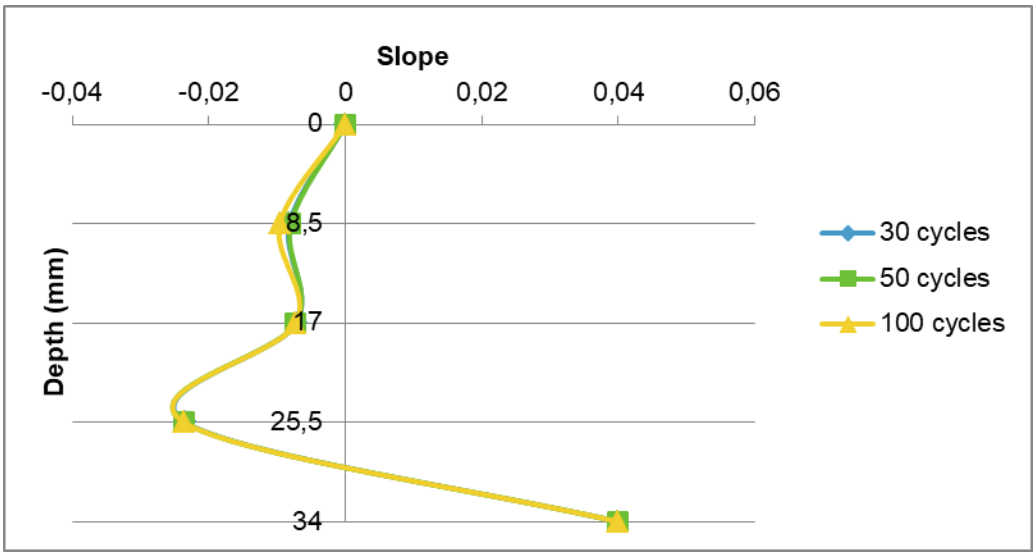

Figure A.26. Slope of the Segmental Pile with Post-Tension Force 750 N in Medium-Dense Soil.

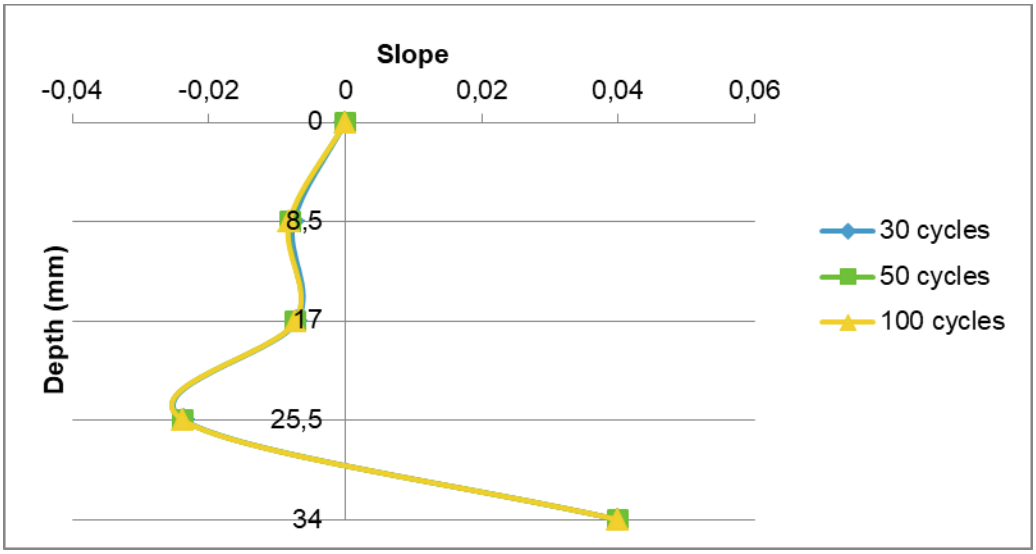

Figure A.27. Slope of the Segmental Pile with Post-Tension Force 750 N in Dense Soil.

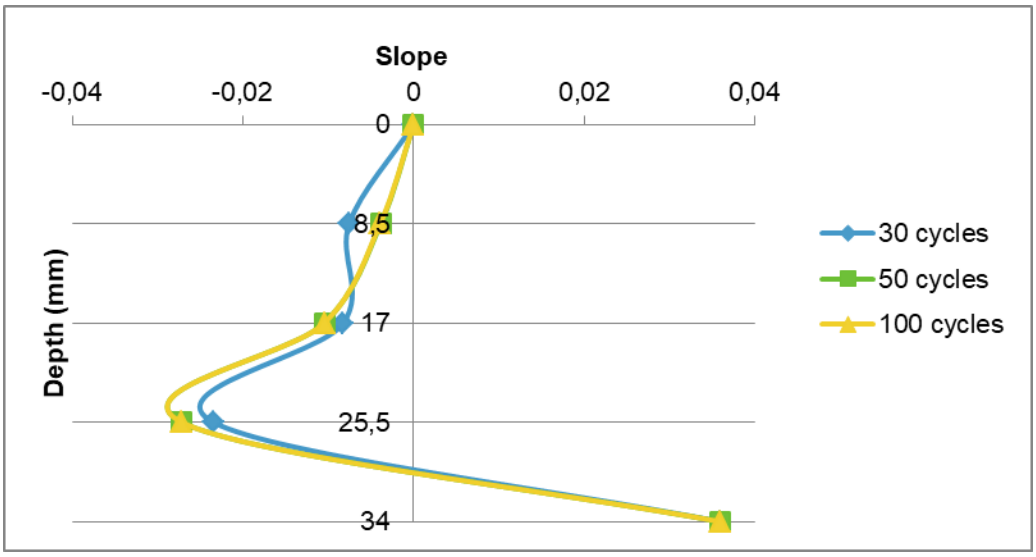

Figure A.28. Slope of the Segmental Pile with Post-Tension Force 1500 N in Loose Soil.

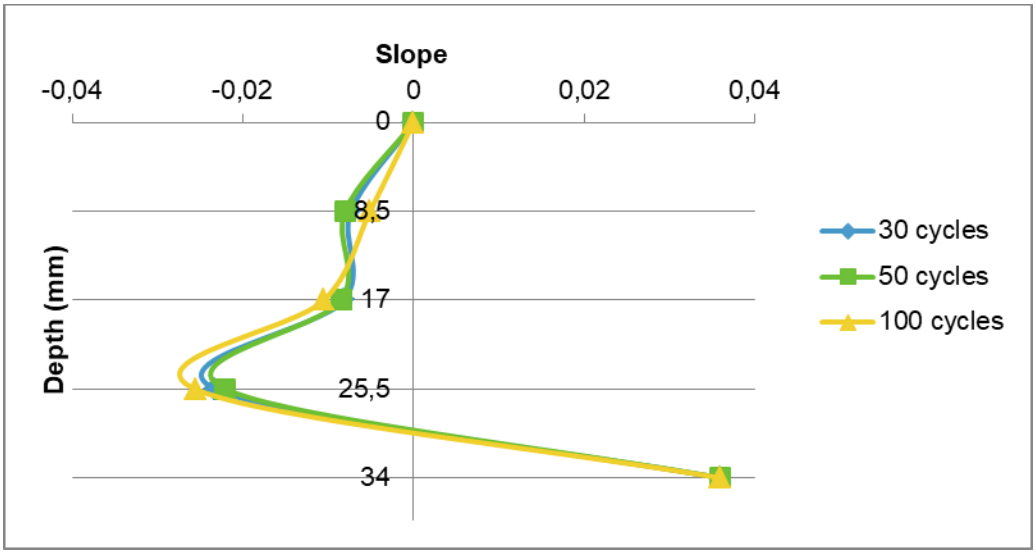

Figure A.29. Slope of the Segmental Pile with Post-Tension Force 1500 N in Medium-Dense Soil.

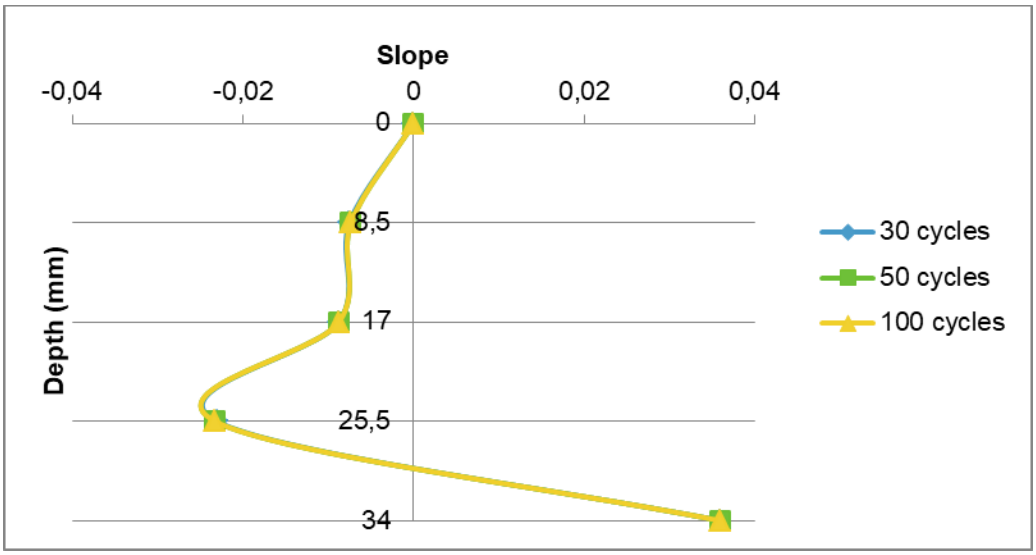

Figure A.30. Slope of the Segmental Pile with Post-Tension Force 1500 N in Dense Soil.

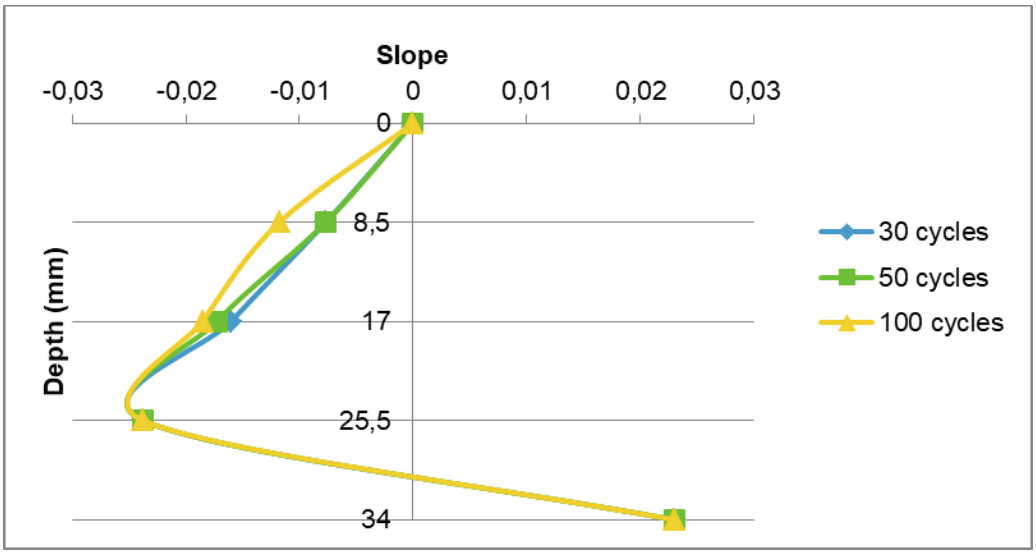

Figure A.31. Slope of the Segmental Pile with Post-Tension Force 2500 N in Loose Soil.

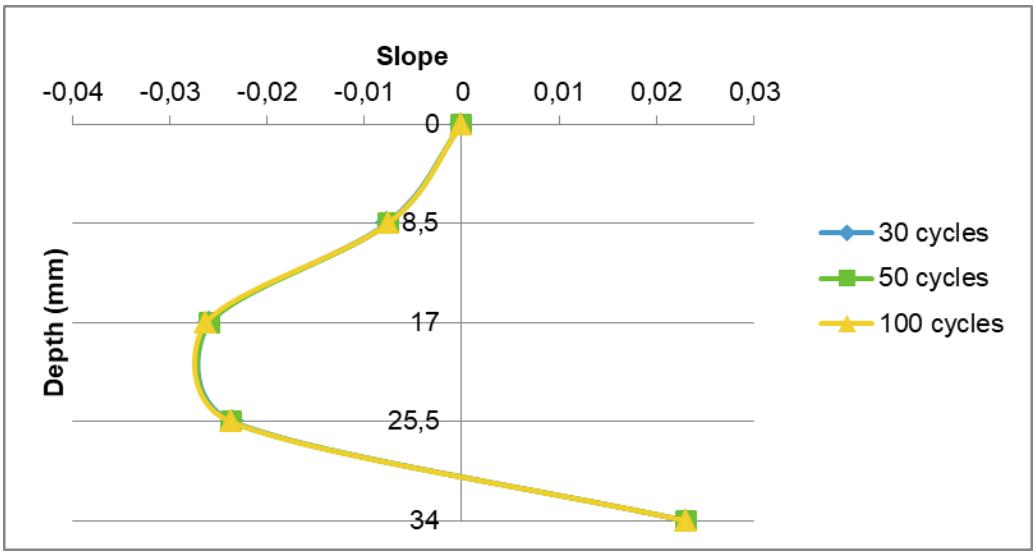

Figure A.32. Slope of the Segmental Pile with Post-Tension Force 1500 N in Medium-Dense Soil.

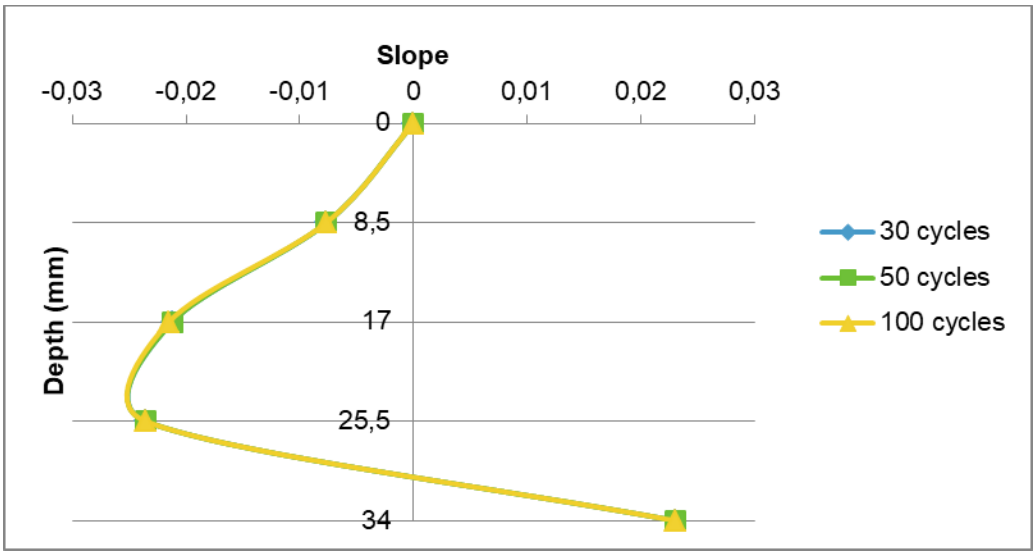

Figure A.33. Slope of the Segmental Pile with Post-Tension Force 2500 N in Dense Soil.

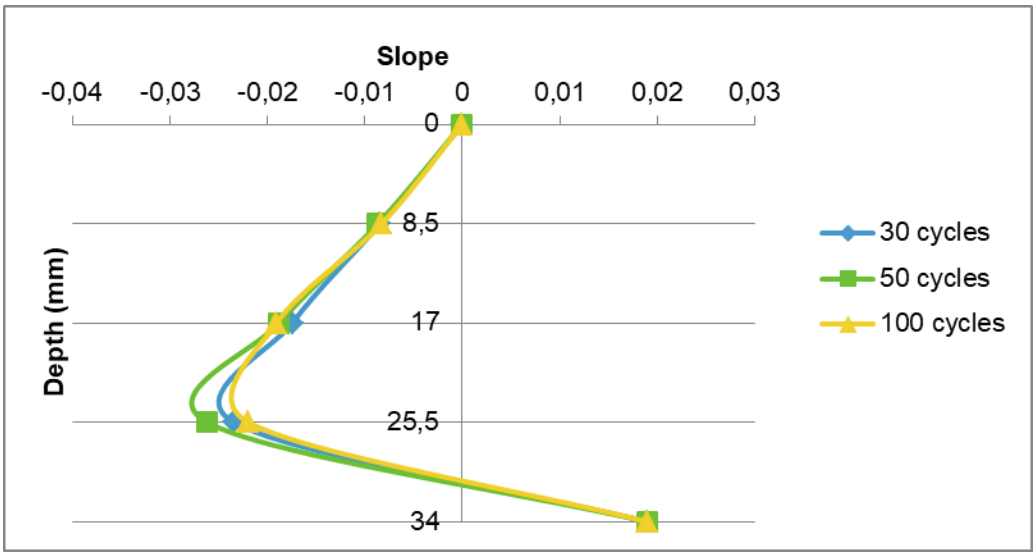

Figure A.34. Slope of the Mortar Beam in Loose Soil.

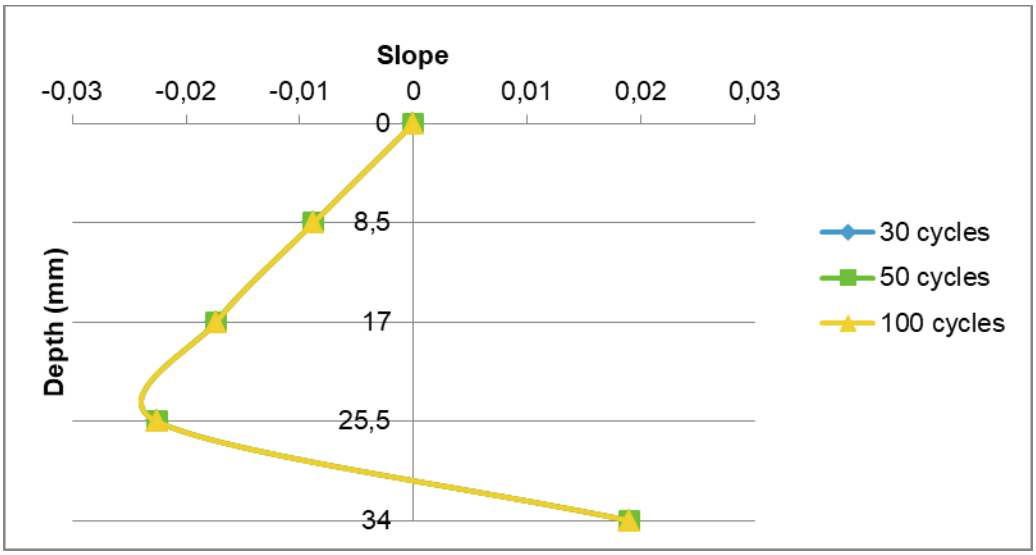

Figure A.35.: Slope of Mortar Beam in Meduim - Dense Soil.

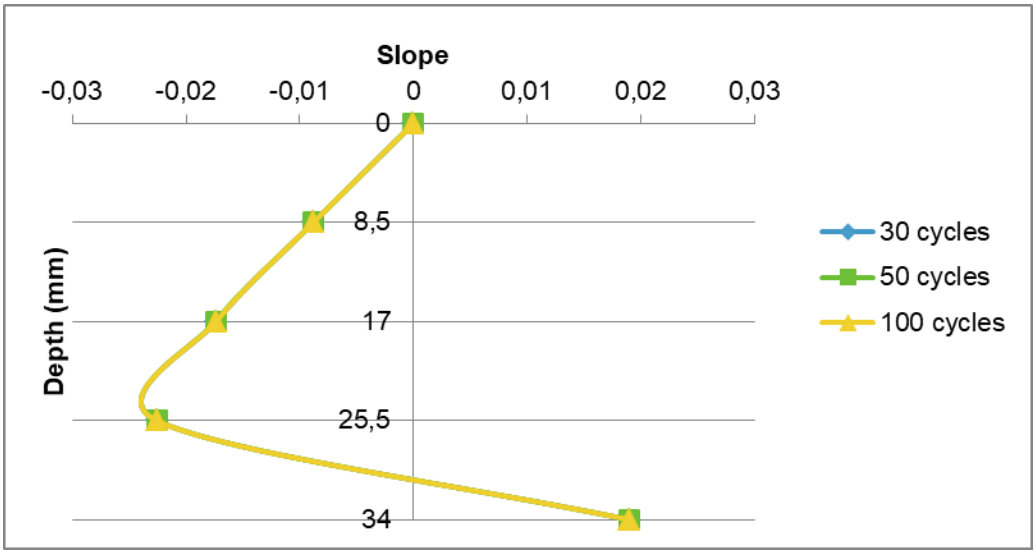

Figure A.36. Slope of the Mortar Beam in Dense Soil.

The table of slope-soil density under various cyclic loads is shown below.

Table A.1. Minimum and Maximum Slope Values of the Piles.

		30 Cycles Slope	50 Cycles Slope	100 Cycles Slope
Post-Tension 750 N	**Loose**	Min: -0,0235	Min: -0,0237	Min: -0,0237
		Max: 0,04	Max: 0,04	Max: 0,041
	Medium-Dense	Min: -0,0234	Min: -0,0236	Min: -0,0236
		Max: 0,04	Max: 0,0405	Max: 0,0405
	Dense	Min: -0,0235	Min: -0,0237	Min: -0,0237
		Max: 0,0405	Max: 0,0408	Max: 0,0407
Post-Tension 1500 N	**Loose**	Min: -0,0234	Min: -0,0271	Min: 0,0271
		Max: 0,036	Max: 0,034	Max: 0,034
	Medium-Dense	Min: -0,0232	Min: -0,0220	Min: -0,0256
		Max: 0,0364	Max: 0,037	Max: 0,0377
	Dense	Min: -0,0230	Min: -0,0232	Min: -0,0232
		Max: 0,036	Max: 0,037	Max: 0,037
Post-Tension 2250 N	**Loose**	Min: -0,0237	Min: -0,0237	Min: -0,0237
		Max: 0,023	Max: 0,023	Max: 0,023
	Medium-Dense	Min: -0,0235	Min: -0,0236	Min: -0,0237
		Max: 0,0229	Max: 0,0229	Max: 0,023
	Dense	Min: -0,0235	Min: -0,0235	Min: -0,0235
		Max: 0,023	Max: 0,023	Max: 0,023
Mortar Beam	**Loose**	Min: -0,0234	Min: -0,0261	Min: -0,0219
		Max: 0,019	Max: 0,017	Max: 0,019
	Medium-Dense	Min: -0,0225	Min: -0,0225	Min: -0,0225
		Max: 0,019	Max: 0,019	Max: 0,019
	Dense	Min: -0,0222	Min: -0,0222	Min: -0,0223
		Max: 0,018	Max: 0,018	Max: 0,0185

Slope values are not effected too much with number of cycles. Also, it is seen that density and rigidity values do not effect the slope value. All the values are quite close to each other.

A.4. Comparison of Cyclic Loading Test Results

In the figures below, displacement results of the cyclic loading tests are shown for each cyclic step and pre-stress value. It is seen that there is no irrelevant value in four test under same conditions. Differences are under one-tenth of milimeter order.

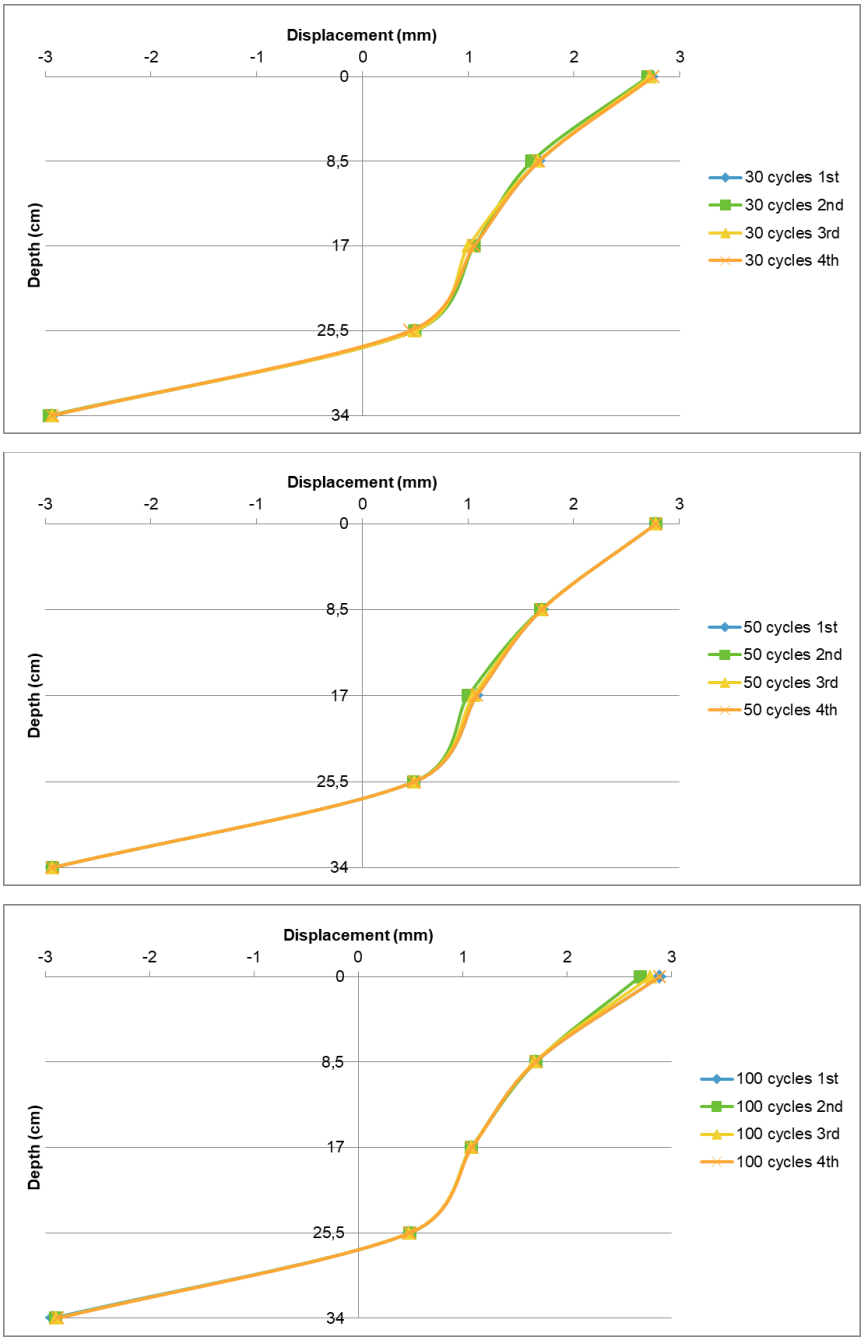

Figure: A.37. All Test Results of Displacement of the Segmental Pile with Post-Tension Force 750 N in Loose Soil.

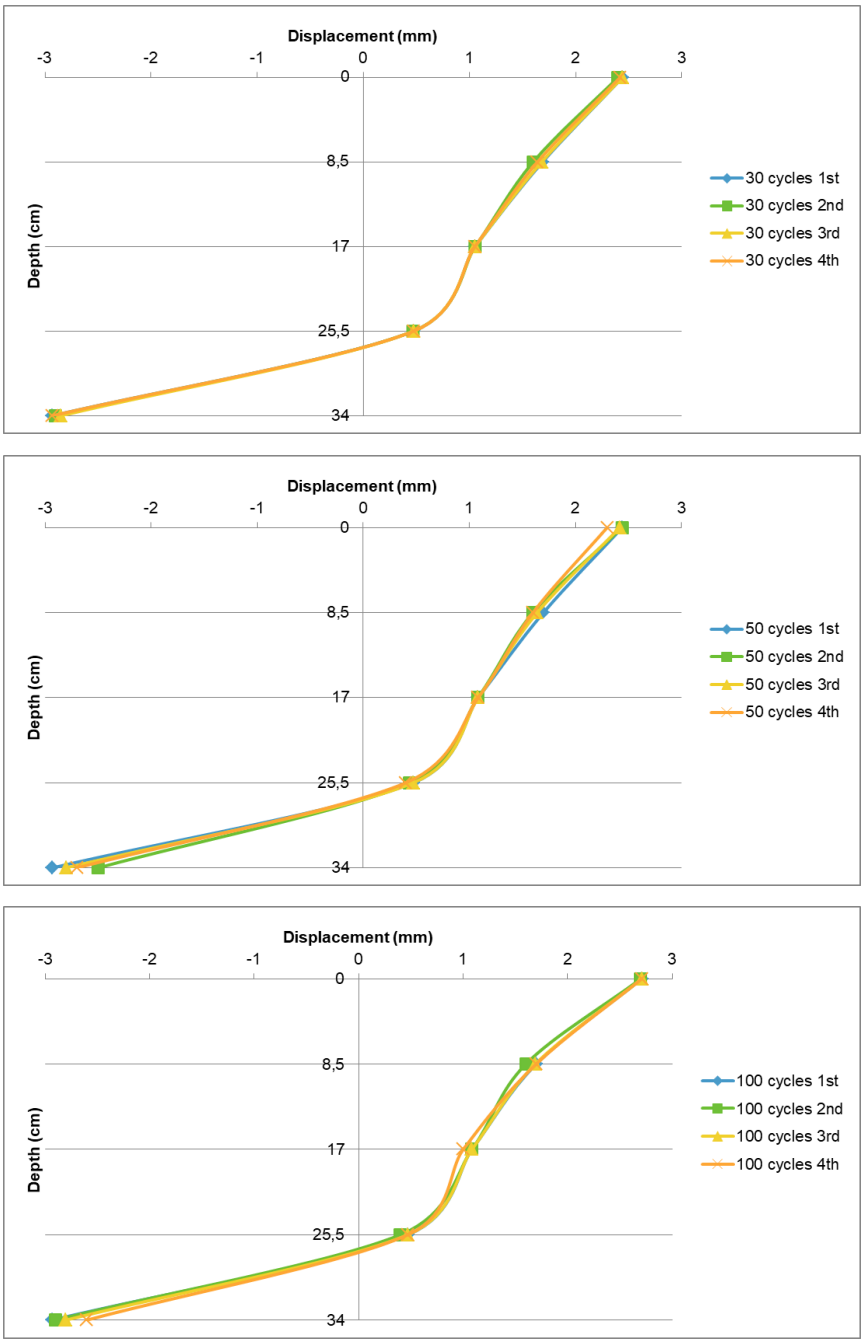

Figure: A.38. All Test Results of Displacement of the Segmental Pile with Post-Tension Force 750 N in Medium - Dense Soil.

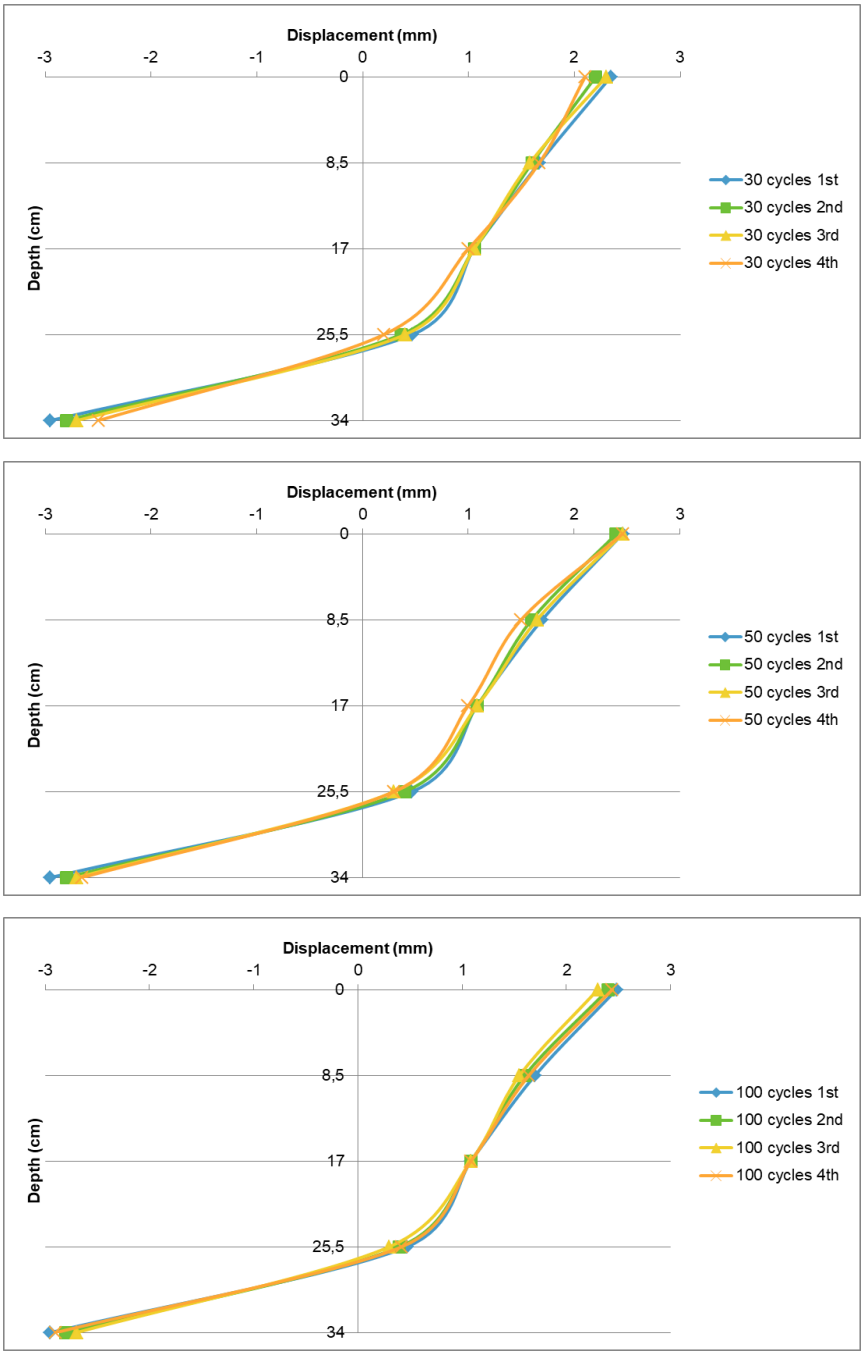

Figure: A.39. All Test Results of Displacement of the Segmental Pile with Post-Tension Force 750 N in Dense Soil.

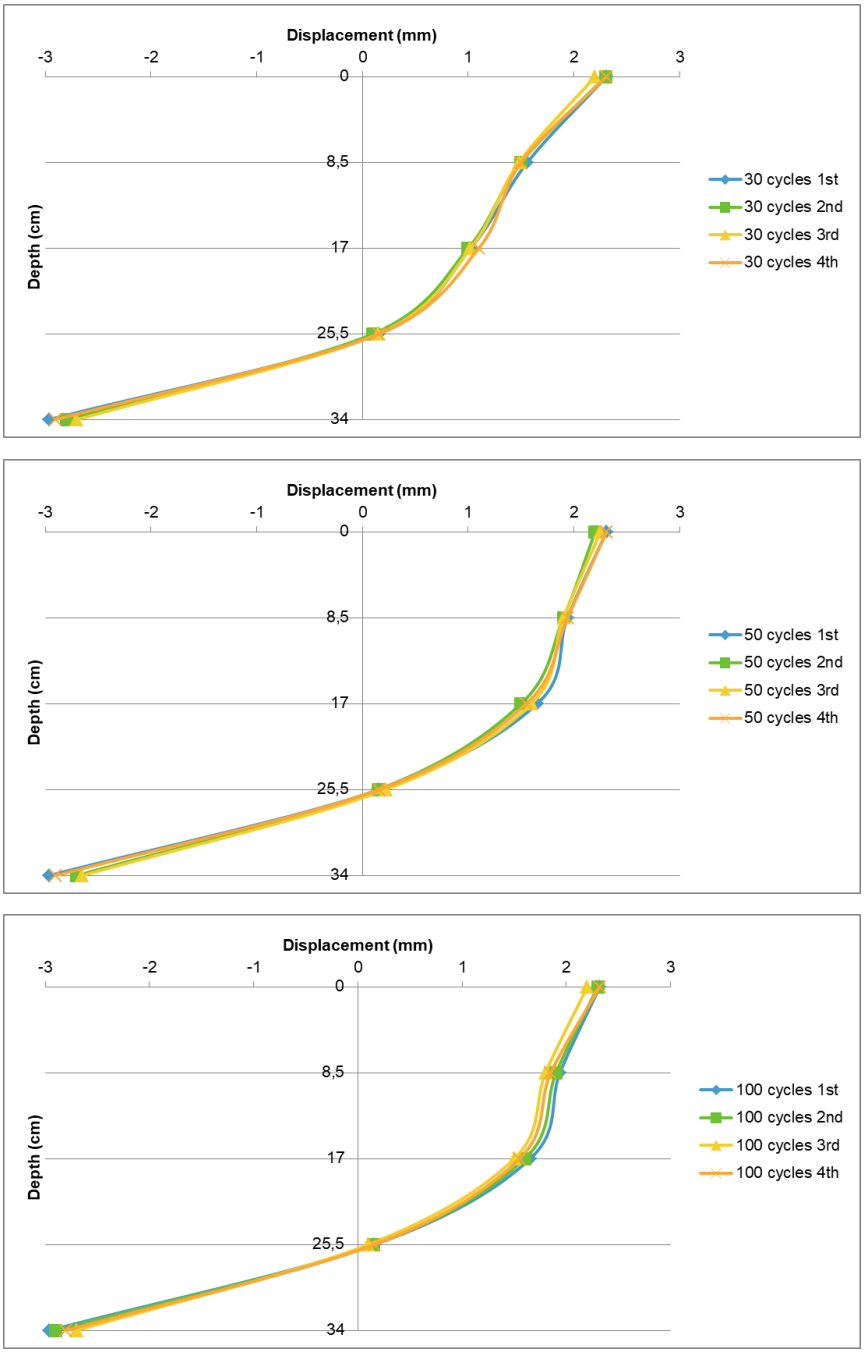

Figure: A.40. All Test Results of Displacement of the Segmental Pile with Post-Tension Force 1500 N in Loose Soil.

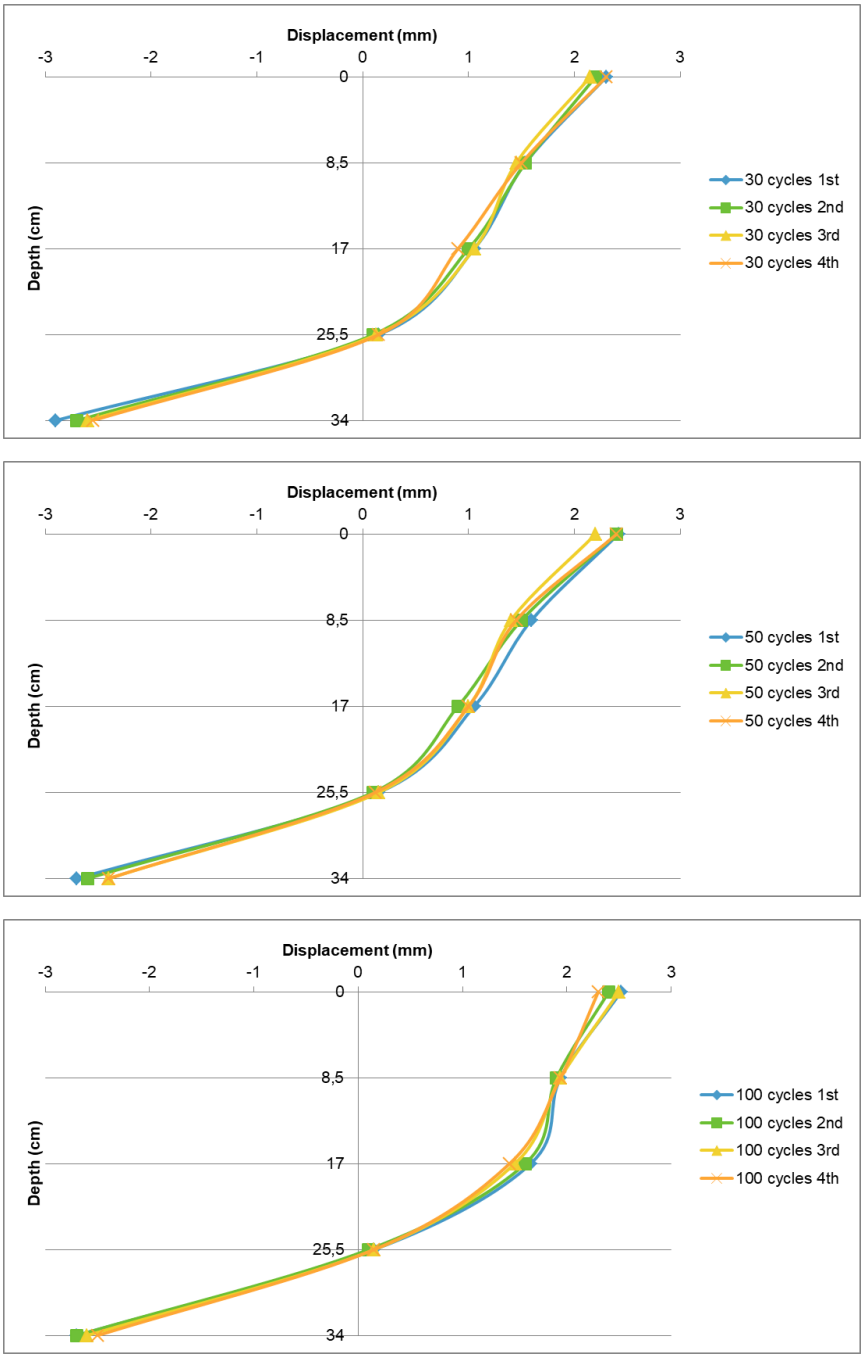

Figure: A.41. All Test Results of Displacement of the Segmental Pile with Post-Tension Force 1500 N in Medium - Dense Soil.

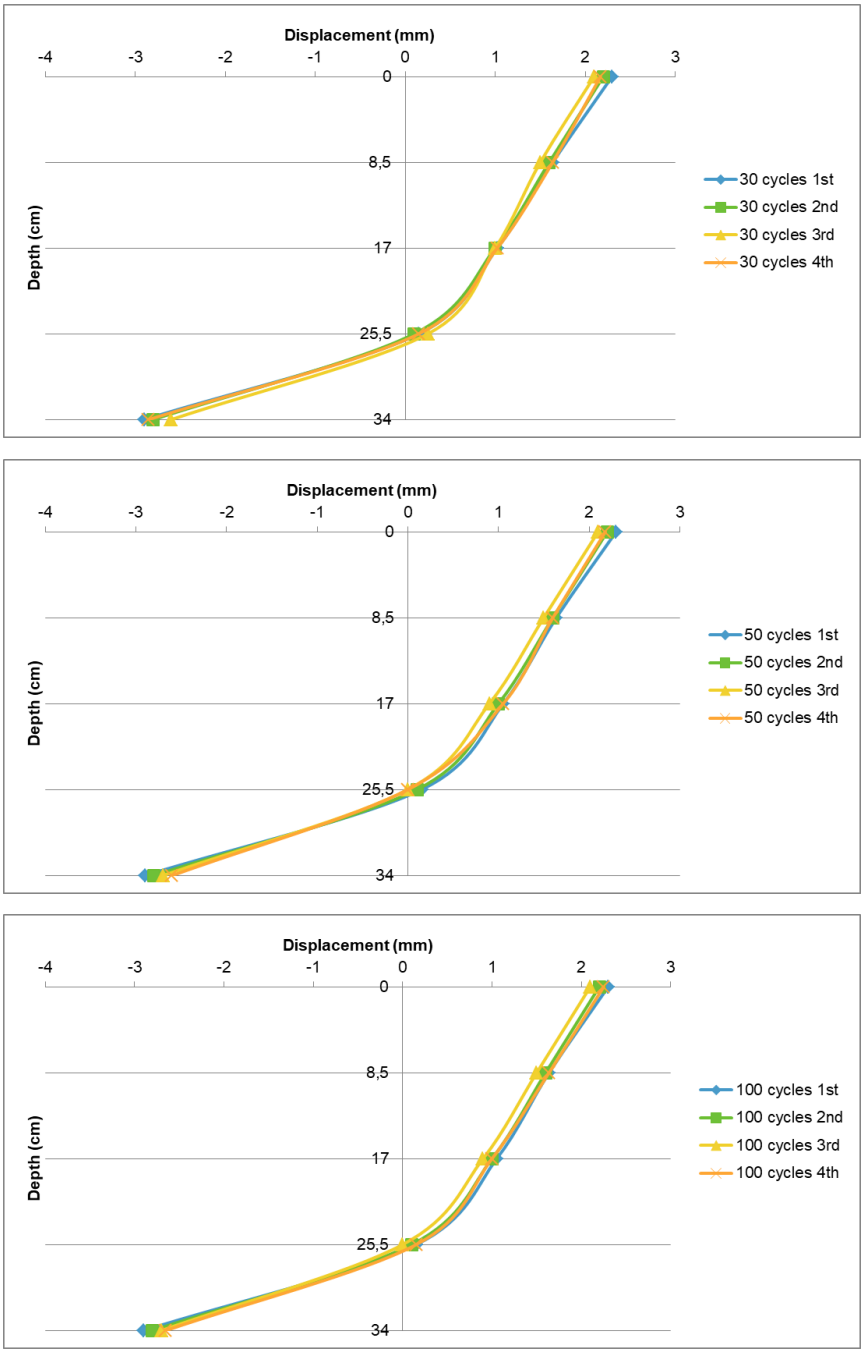

Figure: A.42. All Test Results of Displacement of the Segmental Pile with Post-Tension Force 1500 N in Dense Soil.

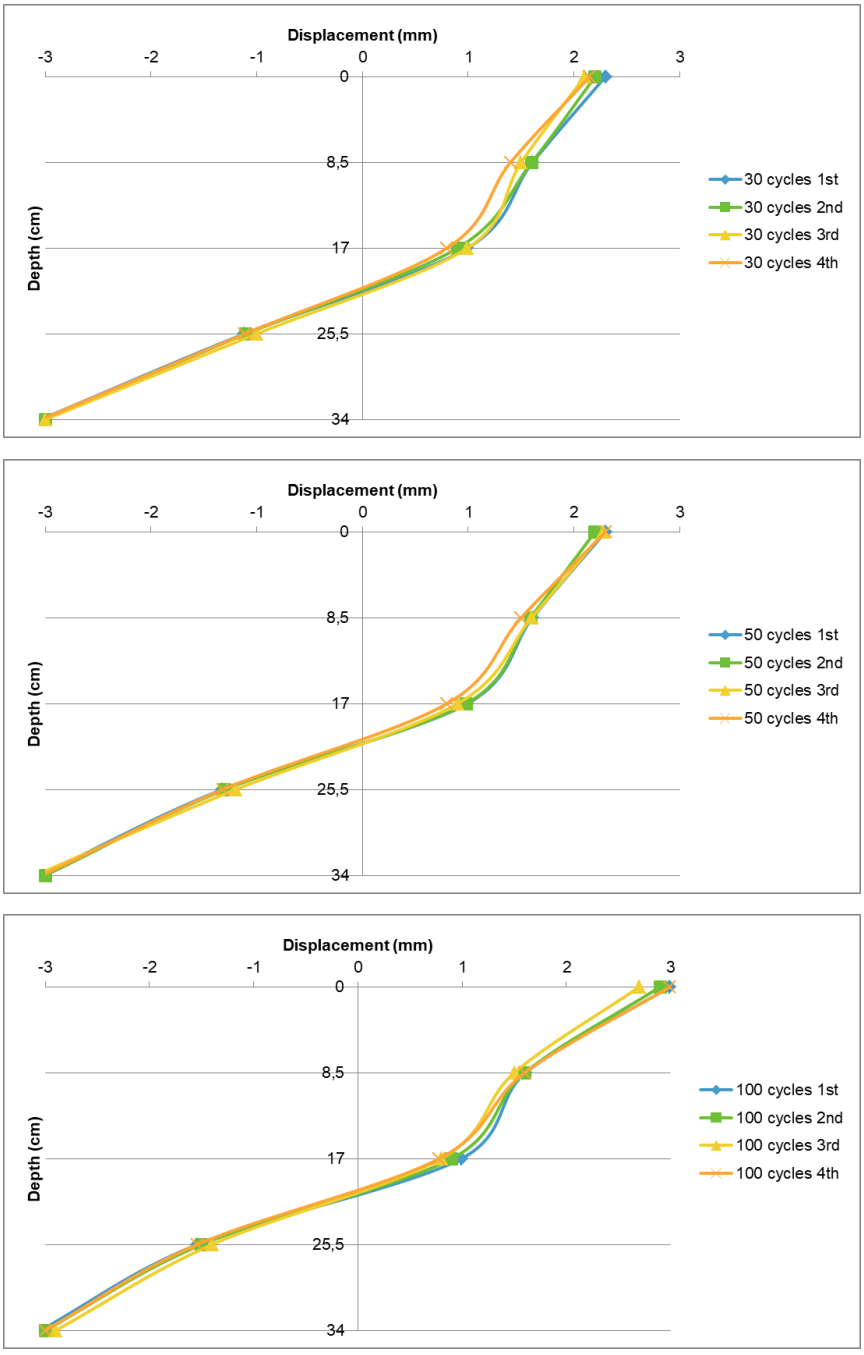

Figure: A.43. All Test Results of Displacement of the Segmental Pile with Post-Tension Force 2250 N in Loose Soil.

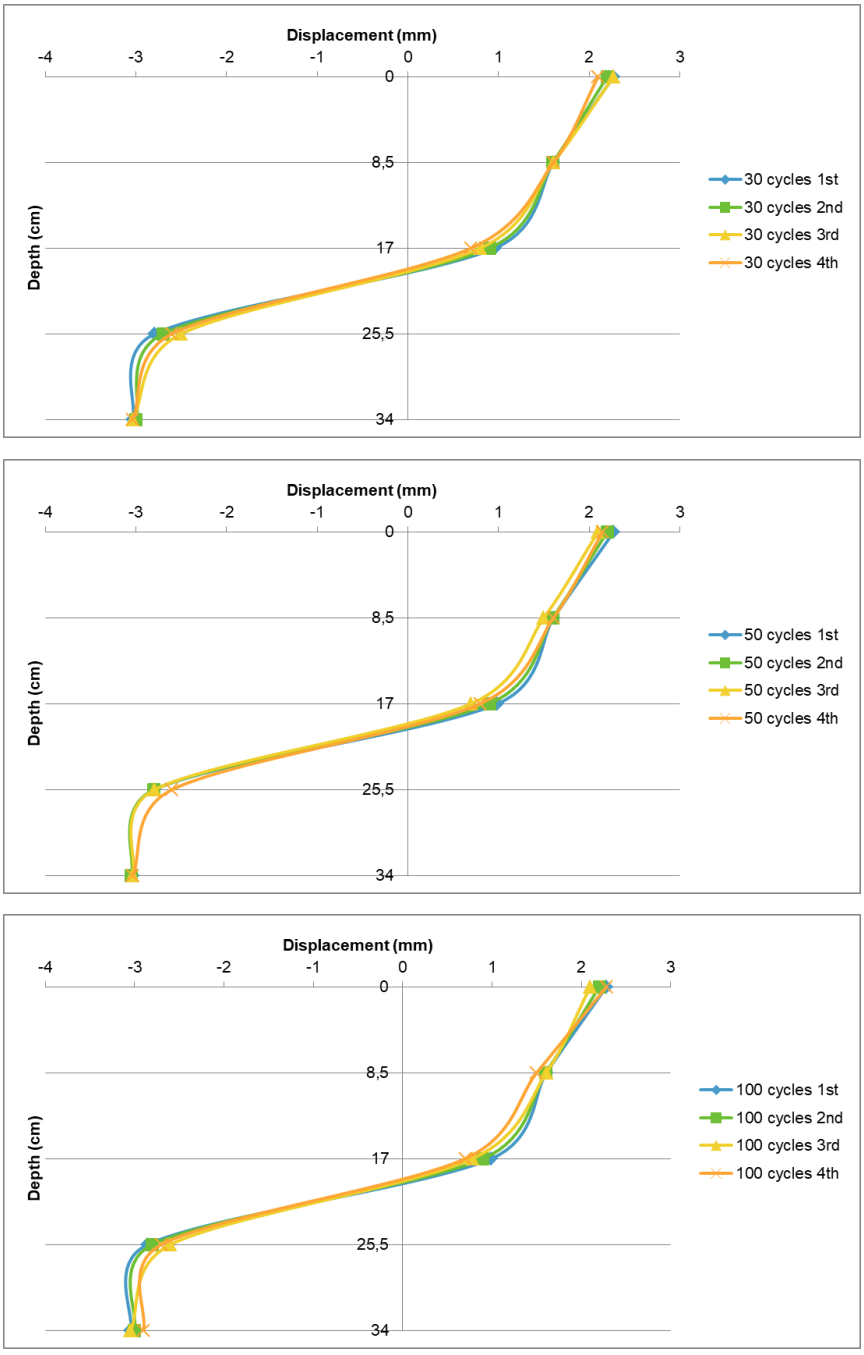

Figure: A.44. All Test Results of Displacement of the Segmental Pile with Post-Tension Force 2250 N in Medium - Dense Soil.

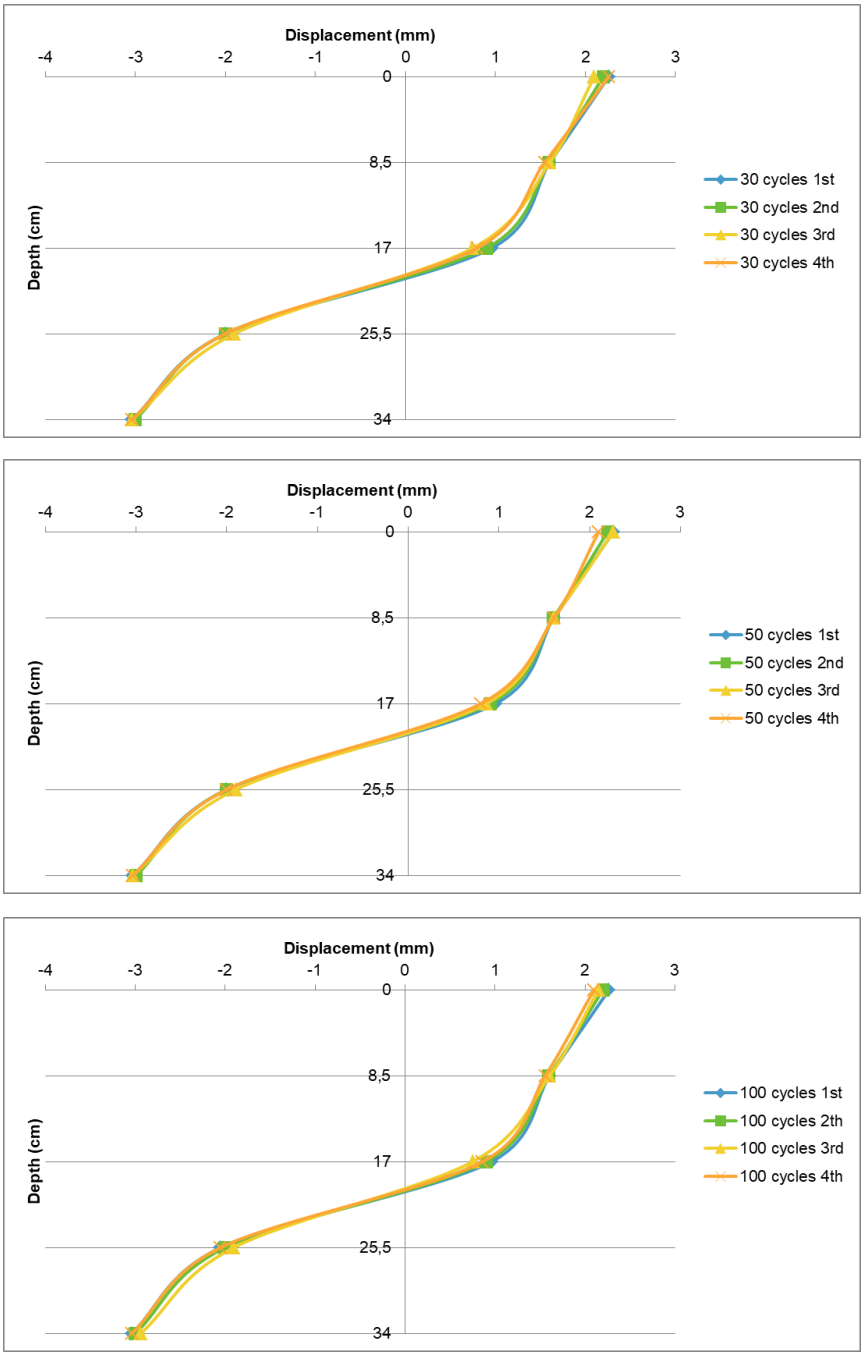

Figure: A.45. All Test Results of Displacement of the Segmental Pile with Post-Tension Force 2250 N in Dense Soil.

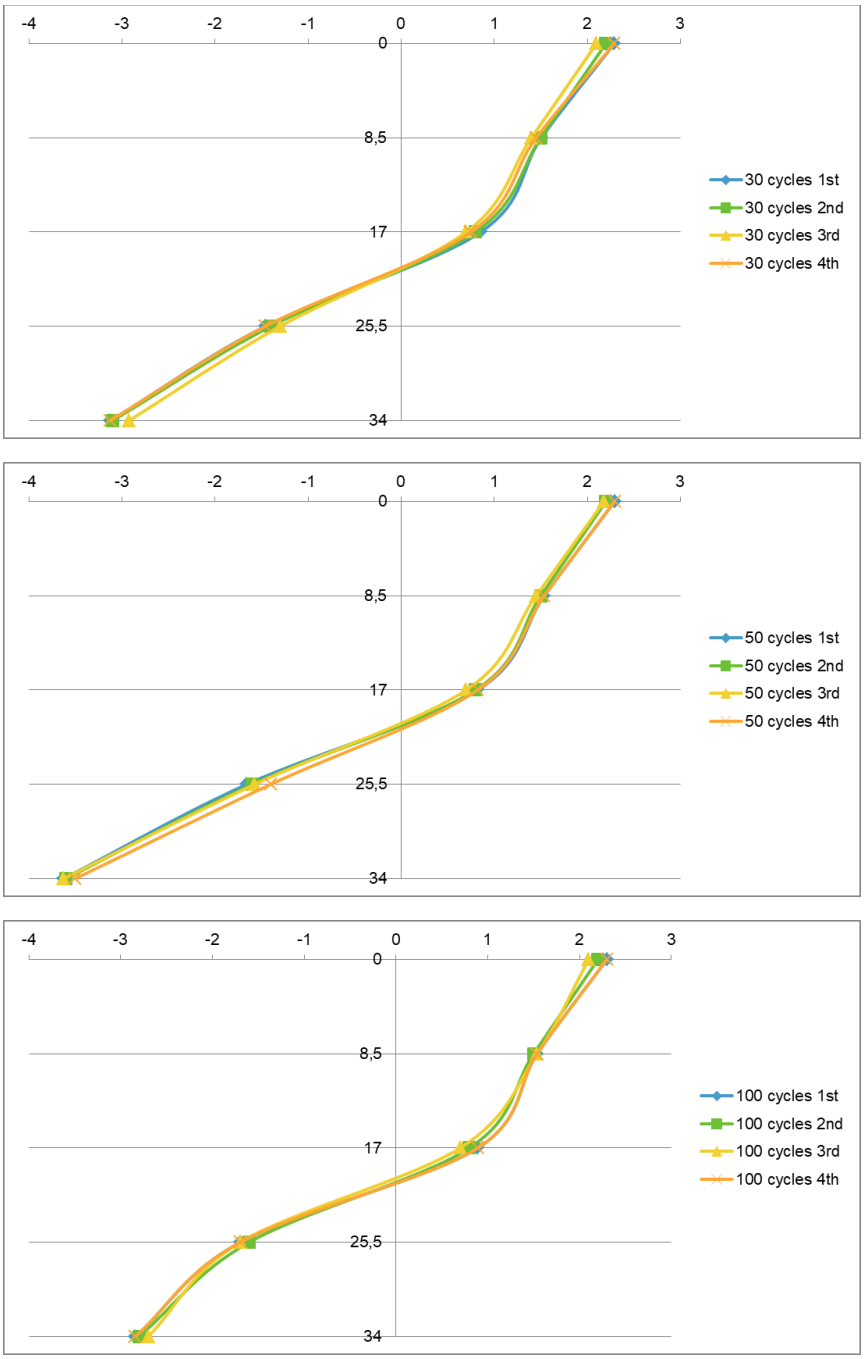

Figure: A.46. All Test Results of Displacement of the Segmental Pile with Post-Tension Force Mortar Beam in Loose Soil.

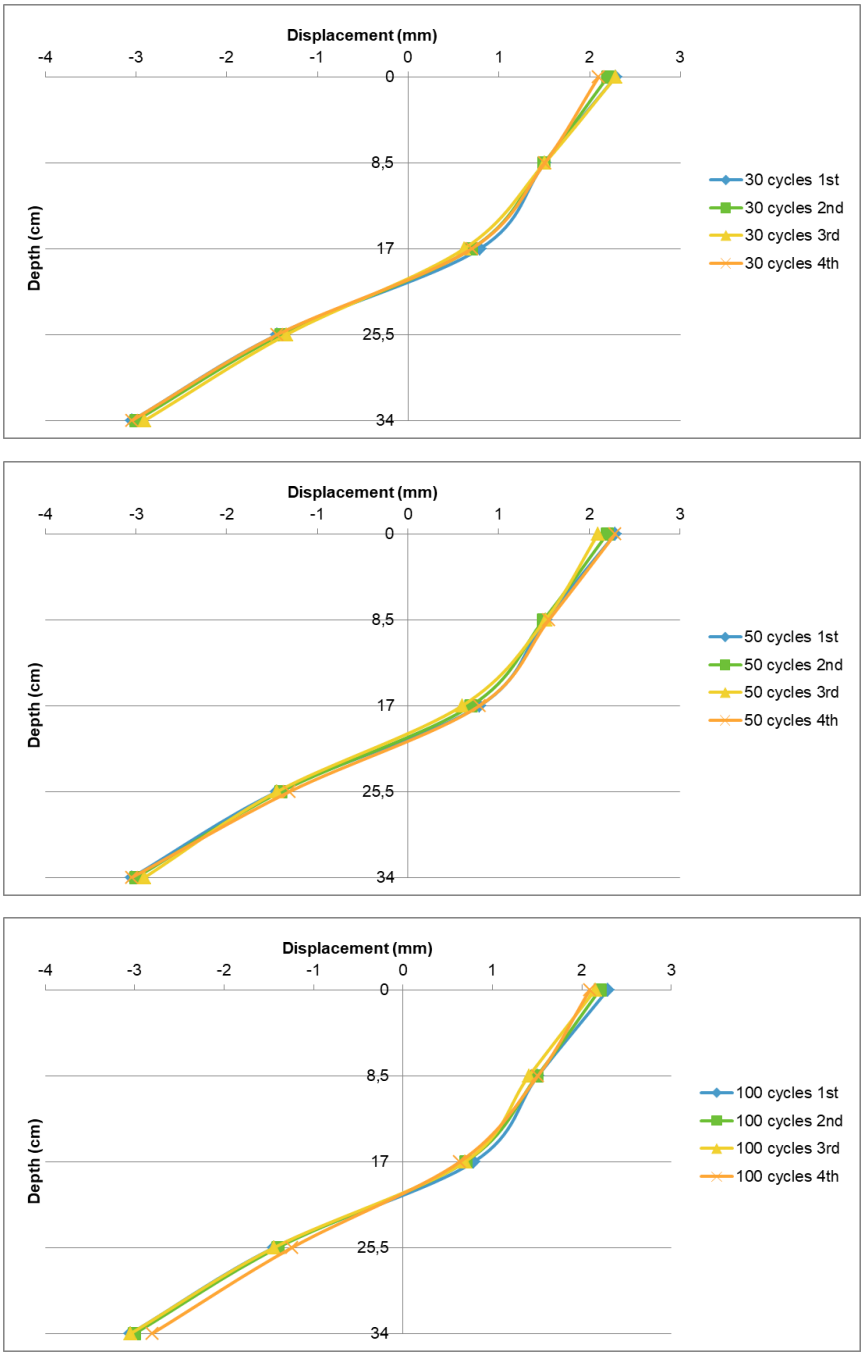

Figure: A.47. All Test Results of Displacement of the Segmental Pile with Post-Tension Force Mortar Beam in Medium - Dense Soil.

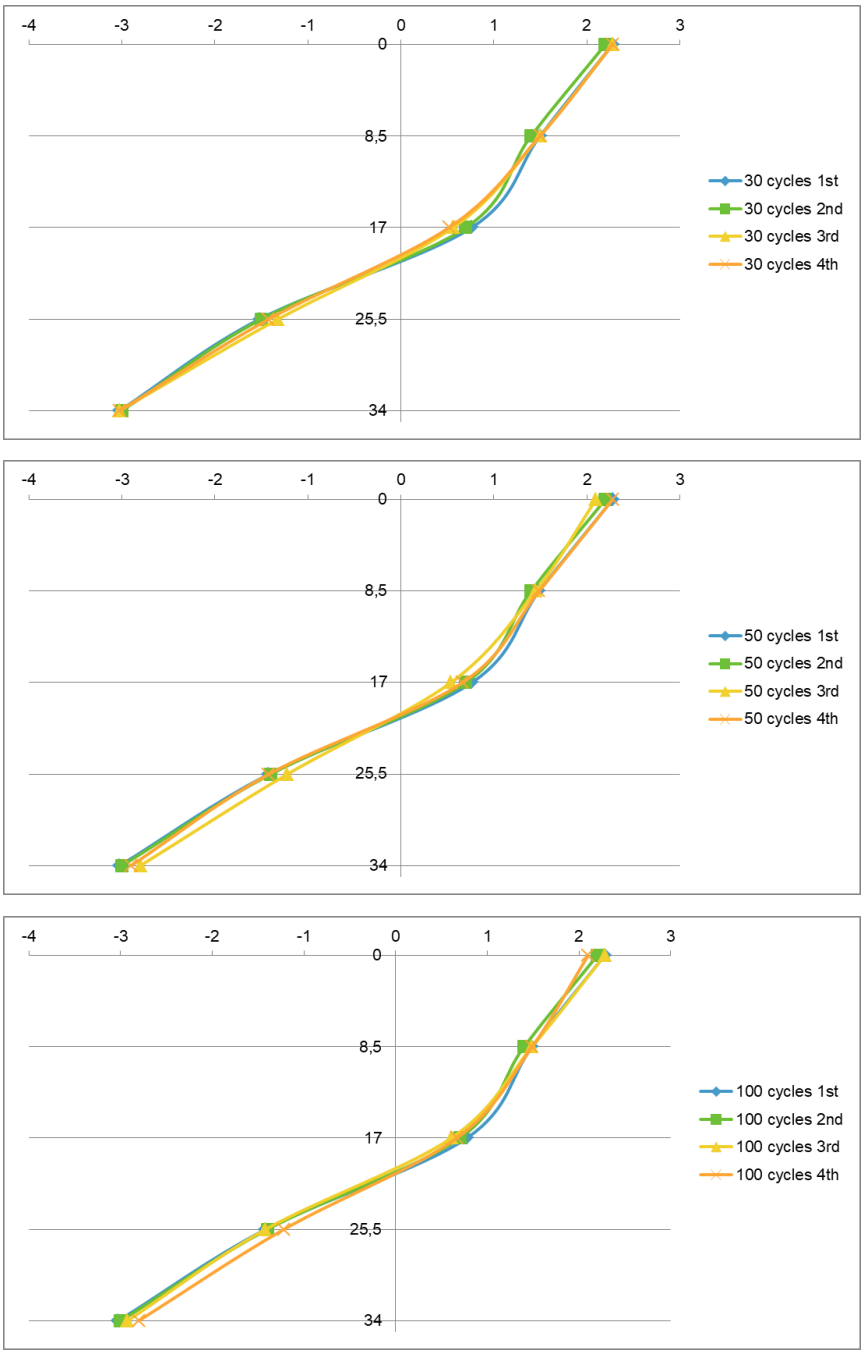

Figure: A.48. All Test Results of Displacement of the Segmental Pile with Post-Tension Force Mortar Beam in Dense Soil.

APPENDIX B: MORTAR BLOCKS PROPERTIES

B.1. Mortar Blocks Dimensions

Dimensions and weight of the blocks are shown in Table B.1. Block width range is between 4,8-5,1 (cm) and the height range is between 1,8-2,15 (cm). The mass of the concrete blocks are between 92,8-108,56 (gr).

Table B.1. Mortar Blocks Properties.

Block No	m (g)	h (cm)	b1 (cm)	b2 (cm)	Area (cm^2)	Volume (cm^3)	γ (g/cm^3)
1	103,2	2	5,05	5	25,25	50,5	2,043
2	104,37	2,06	5	5	25	51,5	2,026
3	106,88	2,1	5,05	5	25,25	53,025	2,015
4	105,96	2,1	5	5	25	52,5	2,018
5	100,4	2,15	5,1	5,1	26,01	55,9215	1,795
6	104,36	2,1	5,05	5	25,25	53,025	1,968
7	100,31	2	5	5	25	50	2,006
8	95,84	1,8	4,85	4,85	23,522	42,340	2,263
9	106,63	2,05	4,8	4,85	23,28	47,724	2,234
10	108,22	2,05	4,8	4,85	23,28	47,724	2,267
11	101,49	1,95	4,9	4,85	23,765	46,341	2,190
12	97,07	1,9	4,85	4,85	23,522	44,692	2,171
13	102,79	2	4,85	4,9	23,765	47,53	2,162
14	100,05	2,1	4,8	4,8	23,04	48,384	2,067
15	106,78	2,1	4,8	4,8	23,04	48,384	2,206
16	101,17	2	4,85	4,85	23,522	47,045	2,150
17	104,39	2	4,9	4,85	23,765	47,53	2,196
18	108,56	2	4,85	4,85	23,522	47,045	2,307
19	105,36	2,1	4,9	4,85	23,765	49,906	2,111
20	98,43	1,95	4,8	4,8	23,04	44,928	2,190
21	106	2	4,85	4,9	23,765	47,53	2,230
22	98,04	1,85	4,8	4,8	23,04	42,624	2,300
23	105,38	2	4,85	4,85	23,522	47,045	2,239
24	106,23	2	4,85	4,85	23,523	47,045	2,258

Table B.1. Mortar Blocks Properties. (cont.)

25	92,8	1,9	4,8	4,8	23,04	43,776	2,119
26	101,47	1,9	4,8	4,8	23,04	43,776	2,317
27	101,45	1,95	4,8	4,8	23,04	44,928	2,258
28	99,58	2	4,85	4,9	23,765	47,53	2,095
29	99,71	1,85	4,8	4,85	23,28	43,068	2,315
30	103,1	2,1	4,85	4,9	23,765	49,906	2,065
31	105,02	2,1	4,85	4,85	23,522	49,397	2,126
32	101,26	2,05	4,85	4,85	23,522	48,221	2,099
33	103,93	2,05	4,8	4,9	23,52	48,216	2,155
34	104,83	1,95	4,8	4,9	23,52	45,864	2,285
35	103,52	2,1	4,85	4,85	23,522	49,397	2,095
36	100,5	2,05	4,85	4,85	23,522	48,221	2,084
37	100,25	1,95	4,8	4,8	23,04	44,928	2,231
38	102,81	2,15	4,85	4,85	23,522	50,573	2,032
39	104,48	1,9	4,8	4,9	23,52	44,688	2,337
40	103,35	2,1	4,85	4,9	23,765	49,906	2,070
41	101,6	2,05	4,85	4,85	23,522	48,221	2,106
42	107,17	2,1	4,8	4,85	23,28	48,888	2,192
43	99,92	2	4,85	4,9	23,765	47,53	2,102
44	104,77	2,1	4,8	4,85	23,28	48,888	2,143
45	105,02	2	4,8	4,9	23,52	47,04	2,232
46	105,86	2,1	4,85	4,8	23,28	48,888	2,165
47	106,31	2,05	4,85	4,9	23,765	48,718	2,182
48	100,75	2,1	4,9	4,9	24,01	50,421	1,998
49	106,53	2,1	4,85	4,85	23,522	49,397	2,156
50	95,22	1,9	4,8	4,85	23,28	44,232	2,152
51	97,77	1,95	4,85	4,85	23,522	45,868	2,131
52	101,4	2,1	4,85	4,85	23,522	49,397	2,052